Past Environmental Change On The Eastern Andean Flank, Ecuador

Thesis

Past environmental change on the eastern Andean flank, Ecuador

---

A thesis presented for the degree of Doctor of Philosophy

By

Hayley Frances Keen

Bachelor of Science with Honours (University of Leicester)

Master of Research (University of Leicester)

March 2015

Department of Environment, Earth and Ecosystems

The Open University

Abstract

The eastern Andean flank of Ecuador (EAF) contains some of the world's most biodiverse ecosystems. Andean montane forests are threatened due to anthropogenic pressures and both current and projected climate change. This thesis examines the palaeoecological history of two stratigraphic sequences (Mera Tigre West [MTW] and Mera Tigre East [MTE]) obtained from the Ecuadorian modern lower montane forest. The sediments preserved were analysed using eight analytical techniques, allowing an insight into the ecosystem's potential response to projected changes derived from their past responses. Palaeoecological studies on the EAF are rare, and those that do exist are debated relating to: i) the inference of robust ecological data from pollen records in floristically diverse locations, and ii) the past source area of sediments preserved in fluvially exposed sequences, potentially leading to contamination with older material.

A statistical sub-sampling tool was developed (debate i), capable of producing statistically robust count sizes for each pollen sample; MTW and MTE count sizes ranged from 196-982 showing the diversity within sequences. The depositional environment of MTE was analysed, investigating sediment provenance throughout (debate ii). Results found that large scale volcanic events were critical in the preservation of the sediments, whereas fluvial influence caused a regional sediment source area in the upper stratigraphy, impacting on the palynological interpretation of MTE. Pollen records demonstrated the presence of a diverse vegetation community with no modern analogue at MTE (abundant taxa (>15 %): *Hedyosmum, Wettinia, Ilex*) and upper montane forest at MTW (*Alnus, Hedyosmum, Podocarpus*). Fire was not the main driver for the vegetation reassortment at either site (MTW correlation coefficient: -0.37, MTE: 0.16). The two sites have demonstrated the EAF plays host to floristically dynamic ecosystems, susceptible to drivers of change (fire and landscape) and should be considered when predicting the montane forests' future response to environmental change.

Acknowledgments

The completion of this thesis would not have been possible without the guidance and support of many people. First and foremost I would like to thank my supervisors Will, Encarni and Sarah, without whom this project would not have existed, nor would I have had the skills and knowledge required to finish it. The support they have provided me with over the last three and a half years has led to the production of the thesis that you are currently reading.

I would also like to thank the various members of the academic community who helped me complete my lab work. Thank you to Alison Halton who helped me with my Argon lab work, remaining patient whilst I covered the pristine white lab benches with piles of mud and then constantly saturated the machine whilst analysing them. Thank you to Andy Carr who performed OSL dating on my samples, despite my difficult samples he still managed to produce two dates from them. I would also like to thank the late John Watson who taught me how to run LOI and XRF on my samples whilst always having an entertaining story to tell. Thanks also go to Michelle Higgins who helped me thin section my wood and then special thanks go to Peter Gasson, Oris Rodriguez Reyes and Imogen Poole who then helped me try and identify them. Thanks also to Pete and Sam who prepped and ran two samples for me on the ICP-MS. Finally I would like to thank Susana León Yánez who helped me to identify my unknown plant pictures, despite only a few of them having pictures of flowers on them. It is definitely not easy identifying tropical plants from pictures of leaves, so I am extremely grateful for your help!

I would also like to thank the people who made the month long fieldwork to Ecuador such an enjoyable experience. I would again like to thank Will and Encarni for the support they gave on this trip, helping to make it so successful. Thanks also go to Frazer who spent many an hour clambering up muddy river banks, Jam who came along to film all of our adventures (and then helped produce a fantastic video from all of the footage) and also Patty who helped identify the

sediments I ended up studying. Since fieldwork Patty has also provided much needed guidance into the many volcanoes of Ecuador, thank you for this as I am no volcanologist.

Thanks also go to the many members of EEE who have made the last few years so enjoyable. There have been many entertaining Friday beers, breakfasts, cricket matches and coffee times which have helped make the process that much easier. Definite thanks go to the lovely people I have shared an office with over my time here, Adele, Alice, Chris, Frazer, Kate, Olu, Pete, Sam and Tom. The Z209 university challenge competition definitely helped by providing some entertainment in the post lunch office slump. Special thanks as well also go to the members of the palaeoenvironmental lab who have always been on hand to offer a listening ear, words of advice, or just a 'palaeo' curry night. Final departmental thanks go to Liz Lomas who was always a great help, no matter what the query.

Last but by no means least; I would like to thank all of my family and friends who have helped me through everything. Mum, thank you for always being there when I need you. Chris, thank you for being so patient and understanding over the last few years, thank you for all of the little things that you have done which have helped make this process easier, you always knew when I would appreciate a bar of chocolate or when to just let me moan it all out. I promise now this is over I will do my fair share of the cooking and the washing up once more! Thank you to all of my friends who have provided me with much needed laughs and days out. We have shared many a good dinner, board game, "Stitch and bitch" and Wednesday pubs, all of which have been great fun!

Thank you once more to all listed above, and to everyone else who has helped in any way, without you all I am not sure I would be anywhere near having a finished thesis in front of me.

Table of Contents

Table of Figures

List of Tables

List of Equations

Previously published material

I confirm that the following chapter has been published:

Chapter 5: A statistical sub-sampling tool for extracting vegetation community and diversity information from pollen assemblage data.

Keen, H.F., Gosling, W.D., Hanke, F., Miller, C.S., Montoya, E., Valencia, B.G. and Williams, J.J. (2014) A statistical sub-sampling tool for extracting vegetation community and diversity information from pollen assemblage data. *Palaeogeography, Palaeoclimatology, Palaeoecology*. **408**, 48-49. DOI:10.1016/j.palaeo.2014.05.001.

Signed..... Dated.....

Chapter 1: Introduction

This chapter introduces the rationale behind this thesis to provide a conceptual background to the approaches and methodologies applied. The specific aims of the research are also introduced along with a structure of the thesis. Further background and details of the conceptual framework are then given in Chapter 2.

1.1. Rationale and research objectives

1.1.1. Current global environmental change

The Earth we know today is changing rapidly under anthropogenic pressures (Cubasch et al., 2013, Eshel et al., 2014, Roberts and Hamann, 2012, Steffen et al., 2015) and also as a result of natural variability (Stouffer et al., 1994). Natural variability within Earth systems occurs on a range of time and spatial scales; for example events such as the El Niño Southern Oscillation (ENSO) acting on small time scales (roughly every three to seven years) whilst glacial/ interglacial cycles occur over much longer time scales (tens –hundreds of thousands of years), both, however, impact global Earth systems (Ghil, 2002). Anthropogenic pressures are, however, expected to accelerate the rate of natural climatic variability (Karl and Trenberth, 2003). Current indications are that atmospheric greenhouse gas concentrations are rising and that this is causing the temperatures of the land and the oceans to increase and the precipitation regime to alter (Cubasch et al., 2013). Alteration in the global climate is subsequently having an effect on global biota, including the vegetation which covers the surface of the Earth (Cubasch et al., 2013, Halofsky et al., 2013, Parmesan and Yohe, 2003). Projected changes in precipitation, temperature and an increase in extreme events (for example increased periods of drought; Rivera and Penalba, 2014 and increased flooding; Espinoza et al., 2014) are expected to have a large influence on vegetation, causing vegetation reassortment and species loss. These changes in climate, in particular, an increased occurrence of drought, is causing a rise in the occurrence of fires, especially in regions that did not use to burn naturally, e.g. the Amazon rainforest (Brando

et al., 2014). These altering drivers of change mean that adaptions in the global vegetation are already being observed, with further variation expected to occur over the next decade and beyond (Hannah et al., 2002). Changing climatic conditions are not, however, the only human induced pressures acting on global vegetation. Increasing populations require increasing resources such as food and shelter which, in turn, is causing an impact on global vegetation cover (Foley et al., 2005, Karl and Trenberth, 2003), with vegetation being cleared to allow space for farming whilst deforestation provides resources, space and capital. Human induced changes in global vegetation cover are occurring rapidly; in the past 2000 years alone, it is estimated that humans have reduced global vegetation cover by 45 %. Fifteen percent of the natural plant cover is estimated to have been removed since 1900, mainly through the mechanisms of deforestation, harvesting for resources and conversion of areas such as wetlands and grasslands to farmland (Goudie, 2013). Vegetation cover is altering all across the globe; however, vegetation in the world's tropical regions is being impacted at an increasing rate (Scholes and van Breemen, 1997). In 2000, it was estimated that 60 % of the world's tropical forest was classified as degraded, meaning that it no longer resembled its natural state (Chazdon, 2003). This large vegetation change means it is important to understand the global impact these changes may have and how best to mitigate impact.

This thesis aims to investigate how future environmental change is likely to impact upon these important tropical ecosystems, with the aim of understanding the global impact these changes may have. By understanding the effect environmental change may have on these ecosystems it will be possible to mitigate the impacts. This thesis also aims to investigate some of the issues regarding palynology (study of pollen and spores used to investigate vegetation change) and then apply palynology (taking into consideration count size issues and preservation problems) to broach some of the knowledge gaps in the investigation of how the tropical ecosystems are being impacted by global environmental change.

1.1.2. Tropical environmental change

Tropical ecosystems (20°N to 20°S) contain the highest level of biodiversity globally and include many endemic species (Barlow et al., 2007, Lewis et al., 2009); however, global environmental change is threatening the existence of these ecosystems (Lewis et al., 2009). Tropical ecosystems are important worldwide as, aside from their high biodiversity value, they play a vital role in terrestrial carbon storage (Denman et al., 2007) and global climate systems (Burn et al., 2010).

Theoretical model based projections indicate that tropical forests are already undergoing major changes to their biodiversity in response to changing environmental conditions (Zuidema et al., 2013). Evidence for these 'future' changes is already being gathered in tropical ecosystems, with a loss of species being observed alongside degradation and fragmentation of these ecosystems (Turner, 1996). However, current understanding of the exact environmental conditions which are impacting tropical ecosystems is poor, with changes attributed variously to altering climate, atmospheric conditions, nutrient deposition, major disturbance recovery and changing land use (Zuidema et al., 2013). In order to correctly protect and manage tropical ecosystems it is essential to fully understand how changing environmental conditions may impact upon them.

One of the best ways to understand how environmental change may impact tropical ecosystems is to look back at how these tropical ecosystems have responded to environmental change in the geological past (Anderson et al., 2006, Moore, 2002, Swetnam et al., 1999). Although we can currently observe tropical ecosystems responding to changing environmental conditions (for example the Amazon drought of 2010 caused an increased fire occurrence in response to decreasing precipitation causing a 31 % loss in canopy cover; (Brando et al., 2014), tropical forests are also known to change over longer time scales (Barlow and Peres, 2008, Joppa et al., 2008, Lewis et al., 2011). Tropical rainforests have existed since the Cretaceous period

(Burnham and Johnson, 2004, Morley, 2000), however, their current vegetation assemblages are estimated to have formed c. 10,000 years ago (Bush et al., 1992, Francisquini et al., 2014). Modern ecological studies often only investigate short time scales (decades), however, this is not long enough to observe change occurring. and in order to fully understand how tropical ecosystems have responded to environmental change in the past it is vital to investigate longer (>1000 year) timescales. By looking back even further (>10,000 years) it is possible to understand how tropical vegetation responded to disturbances prior to human intervention (human arrival >12,000 years BP in the Andes; Borrero et al., 1998, Gosling et al., 2009). Investigating environmental change that occurred greater than 10,000 years ago allows the responses to a wide range of projected environmental changes including glacial-interglacial cycles, global warming and the reassortment of tropical vegetation including taxa turnover and the generation time of a tropical ecosystem (Whitlock, 1992) to be assessed. Aside from providing evidence of responses to these changes, looking back further into geological time provides evidence as to how tropical ecosystems have responded to natural events, e.g. natural burning. The Amazon rainforest does not easily burn naturally today (areas of high precipitation [>2000 mm per annum] are unlikely to burn, however, it is hard to say this for certain due to areas of dense forest being), but it is expected increasingly to burn naturally with a high severity in response to a projected reduction in precipitation (Cochrane and Barber, 2009). Therefore, by observing the vegetation response to past burning events, it is possible to understand how the projected fire increase may impact the modern vegetation assemblage. In order to observe vegetation change that occurred greater than 12,000 years ago a proxy (physical, biological or geochemical archive of the past) of change is required. These proxies are preserved in sedimentary archives (soils, tephra, and fluvial gravels preserved in lakes, swamps and bogs) deposited in the geological past and they can be used to reconstruct how the past environment impacted past ecology (Birks and Birks, 1980).

1.2.1. Palaeoecology

Palaeoecology is concerned with the study of past organisms, or past ecology, and the relationships with the environment that these organisms previously lived in (Birks and Birks, 1980). Palaeoecology can be used to reconstruct past environments, and in a multi proxy approach (analysis of different independent proxies or tools, such as pollen analysis, chironomids and charcoal particles amongst others), it can be used to investigate past environmental change and how the vegetation (or other variable) present was responding to these changes (Birks and Birks, 1980). Without a multi proxy approach in palaeoecology it is hard to reconstruct the environment whilst avoiding circular reasoning (Birks and Birks, 1980). For example, an organism cannot be used to define an environment as cold, if the only reason for that definition is that that organism is cold adapted, a further, independent proxy is required (Battarbee, 2010, Birks and Birks, 1980). In order to avoid circular reasoning, it is important to not only undertake a multi proxy approach, but to provide a chronology for the sediments of interest (Huntley, 1996).

Palaeoecological records are, however, not without their flaws. One problem with palaeoecology is the identification issues that can occur in proxies, in particular with studies involving pollen grains (known as palynology; see section 1.2.2.; Joosten and de Klerk, 2002). Pollen grains preserved in tropical ecosystems are particularly hard to identify due to many similarities in pollen grains leading to difficulty in classification beyond genus, or more often family level (Burn et al., 2010). One example of this is the difficulty separating the Moraceae and Urticaceae families, leading to them being grouped together as one combined pollen taxa (Burn and Mayle, 2008). However, as these two families have many taxa with many different features (e.g. trees, shrubs and cold/warm loving) it is hard to infer anything from such a large group of taxa. A previous lack of reference material did not aid the problems separating pollen taxa, however, a

recent effort has meant that there are now sources to help with pollen identification in tropical ecosystems (Bush and Weng, 2007, Colinvaux et al., 1999, Gosling et al., 2013, Roubik and Moreno, 1991). Despite this increase in reference material, problems still remain in separating pollen grains to species level, meaning that palaeoecological interpretations inferred from pollen grains are best made alongside another proxy (e.g. plant macrofossils). Multi proxy studies are also beneficial when trying to interpret vegetation response to an environmental event as some proxies (e.g. pollen) take longer than others (e.g. chironomids) to respond to an event (e.g. a fire preserved as charcoal particles). With annual life cycles chironomids respond quickly to unfavourable conditions (within a decade), whereas vegetation can take hundreds to thousands of years to respond. This is because, unlike a chironomid, vegetation cannot simply move to another area with more favourable conditions. This means that as a proxy, pollen grains can sometimes look to be taking longer to respond to unfavourable conditions (not always true as if conditions are unfavourable, a plant may simply stop producing pollen), whereas faster acting proxies (e.g. chironomids) can be observed to be altering quickly in response to changing conditions (i.e. they are more sensitive). However, by using a range of proxies, this lag time can be identified.

Palaeoecological studies can also have issues regarding sediment preservation and provenance. Due to the microscopic nature (<100 μm) of many palaeoecological proxies (pollen grains and charcoal particles), they can be easily transported through both fluvial and aeolian transport mechanisms (Birks and Birks, 1980). Mobility of proxies requires all interpretations to be based on a sound understanding of the depositional environment in order to avoid misinterpretation of the signal. Once deposited, subsequent erosion through leaching, sediment reworking, fluvial and volcanic activity can also cause proxies to become hard to interpret due to mixing of the preserved sediment. In order to help solve this issue, careful interpretation of the depositional environment throughout the time of preservation needs to be taken into consideration (see

research aim 3; Section 1.3), in order to be able to make further interpretations based upon palaeoecological proxies.

By taking into consideration identification and preservation issues, palaeoecology can provide a snapshot into the response of vegetation to past environmental change, this can then be extrapolated into the future, providing an idea about how modern vegetation assemblages may react to projected future change (Birks and Birks, 1980). As a tool, palaeoecology can be used in furthering understanding of globally important tropical regions.

1.2.2. Palaeoecology in the tropics

Tropical palaeoecology has provided a vast array of information in an attempt to understand past tropical environmental change; it has provided information on aspects including ecosystem dynamics, landform evolution and the nature and extent of climate change (Colinvaux and de Oliveira, 2000, Haberle and Maslin, 1999, Kumaran and Limaye, 2014). Many studies have used proxies within palaeoecology to aid understanding of changes occurring within these important tropical regions (Behling and Hooghiemstra, 1998, Bhagwat et al., 2012, Kumaran and Limaye, 2014, Rull et al., 2005). However, further knowledge is required to provide a comprehensive insight into long-term (>12,000 year) tropical ecosystem functioning. Current palaeoecological studies undertaken in the tropics are sporadic with few studies focusing on the ecologically important eastern Andean flank (biodiversity hotspot and conservation priority; Myers et al., 2000). One of the main proxies used within palaeoecology to gain an understanding of past vegetation changes within the tropics is palynology.

Palynology is the study of pollen and spores and it can be applied to the fossil record (palaeopalynology) by looking at fossil pollen and spores preserved in sediments (Manten, 1966, Punt et al., 2007). Palynology has been used expansively across the tropics to investigate vegetation change through geological time (Bush, 1990, Colinvaux et al., 1996, Miller and

Gosling, 2014, Van der Hammen, 1991). In addition to the issues described in Section 1.2.1, palynology also has limitations related to investigator effort and effective sampling, i.e. obtaining meaningful pollen counts from diverse tropical pollen assemblages. Count sizes of 300-500 pollen grains have been recommended to correctly classify vegetation preserved as pollen (Birks and Birks, 1980), however, ecosystems with high floral diversity (such as tropical rainforests) may require a higher count size than ecosystems with a lower diversity. Some studies have recommended that a pollen count of greater than 500 grains per sample is a more suitable count size to correctly characterise a past vegetation assemblage (Bennett and Willis, 2001, Moore et al., 1991). This disparity in the appropriate amount of pollen grains to count to be able to correctly characterise a vegetation assemblage is a part of palynology that needs to be investigated further.

Although both tropical palaeoecology and, in particular, tropical palynology have provided evidence of how vegetation has been impacted by global environmental change, much knowledge is still to be obtained, especially in appropriately applying palaeoecological techniques, whilst still ensuring an accurate interpretation can be made. This thesis aims to investigate this using the following aims.

1.3. Research aims

Within this thesis five specific aims are addressed:

1. Correctly characterising a pollen assemblage is essential in order to extract ecologically meaningful data from the pollen record. Research aim 1 is to create a statistical model that can take into account sample richness and evenness and produce a sample specific count size target for each individual pollen sample. This aim is addressed in Chapter 5.

2. Understanding the depositional age of a sedimentary archive is important so that it can be compared with defined climatic events, for example glacial-interglacial cycles.

Research aim 2 is to apply dating methodologies to sediments in order to independently establish the depositional age of the sediments at the sites. Research aim 2 is addressed in Chapter 6.

3. Due to the steep topography and the widespread volcanic activity on the eastern Andean flank sedimentary archives are uncommon. Research aim 3 is to characterise the environmental controls on the deposition and preservation of sedimentary archives on the eastern Andean flank. This research aim is covered in Chapter 7.

4. Palaeoecological records are scarce across the eastern Andean flank (within the Amazon basin), and the few study sites present are situated great distances from each other. Research aim 4 is to generate two new multi-proxy palaeoecological records from the eastern Andean flank of Ecuador. The multi proxy datasets produced (pollen [vegetation], charcoal [fire], x-ray fluorescence [volcanic source], loss-on-ignition [sediment type] and dating techniques [age of deposition]) will provide additional information into a region which is data poor, allowing a greater understanding into the response of this region to environmental change. The multi proxy approach will ensure that as much data as possible can be retrieved from the sediments. This research aim is met throughout the thesis, in particular Chapters 6, 7 and 8.

5. A projected future increased likelihood of natural burning in response to a decrease in precipitation means that it is important to understand how the vegetation of the eastern Andean flank responded to burning events in the past. Research aim 5 is, therefore, to look at charcoal (fire) and pollen (vegetation) records preserved at the two new stratigraphic sequences with the aim of further understanding how the vegetation responded to natural fires. This research aim is addressed in Chapter 8.

1.4. Thesis structure

A range of proxies (pollen, non-pollen-palynomorphs, charcoal, wood macrofossils) archived within two stratigraphic sections from the eastern Andean flank of Ecuador were analysed in order to understand environmental change in this ecologically important region. The data presented in this thesis is structured in the following manor due in part to the inclusion of two scientific papers leading to a particular structure. The structure of the thesis is now described. This introduction chapter precedes Chapter 2 and Chapter 3 which detail the study sites used within this research and some of the previous research performed in this region. Chapter 4 details the range of methodologies used within this research. Chapter 5 has been published as a manuscript in the international journal *Palaeogeography, Palaeoclimatology and Palaeoecology* and it details the methodology employed to generate statistically robust count sizes for pollen samples. This paper has been included in this part of the thesis as pollen counts generated using the model are used in the remaining chapters. Chapter 6 draws together the results from three dating techniques applied in this research. Chapter 7 has been submitted to an international journal (*Journal of South American Earth Science*). Chapter 7 explores in detail one of the stratigraphic sections to investigate how sedimentary sequences can be deposited and preserved on the eastern Andean flank. It has been included at this point in order to check sediment provenance following issues dating sediments in Chapter 6. Chapter 8 provides palaeoecological results derived from the fossil pollen assemblages of the two stratigraphic sections and investigates how fire impacted the eastern Andean vegetation in the past. The final chapter (Chapter 9), summarises the entire thesis, draws conclusions from the research presented, assesses limitations of this research and identifies areas of further work.

References

ANDERSON, J. N., BURGMANN, H., DEARING, J. A. & GAILLARD, M.-J. 2006. Linking palaeoenvironmental data and models to understand the past and to predict the future. *Trends in Ecology & Evolution,* 21**,** 696 - 704.

BARLOW, J., GARDNER, T. A., ARAUJO, I. S., ÁVILA-PIRES, T. C., BONALDO, A. B., COSTA, J. E., ESPOSITO, M. C., FERREIRA, L. V., HAWES, J., HERNANDEZ, M. I. M., HOOGMOED, M. S., LEITE, R. N., LO-MAN-HUNG, N. F., MALCOLM, J. R., MARTINS, M. B., MESTRE, L. A. M., MIRANDA-SANTOS, R., NUNES-GUTJAHR, A. L., OVERAL, W. L., PARRY, L., PETERS, S. L., RIVEIRO-JUNIOR, M. A., DA SILVA, M. N. F., DA SILVA, C. & PERES, C. A. 2007. Quantifying the biodiversity value of tropical primary, secondary, and plantation forests. *Proceedings of the National Academy of Sciences,* 104**,** 18555-18560.

BARLOW, J. & PERES, C. A. 2008. Fire-mediated dieback and compositional cascade in an Amazonian forest. *Philosophical Transactions of the Royal Society B: Biological Sciences,* 363**,** 1787-1794.

BATTARBEE, R. W. 2010. Aquatic Ecosystem variability and climate change - A palaeoecological perspective. *In:* KERNAN, M., BATTARBEE, R. W. & MOSS, B. (eds.) *Climate change impacts on freshwater ecosystems.* Oxford, UK: Wiley-Blackwell.

BEHLING, H. & HOOGHIEMSTRA, H. 1998. Late Quaternary palaeoecology and palaeoclimatology from pollen records of the savannas of the Llanos Orientales in Colombia. *Palaeogeography, Palaeoclimatology, Palaeoecology,* 139**,** 251 - 267.

BENNETT, K. D. & WILLIS, K. J. 2001. Pollen. *In:* SMOL, J. P., BIRKS, J. H. B. & LAST, W. M. (eds.) *Tracking environmental change using lake sediments. Volume 3: Terrestrial, Algal and Siliceous Indicators.* Dordrecht: Kluwer Academic Publishers.

BHAGWAT, S. A., NOGUÉ, S. & WILLIS, K. J. 2012. Resilience of an ancient tropical forest landscape to 7500 years of environmental change. *Biological Conservation,* 153**,** 108-117.

BIRKS, H. J. B. & BIRKS, H., H. 1980. *Quaternary Palaeoecology,* New Jersey, The Blackburn Press.

BORRERO, L. A., ZÁRATE, M., MIOTTI, L. & MASSONE, M. 1998. The Pleistocene-Holocene transition and human occupations in the southern cone of South America. *Quaternary International,* 49/50**,** 191-199.

BRANDO, P. M., BALCH, J. K., NEPSTAD, D. C., MORTON, D. C., PUTZ, F. E., COE, M. T., SILVÉRIO, D., MACEDO, M. N., DAVIDSON, E. A., NÓBREGA, C. C., ALENCAR, A. & SOARES-FILHO, B. S. 2014. Abrupt increases in Amazonian tree mortality due to drought-fire interactions. *Proceedings of the National Academy of Sciences,* 111**,** 6347-6352.

BURN, M. J. & MAYLE, F. E. 2008. Palynological differentiation between genera of the Moraceae family and implications for Amazonian palaeoecology. *Review of Palaeobotany and Palynology,* 149**,** 187-201.

BURN, M. J., MAYLE, F. E. & KILLEEN, T. J. 2010. Pollen - based differentiation of Amazonian rainforest communities and implications for lowland palaeoecology in tropical South America. *Palaeogeography, Palaeoclimatology, Palaeoecology,* 295**,** 1 - 18.

BURNHAM, R. J. & JOHNSON, K. R. 2004. South American palaeobotany and the origins of neotropical rainforests. *Philosophical Transactions of the Royal Society B: Biological Sciences,* 359**,** 1595 - 1610.

BUSH, M. B., PIPERNO, D. R., COLINVAUX, P. A., DE OLIVEIRA, P. E., KRISSEK, L. A., MILLER, M. C. & ROWE, W. E. 1992. A 14 300-YR paleoecological profile of a lowland tropical lake in Panama. *Ecological monographs,* 62**,** 251 - 275.

BUSH, M. B. & WENG, C. 2007. Introducing a new (freeware) tool for palynology. *Journal of Biogeography,* 34**,** 377-380.

BUSH, M. B. C., P.A. 1990. A pollen record of a complete glacial cycle from lowland Panama. *Journal of Vegetation Science,* 105 - 118.

CHAMBERS, J. Q., HIGUCHI, N. & SCHIMEL, J. P. 1998. Ancient trees in Amazonia. *Nature,* 391**,** 135 - 136.

CHAZDON, R. L. 2003. Tropical forest recovery: legacies of human impact and natural disturbances. *Perspectives in Plant Ecology, Evolution and Systematics,* 6**,** 51-71.

COCHRANE, M. A. & BARBER, C. P. 2009. Climate change, human land use and future fires in the Amazon. *Global Change Biology,* 15**,** 601-612.

COLINVAUX, P. A. & DE OLIVEIRA, P. E. 2000. Palaeoecology and climate of the Amazon basin during the last glacial cycle. *Journal of Quaternary Science,* 15**,** 347 - 356.

COLINVAUX, P. A., DE OLIVEIRA, P. E., MORENO, J. E., MILLER, M. C. & BUSH, M. B. 1996. A long pollen record from lowland Amazonia: Forest and cooling in glacial times. *Science,* 274**,** 85 - 88.

COLINVAUX, P. A., DE OLIVEIRA, P. E. & PATIÑO, J. E. M. 1999. *Amazon pollen manual and atlas,* Amsterdam, Harwood Academic Publishers.

CUBASCH, U., WUEBBLES, D., CHEN, D., FACCHINI, M. C., FRAME, D., MAHOWALD, N. & WINTHER, J. G. 2013. Introduction. *In:* STOCKER, T. F., QIN, D., PLATTNER, G.-K., TIGNOR, M., ALLEN, S. K., BOSCHUNG, J., NAUELS, A., XIA, Y., BEX, V. & MIDGLEY, P. M. (eds.) *Climate Change 2013: The physical science basis. Contribution of working group I to the fifth assessment report of the intergovernmental panel on climate change.* Cambridge: Cambridge University Press.

DENMAN, K. L., BRASSEUR, G., CHIDTHAISONG, A., CIAIS, P., COX, P. M., DICKINSON, R. E., HAUGLUSTAINE, D., HEINZE, C., HOLLAND, E., JACOB, D., LOHMANN, U., S., R., DA SILVA DIAS, P. L., WOFSY, S. C. & ZHANG, X. 2007. Couplings between changes in the climate system and biogeochemistry. *In:* SOLOMON, S., QIN, D., MANNING, M., CHEN, Z., MARQUIS, M., AVERYT, K. B., TIGNOR, M. & MILLER, H. L. (eds.) *Climate Change 2007.* Cambridge, United Kingdom: Cambridge University Press.

ESHEL, G., SHEPON, A., MAKOV, T. & MILO, R. 2014. Land, irrigation water, greenhouse gas, and reactive nitrogen burdens of meat, eggs, and dairy production in the United States. *Proceedings of the National Academy of Sciences,* 1 - 6.

ESPINOZA, J. C., MARENGO, J. A., J., R., CARPIO, J. M., FLORES, L. N. & GUYOT, J. L. 2014. The extreme 2014 flood in south-western Amazon basin: the role of tropical-subtropical South Atlantic SST gradient. *Environmental Research Letters,* 9**,** 1-9.

FOLEY, J. A., DEFRIES, R., ASNER, G. P., BARFORD, C., BONAN, G., CARPENTER, S. R., CHAPIN, F. S., COE, M. T., DAILY, G. C., GIBBS, H. K., HELKOWSKI, J. H., HOLLOWAY, T., HOWARD, E. A., KUCHARIK, C. J., MONFREDA, C., PATZ, J. A., PRENTICE, I. C., RAMANJUTTY, N. & SNYDER, P. K. 2005. Global consequences of land use. *Science,* 309**,** 570 - 574.

FRANCISQUINI, M. I., LIMA, C. M., PESSENDA, L. C. R., ROSSETTI, D. F., FRANÇA, M. C. & COHEN, M. C. L. 2014. Relation between carbon isotopes of plants and soils on Marajó Island, a large tropical island: Implications for interpretation of modern and past vegetation dynamics in the Amazon region. *Palaeogeography, Palaeoclimatology, Palaeoecology*.

GHIL, M. 2002. Natural climate variability. *Encyclopedia of global environmental change,* 1**,** 544-549.

GOSLING, W. D., HANSELMAN, J. A., KNOX, C., VALENCIA, B. G. & BUSH, M. B. 2009. Long-term drivers of change in *Polylepis* woodland distribution in the central Andes. *Journal of Vegetation Science,* 20**,** 1041 - 1052.

GOSLING, W. D., MILLER, C. S. & LIVINGSTONE, D. A. 2013. Atlas of the tropical West African pollen flora. *Review of Palaeobotany and Palynology,* 199**,** 1 - 135.

GOUDIE, A. S. 2013. *The human impact on the Natural environment: Past, present and future,* Chichester, Wiley-Blackwell.

HABERLE, S. G. & MASLIN, M. A. 1999. Late Quaternary vegetation and climate change in the Amazon basin based on a 50,000 year pollen record from the Amazon fan, ODP site 932. *Quaternary Research,* 51**,** 27 - 38.

HALOFSKY, J. E., HEMSTROM, M. A., CONKLIN, D. R., HALOFSKY, J. S., KERNS, B. K. & BACHELET, D. 2013. Assessing potential climate change effects on vegetation using a linked model approach. *Ecological modelling,* 266**,** 131 - 143.

HANNAH, L., MIDGLEY, G. F., LOVEJOY, T., BOND, W. J., BUSH, M., LOVETT, J. C., SCOTT, D. & WOODWARD, F. I. 2002. Conservation of biodiversity in a changing climate. *Conservation Biology,* 16**,** 264-268.

HUNTLEY, B. 1996. Quaternary palaeoecology and ecology. *Quaternary Science Reviews,* 15**,** 591 - 606.

JOOSTEN, H. & DE KLERK, P. 2002. What's in a name Some thoughts on pollen classification, identification, and nomenclature in Quaternary palynology. *Review of Palaeobotany and Palynology,* 122**,** 29-45.

JOPPA, L. N., LOARIE, S. R. & PIMM, S. L. 2008. On the protection of "protected areas". *Proceedings of the National Academy of Sciences* 105**,** 6673-6678.

KARL, T. R. & TRENBERTH, K. E. 2003. Modern Global Climate Change. *Science,* 302**,** 1719-1723.

KUMARAN, N. K. P. & LIMAYE, R. B. 2014. Holocene palynology and tropical paleoecology. *Quaternary International,* 325**,** 1 - 2

LEWIS, S. L., BRANDO, P. M., PHILLIPS, O. L., VAN DER HEIJDEN, G. M. F. & NEPSTAD, D. 2011. The 2010 Amazon drought. *Science,* 331**,** 554.

LEWIS, S. L., LLOYD, J., SITCH, S., MITCHARD, E. T. A. & LAURANCE, W. F. 2009. Changing ecology of tropical forests: evidence and drivers. *Annual review of ecology, evolution and systematics,* 40**,** 529 - 549.

MANTEN, A. A. 1966. Half a century of modern palynology. *Earth - Science Reviews,* 2**,** 277 - 316.

MILLER, C. S. & GOSLING, W. D. 2014. Quaternary forest associations in lowland tropical West Africa. *Quaternary Science Reviews,* 84**,** 7 - 25.

MOORE, P. D. 2002. Climate records spruced up. *Nature,* 417**,** 133 - 134.

MOORE, P. D., WEBB, J. A. & COLLINSON, M. E. 1991. *Pollen analysis,* Oxford, Blackwell Scientific.

MORLEY, R. J. 2000. *Origin and evolution of tropical rain forests,* Chichester, John Wiley & Sons.

MYERS, N., MITTERMELER, R. A., MITTERMELER, C. G., DA FONSECA, G. A. B. & KENT, J. 2000. Biodiversity hotspots for conservation priorities. *Nature,* 403**,** 853 - 858.

PARMESAN, C. & YOHE, G. 2003. A globally coherent fingerprint of climate change impacts across natural systems. *Nature,* 421**,** 37 - 42.

PUNT, W., HOEN, P. P., BLACKMORE, S., NILSSON, S. & LE THOMAS, A. 2007. Glossary of pollen and spore terminology. *Review of Palaeobotany and Palynology,* 143**,** 1 - 81.

RIVERA, J. A. & PENALBA, O. C. 2014. Trends and spatial patterns of drought affected area in Southern South America. *Climate,* 2**,** 264-278.

ROBERTS, D. R. & HAMANN, A. 2012. Predicting potential climate change impacts with bioclimate envelope models: a palaeoecological perspective. *Global Ecology and Biogeography,* 21**,** 121-133.

ROUBIK, D. W. & MORENO, J. E. P. 1991. *Pollen and spores of Barro Colorado Island,* United States, Missouri Botanical Garden.

RULL, V., ABBOTT, M. B., POLISSAR, P. J., WOLFE, A. P., BEZADA, M. & BRADLEY, R. S. 2005. 15,000-yr pollen record of vegetation change in the high altitude tropical Andes at Laguna Verde Alta, Venezuela. *Quaternary Research,* 64**,** 308-317.

SCHOLES, R. J. & VAN BREEMEN, N. 1997. The effects of global change on tropical ecosystems. *Geoderma,* 29**,** 9 - 24.

STEFFEN, W., RICHARDSON, K., ROCKSTRÖM, J., CORNELL, S. E., FETZER, I., BENNETT, E. M., BIGGS, R., CARPENTER, S. R., DE VRIES, W., DE WIT, C. A., FOLKE, C., GERTEN, D., HEINKE, J., MACE, G. M., PERSSON, L. M., RAMANATHAN, V., REYERS, B. & SÖRLIN, S. 2015. Planetary boundaries: Guiding human development on a changing planet. *Science,* 347.

STOUFFER, R. J., MANABE, S. & VINNIKOV, K. Y. 1994. Model assessment of the role of natural variability in recent global warming. *Nature,* 367**,** 634-636.

SWETNAM, T. W., ALLEN, C. D. & BETANCOURT, J. L. 1999. Applied historical ecology: Using the past to manage for the future. *Ecological applications,* 9**,** 1189 - 1206.

TURNER, I. M. 1996. Species loss in fragments of tropical rain forest: a review of the evidence. *Journal of applied ecology,* 33**,** 200-209.

VAN DER HAMMEN, T. 1991. Palaeoecology of the neotropics: an overview of the state of affairs. *Boletim do Instituto de Geociências de Universidade de São Paulo,* 8**,** 35 - 55.

WHITLOCK, C. 1992. Vegetational and climatic history of the Pacific Northwest during the last 20,000 years: Implications for understanding present-day biodiversity. *The Northwest Environmental journal,* 8**,** 5-28.

ZUIDEMA, P. A., BAKER, P. J., GROENENDIJK, P., SCHIPPERS, P., VAN DER SLEEN, P., VLAM, M. & STERCK, F. 2013. Tropical forests and global change: filling knowledge gaps. *Trends in Plant Science,* 18**,** 413 - 419.

Chapter 2: Study region and conceptual background

The previous chapter introduced a rationale for this research alongside the five specific aims to be discussed during this thesis. This chapter introduces the study region and reviews the relevant literature to establish the importance of the study region.

2.1. Physical Geography

2.1.1. South America

The geography of western South America is dominated by the Andes mountain range which traverses the continent from North to South (9000 km in length and 750 km at their widest; Graham, 2009). The Andes uplifted 25 million years ago as a result of convergence between the Nazca and the South American plates (Montgomery et al., 2001). Volcanic activity spans the length of the Andes with active volcanoes present throughout four main Volcanic Zones (Figure 2.1): Northern, Central, Southern and Austral (Hall et al., 2008, Ramos, 1999). Fluvial activity also spans the length of South America; with some of the world's largest rivers present (Figure 2.1), including the Amazon, the Orinoco and the Paraná (Holeman, 1968). These rivers cause widespread erosion and are responsible for the transportation of water and sediments from the Andes to the rest of South America (Milliman and Meade, 1983), eventually discharging into the Atlantic Ocean.

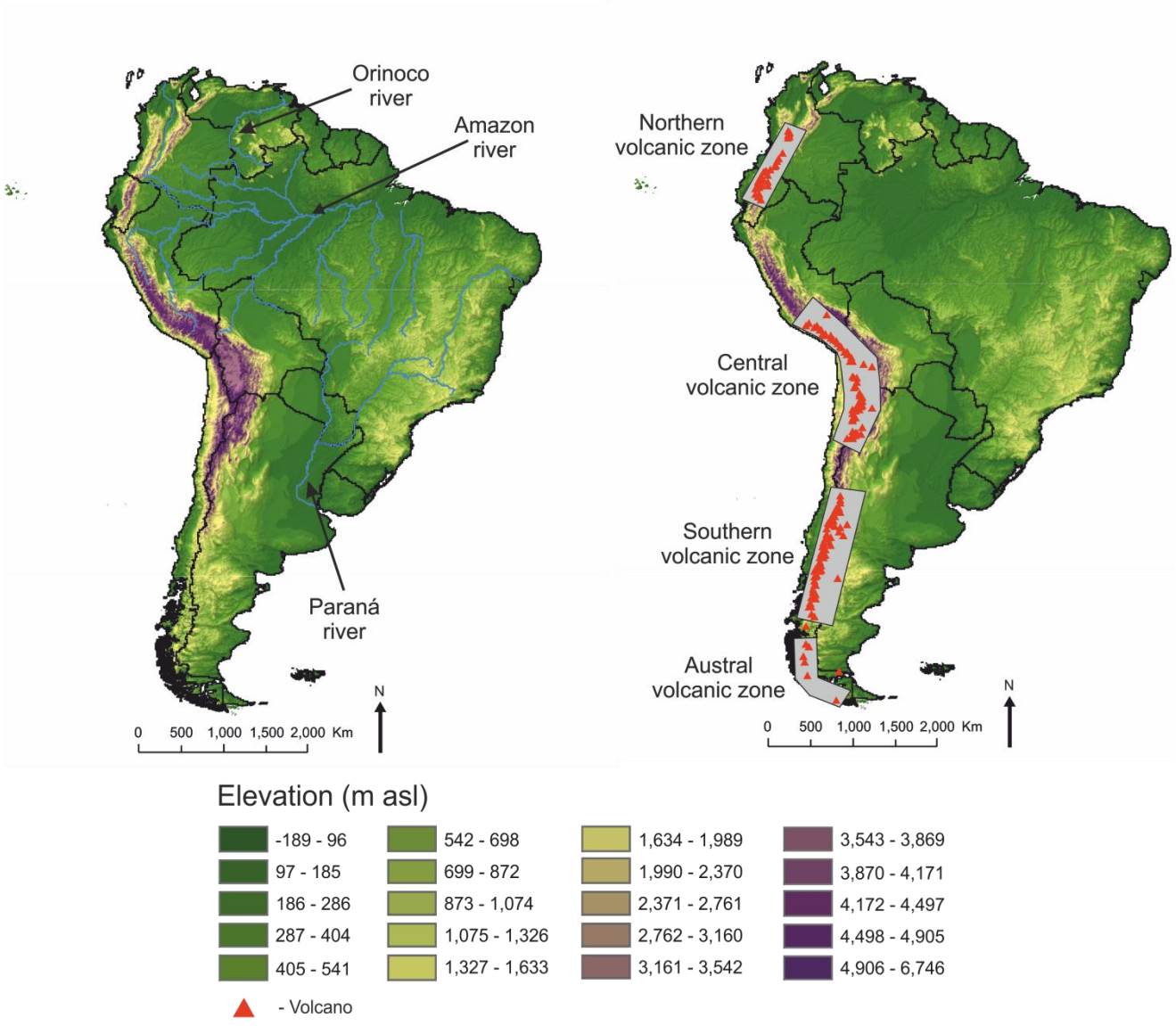

Figure 2.1: Maps showing the major geographic features of South America. The three major rivers are included along with the four volcanic zones. Elevation is also shown on both maps, altitudinal data was obtained from GTOPO30, a 30-arc second digital elevation model (EROS, 1996).

2.1.2. Eastern Andean flank

The eastern Andean flank (extent in Ecuador shown on Figure 2.2) is defined here as the steep elevation gradient (<1000 m - ~4800 m asl) found on the eastern side of the Andes. This flank separates the snowline found at the peaks of the high Andes from the lowland Amazon rainforest. The eastern Andean flank is composed of metamorphic rocks which are of Palaeozoic to Jurassic age (Bès de Berc et al., 2005). The rocks were metamorphosed during the Cretaceous and the Paleocene and they were then overlain by volcanic/volcaniclastic formations from the

late Miocene to Pliocene and also of Quaternary origin (Bernal et al., 2011, Bernal et al., 2012). The surrounding geology is also heavily influenced by nearby volcanic activity. Debris flow deposits, cobbles, sands and silts are widespread across the region, linked to lahars from volcanic events (Bès de Berc et al., 2005). Volcanic activity is widespread across the eastern Andean flank with twenty main Quaternary volcanic edifices present in Ecuador alone (Figure 2.2). Ecuador was chosen to study the eastern Andean flank due to the high biodiversity present (Valencia et al., 1994), the paucity of previous research (Figure 2.2) and the presence of many disturbances (volcanoes and rivers; Figure 2.2). Alongside volcanic activity, the eastern Andean flank is also a highly fluvial area, with many rivers traversing the flank. Riverine activity contributes to erosive processes and can have a large impact on the surrounding landscape e.g. a widespread flood in 2001 in the Atacama desert of northern Chile and southern Peru caused widespread erosion of sediment downstream due to a dramatically increased river flow rate (Houston, 2006, Montgomery et al., 2001).

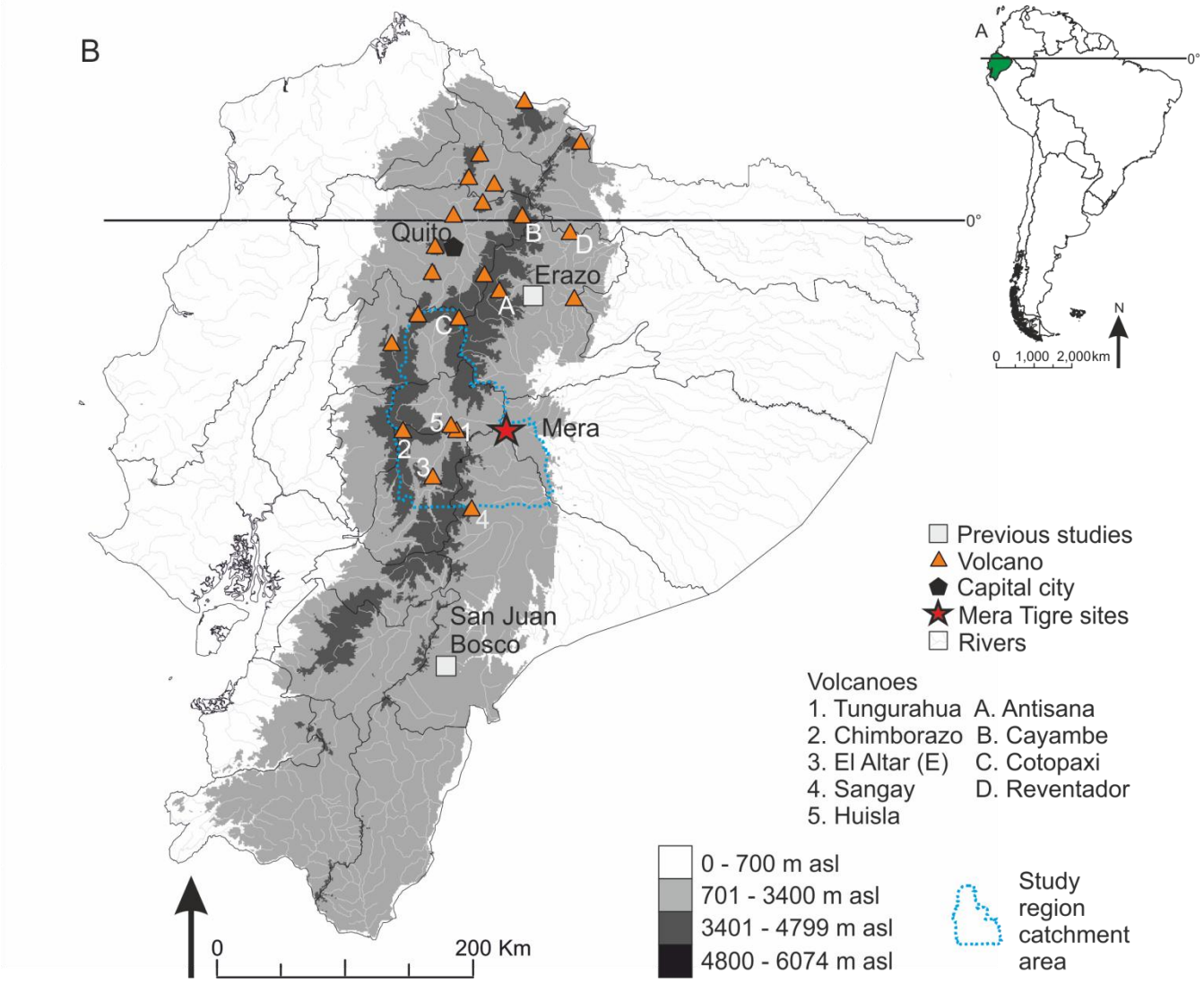

Figure 2.2: Location of Ecuador in relation to South America and location of the study region in Ecuador (catchment of the study sites, to scale). The location of the town of Mera, the study sites, other nearby sites and geographical features discussed are represented. An approximation (based on elevation range of between 1000 m and ~4800 m asl) of the extent of the eastern Andean flank in Ecuador is shown.

2.1.3. Mera region

The rocks that underlay Mera are the same as those described for the eastern Andean flank in section 2.1.2. Many of the Quaternary deposits that surround Mera are derived from volcanic activity, with material arriving through debris flow, ash fall, tephra's and lahar flows. The four closest volcanoes to Mera have the greatest influence on the composition of the landscape and sediments found; these are Tungurahua, Chimborazo, El Altar and Sangay (Figure 2.2). Further

information on the four nearby volcanoes is presented in sections 2.1.3.1. to 2.1.3.4. Fluvial activity is also an important component of the landscape at Mera today. The Río Pastaza, a major tributary of the Amazon, is situated just 1.55 km away from Mera, and three of its smaller tributaries (Río Alpayachu, Chico and Tigre) pass even closer to the town. Abundant fluvial deposits of gravels, silts and sands are visible around Mera, especially in close proximity (within 1 km) to the rivers, providing evidence for considerable landscape modification in the recent geological past.

2.1.3.1. Tungurahua

Tungurahua (01°28'S, 78°27'W) is a highly active stratovolcano (currently erupting, March 2015), with its peak reaching an altitude of 5023 m asl (Biggs et al., 2010, Hall et al., 1999). Tungurahua is situated 37 km away from Mera and its frequent eruptions generate large volumes of volcanic material such as lava, fallout tephra, pyroclastic flows and lahars (Hall et al., 1999). This high volume of volcanic material contributes to sediment accumulation of the surrounding area.

2.1.3.2. Chimborazo

Chimborazo (01°30'S, 78°36'W) is a stratovolcano situated 81 km from Mera. The volcano is characterised by three peaks with the highest peak at 6268 m asl (Barba et al., 2008, Samaniego et al., 2012). Chimborazo has caused large scale debris flows in the past (last eruption AD 550), contributing to the evolution of the surrounding landscape (Barba et al., 2008) through the contribution of 280 km^2 of volcanic material into the landscape (Bernard et al., 2008).

2.1.3.3. Altar

Altar (01°41'S, 78°24'W) is an extinct stratovolcano situated 47.3 km from Mera. It has a cone morphology and stands at an altitude of 5319 m asl (Rosqvist, 1995). The date of the last eruption is unknown but it is thought to have occurred during the Pleistocene (Rosqvist, 1995).

2.1.3.4. Sangay

Sangay (02°00'S, 78°34'W) is an andesitic volcano situated 71.1 km away from Mera. Recent eruptions (last eruption AD 2007) have been characterised by strombolian activity with lava flows, lahars and ash falls, all of which have contributed to the sediment accumulation in the surrounding area (Monzier et al., 1999).

2.2. Modern climate

2.2.1. Climate of South America

The climate of South America is driven by many forcing factors, including, but not limited to, its location on the globe (the continent spans from 12° North to 56° South), the Intertropical Convergence Zone (ITCZ), the South American Summer Monsoon (SASM), the El Niño Southern Oscillation (ENSO) and the South American low level jet (SALLJ; Figure 2.3) (Garreaud et al., 2009, Marengo et al., 2004, Vera et al., 2006, Zhou and Lau, 1998). The ITCZ is the phenomenon in which warm easterly winds from the northern and southern hemispheres (both transporting large amounts of moisture which have evaporated from tropical oceans) converge (Dingman, 2002). In South America this causes the austral winter (June to August) to see increased precipitation North of the Equator, and the austral summer (December – February) to see high precipitation levels on the eastern Andes and the Amazon basin (Bush and Gosling, 2012, Garreaud et al., 2009). The SASM contributes to the precipitation regime in the southern tropical Andes, causing a peak in rainfall during the austral summer. ENSO is responsible for fluctuating cold (La Niña) and warm (El Niño) conditions over the equatorial Pacific (Garreaud et al., 2009). Aside from fluctuating temperatures, ENSO is also responsible for altering precipitation levels, with tropical South America seeing below average rainfall in El Niño episodes and above average rainfall in La Niña episodes (Garreaud et al., 2009). The SALLJ is

responsible for transporting large amounts of moisture from the Amazon to Southern South America; it is also responsible for increased wind strengths, particularly in Bolivia.

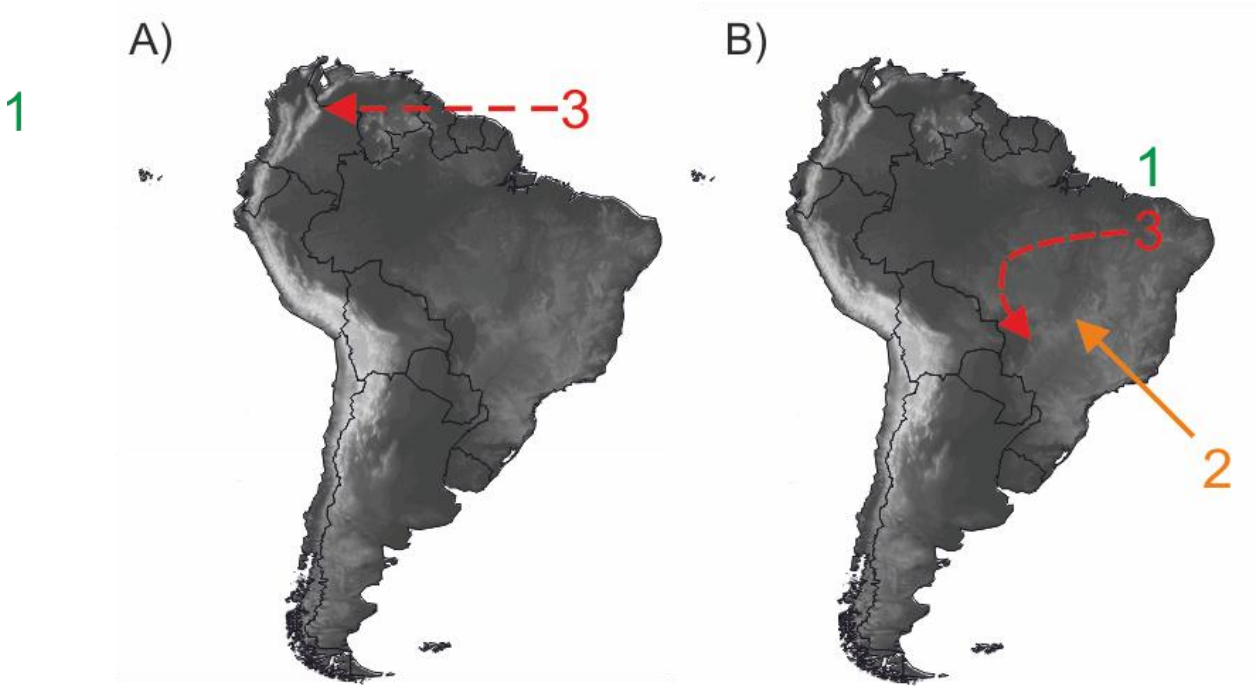

Figure 2.3: A) Location of the ITCZ (1) and the SALLJ (3, red dashed arrow) in the austral summer, B) location of the ITCZ (1), SASM (2, orange solid arrow) and the SALLJ (3, red dashed arrow) in the austral winter. The climate data is, with permission, adapted from Bush and Gosling, 2012. The maps the climate data are overlaid upon are altitudinal maps (white is high elevation, black is low elevation) with data obtained from GTOPO30, a 30-arc second digital elevation model (EROS, 1996).

The Andes mountain range also has a large impact on the climate, acting as a barrier between the climatic conditions of western coast and eastern South America (Garreaud et al., 2009). The Andes play a key role in the South American precipitation regime. They cause a high level of orographic rainfall on the eastern flank of the Andes (Figure 2.4) due to the moist air from the Amazon basin providing the latent energy required to drive precipitation along the Andean flank (Insel et al., 2009).

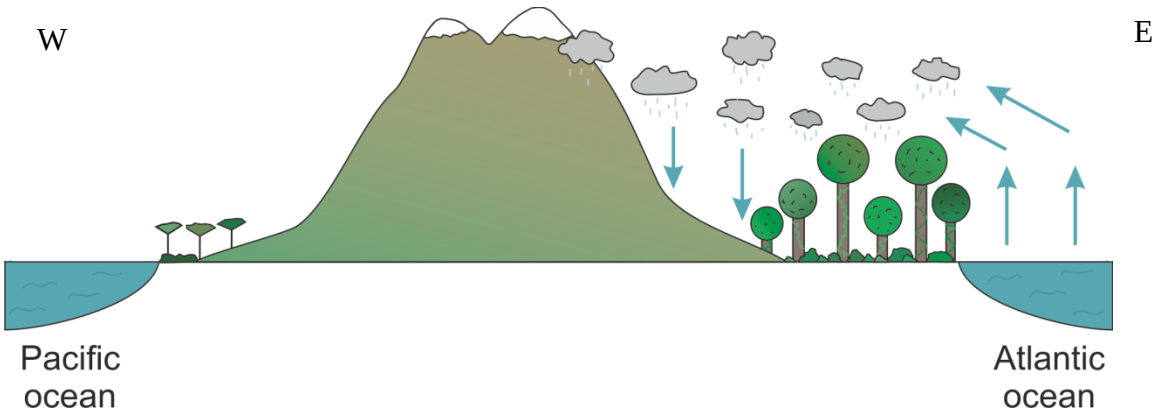

Figure 2.4: Cross section of the Andes (not to scale) representing the moisture transport that occurs from the Atlantic basin to the Andes.

In general, the western side of the Andes receives less precipitation (Figure 2.4 and Figure 2.5), due to the Andean barrier preventing moisture transport from the Amazon (Garreaud et al., 2009). This lower level of precipitation is excluding the region of Chocó, Colombia which receives some of the highest levels of precipitation (8000 to 13,000 mm mean annual precipitation) across the globe; this is due to an enhanced low level westerly jet called Choco (Poveda and Mesa, 2000). However, at 35° South these climatic conditions reverse, with the western slopes seeing the increased precipitation and the eastern slopes having reduced levels of precipitation (likely due to a decrease in average elevation at this point, with the average elevation falling from 4000 m asl to 1500 m asl; Garreaud, 2009). The Amazon basin is another region of South America with high levels of precipitation, as shown in Figure 2.5. The high level of rainfall is generated from the evaporation of recycled moisture from the Amazon basin and moisture transport from the Atlantic Ocean (Fu and Li, 2004).

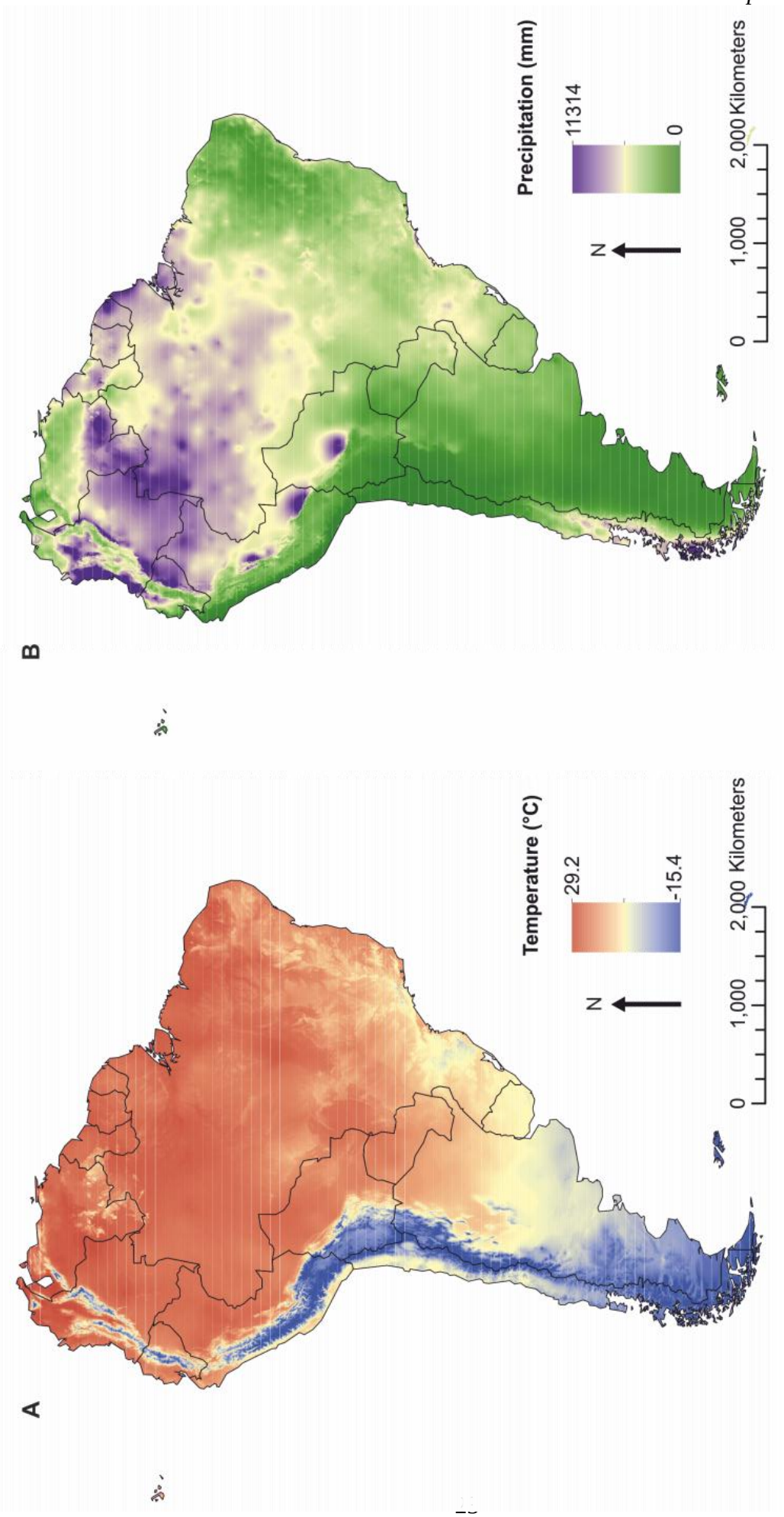
B
Precipitation (mm)
11314
0
N
0
1,000
2,000 Kilometers
A
Temperature (°C)
29.2
-15.4
N
0
1,000
2,000 Kilometers

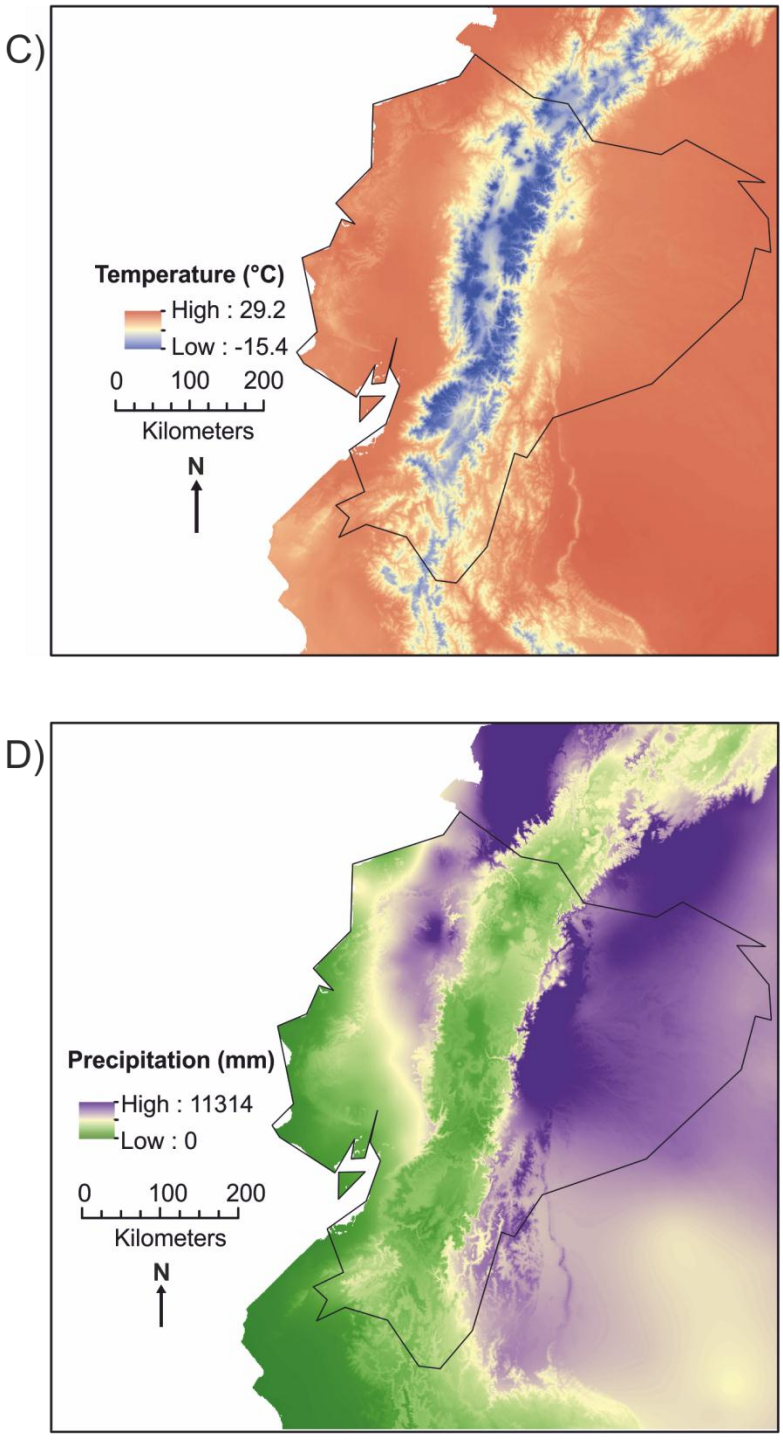

Figure 2.5: (A) Mean annual temperature (°C) for South America, derived from the mean annual temperature between 1950 and 2000 based on monthly temperature data (Hijmans et al., 2005). (B) Mean annual precipitation (mm) for South America, derived from mean annual precipitation between 1950 and 2000 based on monthly precipitation data (Hijmans et al., 2005). (C) Mean annual temperature (°C) for Ecuador (Hijmans et al., 2005). (D) Mean annual precipitation (mm) for Ecuador (Hijmans et al., 2005).

The temperature of South America decreases towards the southern tip of South America, with the tropical regions, especially those closest to the equator being the warmest (Garreaud et al., 2009). The areas of South America located closest to the equator, receive a higher proportion of the suns energy, further away from the equator the rays are distributed further, and as such, temperatures are cooler as the sun's energy is spread over a wider distance. Figure 2.5 represents the warmer northern part of South America, compared to the cooling southern part of the continent. The Andes mountains have different temperature constraints altogether. Based on general/worldwide adiabatic lapse rate trends, the higher the altitude, the cooler the temperature gets in the Andes, meaning the Andes mountain range are clearly visible on Figure 2.5 part A due to their cool temperatures standing out from the lowlands. The latest estimates indicate a lapse rate of ~4.5 °C per 1000 m elevation gain for the Andes (Hertel and Wesche, 2008).

2.2.2. Climate of the eastern Andean flank of Ecuador

The eastern Andean flank of Ecuador is dominated by moist and rainy conditions. This is as a result of orographic rainfall due to the prevailing wind travelling from the Amazon basin (Garreaud, 2009). Similar to the rest of the Andes, the eastern flank sees a decrease in temperature with an increase in elevation (~4.5 °C lost per 1000 m gained; Hertel and Wesche, 2008). The eastern flank is also warmer than the western flank due to the transport of warm air from the Amazon basin (Garreaud, 2009). The eastern Andean flank receives high levels of precipitation (Figure 2.5 part B) due to moist air being transported from the Amazon basin meeting the cooler, heavy air of the Andes mountain range, this creates an orographic rainfall effect (Insel et al., 2009).

2.2.3. Climate of the Mera region

The climate at Mera is largely influenced by a combination of its position on the eastern Andean flank, the ITCZ and the South Atlantic Convergence Zone (Cook, 2009). Temperature at Mera

remains stable throughout the year (mean annual temperature 20.8 °C) due to its close proximity to the equator (01° 27.546" S), meaning, seasonal changes are minimal (Ferdon, 1950). Precipitation at Mera remains high throughout the year (mean annual precipitation >4800 mm), aside from a slightly wetter season from April to July (Ferdon, 1950). Precipitation is caused by air from the Atlantic Ocean and recycled moisture from the Amazon basin colliding, generating a higher level of rainfall for the Mera region than for other parts of the lowlands (Bookhagen and Strecker, 2008, Ferdon, 1950). The prevailing wind direction impacting Mera is from the south east of Ecuador, causing the transportation of warm, moisture laden air from the Amazon rainforest (Garreaud et al., 2009).

2.3. Modern vegetation

2.3.1. Biomes of South America

Containing both the Andes mountain range and the Amazon rainforest amongst others, South America contains extremely high levels of biodiversity, including many endemic species (Daly and Mitchell, 2000, Luteyn and Churchill, 2000, Olson et al., 2001). Figure 2.6 shows the 14 major global biomes (inland water and ice/snow also indicated) and their distribution across South America. The biomes present across South America are composed of ecoregions, an ecoregion being a distinct assemblage of natural communities (Olson et al., 2001). A total of 867 distinct ecoregions have been defined across the globe, however, over half of these are found in the tropics (463 ecoregions found between 23°N and 23°S); many of these ecoregions have been listed as containing outstanding biodiversity, contributing to the designation of the tropics as a high priority for conservation (Olson and Dinerstein, 2002, Olson et al., 2001). The Andes mountain range in particular is of great importance due to the range of ecosystems it contains. Due to its large elevation range (Figure 2.1), great latitudinal extent and wide range of topographic features, a great range of micro climates exist. This great expanse of microclimates contributes to the development of a wide range of ecosystems stretching from the páramo and

glaciated peaks of the high altitudes (>3400 m asl; Harling, 1979) to the lower montane rainforest of the lowlands (>700 m asl; Harling, 1979). The global importance of the eastern Andean flank (between 1000 - ~4800 m asl) has been highlighted by the international scientific community, including the region as a global conservation priority (Myers et al., 2000).

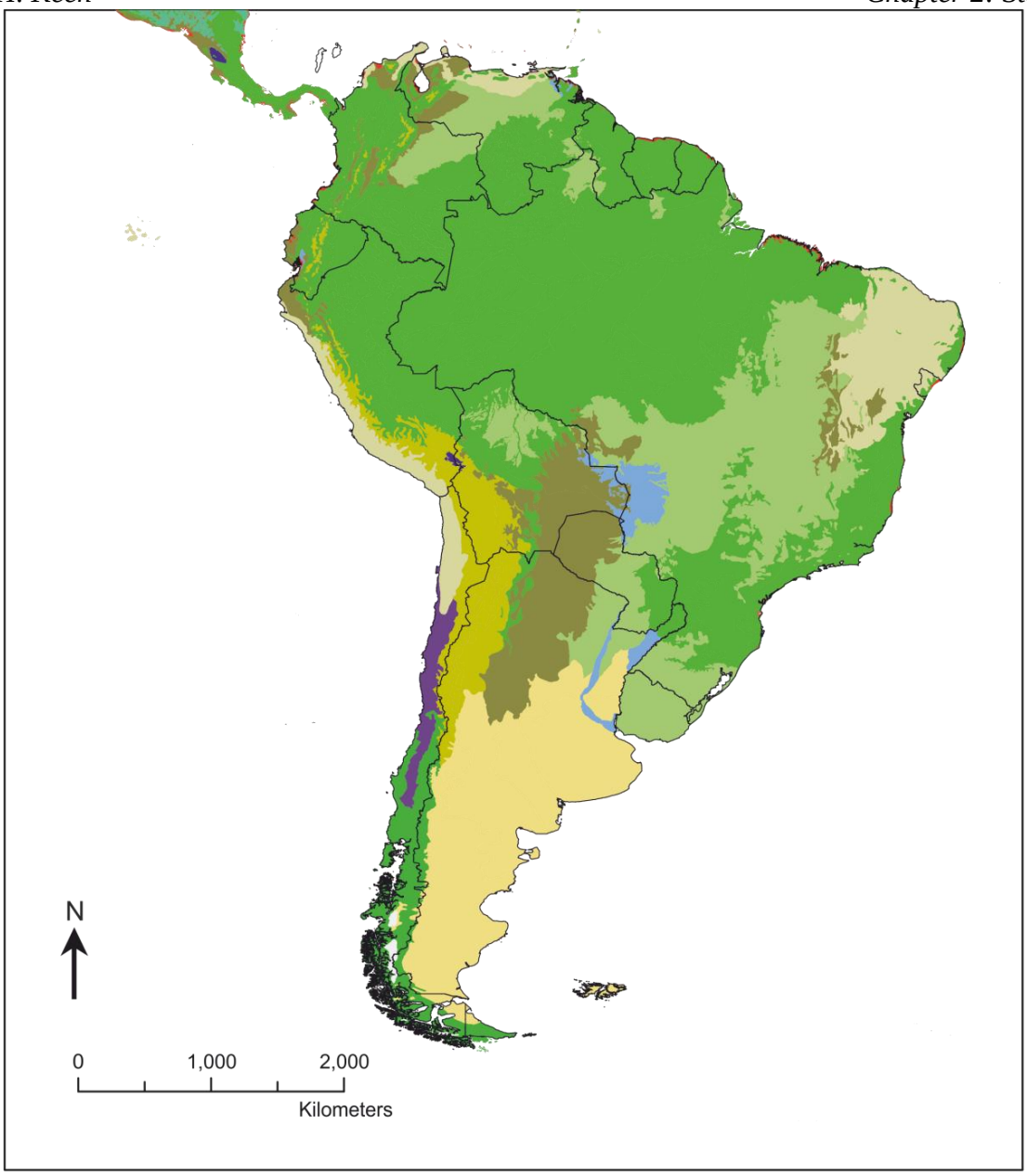

Figure 2.6: Map representing major global biomes found within South America (Olson et al., 2001). A total of 14 major biomes are shown alongside inland water and ice and snow.

2.3.2. Vegetation types of the Eastern Andean flank (Ecuador)

The eastern Andean flank (see Figure 2.2) of Ecuador contains three main vegetation types, these are the lower montane rainforest (700-2500 m asl; Section 2.3.2.1.), the upper montane rainforest (2500-3400 m asl; Section 2.3.2.2.) and the páramo (3400-4800 m asl; Section 2.3.2.3.) (Harling, 1979). These vegetation types are not as clear cut as these elevations suggest, they are a continuum of each other and the altitudinal limits are only approximations, in actual fact they vary along the flank.

2.3.2.1. Lower montane rainforest

The lower montane rainforest (700-2500 m asl) of Ecuador is high in biodiversity, with the floristic composition altering with increasing altitude (Harling, 1979). Up to around 1500 m asl, the floristic composition is mainly comprised of species belonging to the families Myristicaceae, Lecythidaceae and Vochysiaceae. These taxa are slowly replaced by Ericaceae, Melastomataceae, Betulaceae and Cunoniaceae with increasing altitudes (Harling, 1979). Trees found within the lower montane forest are often covered in a range of epiphytes (bryophytes, lichens and vascular plants), the amount of epiphytes being closely related to the air humidity, with an increase in air humidity leading to an increase in epiphytes, in general the higher elevations see a higher rate of epiphyte coverage (Fleischbein et al., 2005).

2.3.2.2. Upper montane rainforest

The upper montane forest (2500-3400 m asl) is also known as the cloud forest due to a persistent cloud cover, often at the level of the canopy (Harling, 1979). The floristic composition of units includes members of the Rosaceae, Ericaceae, Melastomataceae, Rubiaceae and Asteraceae families (Harling, 1979). In addition to these taxa, characteristic genera of the upper montane forest include *Podocarpus* (Podocarpaceae), *Ilex* (Aquifoliaceae), *Hedyosmum* (Chloranthaceae), *Alnus* (Betulaceae) and *Bocconia* (Papaveraceae) (Harling, 1979). Similar to the lower montane forest, the trees present in the upper montane forest play host to a wide variety of epiphytes,

including mosses, bryophytes, ferns and orchids (Fleischbein et al., 2005, Harling, 1979). This is due to the high level of humidity found in the upper montane forest partially related to the presence of clouds in this vegetation type.

The montane rainforests (lower and upper) of the eastern Andean flank are critically endangered, and they are one of the least understood vegetation types of the tropics, meaning it is essential that further study is undertaken on them (Armenteras et al., 2003, Bakker et al., 2008, Olson and Dinerstein, 1998). It is currently thought that only 7 % of the original montane forest of Ecuador still remains, with deforestation being listed as the main cause for its dissapearance (Bakker et al., 2008). Studies providing information about a natural baseline (pre human interference of this vegetation zone) will provide information as to how the taxa currently found on the eastern Andean flank are likely to react to future projected environmental change (drivers such as climate change, increased fire occurrence and landscape change). This allows the opportunity to observe their reactions to events that are beyond the scope of modern (hundreds of years) ecological studies (Willis et al., 2010).

2.3.2.3. Páramo

The Páramo, found between 3400 and 4800 m asl, is split into three different types of páramo (Keating et al., 1999, Sklenář,P. and Jørgensen, P.M., 1999), the grass páramo which is found between 3400 and 4000 m asl, the shrub and cushion páramo between 4000 and 4500 m asl and finally the desert páramo which exists from 4500 m asl to the snowline (Harling, 1979). In general the páramos of South America contain high diversity, including many endemic species (Keating et al., 1999). The grass páramo is distinguished from the other types due to the prevalence of grasses (Poaceae), in particular the genera *Calamagrostis* and *Festuca.* Grass páramo also contains a mixture of herbs and small shrubs, for example *Ranunculus* (Ranunculaceae), *Lupinus* (Faboideae) and *Halenia* (Gentianaceae) (Harling, 1979). The shrub páramo is compositionally similar to the grass páramo but additionally contains small trees

including *Polylepis* (Rosaceae) and a variety of shrubs and herbs. Families present include Asteraceae, Violaceae, Valerianaceae, Lycopodiaceae and Faboideae (Harling, 1979). Genera such as *Plantago* (Plantaginaceae), *Werneria* (Asteraceae) and *Azorella* (Apiaceae) are also common (Sklenář and Jørgensen, 1999). The shrub páramo also plays host to the distinctive *Espeletia* (Asteraceae) which rise above the ground as columnar rosettes (Rull et al., 2005). The desert páramo represents the upper limit of any vegetation found on the Andes, and this vegetation type is predominantly comprised of bare patches of ground which are interspersed with xerophytic grasses (those adapted to little water), mosses, lichens and a few hardy herbs and small shrubs (Harling, 1979). Species often present include *Ephedra americana* (Ephedraceae), *Lupinus microphyllus* (Faboideae) and *Senecio microdon* (Asteraceae) (Harling, 1979).

2.3.3. Mera region

At an altitude of ~1100 m asl the Mera region receives c.4800 mm of precipitation per annum and is within the lower montane rainforest (Harling, 1979, Heine, 1994). The lower montane rainforest around Mera has experienced disturbance in the recent past and consequently, stands of secondary forest are today prevalent amongst the primary forest (Grubb et al., 1963). Both primary and secondary forest of the region are floristically diverse, with an abundance of trees, palms, epiphytes and climbers present, spanning a wide range of families (lists of families can be found in Grubb et al., 1963 and Patzelt, 2008). Appendix C contains photographs of plant taxa (taken by J. Malley) and some of their identifications that were taken at Mera on fieldwork in 2012. Further information on the vegetation at Mera is included in Chapter 3, section 3.2.

2.4. Previous studies of past environmental change

2.4.1. Tropical South America

In 2010 a total of 947 sites containing pollen analysis (including both modern and fossil sites) were included in the Neotoma Latin American Pollen Database (Neotoma, 2010), this is the

entire palaeoecological site coverage for all of South America, a continent which spans >17,779,300 km^2, meaning there is approximately one site per 18,774 km^2 (Eva et al., 2004). Past environmental change research within tropical South America is further limited and irregularly distributed, with few studies undertaken across Amazonia and only slightly more across the Andes (Bush et al., 2011).

The Amazon basin in particular has a paucity of palaeoecological research, this is due in part to the scarcity of lakes present; however, a few studies do exist that have provided palaeoenvironmental data from the region using sediments obtained from lacustrine archives (examples include Bartlett and Barghoorn, 1973, Behling and Hooghiemstra, 2000, Berrio et al., 2000, Mayle et al., 2000, Paduano et al., 2003). Despite the studies which have been undertaken, debate still remains regarding how glacial and interglacial cycles have impacted the palaeoenvironment of the Amazon basin (Bush et al., 2011). In particular, questions have arisen regarding whether or not the Amazon rainforest remained forested during the last glacial, or whether it altered to savanna in response to changing climatic conditions (Hooghiemstra and van der Hammen, 1998). Current consensus is that the Amazon remained mostly forested throughout the last glacial, with some patchy fragmentation of forests occurring (Colinvaux et al., 1996a, Mayle, 2004, Werneck et al., 2011) and also changes to forest structure (Cowling, 2004).

The Andes Mountains have received slightly more attention, due to the presence of more lakes, particularly at higher elevations; records of palaeoenvironmental change include: Bush et al., 2005, Gosling et al., 2009, Grosjean et al., 2001, Mourguiart and Ledru, 2003, Urrego et al., 2010, Valencia et al., 2010, Williams et al., 2011a, Williams et al., 2011b. Results from these studies were varied, with some vegetation responding to environmental drivers (climate, fire) more than that found at other sites, this is due to the different sensitivities of the vegetation. Four of these studies, of particular relevance to the research presented here, are now described in more

detail as they provide an overview of the drivers of change that can impact vegetation; specifically the three drivers of environmental change covered are fire occurrence, moisture availability and temperature change.

Vegetation records (pollen) at Laguna Khomer Kotcha Upper (17°16.514' S, 65°43.945' W, 4153 m asl) in Bolivia is dynamic throughout the last 18,000 years concomitant with periods of increased fire (charcoal) activity (Williams et al., 2011a). It was during these periods of increased fire that the vegetation was most dynamic, without the presence of fires, *Polylepis* woodland formed a major component of the vegetation assemblage (Williams et al., 2011a). The vegetation preserved as pollen, spores and algae at Lake Miscanti (Chile; 22°45'S, 67°45'W, 4140 m asl) was mostly driven by moisture availability (Grosjean et al., 2001). During times of decreased moisture availability, pollen concentrations reduced, whereas times of increased moisture saw the establishment of dense vegetation, these changes took place over the last 22,000 years (Grosjean et al., 2001). Research performed at Lake Pacucha (Peruvian Andes; 13°36'26" S, 73°19'42" W, 3095 m asl) observed a shift from Andean forest (equivalent to the upper montane forest described in this thesis) to Puna brava, a type of Andean grassland (equivalent to the grass páramo described in this thesis). The vegetation shift observed in Pacucha has been related to decreasing temperatures (inferred cooling of 7-8 °C during the last glacial maximum; c. 21,000 years ago) and wetter than modern conditions (Valencia et al., 2010). Vegetation (pollen) preserved at Lake Consuelo (Peru; 13°57.1'S, 68°59.45'W, 1360 m asl) also responded in line with changing moisture availability during the Holocene (Urrego et al., 2010). The main ecological driver of change was found to be moisture availability during the Holocene; dry periods in the mid Holocene caused change in taxa abundance e.g. an increase in *Begonia* (Begoniaceae) and an increase in aquatics representing a lower lake level (Urrego et al., 2010). During the Pleistocene temperature was the main driver of change (Urrego et al., 2010). The studies of Lake Pacucha, Laguna Khomer Kotcha Upper, Lake Miscanti and Lake Consuelo

show the importance of a range of different drivers (temperature, fire, precipitation) in forming and modifying vegetation assemblages. The variability of driving factors amplifies the importance of using multiple proxies as evidence for multiple drivers when investigating vegetation change.

The steep elevation gradient located between the Andes and the Amazon (the eastern Andean flank) has received little study. This is mainly due to lacustrine archives being sparsely distributed on the steep flanks of the Andes. Palaeoenvironmental studies have, however, been undertaken for the mid elevations of western South America, with focus on past vegetation and climatic change (Bush, 2002, Cárdenas et al., 2014, Cárdenas et al., 2011, Urrego et al., 2010). Despite some study, a regional understanding of changes occurring on the eastern Andean flank remains widely understudied (Clapperton, 1993).

2.4.2. Eastern Andean flank of Ecuador

The eastern Andean flank is a biodiversity hotspot, and a conservation priority (Myers et al., 2000). Currently, only a few study sites are in existence for understanding the past environmental change of the eastern Andean flank in Ecuador; further sites are required in order to understand more about this region so as to better protect it in the future. Figure 2.2 shows the location of two other study sites located on the eastern Andean flank (San Juan Bosco; Bush et al., 1990 and Erazo; Cárdenas et al., 2014, Cárdenas et al., 2011). San Juan Bosco (03° 03.45 S, 78° 27.20 W, 970 m asl, 187.62 km away from the presented Mera Tigre sites; Figure 2.2) provided palaeoecological data from c.26,000 years ago based on pollen and fossil wood analysis (Bush et al., 1990). Palaeoecological data obtained from San Juan Bosco indicated the presence of Andean forest (upper montane forest) taxa (including *Alnus*, *Podocarpus* and *Hedyosmum*) now associated with higher elevations, this data was interpreted as a glacial cooling of 7.5 °C from modern temperatures (Bush et al., 1990). This observed cooling is a similar value to the inferred temperature decrease (7-8 °C) observed at Lake Pacucha (Valencia et al., 2010). Lake

Pacucha and San Juan Bosco are at different elevations (970 m asl and 3095 m asl respectively) and they are located in different countries (Peru and Ecuador) suggesting that this cooling could have been common through the Andes during the LGM. The other study performed on the eastern Andean flank investigated sediments obtained from road and river cuttings near the town of Cosanga (Erazo, 0°33.42 S, 77°52.43W, 1914 m asl, ~105 km from the Mera Tigre sites). This site provided past environmental change data dating back from c.192,000 to c.620,000 years ago, further back in time than the other study (San Juan Bosco) undertaken on the eastern Andean flank (Cárdenas et al., 2014, Cárdenas et al., 2011). Fossil pollen and fossil wood data, in particular the presence of *Podocarpus* sp (Podocarpaceae) wood macrofossils, was interpreted as a cooling of c. 5 °C during past glacial periods (Cárdenas et al., 2011). Furthermore, the preservation of fossils at Erazo was also interpreted as indicative of the continuous presence of wet conditions during a c.428,000 year period (Cárdenas et al., 2014, Cárdenas et al., 2011). Palaeoenvironmental data such as that obtained from San Juan Bosco and Erazo are integral in understanding how the eastern Andean flank of Ecuador has responded to drivers of change in the geological past. Despite the data from these sites, it is integral that further sites are found and studied to ensure that more is learnt about this ecologically important region. Further knowledge of how the eastern Andean flank has responded in the past will help us discover how it may react to drivers of change in the future.

2.4.3. Mera region

Scientific study in relation to investigating past environmental change in the Mera region is limited to one major scientific study (Bes de Berc, 2003, Bush et al., 1990, Colinvaux et al., 1996b, Espín, 2014, Heine, 1994, Liu and Colinvaux, 1985). Research was performed on sediments obtained from two road cut sections near the town of Mera and near the Río Pastaza, providing past vegetation data from the last glacial (sediments dated back c. 33,000 years ago; Liu and Colinvaux, 1985). Fossil pollen and fossil wood preserved at the stratigraphic sequence indicated a non-analogous vegetation community with the presence of taxa that are today,

usually associated with higher elevations (Liu and Colinvaux, 1985). *Podocarpus* was preserved at the site as both fossil pollen and fossil wood, the presence of this taxa, usually associated with higher elevations (2000-3500 m asl) was inferred as a temperature depression of >4.5 °C compared to the present day (Liu and Colinvaux, 1985). The amount of cooling observed in Mera during the last glacial is in line with the amount of cooling observed at Erazo from earlier in the Pleistocene, c.620,000 years ago as opposed to 33,000 for Mera; central to arguments for cooler temperatures at both Erazo and Mera was the discovery of *Podocarpus* wood macrofossils. Unlike pollen grains, wood macrofossils are large (>1 cm^3) and as such they are not so easily transportable by fluvial or aeolian mechanisms, they are, therefore, often used to infer local vegetation growth (Pisaric, 2002). However, despite the Mera site having been dated through radiocarbon dating, the age of the Mera site has been contested (Heine, 1994). Questions were raised about the reliability of the ^{14}C dates obtained for sediments and whether or not they had been contaminated by modern material to give artificially young ages (Heine, 1994). Heine performed uranium-thorium dating on a nearby lahar, with reported dates ranging from c. 8000 to 86,000 years BP (Heine, 1994). In a response to this, it was reported that although the dates obtained were at the limit of radiocarbon analysis (at the time of publication), as the analysis was performed on wood, contamination from modern carbon is likely to be reduced when compared to a bulk sediment sample (Colinvaux et al., 1996b). It was also stated that the age range produced by the uranium-thorium dating could not adequately repute the radiocarbon dates, and as such, the original dates and interpretation of the Mera site should be accepted (Colinvaux et al., 1997). The uncertainty surrounding the provenance of the Mera sediments highlighted the importance of fully understanding the depositional environment of a site and source area for the material deposited, enabling possible contamination of past or more recent sediments (Research aim 3; Chapter 7). An understanding of the depositional environment will also allow identifications of local or regional signals, through recognition of the mode of transport by which sediments are reaching the study site. Aside from highlighting this importance, the Heine and

Colinvaux debate regarding the origin of the Mera sediments stresses the importance of finding further sites in this region so that the vegetation dynamics and the response to drivers of change can be observed, providing evidence as to how this region might respond under future drivers of change.

2.6. Summary

In this chapter the study region (Mera) was defined in relation to its physical geography, modern vegetation and modern climate. A conceptual background was also provided, discussing literature presenting palaeoecological data obtained from sites in South America, the eastern Andean flank and finally the Mera region. The next chapter (Chapter 3) will introduce the two sites (Mera Tigre West and Mera Tigre East) used to address the aims outlined in Chapter 1; section 1.3.

References

ARMENTERAS, D., GAST, F. & VILLAREAL, H. 2003. Andean forest fragmentation and the representativeness of protected natural areas in the eastern Andes, Colombia. Biological Conservation, 113, 245 - 256.

BAKKER, J., MOSCOL OLIVERA, M. & HOOGHIEMSTRA, H. 2008. Holocene environmental change at the upper forest line in northern Ecuador. The Holocene, 18, 877-893.

BARBA, D., ROBIN, C., SAMANIEGO, P. & EISSEN, J.-P. 2008. Holocene recurrent explosive activity at Chimborazo volcano (Ecuador). Journal of Volcanology and Geothermal Research, 176, 27 - 35.

BARTLETT, A. S. & BARGHOORN, E. S. 1973. Phytogeographic history of the Isthmus of Panama during the past 12,000 years (a history of vegetation, climate and sea-level change). In: GRAHAM, A. (ed.) Vegetation and vegetational history of northern Latin America. Amsterdam: Elsevier.

BEHLING, H. & HOOGHIEMSTRA, H. 2000. Holocene Amazon rainforest-savanna dynamics and climatic implications: high-resolution pollen record from Laguna Loma Linda in eastern Colombia. Journal of Quaternary Science, 15, 687 - 695.

BERNAL, C., CHRISTOPHOUL, F., DARROZES, J., SOULA, J.-C., BABY, P. & BURGOS, J. 2011. Late Glacial and Holocene avulsions of the Rio Pastaza Megafan (Ecuador–Peru): frequency and controlling factors. International Journal of Earth Sciences, 100, 1759-1782.

BERNAL, C., CHRISTOPHOUL, F., SOULA, J. C., DARROZES, J., BOURREL, L., LARAQUE, A., BURGONS, J., BÈS DE BERC, S. & BABY, P. 2012. Gradual diversions of the Rio Pastaza in the Ecuadorian piedmont of the Andes from 1906 to 2008: role of tectonics, alluvial fan aggradation, and ENSO events. International Journal of Earth Sciences, 101, 1913 - 1928.

BERNARD, B., VAN WYK DE VRIES, B., BARBA, D., LEYRIT, H., ROBIN, C., ALCARAZ, S. & SAMANIEGO, P. 2008. The Chimborazo sector collapse and debris avalanche: Deposit characteristics as evidence of emplacement mechanisms. Journal of Volcanology and Geothermal Research, 176, 36-43.

BERRIO, J. C., BEHLING, H. & HOOGHIEMSTRA, H. 2000. Tropical rain-forest history from the Colombian Pacific area: a 4200-year pollen record from Laguna Jotaordó. The Holocene, 10, 749 - 756.

BES DE BERC, S. 2003. Tectonique de chevauchement, surrection et incision fluviatile (exemple de la Zone Subandine equatorienne, Haut Bassin Amazonien). [Overlapping tectonic uplift and fluvial incision (example of the Sub-Andean Zonem, Ecuadorian upper Amazon basin]. PhD, Universite Toulouse III - Paul Sabatier.

BÈS DE BERC, S., SOULA, J. C., BABY, P., SOURIS, M., CHRISTOPHOUL, F. & ROSERO, J. 2005. Geomorphic evidence of active deformation and uplift in a modern continental wedge-top–foredeep transition: Example of the eastern Ecuadorian Andes. Tectonophysics, 399, 351-380.

BIGGS, J., MOTHES, P., RUIZ, M., AMELUNG, F., DIXON, T. H., BAKER, S. & HONG, S.-H. 2010. Stratovolcano growth by co-eruptive intrusion: The 2008 eruption of Tungurahua Ecuador. Geophysical Research Letters, 37, 1 - 5.

BOOKHAGEN, B. & STRECKER, M. R. 2008. Orographic barriers, high-resolution TRMM rainfall, and relief variations along the eastern Andes. Geophysical Research Letters, 35, 1 - 6.

BUSH, M. B. 2002. Distributional change and conservation on the Andean flank: a palaeoecological perspective. Global Ecology and Biogeography, 11, 463 - 473.

BUSH, M. B., COLINVAUX, P. A., WIEMANN, M. C., PIPERNO, D. E. & LIU, K.-B. 1990. Late Pleistocene temperature depression and vegetation change in Ecuadorian Amazonia. Quaternary Research, 34, 330 - 345.

BUSH, M. B. & GOSLING, W. D. 2012. Environmental change in the humid tropics and monsoonal regions. In: MATTHEWS, J. A. (ed.) The SAGE handbook of environmental change: Volume 2. London: SAGE Publications Ltd.

BUSH, M. B., GOSLING, W. D. & COLINVAUX, P. A. 2011. Climate and vegetation change in the lowlands of the Amazon Basin. In: BUSH, M. B., FLENLEY, J. R. & GOSLING, W. D. (eds.) Tropical rainforest responses to climatic change. 2nd ed. Berlin Heidelberg: Springer- Verlag.

BUSH, M. B., HANSEN, B. C. S., RODBELL, D. T., SELTZER, G. O., YOUNG, K. R., LEÓN, B., ABBOTT, M., SILMAN, M. R. & GOSLING, W. D. 2005. A 17 000-year history of Andean climate and vegetation change from Laguna de Chochos, Peru. Journal of Quaternary Science, 20, 703-714.

CÁRDENAS, M. L., GOSLING, W. D., PENNINGTON, R. T., POOLE, I., SHERLOCK, S. C. & MOTHES, P. 2014. Forests of the tropical eastern Andean flank during the middle Pleistocene. Palaeogeography, Palaeoclimatology, Palaeoecology, 393, 76 - 89.

CÁRDENAS, M. L., GOSLING, W. D., SHERLOCK, S. C., POOLE, I., PENNINGTON, R. T. & MOTHES, P. 2011. The Response of Vegetation on the Andean Flank in Western Amazonia to Pleistocene Climate Change. Science, 331, 1055-1058.

CLAPPERTON, C. M. 1993. Nature of environmental changes in South America at the Last Glacial Maximum. Palaeogeography, Palaeoclimatology, Palaeoecology, 101, 189 - 208.

COLINVAUX, P. A., BUSH, M. B., STEINITZ - KANNAN, M. & MILLER, M. C. 1997. Glacial and postglacial pollen records from the Ecuadorian Andes and Amazon. Quaternary Research, 48, 69 - 78.

COLINVAUX, P. A., DE OLIVEIRA, P. E., MORENO, J. E., MILLER, M. C. & BUSH, M. B. 1996a. A long pollen record from lowland Amazonia: Forest and cooling in glacial times. Science, 274, 85 - 88.

COLINVAUX, P. A., LIU, K.-B., DE OLIVEIRA, P. E., BUSH, M. B., MILLER, M. C. & STEINITZ - KANNAN, M. 1996b. Temperature depression in the lowland tropics in glacial times. Climatic Change, 32, 19 - 33.

COOK, K. H. 2009. South American climate variability and change: remote and regional forcing processes. In: VIMEAUX, F. S., F. & KHODRI, M. (eds.) South American climate variability and change: remote and regional forcing processes. Paris: Springer.

COWLING, S. A. 2004. Tropical forest structure: a missing dimension to Pleistocene landscapes. Journal of Quaternary Science, 19, 733-743.

DALY, D. C. & MITCHELL, J. D. 2000. Lowland vegetation of tropical South America. In: LENTZ, D. L. (ed.) Imperfect balance: Landscape transformations in the precolumbian Americas. New York: Columbia University Press.

DINGMAN, S. L. 2002. Physical Hydrology, New Jersey, Prentice Hall.

EROS, U. S. G. S. S. C. F. E. R. O. A. S. 1996. 30 arc-second DEM of South America [Online]. [Accessed 23/10/2014 2914].

ESPÍN, B. P. A. 2014. Caracterizacin geológica y litoógica de los depósitos laháricos de Mera, provincia de Pastaza (Geological and lithological characterisation of lahar deposits, Mera province of Pastaza). Escuela Politécnica Nacional, Quito.

EVA, H. D., BELWARD, A. S., DE MIRANDA, E. E., DI BELLA, C. M., GONDS, V., HUBER, O., JONES, S., SGRENZAROLI, M. & FRITZ, S. 2004. A land cover map of South America. Global Change Biology, 10, 731-744.

FERDON, E. N. J. 1950. Studies in Ecuadorian Geography, Santa Fe, New Mexico, School of American Research and University of Southern California.

FLEISCHBEIN, K., WILCKE, W., GOLLER, R., BOY, J., VALAREZO, C., ZECH, W. & KNOBLICH, K. 2005. Rainfall interception in a lower montane forest in Ecuador: effects of canopy properties. Hydrological processes, 19, 1355 - 1371.

FU, R. & LI, W. 2004. The influence of the land surface on the transition from dry to wet season in Amazonia. Theoretical and Applied Climatology, 78, 97 - 110.

GARREAUD, R. D. 2009. The Andes climate and weather. Advances in Geosciences., 22, 3 - 11.

GARREAUD, R. D., VUILLE, M., COMPAGNUCCI, R. & MARENGO, J. 2009. Present-day South American climate. Palaeogeography, Palaeoclimatology, Palaeoecology, 281, 180-195.

GOSLING, W. D., HANSELMAN, J. A., KNOX, C., VALENCIA, B. G. & BUSH, M. B. 2009. Long-term drivers of change in Polylepis woodland distribution in the central Andes. Journal of Vegetation Science, 20, 1041 - 1052.

GRAHAM, A. 2009. The Andes: A geological overview from a biological perspective. Annals of the Missouri Botanical Garden, 96, 371 - 385.

GROSJEAN, M., VAN LEEUWEN, J. F. N., VAN DER KNAAP, W. O., GEYH, M. A., AMMANN, B., TANNER, W., MESSERLI, B., NÚÑEZ, L. A., VALERO-GARCÉS, B. L. & VEIT, H. 2001. A 22,000 ^{14}C year BP sediment and pollen record of climate change from Laguna Miscanti (23°S), northern Chile. Global and planetary change, 28, 35-51.

GRUBB, P. J., LLOYD, J. R., PENNINGTON, R. T. & WHITMORE, T. C. 1963. A comparison of montane and lowland rain forest in Ecuador I. The forest structure, physiognomy and floristics. Journal of Ecology, 51, 567 - 601.

HALL, M. L., ROBIN, C., BEATE, B., MOTHES, P. & MONZIER, M. 1999. Tungurahua Volcano, Ecuador: structure, eruptive history and hazards. Journal of Volcanology and Geothermal Research, 91, 1 - 21.

HALL, M. L., SAMANIEGO, P., LE PENNEC, J. L. & JOHNSON, J. B. 2008. Ecuadorian Andes volcanism: A review of Late Pliocene to present activity. Journal of Volcanology and Geothermal Research, 176, 1 - 6.

HARLING, G. 1979. The vegetation types of Ecuador - A brief survey. In: LARSEN, K. & HOLM-NIELSEN, L. B. (eds.) Tropical Botany. London: Academic press.

HEINE, K. 1994. The Mera site revisited: Ice - age Amazon in the light of new evidence. Quaternary International, 21, 113 - 119.
HERTEL, D. & WESCHE, K. 2008. Tropical moist Polylepis stands at the treeline in East Bolivia: the effect of elevation on stand microclimate, above- and below-ground structure, and regeneration. Trees, 22, 303-315.
HIJMANS, R. J., CAMERON, S. E., PARRA, J. L., JONES, P. G. & JARVIS, A. 2005. Very high resolution interpolated climate surfaces for global land areas. International Journal of Climatology, 25, 1965 - 1978.
HOLEMAN, J. N. 1968. The sediment yield of major rivers of the world. Water resources research., 4, 737 - 747.
HOOGHIEMSTRA, H. & VAN DER HAMMEN, T. 1998. Neogene and Quaternary development of the neotropical rain forest: the forest refugia hypothesis, and a literature overview. Earth - Science Reviews, 44, 147 - 183.
HOUSTON, J. 2006. The great Atacama flood of 2001 and its implications for Andean hydrology. Hydrological processes, 20, 591-610.
INSEL, N., POULSEN, C. J. & EHLERS, T. A. 2009. Influence of the Andes Mountains on South American moisture transport, convection, and precipitation. Climate Dynamics, 35, 1477 - 1492.
KEATING, P.L. 1999. Changes in páramo vegetation along an elevation gradient in southern Ecuador. Journal of the Torrey Botanical Society. 126, 159-175.
LIU, K.-B. & COLINVAUX, P. A. 1985. Forest changes in the Amazon Basin during the last glacial maximum. Nature, 318, 556 - 557.
LUTEYN, J. L. & CHURCHILL, S. P. 2000. Vegetation of the Tropical Andes. In: LENTZ, D. L. (ed.) Imperfect balance: Landscape transformations in the precolumbian Americas. New York: Columbia University Press.
MARENGO, J. A., SOARES, W. R., SAULO, C. & NICOLINI, M. 2004. Climatology of the low-level jet east of the Andes as derived from the NCEP-NCAR reanalyses: Characteristics and temporal variability. Journal of Climate, 17, 2261-2280.
MAYLE, F. E. 2004. Assessment of the Neotropical dry forest refugia hypothesis in the light of palaeoecological data and vegetation model simulations. Journal of Quaternary Science, 19, 713-720.
MAYLE, F. E., BURBRIDGE, R. & KILLEEN, T. J. 2000. Millennial- Scale Dynamics of Southern Amazonian Rain Forests. Science, 290, 2291 - 2294.
MILLIMAN, J. D. & MEADE, R. H. 1983. World-Wide Delivery of River Sediment to the Oceans. The journal of Geology, 91, 1 - 21.
MONTGOMERY, D. R., BALCO, G. & WILLETT, S. D. 2001. Climate, tectonics, and the morphology of the Andes. Geology, 29, 579 - 582.
MONZIER, M., ROBIN, C., SAMANIEGO, P., HALL, M. L., COTTEN, J., MOTHES, P. & ARNAUD, N. 1999. Sangay volcano, Ecuador: structural development, present activity and petrology. Journal of Volcanology and Geothermal Research, 90, 49 - 79.
MOURGUIART, P. & LEDRU, M.-P. 2003. Last Glacial Maximum in an Andean cloud forest environment (Eastern Cordillera, Bolivia). Geology, 31, 195-198.
MYERS, N., MITTERMELER, R. A., MITTERMELER, C. G., DA FONSECA, G. A. B. & KENT, J. 2000. Biodiversity hotspots for conservation priorities. Nature, 403, 853 - 858.
NEOTOMA. 2010. Neotoma Paleoecology Database (http://www.neotomadb.org/) [Online]. Available: http://www.neotomadb.org/ [Accessed 11/02/2015 2015].
OLSON, D. M. & DINERSTEIN, E. 1998. The global 200: A representation approach to conserving the Earth's most biologically valuable ecosystems. Conservation Biology, 12, 502 - 515.
OLSON, D. M. & DINERSTEIN, E. 2002. The Global 200: Priority ecoregions for global conservation. Annals of the Missouri Botanical Garden, 89, 199 - 224.

OLSON, D. M., DINERSTEIN, E., WIKRAMANAYAKE, E. D., BURGESS, N. D., POWELL, G. V. N., UNDERWOOD, E. C., D'AMICO, J. A., ITOUA, I., STRAND, H. E., MORRISON, J. C., LOUCKS, C. J., ALLNUTT, T. F., RICKETTS, T. H., KURA, Y., LAMOREUX, J. F., WETTENGEL, W. W., HEDAO, P. & KASSEM, K. R. 2001. Terrestrial ecoregions of the world: a new map of life on Earth. Bioscience, 51, 933 - 938.

PADUANO, G. M., BUSH, M. B., BAKER, P. A., FRITZ, S. C. & SELTZER, G. O. 2003. A vegetation and fire history of Lake Titicaca since the Last Glacial Maximum. Palaeogeography, Palaeoclimatology, Palaeoecology, 194, 259-279.

PATZELT, E. 2008. Flora del Ecuador, Quito - Ecuador, Imprefepp.

PISARIC, M. F. J. 2002. Long-distance transport of terrestrial plant material by convection resulting from forest fires. Journal of Paleolimnology, 28, 349-354.

POVEDA, G. & MESA, O. J. 2000. On the existence of Lloró (the rainiest locality on Earth): Enhanced ocean-land-atmosphere interaction by a low-level jet. Geophysical Research Letters, 27, 1675-1678.

RAMOS, V. A. 1999. Plate tectonic setting of the Andean Cordillera. Episodes, 22, 183 - 190.

ROSQVIST, G. C. 1995. Proglacial lacustrine sediments from El Altar, Ecuador: evidence for late - Holocene climatic change. The Holocene, 5, 111-117.

RULL, V., ABBOTT, M.B., POLISSAR, P.J., WOLFE, A.P., BEZADA, M., BRADLEY, R.S. 2005. 15,000-yr pollen record of vegetation change in the high altitude tropical Andes at Laguna Verde Alta, Venezuela. Quaternary Research. 64, 308-317.

SAMANIEGO, P., BARBA, D., ROBIN, C., FORNARI, M. & BERNARD, B. 2012. Eruptive history of Chimborazo volcano (Ecuador): A large, ice - capped and hazardous compound volcano in the Northern Andes. Journal of Volcanology and Geothermal Research, 221 - 222, 33 - 51

SKLENÁŘ, P. & JØRGENSEN, P. M. 1999. Distribution patterns of páramo plants in Ecuador. Journal of Biogeography, 26, 681-691.

URREGO, D. H., BUSH, M. B. & SILMAN, M. R. 2010. A long history of cloud and forest migration from Lake Consuelo, Peru. Quaternary Research, 73, 364-373.

VALENCIA, B. G., URREGO, D. H., SILMAN, M. R. & BUSH, M. B. 2010. From ice age to modern: a record of landscape change in an Andean cloud forest. Journal of Biogeography, 37, 1637-1647.

VALENCIA, R., BALSLEV, H. & PAZ Y MIÑO C, G. 1994. High tree alpha-diversity in Amazonian Ecuador. Biodiversity & Conservation, 3, 21-28.

VERA, C., HIGGINS, W., AMADOR, J., AMBRIZZI, T., GARREAUD, R. & GOCHIS, D. 2006. Toward a unified view of the American monsoon systems. Journal of Climate, 19, 4977-5000.

WERNECK, F. P., COSTA, G. C., COLLI, G. R., PRADO, D. E. & SITES JR, J. W. 2011. Revisiting the historical distribution of Seasonally Dry Tropical Forests: new insights based on palaeodistribution modelling and palynological evidencegeb. Global Ecology and Biogeography, 20, 272-288.

WILLIAMS, J. J., GOSLING, W. D., BROOKS, S. J., COE, A. L. & XU, S. 2011a. Vegetation, climate and fire in the eastern Andes (Bolivia) during the last 18,000years. Palaeogeography, Palaeoclimatology, Palaeoecology, 312, 115-126.

WILLIAMS, J. J., GOSLING, W. D., COE, A. L., BROOKS, S. J. & GULLIVER, P. 2011b. Four thousand years of environmental change and human activity in the Cochabamba Basin, Bolivia. Quaternary Research, 76, 58-68.

WILLIS, K. J., BAILEY, R. M., BHAGWAT, S. A. & BIRKS, H. J. B. 2010. Biodiversity baselines, thresholds and resilience: testing predictions and assumptions using palaeoecological data. Trends in Ecology & Evolution, 25, 583 - 591.

ZHOU, J. & LAU, K.-M. 1998. Does a monsoon climate exist over South America? Journal of Climate, 11, 1020-1040.

Chapter 3: Study sites

The previous chapter introduced the study region (eastern Andean flank and the Mera region), and also identified this region as important for further study by reviewing the current literature. This chapter goes on to introduce the generalities (catchment area, local vegetation and local climate) of the two study sites used to answer the aims set out in Chapter 1, and then the two stratigraphic sequences are discussed. The two stratigraphic sequences that are discussed in the latter part of this chapter are Mera Tigre West (sampled in October 2008) and Mera Tigre East (sampled in September 2012).

3.1. Study sites

Two stratigraphic sequences exposed by fluvial processes were sampled from the Mera region of Ecuador (Mera Tigre West (MTW), 01° 27.546 S, 78° 06.791 W, 1117 m asl and Mera Tigre East (MTE), 01° 27.546 S, 78° 06.199 W, 1117 m asl). The stratigraphic sections are situated in central Ecuador, South America, 144 km southeast of Quito, the capital city of Ecuador (Figure 3.1). The sites are situated within the biodiversity hotspot of the eastern Andean flank (Myers et al., 2000).

The MTW and MTE stratigraphic sections are situated 0.38 km away from each other, located on opposing sides of the Río Alpayacu river valley (Figure 3.2 and Figure 3.3). The Río Alpayacu is part of a complicated system of tributaries. Before it reaches the stratigraphic sections the Río Alpayacu is intersected by the Río Tigre. The Río Tigre has been dammed to create a water park (el Dique de Mera) and as such today the Río Alpayacu receives a partially reduced water input from the Río Tigre. Due to the fluvial environment of the stratigraphic sections, the catchment area was calculated based on elevation data (compiled from a mosaic of twelve digital elevation models surrounding the site) and the rivers and streams of the area (Figure 3.1).

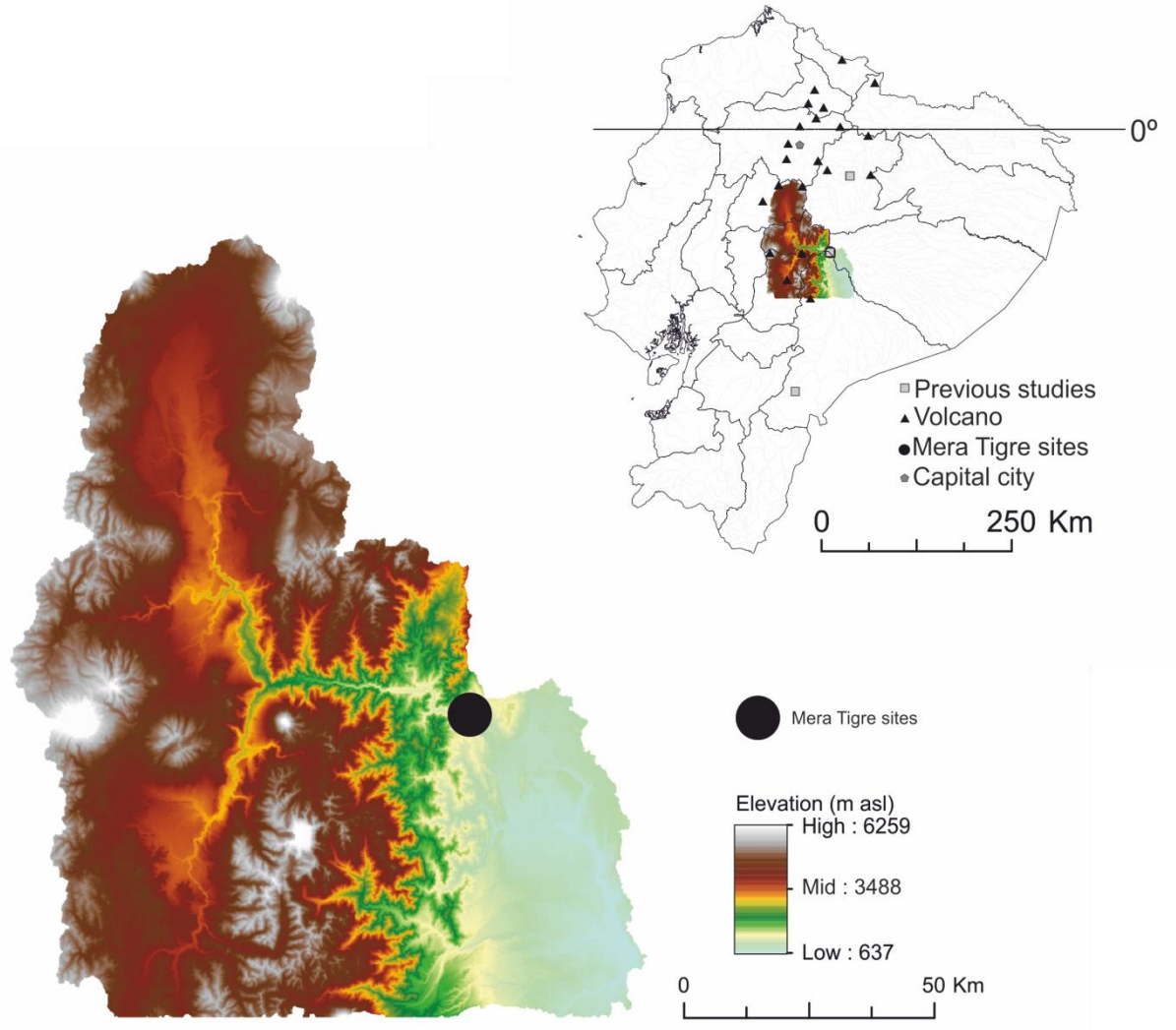

Figure 3.1: Catchment area map for Mera Tigre West and Mera Tigre East. The catchment was generated using elevation data (Hijmans et al., 2004) and tools available in ArcHydro and ArcGIS 10.1. The catchment area is also shown relevant to Ecuador.

The catchment area generated (Figure 3.1) was approximately 15,000 km^2, covering roughly 5 % of Ecuador's land surface. The large size of this catchment area means that a lot of sediment could be transported into the sample sites, bringing sediment from a wide range of vegetation types. The sediment transported through the large catchment area above Mera highlights the extent of the potential source area for sediments found at the MTW and MTE stratigraphic sequences.

Despite the large catchment area, based on the sediment type present in the stratigraphic sequences, it is expected that the source area for MTW is local (no fluvial evidence present in the sequence). MTE contained a more varied sediment type, including evidence of fluvial sediments in the upper part of the sequence. Due to this, the source area of MTE is discussed in detail in Chapter 7 of this thesis, however, the majority of MTE has no evidence of fluvial sequences meaning it is likely that most of this sequence is of local origin.

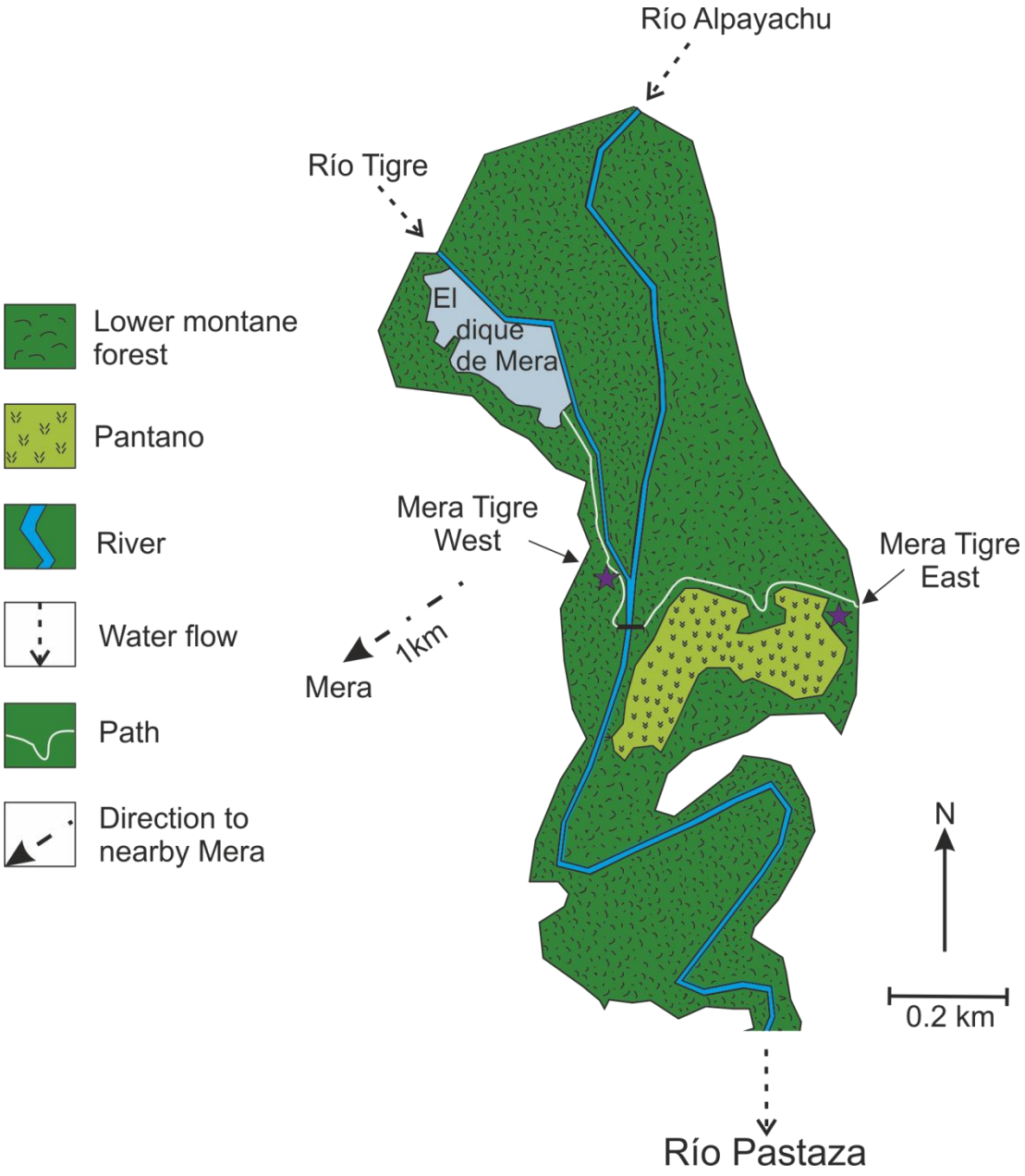

Figure 3.2: Location of study sites (Mera Tigre West and Mera Tigre East) relative to the town of Mera and nearby geographic features including el Dique de Mera, Río Tigre, Río Alpayacu and the paths that run past the study sites. The map is based on an aerial photograph (number 29705) taken by Proyecto Carta Nacional on 22nd January 2013 (Figure 3.3).

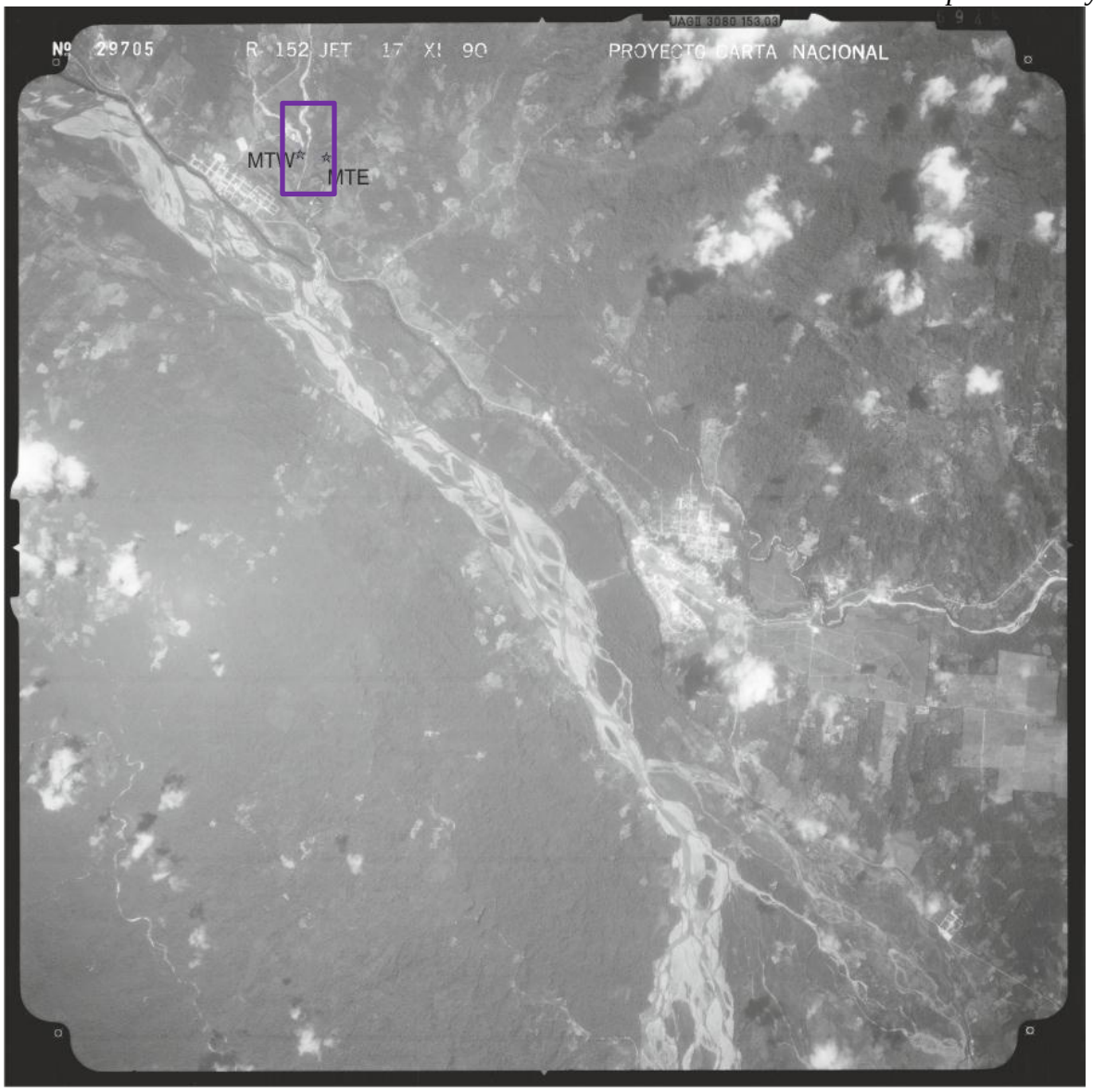

Figure 3.3: Aerial photograph of the area surrounding the Mera Tigre sites. The aerial photograph (number 29705) was taken by Proyecto Carta Nacional on 22nd January 2013. Mera Tigre West and Mera Tigre East are included on the map as a point of reference. The purple rectangle represents the extent of Figure 3.2.

3.2. Local vegetation

The Mera Tigre study sites are located at 1117 m asl, meaning the vegetation type present is the lower montane rainforest (see Section 2.3.2.1, found up to 2500 m asl; Harling, 1979). Many species of trees, palms, shrubs, grasses, epiphytes and bryophyte are present (Liu and Colinvaux, 1985). During fieldwork in 2012, the following taxa were noted as present: Apiaceae, *Asplenium* spp. (Aspleniaceae), Bromeliaceae, *Cecropia* spp. (Urticaceae), Cyperaceae, *Lycopodium* spp.

(Lycopodiaceae), Melastomataceae, Orchidaceae, Poaceae, *Polypodium* spp. (Polypodiaceae), and Sapindaceae. A total of 51 photographs were also taken during fieldwork for identification by tropical botanist Susana León Yanez, currently based at Pontificia Universidad Católica del Ecuador. The photographs of the 51 taxa taken at the stratigraphic sequences are included in Appendix C for reference purposes.

The modern floristic composition at the Mera Tigre sites reflects recent disturbance (likely to be as a result of human or fluvial disturbance mechanisms), for example the presence of the disturbance indicator *Cecropia* (Berrío et al., 2002, Colinvaux et al., 1999). *Cecropia* is a pioneer taxa, it has an almost continuous seed production, the ability of seeds to be dormant and a rapid growth rate, especially in the high light levels that follow landscape disruption, these adaptations mean it can rapidly colonise an area following a disturbance (Guariguata and Ostertag, 2001, Hartshorn, 1980). Pioneer taxa such as *Cecropia* are often the first taxa to take over an area following a perturbation, because of this they are primary components of secondary forests (forests in which the floristic structure of a forest has been altered by a disturbance, often through anthropogenic mechanisms; Corlett, 1994). Evidence of secondary forest is present at the Mera Tigre sites, with taxa such as Poaceae, *Cecropia* spp. and *Heliocarpus* spp. (Malvaceae) present (Grubb et al., 1963), these taxa are found alongside a variety of ferns, another indicator of disturbance and secondary forests (Martin et al., 2007). Recent disturbance could be due to the sites close location to el Dique de Mera waterpark (0.34 km away from Mera Tigre West and 0.72 km away from Mera Tigre East) and the nearby town of Mera (1 km away; Figure 3.2), meaning there is a possible anthropogenic input in the area. Footpaths run past both sites, leading to the occurrence of erosive processes caused by people walking on the path. However, this is kept to a minimal level as both of the stratigraphic sequences are above and below the paths. Divergence from the path is limited by vegetation and as such the sediments of the stratigraphic sequences remain untouched and intact.

3.3. Local climate

Local climate at the Mera Tigre sites is influenced by their location on the eastern Andean flank, with the same controlling mechanisms as described in section 2.3.3. The study sites have a mean annual temperature of c. 20.8 °C and a mean annual precipitation of >4800 mm (Ferdon, 1950, Liu and Colinvaux, 1985). At Mera precipitation remains constantly high throughout the year with no dry season; however, there is a slightly wetter season during the months of April and July (Figure 3.4; Ferdon, 1950).

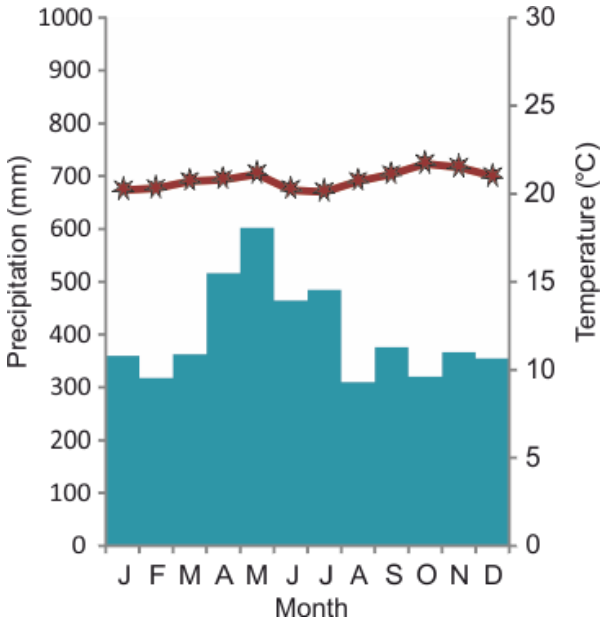

Figure 3.4: Climate graph representing monthly values for temperature (°C; stars) and precipitation (mm; bars). Values obtained from Mera climate station. Original data from Ferdon, 1950.

3.4. Sedimentary sequences

3.4.1. Mera Tigre West

Mera Tigre West is an 8.49 m vertical stratigraphic section (Figure 3.5) exposed by fluvial down cutting of the present day Río Alpayacu.

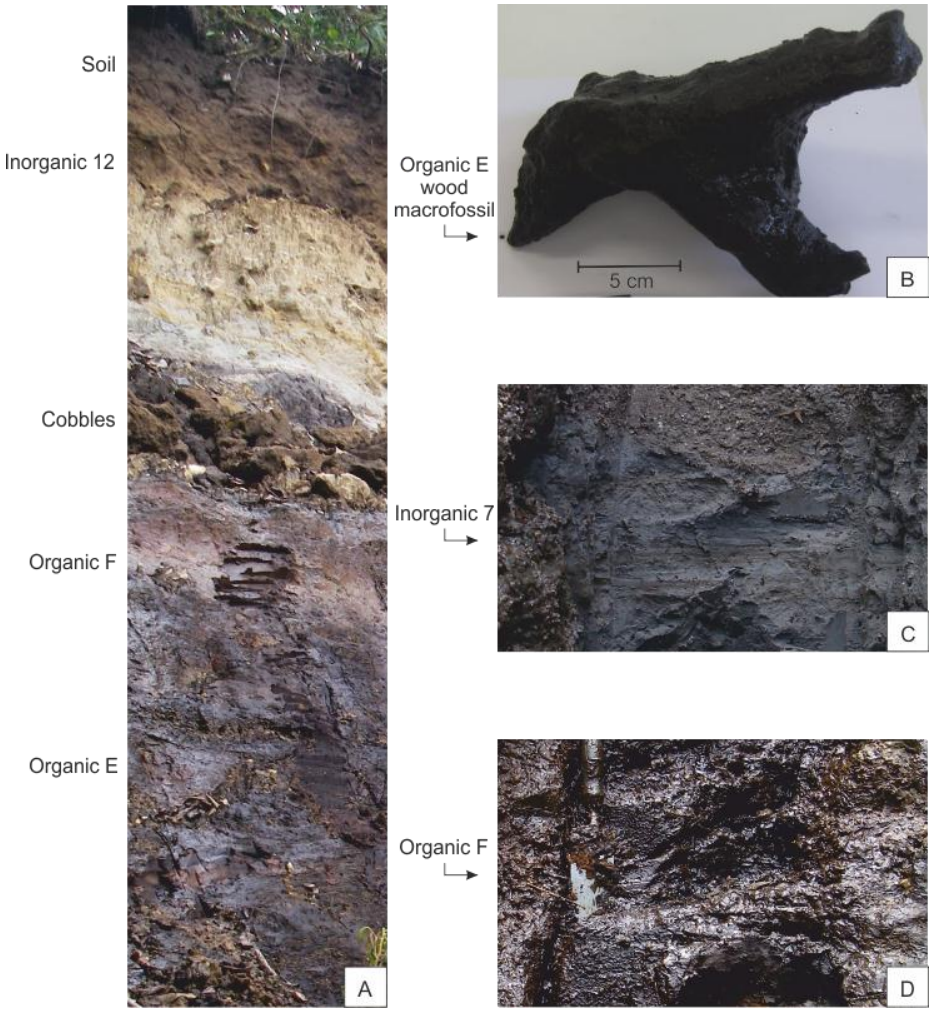

Figure 3.5: (A) Upper portion of the Mera Tigre West stratigraphic section. Organic (dark in colour) and inorganic (light in colour) layers are visible. Distinguishable layers have been identified. (B) A wood macrofossil recovered from Mera Tigre West, organic layer E. (C) Inorganic layer sampled from Mera Tigre West. (D) Organic layer F sampled at Mera Tigre West. Photographs A, C and D courtesy of William Gosling and photograph B taken by Hayley Keen.

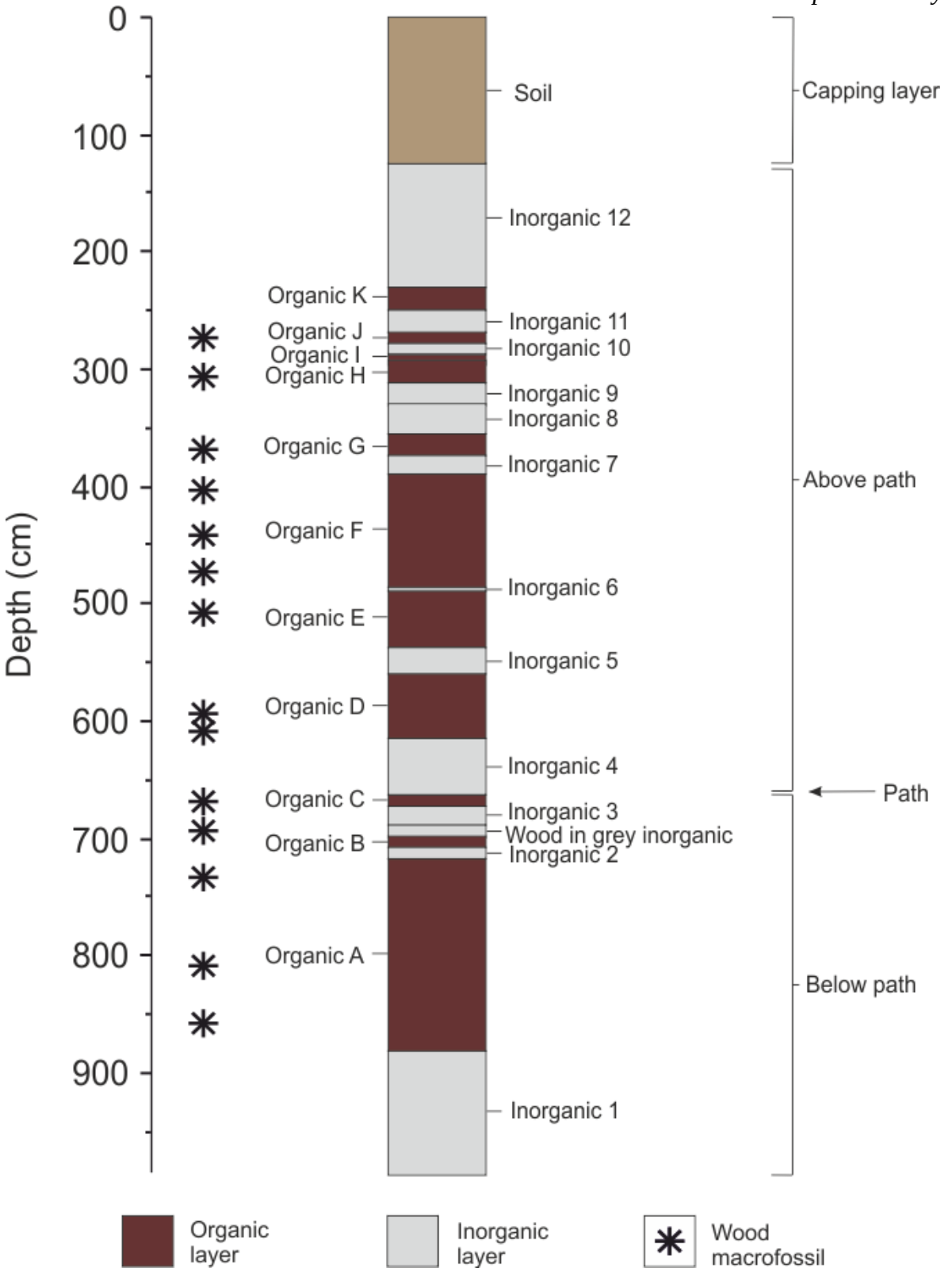

Figure 3.6: Stratigraphic column for Mera Tigre West. The column represents the interspersed organic (brown) and inorganic (grey) layers and also the presence of wood macrofossils (star). Despite the presence of a path in the middle of the section, the sequences are deemed continuous due to the similarity of the sediment before and after the path. There was also no break in pollen types before and after the sequence (Figure 8.1).

The stratigraphic sequence is composed of 11 organic layers and 13 inorganic layers, capped by a thick layer of soil intermixed with inorganic material (Figure 3.6). A total of 14 wood macrofossils were recovered from the stratigraphic section. The section was accessed via a path leading from the nearby el Dique de Mera waterpark. At the time of sample collection, in October 2008, the section was exposed due to a recent landslip. On a return visit in September 2012 the upper part of the section (above path) was completely vegetated. The lower part of the section (below path) no longer existed due to a landslip into the Río Alpayacu below removing the material. Consequently, the MTW section could not be resampled in September 2012 due to vegetation cover and loss of sediment.

3.4.2. Mera Tigre East

Mera Tigre East is a 12.83 m vertical stratigraphic section, situated on the opposite side of the Río Alpayacu river valley, 0.29 km away from the active stream channel. The site is above a swampy (pantano) area and the section is split into two parts by a small path (Figure 3.7 shows the above and below path parts of the section).

Figure 3.7: (A) Lower portion of the stratigraphic section (below path). Organic layers are identifiable by their dark colour; inorganic layers by their lighter colour, distinguishable layers are labelled. (B) Upper portion of the stratigraphic section (above path). Organic layers (dark in colour) and inorganic layers (light in colour) are visible. Distinguishable layers are labelled. (C) The basal inorganic layer, sampled from Mera Tigre East (D) Organic layer B sampled from Mera Tigre East shown. Photographs all courtesy of James Malley.

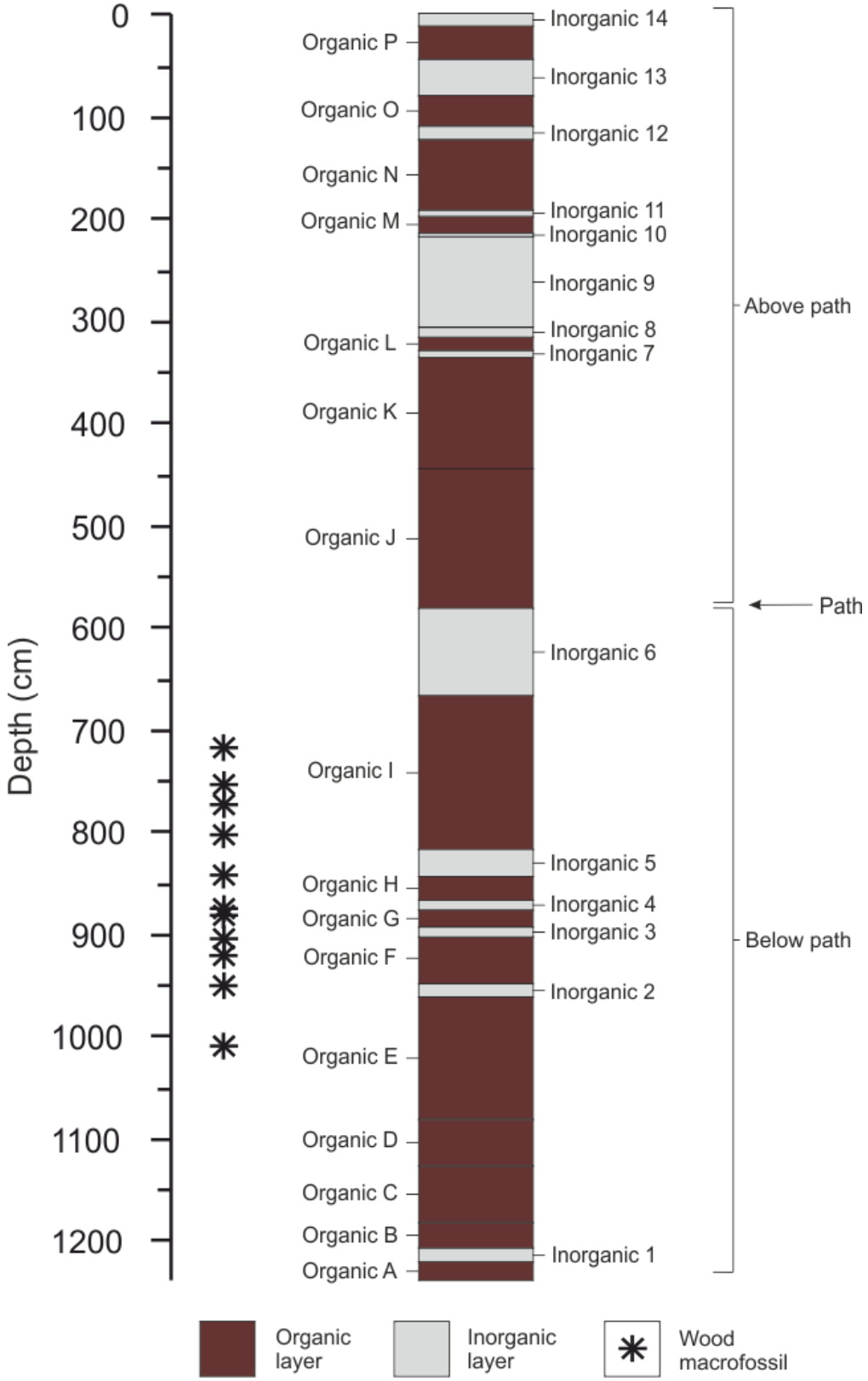

Figure 3.8: Stratigraphic column for Mera Tigre East. The column represents the interspersed organic (brown) and inorganic (grey) layers. The presence of wood macrofossils (star) is also indicated. Despite the presence of a path in the middle of the section, the sequences are deemed continuous due to the similarity of the sediment before and after the path. There was also no break in pollen types before and after the sequence (Figure 8.4).

The stratigraphic sequence is composed of 16 organic layers, 14 inorganic layers (Figure 3.8). A total of 11 wood macrofossils were also recovered from within the stratigraphic section. At the time of collection in September 2012 the site was partially vegetated with a few sections exposed. At a return visit in January 2013 the site was more vegetated with rapidly colonising plant taxon, such as Poaceae, dominant (Figure 3.9).

Figure 3.9: (A) Mera Tigre East photographed in September 2012, photograph courtesy of James Malley. (B) Mera Tigre East photographed in January 2013, photograph courtesy of Encarni Montoya. Both photographs show Organic J.

3.5. Summary

In this chapter the study sites Mera Tigre West and Mera Tigre East were defined, including information about the local vegetation and the climate. In the next chapter (Chapter 4) the methodologies employed in this research to address the scientific aims (see Section 1.3) will be explained and justified.

References

BERRÍO, J. C., HOOGHIEMSTRA, H., MARCHANT, R. & RANGEL, O. 2002. Late-glacial and Holocene history of the dry forest area in the south Colombian Cauca Valley. *Journal of Quaternary Science*, 17**,** 667-682.

COLINVAUX, P. A., DE OLIVEIRA, P. E. & PATIÑO, J. E. M. 1999. *Amazon pollen manual and atlas,* Amsterdam, Harwood Academic Publishers.
CORLETT, R. T. 1994. What is secondary forest? *Journal of Tropical Ecology,* 10**,** 445-447.
FERDON, E. N. J. 1950. *Studies in Ecuadorian Geography,* Santa Fe, New Mexico, School of American Research and University of Southern California.
GRUBB, P. J., LLOYD, J. R., PENNINGTON, R. T. & WHITMORE, T. C. 1963. A comparison of montane and lowland rain forest in Ecuador I. The forest structure, physiognomy and floristics. *Journal of Ecology,* 51**,** 567 - 601.
GUARIGUATA, M. R. & OSTERTAG, R. 2001. Neotropical secondary forest succession: changes in structural and functional characteristics. *Forest ecology and management,* 148**,** 185-206.
HARLING, G. 1979. The vegetation types of Ecuador - A brief survey. *In:* LARSEN, K. & HOLM-NIELSEN, L. B. (eds.) *Tropical Botany.* London: Academic press.
HARTSHORN, G. S. 1980. Neotropical forest dynamics. *Biotropica,* 12**,** 23-30.
HIJMANS, R. J., GUARINO, L., BUSSINK, C., MATHUR, P., CRUZ, M., BARRENTES, I. & ROJAS, E. 2004. *DIVA-GIS. Vsn. 5.0. A geographic information system for the analysis of species distribution data.* [Online]. Available: http://www.diva-gis.org.
LIU, K.-B. & COLINVAUX, P. A. 1985. Forest changes in the Amazon Basin during the last glacial maximum. *Nature,* 318**,** 556 - 557.
MARTIN, P. H., SHERMAN, R. E. & FAHEY, T. J. 2007. Tropical montane forest ecotones: climate gradients, natural disturbance, and vegetation zonation in the Cordillera Central, Dominican Republic. *Journal of Biogeography,* 34**,** 1792-1806.
MYERS, N., MITTERMELER, R. A., MITTERMELER, C. G., DA FONSECA, G. A. B. & KENT, J. 2000. Biodiversity hotspots for conservation priorities. *Nature,* 403**,** 853 - 858.

Chapter 4: Field and laboratory methodologies

In the previous chapter, the two stratigraphic sections, Mera Tigre West and East, which are the focus of this research, were introduced. This chapter provides details on the methodologies used during fieldwork (including discovery, description and sampling of study sites), and in the laboratory (including physical and biological proxies and dating techniques). Fieldwork was undertaken in Ecuador during 2008 and 2012 and all laboratory procedures were completed between 2011 and 2014. Full details of all analytical protocols can be found in Appendix 1. A range of methods were applied in this study (multi proxy approach), some of the proxies used are dependent on each other, however, despite this a whole range of data has been produced from this study which is useful to palaeoecology. It was not possible to use more independent variables due to their lack of presence in the sediments, for example there were no chironomids preserved in the samples, meaning it was not possible to use chironomids as an indicator of temperature.

H. Keen led, wherever possible, the field and laboratory work. Notable exceptions were: (i) fieldwork in 2008 (Mera Tigre West section; H. Keen had not yet been recruited to the project), (ii) radiocarbon dating for Mera Tigre West (dating was performed at external laboratories prior to the involvement of H. Keen with the project). Radiocarbon dating for Mera Tigre East was performed at an external laboratory. (iii) Optically stimulated luminescence (OSL) dating for Mera Tigre East was performed at an external laboratory due to the time restraints for the project not allowing time to learn the entire complex procedure required for OSL. Where analysis was not conducted by H. Keen all other scientists and laboratories involved have been fully acknowledged below.

4.1. Fieldwork

A video containing information about the study area and the sampling methodologies is included in Appendix A. The video contains footage of Mera Tigre East (filmed during fieldwork in 2012) and the area surrounding both Mera Tigre East and West. The video was put together by Hayley Keen, James Malley and Frazer Matthews-Bird. The video was entered into the American Geophysical Union (AGU) student video competition 2014 and won the competition.

4.1.1. Study site discovery

William Gosling and two PhD students (Macarena Cárdenas and Joseph Williams) undertook a field expedition to the Mera region in 2008 in search of deposits discussed in research by Liu and Colinvaux (Liu and Colinvaux, 1985). The original deposits could not be found, however, a similar sedimentary sequence was discovered and sampled nearby; this section is below referred to as Mera Tigre West.

In 2012 Hayley Keen led fieldwork back to the Mera region in search for a sedimentary sequence similar to Mera Tigre West so that a comparative study could be performed. Mera Tigre East was discovered and sampled by Hayley Keen with the assistance of William Gosling, Frazer Matthews-Bird (PhD student) and James Malley (technician).

4.1.2. Stratigraphic section description

Field descriptions of both the Mera Tigre West and East stratigraphic sections were made before sampling of the sediments, following clearance of overhanging vegetation. The front faces of both sections were cleaned using a spade to remove at least the first two centimetres of material. The removal of surface material allowed the sediment structure to be revealed whilst also preventing the samples being contaminated with modern material. Preliminary notes were taken for all sections; noting sediment type present, local vegetation type and any other useful observations.

4.1.3. Sampling of stratigraphic sections

The Mera Tigre West section was collected in two parts (see Figure 3.6). A tape measure was used to locate samples relative to the river (lower part) and the path (upper part). The tape measure was left in situ throughout the sampling process. Where sediments allowed, the organic sections were sampled at a five centimetre resolution. Organic samples were carefully extracted from the exposed sediment using a spatula and a knife. In each case the organic sample was cut out of the section and placed into a pre-labelled bag, sediments were not handled if possible to prevent contamination. Inorganic layers (differentiated in the field by their light colour and uniform texture) were sampled in bulk. Inorganic samples were taken using a spatula and 'scooped' into the bag with no handling, Wood macrofossils were removed from the section wherever they were found using a spade and were placed into pre-labelled bags. The samples were not touched at all, to prevent contamination so radiocarbon dating could be performed.

The Mera Tigre East section was sampled in two separate parts (see Figure 3.8), above the road and below the road (road meaning a small track intersecting the section which was used by people only). A tape measure was used to measure the position of samples relative to the track. Where sediments allowed, samples were obtained at a five cm resolution throughout organic layers. Organic samples were extracted using a spatula and a knife and placed into pre-labelled bags with minimal handling. Inorganic layers in the sediment were bulk sampled using a spade for the larger layers, and a spatula for smaller layers. Wood macrofossils were extracted from the sediment using a knife and a spade, and then placed into labelled bags. Sediment short cores for modern pollen analysis were also retrieved from the Mera Tigre area from the pantano; the sampling methodology for this is covered in Section 4.1.4. Samples for Optically stimulated luminescence (OSL) analysis were also retrieved; the methodology for this is covered in Section 4.1.5.

All samples (organic, inorganic and wood macrofossils) were carefully sealed in plastic grip lock bags and then placed in a cool location before they were transported back to The Open University's cold store which is kept at a constant 4 °C.

4.1.4. Short core – modern pollen sampling

Short cores were obtained in two locations in the pantano (see Figure 3.2.) to provide an insight into the modern depositional environment and microfossil representation of the environment. The sediment-water interface was sampled using a plastic tube dropped into the sediment; core one recovered 4 cm of sediment and core two (Figure 4.1) recovered 23 cm of sediment. The surface sediment cores were extruded from the plastic tube on site and every 1 cm was carefully sliced off using a spatula and placed into individual labelled sample bags. Samples were kept cool until they were transported back to The Open University, where they were then placed into cold storage (4 °C).

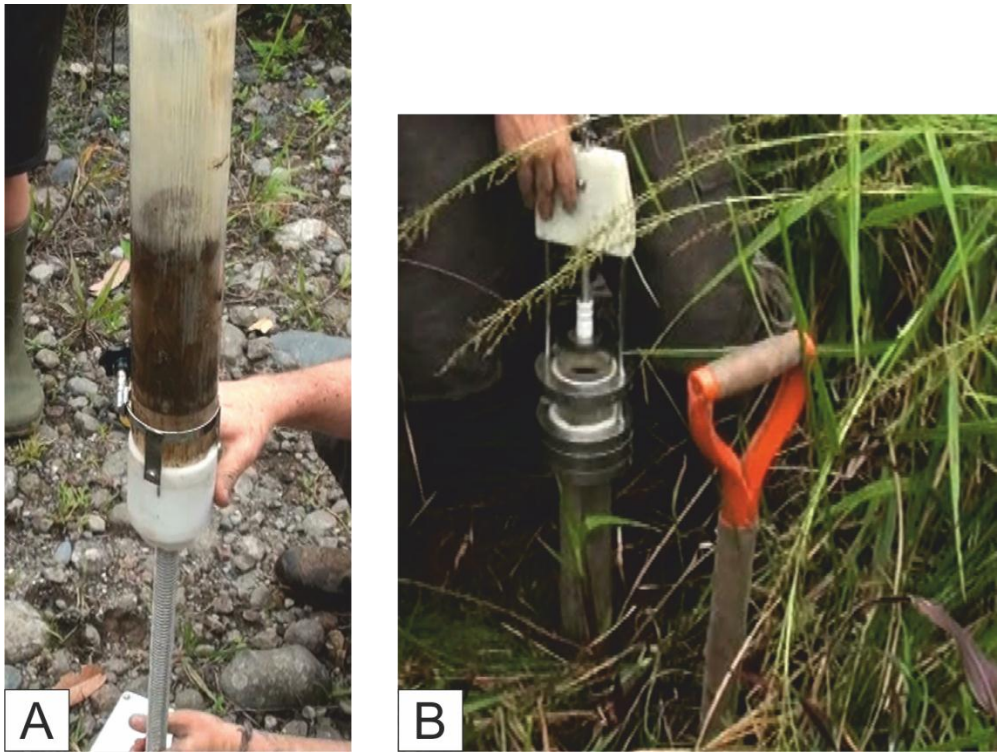

Figure 4.1: A) Core 2 being extruded from the pantano it was cored from. B) Core 2 being extracted from the pantano.

4.1.5. OSL sampling

Samples for optically stimulated luminescence dating were collected from Mera Tigre East on a subsequent field trip by Encarni Montoya and Frazer Matthews-Bird in January 2013. Nine 30 cm long metal tubes were inserted into the sediment at selected points (~1.5 m resolution throughout the site) and were then carefully extracted to ensure no light reached the sediments. The tubes were sealed at the top and the bottom of the tube and then wrapped with duct tape. The tubes were labelled and the samples were then placed in a cool dark place. They were posted back to The Open University and then placed in cold storage at 4 °C until required for analysis.

4.2. Laboratory analysis of physical properties

Two techniques (Loss-on-ignition and X-ray fluorescence analysis) were applied to sediments from Mera Tigre West and East to understand the physical properties of sediments sampled including organic content of the samples and the composition of inorganic sediments respectively.

4.2.1. Loss-on-ignition

4.2.1.1. Rationale

Loss-on-ignition (LOI) is widely used in order to gain an understanding of the depositional environment by quantifying the relative proportion of organic and carbonate sediment present (Birks and Birks, 2006). LOI is a simple and fast technique that provides insight into the sediment composition; however, care does have to be applied when using this technique as it does contain some analytical issues. It has been found that changes in a combination of factors such as sample size, exposure time, and even the position in the furnace can alter the results obtained (Heiri et al., 2001). Due to this, it is important that the same sample protocol is applied throughout the use of LOI in order to obtain the most accurate results.

4.2.1.2. Methodology

Sub-samples of 1 cm^3 were taken from all organic samples (66 samples for Mera Tigre West and 180 samples for Mera Tigre East) within both of the Mera Tigre sections in order to gain a comprehensive as possible understanding of sediment composition changes. Following standard protocol, sub-samples were dried at 105 °C for 12 hours and ignited at 550 °C and 925 °C in a muffle furnace for two and four hours respectively (Dean, 1974, Heiri et al., 2001). The full analytical procedure followed is included in Appendix 1.

4.2.2. X-ray fluorescence analysis – major element

4.2.2.1. Rationale

Major element X-ray fluorescence analysis (XRF) was selected as a quick analytical technique to identify similarities between inorganic deposits at the two different Mera Tigre sites and potential source area sizes for the inorganic deposits. XRF major element analysis measures the following elements (SiO_2, TiO_2, Al_2O_3, Fe_2O_3, MnO, CaO, Na_2O, K_2O and P_2O_5) of a sample. XRF major element analysis is a well-established technique (Thomas and Haukka, 1978) that is routinely used within multi proxy palaeoecological studies, e.g. Brunschön et al., (2010) and Niemann et al., (2013). XRF provides accurate data which can be used alongside palaeoecological data to provide evidence on the depositional environment and sediment type in a multi proxy approach.

4.2.2.2. Methodology

Major element XRF analysis was undertaken on 23 inorganic layers (12 for Mera Tigre West and 11 for Mera Tigre East). Three grams of each sample were dried overnight at 110 °C; sub-samples were then crushed to a fine powder. Loss-on-ignition was performed on 1.2 g of the powdered sub-sample; the sub-sample was ignited for one hour in a furnace set at 1000 °C. This

provided a percentage loss (Equation 4.1) for the major components (H_2O and CO_2), that cannot be measured using XRF.

$$Percentage\ Loss\ on\ Ignition = \frac{weight\ change\ of\ sample\ powder\ x\ 100}{original\ weight\ of\ sample\ powder} \quad \text{Equation 4.1:}$$

Glass discs were then created using 0.7000 g of the remaining powdered sub-sample and 3.6300 g of lithium metaborate flux. These were accurately weighed into platinum crucibles and then stirred together. The powder/flux mix was then placed into a muffle furnace at 1100 °C for 20 minutes in order to melt the mixture. When homogenised, the melt was poured into a heated brass mould and a plunger was pressed down steadily, forming the glass disc. Once glass discs had been created and the loss-on-ignition values had been determined, the samples were analysed on an ARL 8420+ dual goniometer wavelength dispersive XRF spectrometer. A detailed analytical procedure is included in Appendix 1.

4.3. Laboratory analysis of biological proxies

4.3.1. Fossil pollen and non-pollen-palynomorphs

4.3.1.1. Rationale

The analysis of fossil pollen and spores (palaeopalynology) has been widely adopted to investigate the past history of Earth's climate and ecology since its introduction in 1929 (Von Post, 1929, Von Post, 1946). Pollen grains are produced by plants in varying abundances and many of these preserve in sediments. The pollen exine contains sporopollenin, a resistant organic material, possibly an oxidative polymer or carotenoids and carotenoid esters (Kawase and Takahashi, 1995), meaning the pollen grain can preserve in sediments (providing oxidation does not occur, as oxidation impacts the sporopollenin meaning the exine will degrade and the pollen

grain will not be preserved) and then can survive the harsh chemical processes undergone in laboratory preparation (Birks and Birks, 1980). By analysing accumulated archives preserved through time in bog, lake and river sediments, they provide a detailed sedimentary record on how regional and local past vegetation has altered in response to drivers of change (both natural and anthropogenic).

Due to their small size (c. <100 µm) pollen grains are easily transportable by aeolian and fluvial transport mechanisms (Birks and Birks, 1980). Pollen grains are easily transported in suspension by rivers and streams, and by this mechanism they can be transported through entire catchment areas, providing difficulties to palynologists trying to interpret local vegetation from preserved pollen. Erosive processes can also move pollen grains once they have been deposited, particularly important to take into consideration in open stratigraphic sections such as Mera Tigre West and East. Due to this potential transportation by aeolian and fluvial mechanisms, care must be taken when interpreting pollen signals. The depositional environment of a site should also be considered to ensure that influences such as fluvial transport are noted.

Aside from pollen grains, non-pollen-palynomorphs (NPPs) are also preserved in sediments. NPPs are comprised of anything in a sample which is not a pollen grain, and these can include fungal spores, insect parts and other plant remains, for example the xylem and phloem of a plant (Van Geel, 2001).

4.3.1.2. Methodology (preparation and identification)

From both the Mera Tigre West (30 samples) and the Mera Tigre East (67 samples) stratigraphic sequences 0.5 cm^3 sub-samples were retrieved at a ~10 cm resolution throughout the organic sediments. Each sub-sample was spiked with the exotic marker spore *Lycopodium* (batch 124961, Lund University) to allow pollen concentrations to be calculated (Maher, 1972, Stockmarr, 1971). Sub-samples were prepared following standard analytical procedures,

involving acetolysis and digestions in Hydrochloric acid, Hydrofluoric acid and Potassium hydroxide (Moore et al., 1991). A detailed analytical procedure can be found in Appendix 1.

After processing, sub-samples were then mounted on microscope slides using glycerol and covered with a cover slip to prevent contamination. Pollen and spores were then counted and identified using a Nikon Eclipse 50*i* microscope at x20 and x40 magnification. Pollen grains and spores were described and identified using distinctive morphological features including size, shape, surface pattern and number of pores (Figure 4.2). Identifications were based on comparison of fossil material with published material (Bush and Weng, 2007, Colinvaux et al., 1999, Hooghiemstra, 1984, Roubik and Moreno, 1991) and a reference collection held at The Open University. Unidentified pollen grains were photographed using an Infinity 1 digital camera and assigned a pollen "type" number, for example 'Pollen unknown OU 48'. Unidentified NPPs were assigned a reference, for example 'Spore unknown OU 17'.

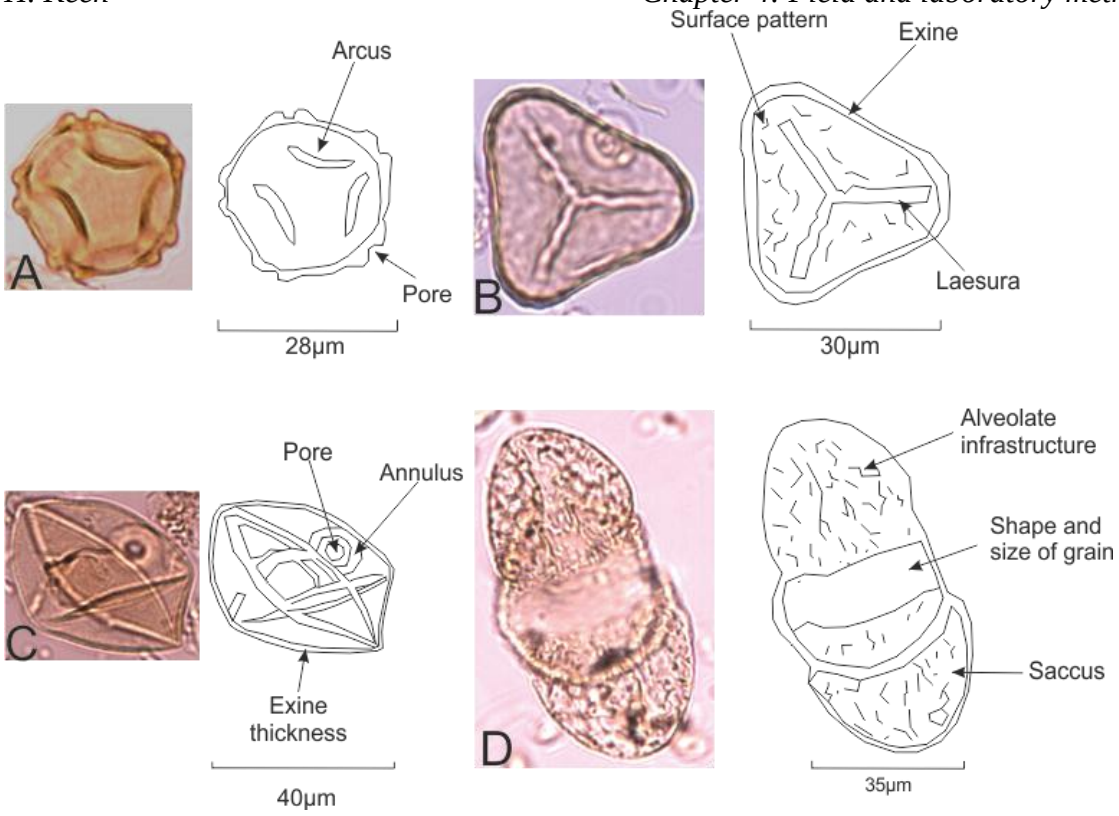

Figure 4.2: Examples of key morphometric features used for identification of pollen and spores are shown. Pollen grains A to D shown here are from the Mera Tigre sites, and represent the following taxa: A – *Alnus* sp, B – Trilete fern spore, C – Poaceae and D – *Podocarpus* spp.

4.3.1.3. Methodology (pollen and spore counting)

Counts were achieved by traversing across the microscope slide, noting the presence of all pollen grains and spores until the appropriate count size was achieved. The presence of grains was recorded on a pollen count sheet (an example of which can be found in Appendix 1; Section A.1.2). Each sub-sample was counted using a sample specific count size, generated using a statistical approach, designed to ensure the major elements of the pollen assemblage were robustly characterised (Model 1; Chapter 5), count sizes varied from 196-982. Count sizes were generated taking into consideration the richness and evenness (see 5.3.1. and 5.3.2.) of a provisional input of 100 pollen grains. The sub-sampling tool uses a Monte Carlo simulation (multiple random sampling to obtain the best suited count size). The sub-sampling tool was created based on extended empirical counting for six samples from Mera Tigre West and four

other tropical sites. The full methodology for the development of the sub-sampling tool is presented in Chapter 5 (Keen et al., 2014).

4.3.2. Charcoal particle analysis

4.3.2.1. Rationale

The analysis of charcoal particles is regularly included in palaeoecological studies as a method to determine fire occurrence in the landscape (Niemann and Behling, 2008, Taylor et al., 2010, Whitlock and Larsen, 2001). Charcoal particles remain in the environment following fires and, similar to pollen and non-pollen-palynomorphs, can be preserved in sedimentary sequences. Alongside climate, fire is one of the biggest drivers of ecosystem change (Thonicke et al., 2001), and as such exploring fire in the palaeoecological record provides further understanding into mechanisms of change (Seppä and Bennett, 2003, Whitlock and Larsen, 2001). By including charcoal alongside pollen records, shifts in the vegetation corresponding to fire events can be explored.

Charcoal particles can be transported by aeolian and fluvial transport mechanisms, however, the larger a particle of charcoal is, the smaller the distance it is likely to have travelled (Whitlock and Larsen, 2001). As such, the investigation of macro charcoal particles is more likely to provide a local fire signal. Debate, does, however, exist into how far particles are likely to travel via aeolian transport mechanisms, with a correlation between the intensity and severity of the fire and the distance the particles are transported (Higuera et al., 2007). Alongside aeolian transportation, charcoal particles are also subject to fluvial transport. Charcoal particles can float on the surface of water for a few weeks before they sink down to the sediment layer, and, therefore, it can be transported a long distance via fluvial transport (Scott, 2010). Due to this potential long distance travel, care must be taken when interpreting charcoal particle concentrations from fluvial sites, as is the case with pollen analysis (see Section 4.3.1.1).

4.3.2.2. Methodology

Sub-samples of 0.5 cm^3 were taken from both Mera Tigre sites at a 10 cm resolution (same sub-samples as those taken for pollen analysis: 30 samples for Mera Tigre West and 67 for Mera Tigre East). To each sample, 8-10 ml of 10 % Potassium hydroxide (KOH) was added in order to deflocculate the sediment; sub-samples were left in KOH for 24 hours. Sub-samples were then sieved through 100 µm mesh sieves and washed with deionised water until the run off was clear. Sub-samples were then transferred to a Bogorov counting chamber. All charcoal particles within the sediment were counted using a binocular dissecting microscope (Nikon SMZ745) and a charcoal concentration per cm^3 was calculated. Charcoal particles (Figure 4.3) were identified due to their angular structure, high reflectivity (Clark and Royall, 1995), and their readiness to fragment when pressed.

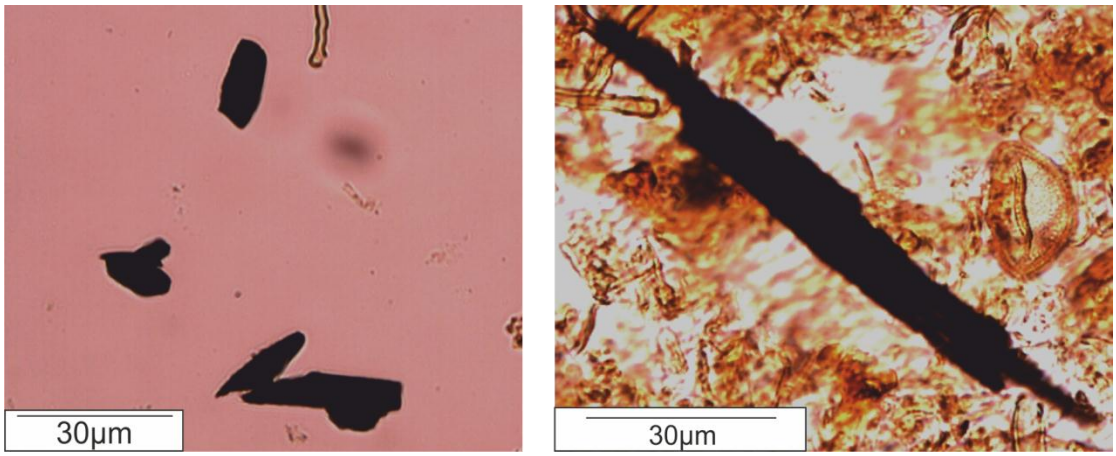

Figure 4.3: Micro charcoal particle examples from Mera Tigre West sediments.

Micro charcoal particles (<100 µm) were also counted in palynological slides under the microscope. Particles were identified in the same way as for the macro charcoal, the particles were just smaller (<100 µm). Micro charcoal particle concentrations were calculated against a known number of *Lycopodium* spores which were added to the pollen sub-samples. By using two separate methods (micro, <100 µm and macro, >100 µm) it means that no particles are missed,

by using a 100 µm sieve it means that no particles are missed between those captured in the pollen slides and the macro charcoal particles found when sieved at 100 µm.

4.3.3. Wood macrofossil thin sections

4.3.3.1. Rationale
The use of wood macrofossils within all palaeoecological studies is expanding, as they can provide an excellent insight into local vegetation (Brea et al., 2015, Cárdenas et al., 2014, Cárdenas et al., 2011, IAWACommittee, 1989, Morales-Molino et al., 2011). By identifying wood macrofossils deposited at the stratigraphic section, they can be used to provide an indicator of more local vegetation, due to their large size meaning it is harder for them to be transported by aeolian and fluvial transport mechanisms, issues which are widespread with pollen analysis. Alongside the fact they are harder to transport, wood macrofossils can be more easily identifiable to species level if preservation is suitable, meaning a greater understanding can be obtained of the ecosystem (Birks and Birks, 1980). As such, when used alongside pollen analysis they provide a reliable proxy.

4.3.3.2. Methodology
A 3 cm^3 sub-sample of wood was taken from each of the fourteen wood macrofossils collected from the two Mera Tigre sites. The sub-samples were then air dried in a sterile environment for approximately two weeks. Sub-samples were then soaked in epoxy resin under vacuum for 10 minutes in order to prevent fragmentation when thin sectioning. The sub-samples were then left to air cure. Once the resin had cured, the sub-samples of wood were then sliced in as many ordinations as possible to try and capture the transverse, radial and tangential planes needed for identification (Figure 4.4). These were then mounted onto individual slides and thinned until they were between 20 and 30 µm thick. The slides were then sealed with cover slips.

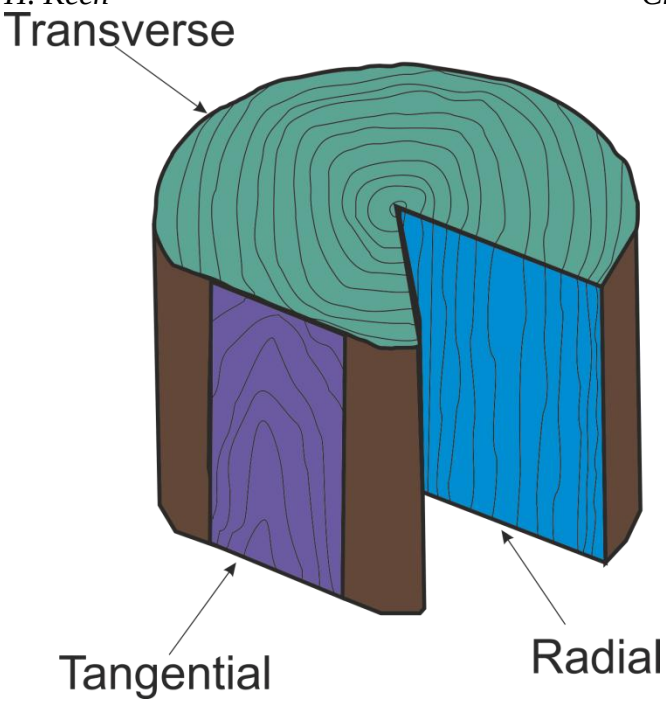

Figure 4.4: Diagrammatic representation of the three planes needed for successful wood macrofossil identification from thin section. It is important to get all three planes as each has its own individual features used for identification. The transverse plane is taken as if you were looking at the end of a log, the tangential is taken perpendicular to the direction of the wood rays and the radial is taken as if the log has been cut in half.

Wood macrofossil identifications were made from microscope slides (Figure 4.5) of thin sections and was based on distinguishing morphometric features, identified from the three planes (transverse, radial and tangential). Features of importance were identified under a Nikon Eclipse 50*i* microscope at x20 magnification and an Olympus BH-2 binocular microscope at x10 magnification. Features were described using the International Association of Wood Anatomists (IAWA) list of microscopic features for hardwood identification (IAWACommittee, 1989) and then keyed into the online database inside wood (IAWA, 2004). To aid identification the reference collection at the Jodrell laboratory in Kew and an Amazon tree identification book were used (Détienne and Jacquet, 1983). Help was also provided by Peter Gasson (Kew Royal Botanic Gardens) and Imogen Poole (Aberdeen/Shell).

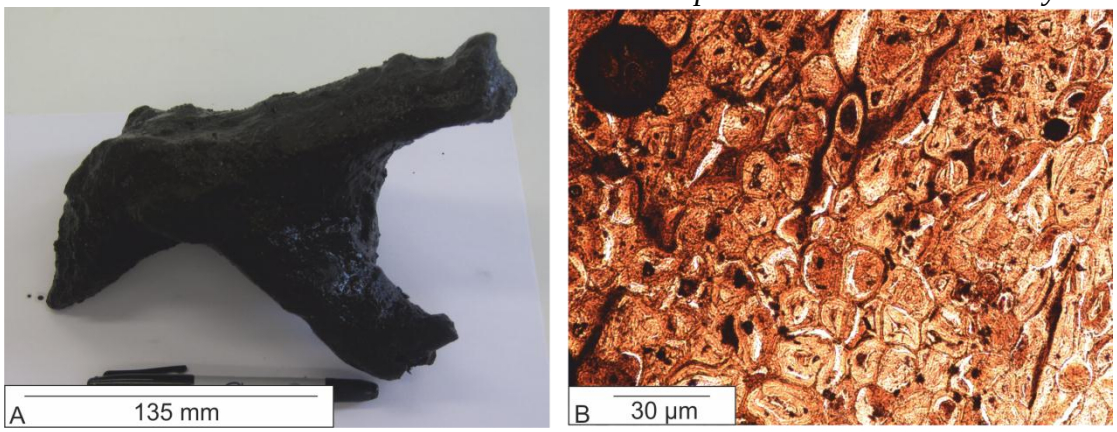

Figure 4.5: A) Wood macrofossil from Mera Tigre West. B) Thin sectioned wood macrofossil from Mera Tigre West. Picture taken at a x20 resolution on a Nikon Eclipse 50*i* microscope.

4.4. Dating techniques

Three dating techniques were applied to different material obtained from the Mera Tigre sediments (wood macrofossils, inorganic and organic sediments) to obtain an independent estimate on the age of deposition. Radiocarbon dating (^{14}C), Argon-Argon ($^{40}Ar/^{39}Ar$) and optically stimulated luminescence dating (OSL) were applied to sediments. Radiocarbon dating and $^{40}Ar/^{39}Ar$ were used for Mera Tigre West whilst radiocarbon, $^{40}Ar/^{39}Ar$ and OSL were applied to Mera Tigre East.

4.4.1. Radiocarbon dating

Radiocarbon dating was carried out at two external laboratories (Lawrence Livermore laboratory for Mera Tigre West, and the Beta Analytic facility for Mera Tigre East). Sample preparation and processing for the Mera Tigre West samples was performed prior to the arrival of H. Keen on the project, as such she did not do this work. Sample preparation and pre-processing was performed by H. Keen for the Mera Tigre East sample.

4.4.1.1. Rationale

Radiocarbon dating is based on the decay of ^{14}C to a stable form of nitrogen (^{14}N) through the release of beta particles (one particle is released for every atom of ^{14}C that decays). ^{14}C is

produced in the upper atmosphere and it reaches the earth by combining with oxygen to produce $^{14}CO_2$ (Walker, 2005). Through this, the ^{14}C makes its way into the global carbon cycle and subsequently into plants and animals. After the plant or animal dies no more ^{14}C can be taken up and from that point ^{14}C decay starts, and by measuring how much the ^{14}C has decayed (half-life 5730 years) the time passed since death can be calculated (Walker, 2005).

Radiocarbon dating was chosen due to its success when applied in other palaeoecology studies (Cole et al., 2015, D'Apolito et al., 2013, Das, 2014, Roucoux et al., 2013, Urrego et al., 2005). It is the radiometric dating technique that is used most often in Late Quaternary palaeoecology studies and it can be used to date sediments back to around 50,000 years ago (Walker, 2005). Wood macrofossils distributed through Mera Tigre West provided suitable material in which to perform radiocarbon dating upon (Galka et al., 2014). Mera Tigre East only had the presence of wood macrofossils in the lower part of the section so pollen residues (bulk samples) were used for the top most part of the section (Berrío et al., 2002).

4.4.1.2. Methodology

Radiocarbon dating for Mera Tigre West was undertaken at Lawrence Livermore laboratory by Dr Tom Guilderson in the Center for Accelerator Mass Spectrometry (CAMS) in 2010. Three wood macrofossils were prepared and analysed followed standard procedure (Taylor, 1997).

Radiocarbon dating for Mera Tigre East was performed on one pollen residue sample from Mera Tigre East. The pollen residue was removed from a $2cm^3$ organic sample following most steps of the protocol for pollen analysis outlined in section 4.3.1.2. and Appendix 1, however, for radiocarbon analysis modifications were made to the process. *Lycopodium* spp. spores were not added to the sample for radiocarbon dating as these would have influenced the age of the sample and no marker grains are required for radiocarbon dating. Acetolysis and the two CH_3COOH (acetic acid) washes were not undertaken on the sample so as not to damage the pollen or

organics needed for the radiocarbon dating. Radiocarbon dating was undertaken at the Beta Analytic facility in Miami, Florida in December 2014. Radiocarbon results for MTE are presented as calibrated ages. These have been calibrated using the programme CALIB to a 2 sigma (95 % confidence) calibration using the Southern hemisphere calibration curve (Reimer et al., 2013). The radiocarbon results for MTE were also calibrated to the Northern hemisphere calibration curve (IntCAL), however, the difference between the two ages produced at a 2sigma calibration was negligible so as the sample sites are in the Southern hemisphere, it was decided to use the Southern hemisphere curve for calibration (Reimer et al., 2013).

4.4.2. $^{40}Ar/^{39}Ar$ dating

4.4.2.1. Rationale

$^{40}Ar/^{39}Ar$ dating was selected as a technique to provide an age for the Mera Tigre sediments in an effort to constrain the deposits beyond the limits of radiocarbon dating and following the successful application to the similar deposits at Erazo nearby (Cárdenas et al., 2014, Cárdenas et al., 2011).

$^{40}Ar/^{39}Ar$ is applicable to inorganic sediments of volcanic origin because ^{40}Ar is trapped in minerals once rocks have cooled and are no longer in a molten state (molten during volcanic processes). Once cooled, the argon can no longer leave the mineral lattice, meaning that these inorganic rocks are perfect for radiometric dating of this argon (Walker, 2005). $^{40}Ar/^{39}Ar$ is based on the decay of the radioactive parent ^{40}K to the stable ^{40}Ar (half-life $1.2x10^{9}$). The ^{40}Ar content is measured directly from the sample using a mass spectrometer; however, the ^{40}K content is measured indirectly through the use of known proportions between potassium and argon isotopes. To do this, ^{39}K within the samples is transformed to ^{39}Ar by fast neutron bombardment during irradiation in a nuclear reactor. As the ^{39}Ar content is proportional to the content of ^{39}K and the ^{39}K ratio is proportional to the ^{40}K ratio [$^{39}K/^{40}K$ ratio is assumed stable at

0.0001167 (Steiger and Jäger, 1977)] the $^{40}Ar/^{40}K$ ratio can be inferred, and it can be used to calculate the age of the sediments (Walker, 2005).

The widespread inorganic layers present throughout both of the Mera Tigre sections meant that $^{40}Ar/^{39}Ar$ dating was suitable, dependent on the presence of suitable minerals (potassium rich feldspars and biotite) within the inorganic layers.

Due to the young (<1 million years due to presence of the pollen grain *Alnus* spp.; Hooghiemstra, 1984) estimated age of the Mera Tigre sediments, a large amount of mineral grains were required for $^{40}Ar/^{39}Ar$ analysis (0.2-0.25 g), because of the low amount of ^{39}K present in the sediments (sample >1 million years). As such a large amount of inorganic sediment (~0.5-1kg) was required from the field site to ensure an appropriate amount of mineral grains could be picked from the sample ensuring a large enough amount of ^{39}K will be present.

4.4.2.2. Methodology

One hundred grams of sediment was extracted from each inorganic layer, and this sub-sample was then air dried. Once dried, sub-samples were crushed using a pestle and mortar. The crushed sub-samples were then sieved in three size fractions between 0 and 250 μm (0-125 μm, 125-250 μm and 250 μm). The 250 μm and the 125-250 μm fractions were retained for picking of individual mineral grains. All inorganic layer sub-samples were picked for potassium rich feldspar or biotite minerals. Once 0.25 g of either feldspar and/or biotite had been picked the mineral grains were then washed in acetone and distilled water. They were then packed in foil and sent for irradiation at the McMaster medium flux nuclear fission reactor in Canada for a one hour irradiation. Irradiation transforms ^{39}K into ^{39}Ar meaning the decay ratio can be measured. Once transported back to The Open University, samples were then analysed using the Map 215-50 noble gas spectrometer with a SPI 25W Infra-Red fibre laser. Peaks of ^{35}Ar, ^{36}Ar, ^{37}Ar, ^{38}Ar, ^{39}Ar, ^{40}Ar and ^{41}Ar were analysed. Standards of known age were processed through the entire

process, meaning corrections could be made based on whether or not the age of the standard deviated from its known age. Ages were generated using the programme ArMaDiLo v 1.0.1. A full analytical procedure is included in Appendix 1.

4.4.3. Optically stimulated luminescence

Optically stimulated luminescence (OSL) dating was undertaken at the University of Leicester by Dr Andrew Carr. The entire process was performed by Dr Carr due to the time requirements to learn the process and carry out both the preparation procedure and the analysis being beyond the time limits for this PhD research.

4.4.3.1. Rationale

OSL dating is based on materials containing naturally occurring radioactive isotopes (uranium, thorium and potassium). It is a dating technique that can be used to measure the burial age of sediments (the last exposure to light). The process relies upon minerals being subject to low radiation (from the sun) causing the ionisation of atoms in the minerals, leading to electrons being freed. These electrons become trapped in the crystal lattice of a host mineral once buried (e.g. feldspar or quartz) and when a beam of light is focused on these crystal lattices, the luminescence signal or amount of electrons released provides the time since burial (or the last time the mineral was exposed to light; Walker, 2005). OSL dating was selected as a potential dating technique in case radiocarbon dating and $^{40}Ar/^{39}Ar$ were unsuccessful. Unlike radiocarbon dating but similar to $^{40}Ar/^{39}Ar$, this technique can be applied to sediments older than 50,000 years old.

4.4.3.2. Methodology

All sample preparation took place under red light conditions so that any light does not reset the burial signal that is being measured. Samples were treated with Hydrochloric acid and Hydrogen peroxide to remove carbonates and organic matter, samples were then wet sieved (two size fractions 90-180 µm and 180-250 µm). Quartz crystals were isolated by density separation

(quartz found between 2.58 and 2.70 g cm^{-3}). The 180-250 μm fraction was chosen for quartz and this was etched in Hydrofluoric acid for 1 hour and then washed in Hydrochloric acid to remove residue fluorides. Small aliquots of quartz (approximately 2 mm diameter area at the centre of a 9 mm disk) were then measured on a Risø TL – DA 20TL/OSL reader. Estimates of acquired dose were made using the single aliquot regeneration (SAR) protocol (Murray and Wintle, 2000). Alongside the acquired dose rate, the environmental dose rate (or annual dose rate) was also calculated (Walker, 2005). The environmental dose rate includes factors determining the radiation dose per unit of time for the mineral of interest since burial, it includes factors such as water content, latitude and longitude, altitude and uranium, thorium and potassium content of the samples (Walker, 2005). To calculate the uranium, thorium and potassium content of the samples for the environmental dose rate, Inductively Coupled Mass Spectrometry (ICP-MS) was used; this process is described in Section 4.4.3.3. A methodological process has been included in Appendix 1.

4.4.3.3. Inductively Coupled Mass Spectrometry

The ICP-MS process was performed at the Open University by Dr Samantha Hammond. The samples were crushed by H. Keen, and due to only two samples being processed, H. Keen only observed the ICP-MS process, this meant that the samples were processed in a time efficient manner and H. Keen learnt the process at the same time.

In order to calculate the uranium, thorium and potassium values for the environmental dose rate, ICP-MS was used. Following standard protocol (Bailey et al., 2003) 20 g of dry sediment was powdered using a tema ball mill and then 0.1 g of this was sampled for digestion. Before the process began, Teflon® beakers were thoroughly cleaned following a five stage process of deionised water and acid washes (see Appendix 1). Following the full cleaning procedure for Teflon® beakers, the processing of samples for ICP-MS could take place. The sample processing involved the dissolution of samples in Nitric acid, Hydrofluoric acid, Hydrochloric acid and

deionised water. A full methodology for this is outlined in Appendix 1. Following the sample pre-processing the sample could then be measured on an Agilent 7500a ICP-MS fitted with a standard quartz spray chamber and a Babington nebuliser. To check prevision and accuracy of data collection, five standard samples (BIR-1, W2, DNC-1, BHVO-2 and AGV-1) were run before the Mera Tigre East samples, allowing errors for each of the two samples to be calculated.

4.5. Summary

In this chapter the field and eight laboratory methodologies (LOI, XRF, pollen and NPP analysis, charcoal analysis, wood macrofossil analysis, radiocarbon dating, $^{40}Ar/^{39}Ar$ dating and OSL) used to provide information on past environmental change were justified and described. Only seven of these methodologies were applied in the thesis, due to issues with the sample preservation preventing identification, wood macrofossil analysis was not applied in this thesis. Photographs of wood macrofossil thin sections were included in Appendix C. The next chapter, Chapter 5, will cover a technique used to create a statistically reliable count size for each individual pollen sample; this was briefly introduced in Section 4.3.1.3.

References

BAILEY, R. M., STOKES, S. & BRAY, H. 2003. Inductively- Coupled Plasma Mass Spectrometry (ICP - MS) for dose rate determination: some guidelines for sample preparation and analysis. Ancient TL, 21, 11 - 15.

BERRÍO, J. C., HOOGHIEMSTRA, H., MARCHANT, R. & RANGEL, O. 2002. Late-glacial and Holocene history of the dry forest area in the south Colombian Cauca Valley. Journal of Quaternary Science, 17, 667-682.

BIRKS, H., H. & BIRKS, H. J. B. 2006. Multi-proxy studies in palaeolimnology. Vegetation History and Archaeobotany, 15, 235 - 251.

BIRKS, H. J. B. & BIRKS, H., H. 1980. Quaternary Palaeoecology, New Jersey, The Blackburn Press.

BREA, M., ARTABE, A. E., FRANZESE, J. R., ZUCOL, A. F., SPALLETTI, L. A., MOREL, E. M., VEIGA, G. D. & GANUZA, D. G. 2015. Reconstruction of a fossil forest reveals details of the palaeoecology, palaeoenvironments and climatic conditions in the late Oligocene of South America. Palaeogeography, Palaeoclimatology, Palaeoecology, 418, 19-42.

BRUNSCHÖN, C., HABERZETTL, T. & BEHLING, H. 2010. High-resolution studies on vegetation succession, hydrological variations, anthropogenic impact and genesis of a subrecent lake in southern Ecuador. Vegetation History and Archaeobotany, 19, 191 - 206.

BUSH, M. B. & WENG, C. 2007. Introducing a new (freeware) tool for palynology. Journal of Biogeography, 34, 377-380.

CÁRDENAS, M. L., GOSLING, W. D., PENNINGTON, R. T., POOLE, I., SHERLOCK, S. C. & MOTHES, P. 2014. Forests of the tropical eastern Andean flank during the middle Pleistocene. Palaeogeography, Palaeoclimatology, Palaeoecology, 393, 76 - 89.

CÁRDENAS, M. L., GOSLING, W. D., SHERLOCK, S. C., POOLE, I., PENNINGTON, R. T. & MOTHES, P. 2011. The Response of Vegetation on the Andean Flank in Western Amazonia to Pleistocene Climate Change. Science, 331, 1055-1058.

CLARK, J. S. & ROYALL, P. D. 1995. Particle-Size evidence for source areas of charcoal accumulation in Late Holocene sediments of Eastern North American Lakes. Quaternary Research, 43, 80 - 89.

COLE, L. E. S., BHAGWAT, S. A. & WILLIS, K. J. 2015. Long-term disturbance dynamics and resilience of tropical peat swamp forests. Journal of Ecology, 103, 16-30.

COLINVAUX, P. A., DE OLIVEIRA, P. E. & PATIÑO, J. E. M. 1999. Amazon pollen manual and atlas, Amsterdam, Harwood Academic Publishers.

D'APOLITO, C., ABSY, M. L. & LATRUBESSE, E. M. 2013. The Hill of Six Lakes revisited: new data and re-evaluation of a key Pleistocene Amazon site. Quaternary Science Reviews, 76, 140-155.

DAS, S. 2014. Palaeo-palynology of late Quaternary peat deposit from Lower Bengal Basin, India: A palaeoecological approach. Quaternary International, 325, 197 - 204.

DEAN, W. E. 1974. Determination of carbonate and organic matter in calcaerous sediments and sedimentary rocks by loss on ignition: comparison with other methods. Journal of Sedimentary Research (SEPM), 44, 242 - 248.

DÉTIENNE, P. & JACQUET, P. 1983. Atlas d'identification des bois de l'Amazonie et des régions voisines., Centre technique forestier tropical, Nogent - sur - Marne.

GALKA, M., TOBOLSKI, K. & BUBAK, I. 2014. Late Glacial and Early Holocene lake level fluctuations in NE Poland tracked by macro-fossil, pollen and diatom records. Quaternary International.

HEIRI, O., LOTTER, A. & LEMCKE, G. 2001. Loss on ignition as a method for estimating organic and carbonate content in sediments: reproducibility and comparability of results. Journal of Paleolimnology, 25, 101-110.

HIGUERA, P. E., PETERS, M. E., BRUBAKER, L. B. & GAVIN, D. G. 2007. Understanding the origin and analysis of sediment-charcoal records with a simulation model. Quaternary Science Reviews, 26, 1790 - 1809.

HOOGHIEMSTRA, H. 1984. Vegetational and climatic history of the high plain of Bogotá, Colombia: a continuous record of the last 3.5 million years. . Dissertationes Botanicae, 79, 1 - 138.

IAWA. 2004. InsideWood [Online]. Available: http://insidewood.lib.ncsu.edu/search [Accessed 10/6/2014.

IAWACOMMITTEE 1989. IAWA list of microscopic features for hardwood identification. IAWA Bulletin, 10, 219 - 332.

KAWASE, M. & TAKAHASHI, M. 1995. Chemical composition of Sporopollenin in Magnolia Grandiflora (Magnoliaceae) and Hibiscus Syriacus (Malvaceae). Grana, 34, 242-245.

KEEN, H. F., GOSLING, W. D., HANKE, F., MILLER, C. S., MONTOYA, E., VALENCIA, B. G. & WILLIAMS, J. J. 2014. A statistical sub-sampling tool for extracting vegetation community and diversity information from pollen assemblage data. Palaeogeography, Palaeoclimatology, Palaeoecology, 408, 48 - 59.

LIU, K.-B. & COLINVAUX, P. A. 1985. Forest changes in the Amazon Basin during the last glacial maximum. Nature, 318, 556 - 557.

MAHER, L. J. 1972. Nomograms for computing 0.95 confidence limits of pollen data. Review of Palaeobotany and Palynology, 13, 85-93.

MOORE, P. D., WEBB, J. A. & COLLINSON, M. E. 1991. Pollen analysis, Oxford, Blackwell Scientific.

MORALES-MOLINO, C., POSTIGO-MIJARRA, J. M., GARCÍA-ANTÓN, M. & ZAZO, C. 2011. Vegetation and environmental conditions in the Doñana Natural Park coastal area (SW Iberia) at the beginning of the last glacial cycle. Quaternary Research, 75, 205-212.

MURRAY, A. S. & WINTLE, A. G. 2000. Luminescence dating of quartz using an improved single-aliquot regenerative-dose protocol. Radiation Measurements, 32, 57 - 73.

NIEMANN, H. & BEHLING, H. 2008. Late Quaternary vegetation, climate and fire dynamics inferred from the El Tiro record in the southeastern Ecuadorian Andes. Journal of Quaternary Science, 23, 203-212.

NIEMANN, H., MATTHIAS, I., MICHALZIK, B. & BEHLING, H. 2013. Late Holocene human impact and environmental change inferred from a multi-proxy lake sediment record in the Loja region, southeastern Ecuador. Quaternary International, 308 - 309, 253 - 264.

REIMER, P. J., BARD, E., BAYLISS, A., BECK, J. W., BLACKWELL, P. G., RAMSEY, C. B., BUCK, C. E., CHENG, H., EDWARDS, R. L., FRIEDRICH, M., GROTTES, P. M., GUILDERSON, T. P., HAFLIDASON, H., HAJDAS, I., HATTÉ, C., HEATON, T. J., HOFFMANN, D. L., HOGG, A. G., HUGHEN, K. A., KAISER, K. F., KROMER, B., MANNING, S. W., NIU, M., REIMER, R. W., RICHARDS, D. A., SCOTT, E. M., SOUTHON, J. R., STAFF, R. A., TURNEY, C. S. M. & VAN DER PLICHT, J. 2013. IntCal13 and Marine13 Radiocarbon Age Calibration Curves 0-50,000 Years cal BP. *Radiocarbon,* 55.

ROUBIK, D. W. & MORENO, J. E. P. 1991. Pollen and spores of Barro Colorado Island, United States, Missouri Botanical Garden.

ROUCOUX, K. H., LAWSON, I. T., JONES, T. D., BAKER, T. R., CORONADO, E. N., GOSLING, W. D. & LÄHTEENOJA, O. 2013. Vegetation development in an Amazonian peatland. Palaeogeography, Palaeoclimatology, Palaeoecology, 374, 242 - 255.

SCOTT, A. C. 2010. Charcoal recognition, taphonomy and uses in palaeoenvironmental analysis. Palaeogeography, Palaeoclimatology, Palaeoecology, 291, 11 - 39.

SEPPÄ, H. & BENNETT, K. D. 2003. Quaternary pollen analysis: recent progress in palaeoecology and palaeoclimatology. Progress in Physical Geography, 27, 548 - 579.

STEIGER, R. H. & JÄGER, E. 1977. Subcomission on geochronology: convention on the use of decay constants in geo- and cosmochronology. Earth and Planetary Science Letters, 36, 359 - 362.

STOCKMARR, J. 1971. Tablets with spores used in absolute pollen analysis. Pollen et spores, 13, 615 - 621.

TAYLOR, R. E. 1997. Chapter 3: Radiocarbon Dating. In: TAYLOR, R. E. & AITKEN, M. J. (eds.) Chronometric dating in archaeology. Advances in archaeological and museum science, volume 2. New York: Plenum Press.

TAYLOR, Z. P., HORN, S. P., MORA, C. I., ORVIS, K. H. & COOPER, L. W. 2010. A multi-proxy palaeoecological record of late-Holocene forest expansion in lowland Bolivia. Palaeogeography, Palaeoclimatology, Palaeoecology, 293, 98 - 107.

THOMAS, I. L. & HAUKKA, M. T. 1978. XRF determination of trace and major elements using a single - fused disc. Chemical Geology, 1978, 39 - 50.

THONICKE, K., VENEVSKY, S., SITCH, S. & CRAMER, W. 2001. The role of fire disturbance for gloval vegetation dynamics: coupling fire into a Dynamic Global Vegetation Model. Global Ecology and Biogeography, 10, 661 - 677.

URREGO, D. H., SILMAN, M. R. & BUSH, M. B. 2005. The Last Glacial Maximum: stability and change in a western Amazonian cloud forest. Journal of Quaternary Science, 20, 693-701.

VAN GEEL, B. 2001. Non-Pollen Palynomorphs. In: SMOL, J., BIRKS, H. J., LAST, W., BRADLEY, R. & ALVERSON, K. (eds.) Tracking Environmental Change Using Lake Sediments. Springer Netherlands.

VON POST, L. 1929. Die Zeichenschrift der Pollenstatistik. Geologiska Föreningens i Stockholm Förhandlinger, 4, 543 - 565.

VON POST, L. 1946. The prospect of pollen analysis in the study of the earth's climatic history. New Phytologist, 45, 193 - 217.

WALKER, M. J. C. 2005. Quaternary Dating Methods, Chichester, West Sussex, John Wiley & Sons.

WHITLOCK, C. & LARSEN, C. 2001. Charcoal as a fire proxy. In: SMOL, J. P., BIRKS, H. J. B. & LAST, W. M. (eds.) Tracking environmental change using lake sediments: Volume 3: terrestrial, algal, and siliceous indicators. Dordrecht: Kluwer academic publishers.

Chapter 5: A statistical sub-sampling tool for extracting vegetation community and diversity information from pollen assemblage data.

In this chapter a new statistical sub-sampling tool developed to create a statistically reliable count size for each individual pollen sample will be introduced. This chapter has been published separately in an international journal. This chapter was the work of all of the co-authors listed in the reference below. The contribution of H. Keen was the collation of all of the data, counting the pollen for the six Mera Tigre samples and writing the manuscript. F. Hanke created the statistical model used and published in this chapter, H. Keen applied the model to the pollen data from all named sites. Data from other sites to test the model was provided by co-authors: Miller (Bosumtwi), Valencia (Pacucha) and Williams (Khomer Kotcha Upper and Vacas). Co-authors also contributed to editing the manuscript.

Keen, H.F., Gosling, W.D., Hanke, F., Miller, C.S., Montoya, E., Valencia, B.G. and Williams, J.J. (2014) A statistical sub-sampling tool for extracting vegetation community and diversity information from pollen assemblage data. *Palaeogeography, Palaeoclimatology, Palaeoecology*. 408, 48 – 59. DOI:10.1016/j.palaeo.2014.05.001.

Highlights

- A statistically based model is proposed for calculation of pollen count sizes.
- Count sizes are predicted based on samples richness and evenness values.
- A preliminary input of 100 pollen grains is required to calculate count sizes.
- Counts required to detect major vegetation components and rare taxa can be easily obtained.
- The statistical sub-sampling tool is downloadable via supplementary material.

Abstract

Pollen assemblages are used extensively across the globe, providing information on various characteristics of the vegetation communities that originally produced them, and how these vary temporally and spatially. However, anticipating a statistically based robust pollen count size, sufficient to characterise a pollen assemblage is difficult; particularly with regard to highly diverse pollen assemblages. To facilitate extraction of ecologically meaningful information from pollen assemblage data, a two part statistical sub-sampling tool has been developed (Models 1 and 2), which determines the pollen count size required to capture major vegetation communities of varying palynological richness and evenness, and the count size required to find the next not yet seen (rare) pollen taxa. The sub-sampling tool presented here facilitates the rapid assessment of individual pollen samples (initial information input of 100 pollen grains) and can, therefore, on a sample by sample basis achieve maximum effectiveness and efficiency. The sub-sampling tool is tested on fossil pollen data from five tropical sites.

Results demonstrate that Model 1 predicts count sizes relating to palynological richness and evenness consistently. To characterise major vegetation community components model 1 indicates that, for samples with a lower richness and higher evenness lower count sizes than are considered standard can be used (< 300, e.g. 122); however, for samples of high richness and low evenness, higher count sizes are required (> 300, e.g. 870). Model 2 calculates the additional number of pollen grains needed to be counted to detect the next not yet seen pollen taxa, outputs were strongly related to input data count size as well as richness and evenness characteristics. We conclude that, given the temporal and spatial variations in vegetation communities and also pollen assemblages, pollen count sizes should be determined for each individual sample to ensure that effective and efficient data are generated and that detection of rare taxa is checked iteratively throughout the counting process.

Keywords

Palynology; Count size; Evenness; Richness; Sub-sampling; Tropical

5.1. Introduction

Fossil pollen contained within natural sedimentary records can be used to reconstruct past vegetation communities and assess how they have changed through time. The type of ecological information extracted from fossil pollen records includes: i) identifying large-scale shifts between biomes (defined here as a large array of flora and fauna within one major habitat), e.g. shifts between woodland and grassland (Rull et al., 2005), or shifts between deciduous forest and boreal forest (Fréchette and de Vernal, 2013), ii) determining first arrival or introduction of species (Hooghiemstra and Cleef, 1995, Van der Knaap et al., 2012), and iii) characterising shifts in criteria important for conservation, e.g. assemblage richness or the discovery of rare taxa (Bush and Colinvaux, 1988). Furthermore, examination of modern pollen-vegetation relationships can be used to address biogeographic and ecological questions (Jantz et al., 2014). Understanding the nature and dynamics of vegetation communities through time and space is essential in order to anticipate the likely response of modern vegetation to human activity, and on-going/projected climate changes (Jackson, 2012).

To be confident that the inferences being drawn about vegetation communities from the pollen assemblage data are valid, it is necessary to consider several key factors including: i) pollen production (Bush, 1995, Gosling et al., 2005), ii) pollen transport (Gosling et al., 2009, van der Knaap, 2009), iii) pollen preservation (Havinga, 1964, Havinga, 1984), iv) distribution of pollen grains on the slide (Brooks and Thomas, 1967, Holt et al., 2011), v) taxonomic classification of pollen types and the relationship with the taxonomic classification of the parent vegetation (Odgaard, 1999), and vi) efficiency of sampling (Moore et al., 1991, Rull, 1987). Furthermore,

consideration of other proxies (e.g. macrofossils) is also important, as these can provide further insight into the vegetation communities (Birks and Birks, 2006). In this paper we focus on sampling efficiency only and present a new methodology for sub-sampling (by means of pollen counting) pollen assemblages. The method presented allows the researcher to: i) tailor their sampling strategy to the scientific question being asked, and ii) account for variation in the pollen assemblages throughout time and space. This method ensures that if a vegetation change occurs, a statistically robust count size appropriate for its detection will be achieved.

5.2. Considerations for pollen counting

To establish a robust link between fossil pollen data and past vegetation communities, it is necessary for the researcher to consider the question(s) posed and balance the investigator effort required (time consumed), against time available. Next we consider two key factors related to effective and efficient pollen counting: i) determining an appropriate pollen count size, and ii) the application of the determined pollen count size to a study site.

5.2.1. Determining pollen count size

Research based on percentage rarefaction curves of pollen assemblages from temperate regions indicates that pollen count sizes (target amount of pollen grains to count within a single sample) of between 300 and 500 grains (excluding aquatic taxa) are often enough, dependent on the question being investigated (Birks and Birks, 1980). However, larger count sizes (>500 grains) have also been recommended as a more suitable count size to characterise past vegetation composition (Bennett and Willis, 2001, Moore et al., 1991). Within more floristically diverse tropical regions, studies establishing an effective pollen count size are scarce (Rull, 1987); although pollen counts of >500 grains were found to be sufficient to characterise the major components of pollen assemblages in a study of modern pollen-vegetation relationships in Neotropical forests and savannahs (Gosling, 2004, Gosling et al., 2005).

Most investigations into past vegetation change are concerned with large scale characterisation of the vegetation and, therefore, pollen sums of >300 grains are widely used (following Birks & Birks, 1980); i.e. 74% percent of the top 50 most cited papers returned within Scopus (http://www.scopus.com) for the search term 'Quaternary fossil pollen' indicated that count sizes of at least 300 were targeted (25th October 2013). However, variance in either the richness (amount of taxa within an ecosystem), or evenness (representation of taxa within an ecosystem) of how the parent vegetation is expressed in the pollen assemblage could result in pollen sums of >300 being insufficient or in excess. The potential for variance in richness and evenness to hinder pollen counting accuracy is of particular concern when trying to reconstruct past vegetation from the tropics, mainly due to the high floristic diversity within these ecosystems. Consequently, tropical vegetation is more difficult to reconstruct (Odgaard, 2001). For example, in a fossil pollen assemblage sub–sample from the tropical eastern Andean flank, diversity characteristics (Figure 5.1A) and relative taxon abundances (Figure 5.1B) are shown to vary markedly dependent on count size.

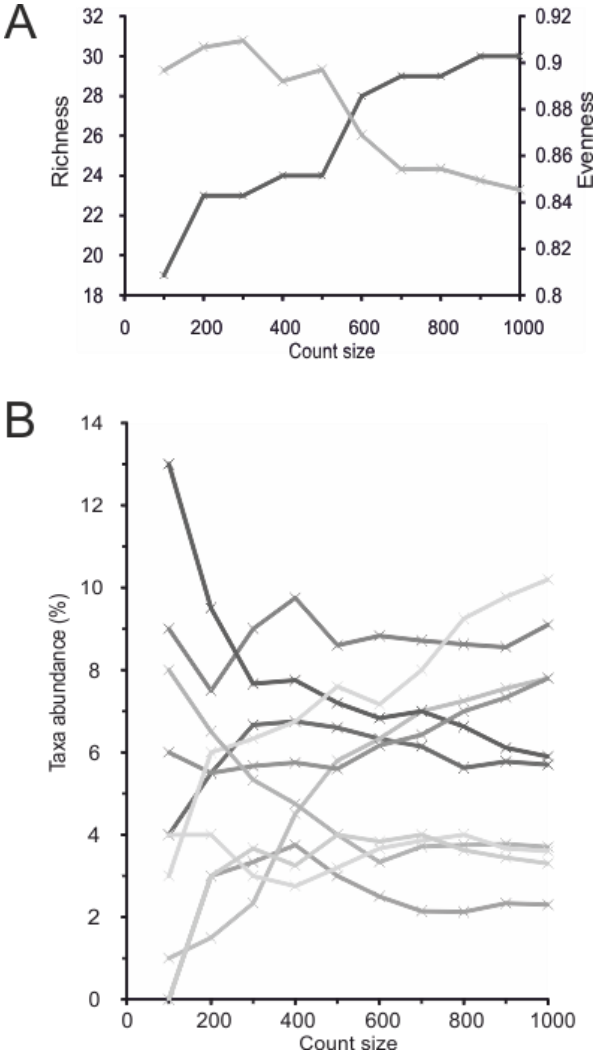

Figure 5.1: Ecological descriptors of a fossil pollen assemblage from the tropical eastern Andean flank (Mera Tigre East) as a function of increasing sample size (increments of 100 grains). A) Diversity: total sub-sample richness (black line) and evenness (grey line). B) Assemblage composition: percentage cumulative taxa abundance for ten selected taxa.

5.2.2. Applying pollen count sizes to a study site

Currently, standard research practice is to apply an identical count size target for an entire study i.e. throughout a sedimentary sequence for fossil pollen, or across a series of vegetation plots for modern pollen studies. In a setting where the richness and/or evenness characteristics of the various vegetation communities being examined are roughly similar, the application of a uniform count size is more applicable, e.g. comparison of two types of temperate forest. However, if the time period, or area, being studied covers a shift in richness or evenness characteristics of the

parent vegetation community, the use of a single count size could result in false inferences due to under or over sub-sampling (hereafter interchangeable sample/ sub- sampling), and although over sampling is not a statistical issue, it does mean wasted investigator effort. For example, to characterise the major components of a savannah with low palynological richness, a lower pollen count size would be required in comparison to a palynologically diverse tropical forest (high richness). Richness changes could occur within an individual sedimentary sequence or study region, making it important to identify a count size appropriate for each sample. Consequently, a methodology is required to determine appropriate pollen count sizes on a sample-by-sample basis.

5.2.3. Improving statistical sub-sampling of pollen assemblages

In this paper we present a statistical methodology (sub-sampling tool), which allows preliminary pollen count data to be used to assess the ideal pollen count required to address three ecological questions: i) what are the major components of the parent vegetation community (biome), ii) what is the richness of the sample (including rare taxa), and iii) when is it probable that the next not yet seen pollen grain has been sampled? The statistical model presented takes into account the richness and evenness of a sample through the input of an initial pollen count of 100 pollen grains (see Section 5.1). To test the robustness of the model, extended fossil pollen count data from three tropical regions are compared against the model output: i) the high elevation central Andes (Bolivia and Peru), ii) mid-elevation eastern Andean flank (Ecuador), and iii) lowland West Africa (Ghana).

5.3. Ecological parameters

5.3.1. Richness

For the purpose of this paper, richness (R) is defined as the amount of taxa within an ecosystem and it is calculated as the total number of palynological taxa within a sample. R can only be used

as a measure of palynological richness if the pollen count numbers are standardised, as such a fixed amount of grains (100 grains – see section 5.1) is used to enter data into the statistical model so that R can be calculated. Rarefaction analysis can be used for standardisation purposes if the count sizes are different (Birks and Line, 1992).

In general for any given pollen assemblage a parent vegetation community with a high richness will have a greater number of different pollen taxa than a vegetation community with a low richness. However, due to the variances in pollen production for each taxon, the pollen assemblage does not always directly reflect the richness of the parent vegetation (Bush, 1995, Odgaard, 2001). Some taxa present in the vegetation can be under represented in the pollen assemblage, or even be absent (e.g. Orchidaceae), and consequently, the vegetation community richness may not be fully represented by pollen richness (Goring et al., 2013, Odgaard, 1999). Conversely long-distance transport of pollen grains into the study site from extra-regional vegetation communities could result in an artificially elevated palynological richness in comparison to the local parent vegetation community (Gosling et al., 2009).

5.3.2. Evenness

For the purpose of this paper, evenness (E) describes the distribution of pollen taxa within the pollen assemblage. In this sense, a sample with a dominant taxon (high number of pollen grains of the same type) would be considered low evenness, whereas a sample without dominant taxa (pollen grains similarly/ equally distributed amongst all taxa) would represent high evenness (Smith and Wilson, 1996). In a pollen assemblage, understanding evenness is not always straightforward as different taxa produce varying amounts of grains and distribute pollen grains differently, e.g. anemophilous vs. entomophilous taxa (Bush, 1995, Gosling et al., 2009, Sugita, 1994). The variance in production and distribution can occasionally lead to difficulties in linking evenness within a pollen assemblage, to that of the parent vegetation. Nevertheless, the sub-sampling tool uses evenness in the pollen assemblage, so this does not affect model performance,

i.e. the relationship between palynological evenness and the parent vegetation evenness still needs to be considered as usual when interpreting the pollen and vegetation relationship.

Evenness (E) is calculated using the following formulae (Equations 5.1-3), where two variables are required: i) richness (R) (defined in Section 5.3.1) which is not heavily dependent on evenness, and ii) the Shannon–Wiener index (H), which is an index used to measure biodiversity, and is strongly influenced by evenness within the pollen assemblage.

$$P_i = \frac{number\ of\ grains\ for\ an\ individual\ taxa}{total\ number\ of\ grains\ for\ all\ taxa} \quad \text{(Equation 5.1)}$$

P_i is the proportion of a total sample belonging to the i^{th} taxa. (Krebs, 2014), and it is a variable used within the calculation of H.

$$H = -\sum_{i=1}^{S}(P_i * \ln[P_i]) \quad \text{(Equation 5.2)}$$

Where Σ represents the sum, *S* is the number of taxa within the sample, $_i$ is a single taxa within the sample, ln represents the natural logarithm, and P_i is as defined above (Equation 5.1). Equation 5.2 must be applied to all taxa individually and the summation of these calculations used for the calculation of H for the entire pollen assemblage.

Once R (richness) and H (Shannon – Wiener index) have been calculated the following formula can be applied to produce an E (evenness) value.

$$E = \frac{H}{\ln(R)} \quad \text{(Equation 5.3)}$$

The value of E can vary between 0 (low evenness) and 1 (high evenness).

5.4. Methodology

In order to develop and verify a robust methodology for determining appropriate count sizes for pollen assemblages of varying richness and evenness, the following steps were applied: i) selection of study sites with vegetation of varying richness and evenness, ii) generation of empirical data (pollen preparation, identification and counting), iii) generation of statistically

modelled pollen counts (sub-sampling tool), and iv) consideration of how to apply count size estimations to address particular ecological questions.

5.4.1. Study sites

To capture a wide range of evenness and richness values within pollen assemblage data, ten samples were analysed from three different tropical regions: i) high central Andes, ii) eastern Andean flank, and iii) lowland West Africa. Sites from high (three sites), mid (one site) and low (one site) elevations were selected for study to provide insight into a range of tropical vegetation communities. One sample was analysed for each site, except for the mid elevation site where six samples were analysed to investigate variance within one region through time. All samples were obtained from sedimentary sequences (fossil pollen records).

5.4.1.1. High elevation, central Andes, Bolivia and Peru, South America

Three high elevation study sites (Lakes Khomer Kotcha Upper, Challacaba and Pacucha) were used in this study and provide an opportunity to test the model output against a range of different richness and evenness values. The sediment cores from all three high elevation sites were collected using a Colinvaux modified Livingstone corer (Valencia et al., 2010, Williams et al., 2011a, Williams et al., 2011b).

Khomer Kotcha Upper is a glacier formed lake situated in Bolivia (17°16.514'S, 65°43.945'W, 4153 m asl [above sea level]). Today the site has a mean annual temperature (MAT) of 4.5°C to 7.6°C and mean annual precipitation (MAP) of 772 mm. Modern vegetation present at the region transitions between puna grassland and punean woodland (Williams et al., 2011a). The sample chosen for this study from Khomer Kotcha Upper is from the Early Holocene (c. 9360 cal yr BP [calibrated years before present]).

Challacaba is a freshwater lake located in the Andes of Bolivia (17°33.257'S, 65°34.024'W, 3400 m asl). The MAT of the site varies from 7.2°C to 11.3°C annually and the precipitation varies seasonally between 2.6 mm and 114 mm per month. Current vegetation at the site is a patchwork of grassland, shrub and *Polylepis* spp. dominated woodland (Williams et al., 2011b). The sample chosen for this study from Challacaba is from the Late Holocene (c. 3270 cal yr BP).

Lake Pacucha is located in the Peruvian high Andes (13°36.384'S, 73°19.690'W, 3095 m asl). MAT is 13ºC and MAP is <700 mm (Valencia et al., 2010). Human activity around the lake has resulted in a shift from native *Polylepis* spp. woodland to *Eucalyptus* spp. plantations and crops (mainly potatoes and barley). The sample chosen for this study from Pacucha is from the last glacial maximum (c. 22,400 cal yr BP).

5.4.1.2. Mid elevation, eastern Andean flank, Ecuador, South America

Mera Tigre East is located on the eastern Andean flank in the Pastaza province of Ecuador (01º 27.546'S, 78º 06.199'W, 1117 m asl). Today, the Mera region has a MAT of 20.8ºC and MAP of >4800 mm (Ferdon, 1950, Liu and Colinvaux, 1985), and diverse vegetation including different degrees of disturbed rainforests. Sediments were recovered from an 8.49 m vertical section exposed by the down cutting of the Rio Tigre. The six samples selected for this study are all of Pleistocene age (younger than 1 Ma due to the presence of *Alnus* in the pollen assemblage (Hooghiemstra, 1984), but beyond the limit of radiocarbon dating, i.e. >50,000 years old). The six samples from Mera Tigre East were selected for analysis because they presented an opportunity to test the model against multiple samples with high palynological diversity (richness).

5.4.1.3. Low elevation, central Ghana, West Africa

Lake Bosumtwi is located in the lowlands of Ghana, Africa (6° 30.000' N, 1°25.000'W, 97 m asl). The MAT is 26°C and the MAP is 1260 mm (Shanahan et al., 2008). Prior to the

degradation of the natural vegetation by human settlement and cultivation, the lake was surrounded by moist semi–deciduous forest (Gill, 1969, Rebelo and Siegfried, 1990), with a dominant canopy comprised of trees from the Ulmaceae and Sterculiaceae families (Beuning et al., 2003, Hall and Swaine, 1981). In 2004, 1833 m of sediments were recovered from Bosumtwi as part of the International Continental Drilling Program (Koeberl et al., 2007). The sample chosen from Bosumtwi was from the last glacial period (Miller and Gosling, 2014). The glacial sample from Bosumtwi was selected for analysis because of its low palynological richness.

5.4.2. Pollen preparation and identification

Pollen preparation at all sites followed standard procedure, including acetolysis and digestions with Hydrochloric acid, Potassium hydroxide and Hydrofluoric acid (Moore et al., 1991). Samples were spiked with an exotic marker to: i) allow the calculation of pollen concentrations (Maher, 1972, Stockmarr, 1971), and ii) provide a reference marker for the extended pollen counts. The samples were mounted on slides using glycerol and pollen was identified from their distinguishing morphometric features using reference material held at The Open University and Florida Institute of Technology, open access online pollen databases (Bush and Weng, 2007, Gosling et al., 2013), and published pollen atlases (Colinvaux et al., 1999, Gosling et al., 2009, Hooghiemstra, 1984, Lézine, 2005, Reille, 1995, Roubik and Moreno, 1991).

5.4.2.1. Extended pollen counts

Extended pollen counts for the six Mera Tigre East samples followed a protocol designed to assist in the development of the statistical model. Samples were counted until a total of 300 exotic markers (*Lycopodium* spp. spores, batch 124961, Lund University) were reached. *Lycopodium* spores were counted in batches of twenty and all terrestrial pollen grains were counted within the batches. Once a count of 300 *Lycopodium* spores had been achieved the analysis stopped and the percentage abundance for the terrestrial pollen grains was calculated.

By counting to 300 *Lycopodium* marker spores, roughly 2000 terrestrial pollen grains were counted for each sample.

Lakes Khomer Kotcha Upper, Challacaba and Lake Bosumtwi were extensively counted until a total of 1000 terrestrial pollen grains had been reached as suggested by Moore et al. (1991). Pacucha was not counted extensively, but a 'standard' count of 300 pollen grains was achieved.

5.4.3. Modelled pollen counts

The statistical model (sub-sampling tool) requires the input of empirical pollen count data for each pollen sub-sample being considered. The statistical model generates multiple simulations of the possible permutations for pollen assemblages based on the input data, and then assesses the most probable count size required to capture the ecological characteristics (assemblage composition and diversity).

The primary aim of the model is to estimate the required count size that would reliably characterise the major components of the parent vegetation community (hereafter Model 1). The secondary aim of the model is to estimate how many more pollen grains would be needed before a not yet found pollen type was detected, i.e. a taxa not already seen is found (hereafter Model 2). This count size estimate will depend on the richness, as well as the evenness, of the sample based on the initial input data. However, it is important to note that the outputs are modelled probabilities, and that there are many complexities that mean the translation of modelled estimates to 'real world' pollen assemblages will not be perfect. The purpose of the model is, therefore, to provide statistically-based support for the researcher to help ensure the data generated have the best possible chance of addressing the question(s) posed.

5.4.3.1. Model methodology

The statistical model (sub-sampling tool) takes empirical pollen assemblage input data and runs a simple Monte Carlo simulation (a method involving running a simulation multiple times to assess the likely outcomes) one hundred times in succession. The multiple model runs allow the pollen count required to determine the ecological characteristics (assemblage composition and diversity) within a sub-sample to be estimated. The target amount of empirical pollen count data that should be examined to capture this can then be calculated.

The model pollen count simulations work by assigning each pollen grain with a random number. For a given distribution of taxa the simulation then has to determine which taxa corresponds to the chosen random number. By repeatedly choosing random numbers, the model mimics the empirical pollen counting process.

In practice, the pollen count model procedure is as follows. At the beginning of each run, the relative abundance of each taxon is obtained (p_i), ensuring that the sum of p_i is 1. A cumulative amount $r_i = p_i + r_{i-1}$ (sum of all p_j for $i < j$) is determined for each taxon. Each modelled pollen grain is described by obtaining a single random *s* number between 0 and 1. The taxa index *i* of this pollen grain is obtained by working out which cumulative fraction corresponds to the random number, e.g. by testing for $p_i < s < p_{i-1}$. By repeating this process for each pollen grain, a randomised counting is achieved, corresponding to the suggested input data when a sufficient amount of pollen grains are counted.

Once these data have been generated within the model environment, the model then 'bins' the simulation data. Binning is a process simply used to group individual data values into one place; this is instead of displaying a large amount of data separately. In this statistical model, the simulation data can be binned using two different methods, either by a pre-defined number of pollen grains per bin, or by counting up to a fixed number of exotic markers in each bin. The

method of binning can be chosen when using the model. The operator chooses a binning method and then 'turns off' the other method, meaning only one is used during any one model run. For the model runs used to generate the results in Figures 5.2-5.6, the simulation data were binned using a fixed number of exotic markers (*Lycopodium* spp. spores) per bin. The other method, using a predefined number of pollen grains per bin, is useful if a low number of exotic markers have been counted, i.e. when the pollen concentration is high.

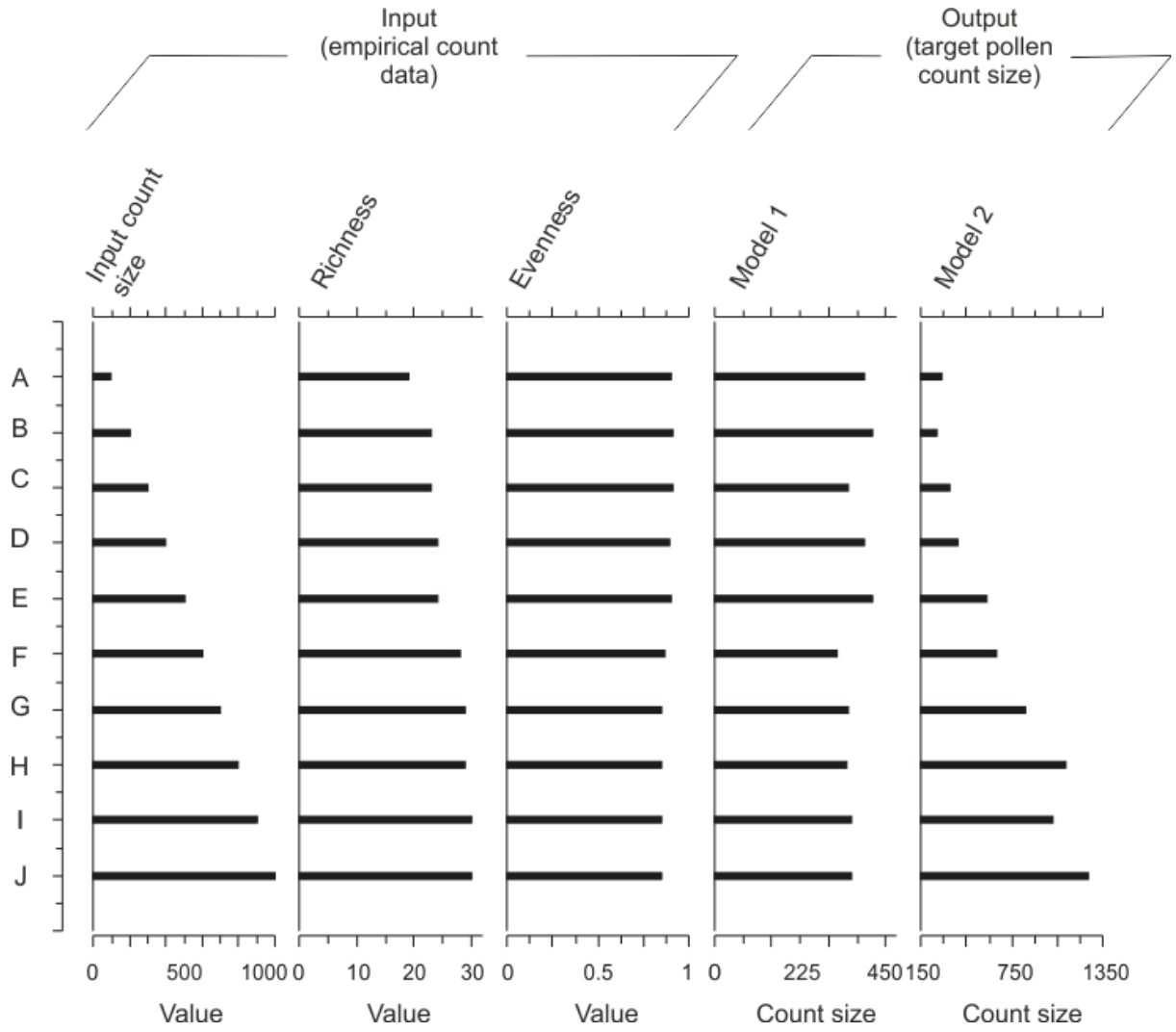

Figure 5.2: Model response to increasing amount of pollen count input data from a fossil pollen assemblage from the eastern Andean flank (Mera Tigre East). The amount of pollen count input data varies from 100 grains (sub-sample A) to 1000 grains (sub-sample J) in increments of 100 grains. Count size outputs for detecting major vegetation composition (biome) Model 1 (Section 4.4.1.) and the next not yet seen pollen taxa Model 2 (Section 4.4.2.) for each sample are shown.

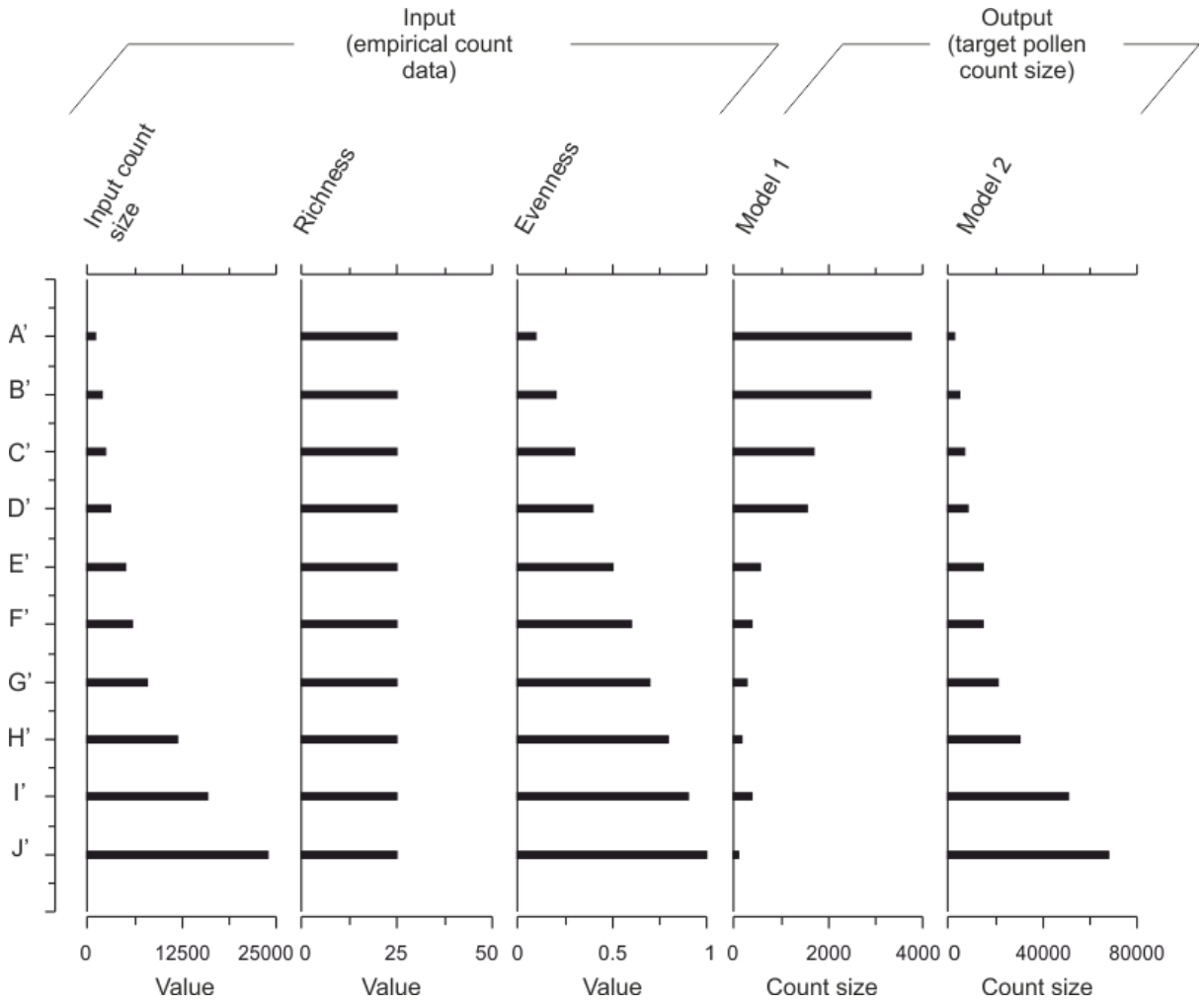

Figure 5.3: Model response to increasing evenness in pollen assemblage composition. The richness value was kept the same (25) and the evenness increased from 0.1 (sub-sample A') to 1.0 (sub-sample J') in increments of 0.1. To maintain richness and evenness values it was necessary to use different input count size values. Count size outputs for detecting major vegetation composition (biome) Model 1 (Section 5.4.4.1.) and the next not yet seen pollen taxa Model 2 (Section 5.4.4.2.) for each sample are shown. Data used is from a random generation and is not indicative of any of the study sites.

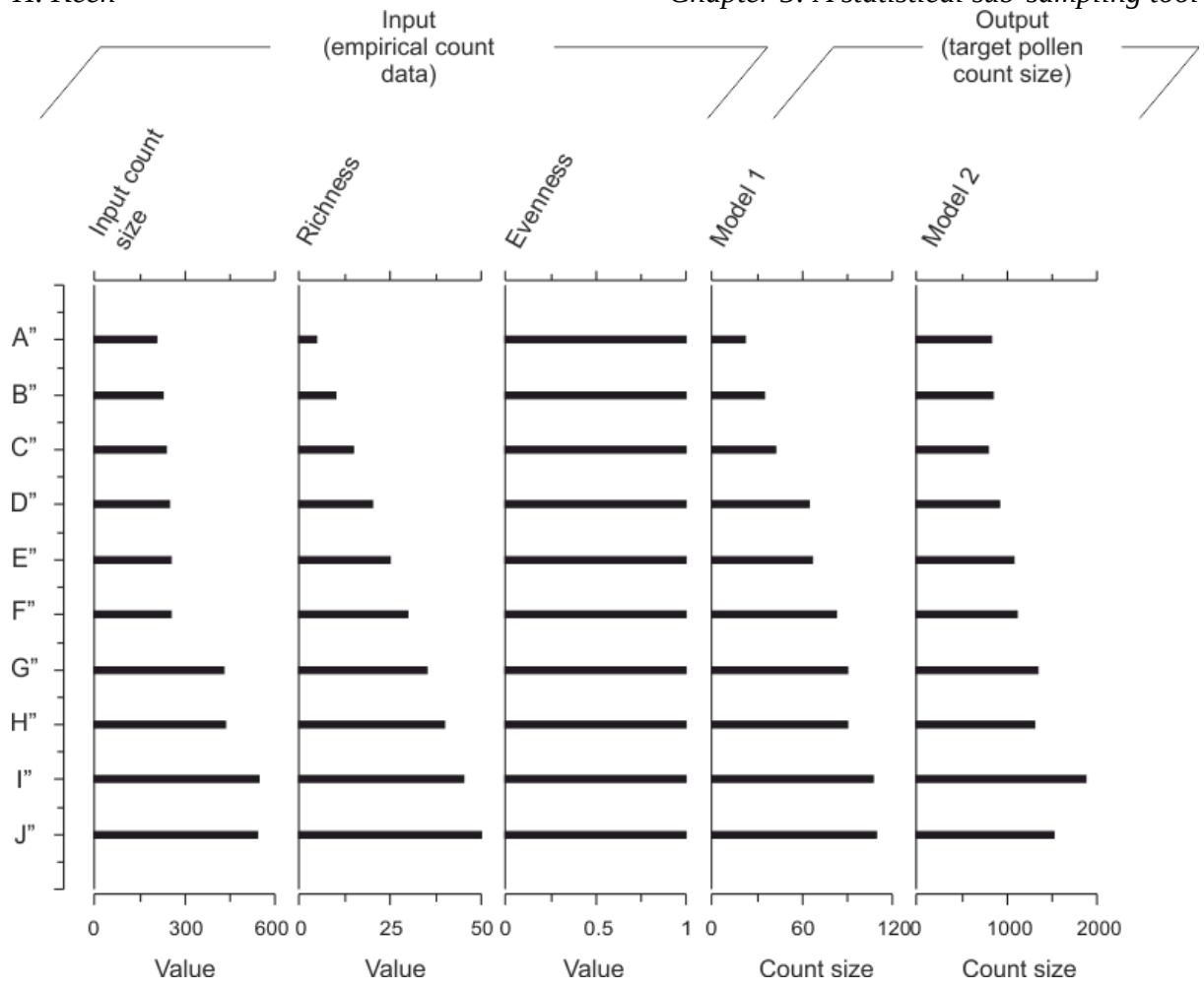

Figure 5.4: Model response to increasing richness in pollen assemblage composition. The evenness value was kept the same (1.0) and the richness increased from 5 (sub-sample A”) to 50 (sub-sample J”) in increments of 5. To maintain richness and evenness values it was necessary to use different input count size values. Count size outputs for detecting major vegetation composition (biome) Model 1 (Section 5.4.4.1.) and the next not yet seen pollen taxa Model 2 (Section 5.4.4.2.) for each sample are shown. Data used is from a random generation and is not indicative of any of the study sites.

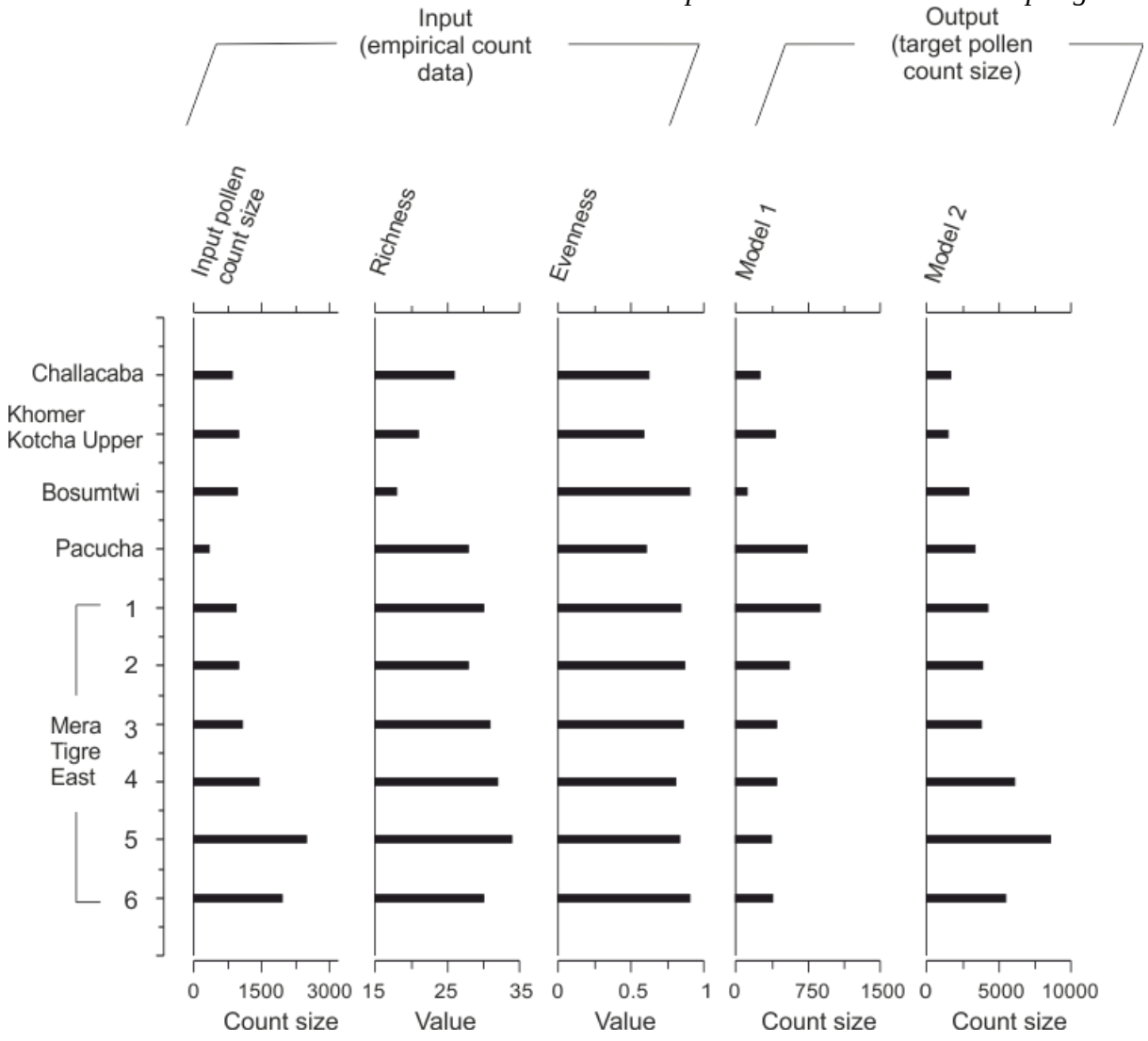

Figure 5.5: Model count size estimates for ten fossil pollen assemblages obtained from five different tropical study sites. Each fossil pollen assemblage has different ecological characteristics (richness and evenness). The pollen count size outputs for detecting major vegetation composition (biome) Model 1 (section 5.4.4.1.) and the next not yet seen pollen taxa Model 2 (Section 5.4.4.2.) for each sample are shown, alongside the empirical pollen count achieved through extended pollen counting.

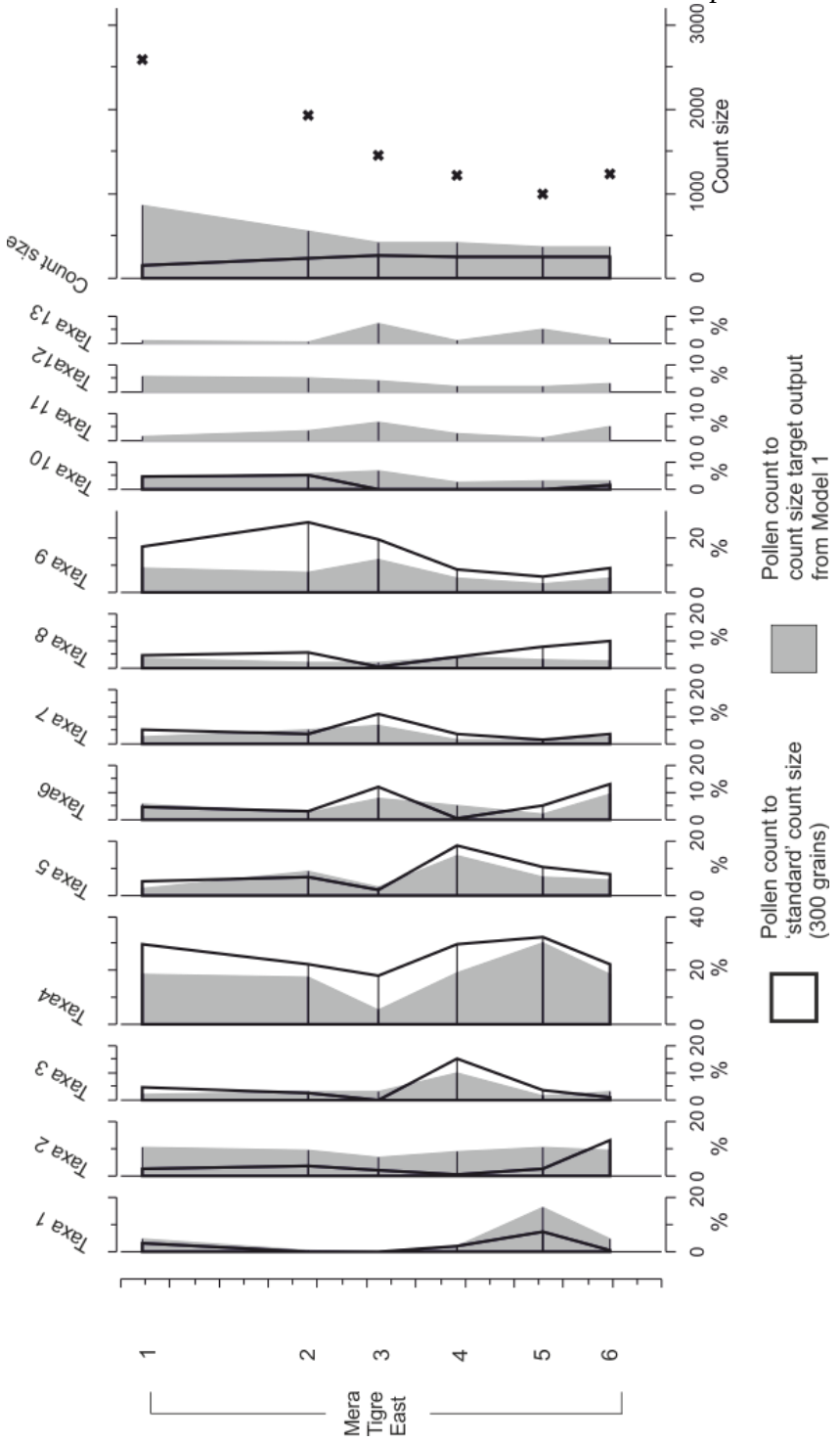

Figure 5.6: Pollen assemblage data from a mid-elevation site on the eastern Andean flank (Mera Tigre East) for pollen count sizes of: i) 300 grains (black outline) and ii) extended counts based on statistical sub-sampling tool estimates (Model 1), count size estimates required to detect the next not yet seen taxa (Model 2) are also shown (black crosses); Model 2 estimates are based on an input of the extended pollen assemblage count data generated when counting to the target output from Model 1. All taxa >5% abundance are shown.

A single model count run takes no more than a few seconds; therefore, generating multiple model runs simultaneously is possible, and so statistical information can be obtained from the aggregated output. This allows the multiple runs necessary for the Monte Carlo simulation to be produced in a minimal time (c. 20 s). Data from multiple model runs allow an error estimate for the counted distribution to be calculated and, therefore, a pollen count size suitable for each specific sample to within a 95% confidence interval to be determined (see section 8 for further information on output data).

5.4.3.2. Model parameters

For each model run the statistical sub-sampling tool simulates the equivalent of an empirical pollen count size of 2000 grains. The model is then run one hundred times in succession (multiple simulations needed for the Monte Carlo simulation) for the individual sub-sample being considered; the equivalent of considering the possible combination of 200,000 pollen grains. Generating an empirical pollen count of 200,000 grains from any one sample would take weeks, and so, is impractical. Therefore, the model provides an opportunity to explore the characteristics of pollen assemblage data which was not previously practical.

5.4.4. Determining appropriate count sizes for specific scientific questions

Two different statistical approaches are presented to address three questions (listed in section 5.2.3) which can be asked of the pollen data. The first statistical approach (Model 1) determines the probability that the pollen count has correctly characterised the major components of the pollen assemblage (Question i). The second (Model 2) assesses the likely investigator effort required (number of additional pollen grains that must be counted) to detect an as yet undiscovered taxa within the pollen assemblage (Questions ii and iii).

5.4.4.1. Characterising major vegetation components (Model 1)

To determine statistically if the major components of the pollen assemblage have been characterised, the rank abundance of taxa within a sample was examined, i.e. has the pollen count been of a sufficient size to arrange the major components of the pollen assemblage in the 'correct' order. To assess the rank abundance, the Spearman's rank correlation coefficient (a method of assessing the link between two different variables) was calculated for a series of modelled count sizes (100, 200, 300 grains continuing up to 1000 grains) and compared against the model endpoint (equivalent count size 200,000 pollen grains).

Once a Spearman's rank value of over 0.95 (standard statistical 95% confidence level) is attained, then a reliable count is considered to have been reached. Therefore, when the determined count size has been achieved it can be considered that all major taxa have been correctly characterised in terms of rank abundance, i.e. characterised when the relative abundance of each of the major taxa (>5% abundance) has met the proposed model proportion estimate within the sample. This way of establishing a vegetation community representation in the pollen record (through means of key taxa) is used hereafter. However, in certain circumstances (e.g. very high richness) the Spearman's rank correlation coefficient can never reach 0.95. This is because although major components of the rank correlation will look identical, small differences in low abundance (minor) taxa can mean the Spearman's rank correlation coefficient will not increase to a value of 0.95. In this scenario the standard deviation of the Spearman's rank correlation coefficient can be considered, i.e. the major components have been characterised, but there is still uncertainty within the minor taxa, leading to lower Spearman's rank correlation coefficient values. To circumvent the statistical problem caused by the low abundance taxa, a secondary threshold has been established at the point when the standard deviation of the Spearman's rank correlation coefficient reaches less than 0.05 for all taxa. The standard deviation determines how far the Spearman's rank correlation coefficient value deviates from the average. Once the standard deviation has reached a low level (<0.05), it

indicates that the relative proportions of the majority of the taxa within the pollen assemblage have been successfully determined. The standard deviation is calculated automatically within the model and it is taken across all of the model runs and calculated for each Spearman's rank coefficient, for each of the separate count size bins. Unfortunately, it is not possible to calculate standard deviations for empirical pollen count data in the same way because it is not practical to generate an equivalent quantity of data.

5.4.4.2. Determining sample richness and detecting rare and first occurrence of taxa (Model 2)

To address ecological questions regarding diversity, and for the detection of rare taxa, a different form of statistical assessment is required, i.e. to determine how many more pollen grains would have to be examined to discover the next as yet unseen pollen taxa. An estimation of the investigator effort required to detect the next 'missing' taxa from any sub-sample, can be obtained as follows.

The unknown taxa is defined as taxa x, something likely to be there, but not yet discovered. If the aim is to find taxa x within the sample, then a high enough total count (N_{tot}) needs to be achieved. This experimental set up follows a Poisson distribution (probability of a given number of the unknown taxa x occurring in a fixed interval, in this case a total count size), meaning the variance on the number of unknown pollen grains within a sample is xN_{tot} and the standard deviation of the unknown count size is $\sqrt{xN_{tot}}$. It is also known that within each pollen sample, there will be a number of difficult to identify pollen grains (N_{unc}), this could be known as the unknown taxa x. In many cases the value N_{unc} can be set to equal 1, simply corresponding to the next (unknown) pollen grain at the end of the sample. The aim is to know to within *S* standard deviations how many pollen grains need to be counted for it to be likely that the number of unknown pollen grains in the sample is smaller than N_{unc} given a total N_{tot} and an unknown

x. These numbers have to satisfy the following inequality (Equation 5.4) which can then be solved as an equality for xN_{tot} (Equation 5.5).

$$N_{unc} < xN_{tot} - S\sqrt{xN_{tot}} \quad \text{(Equation 5.4)}$$

To solve this inequality, solving for $S\sqrt{xN_{tot}}$ followed by squaring both sides will give a quadratic equation in xN_{tot} with the following solution:

$$xN_{tot} > N_{unc} > + \frac{S^2}{2} + \frac{S}{2}\sqrt{S^2 + 4N_{unc}} \quad \text{(Equation 5.5)}$$

If it is hypothesised that we have no more than one pollen unidentified grain (e.g. the next not yet seen taxa) then, to within one standard deviation S, the number of N_{tot} counts required to ensure that unknown taxa make up no more than a fraction *x* of the total sample is represented in Equation 5.6.

$$xN_{tot} > \frac{3+\sqrt{5}}{2} = 2.618 \quad \text{(Equation 5.6)}$$

As a simple example, let's consider a pollen sample in which, to one standard deviation, it is important to make sure that no more than 0.1% of pollen grains belong to an unknown taxa (i.e. *x*=0.001 and *S*=1). If every pollen grain can be identified, the required count size is $N_{tot} = 2.618/0.001$ = a minimum count size of 2618 pollen grains. If there are N_{unc}unidentified grains, then the inequality (Equation 5.5) can be applied instead to find the required count size N_{tot} for a given fraction of unknown taxa *x*.

5.5. Results

Ideal count size estimates were produced from the examination of both empirical data generated from extended pollen counts and the sub-sampling tool outputs (Figure 5.5).

5.5.1. Assessment of preliminary data input into the model

Pollen assemblage data for input into the model must be done at a consistent taxonomic level. Some plant families produce pollen grains which are hard to separate taxonomically (e.g.

Poaceae), and thus are often classified only to family level within pollen assemblage data (Jantz et al., 2014). Keeping the taxonomic classification level of model input data standard between samples allows values obtained from different sub-samples to be compared. This does not mean that the palynologist needs to ignore the opportunity to classify pollen grains at a finer taxonomic level; it simply means that once classified and counted, the grains should be grouped into a consistent taxonomic level for input into the model for the different sub-samples being studied. If the grains in some sub-samples cannot be classified to the same taxonomic level, then taxa should be grouped together into the appropriate genus/family to keep the input consistent.

In order for each model run (each individual sample) to be comparable, it is also important to have comparable input variables, specifically, the amount of empirical pollen count data that are input into the model. A test run was performed using an extended count from the eastern Andean flank (Mera Tigre East) to see whether variations in the quantity of pollen count data input affected the model output target pollen count size. Due to the extended count being performed in stages, it was possible to input pollen grain counts of increasing increments (100, 200, 300 and so on.) into the model sequentially.

Regardless of how much empirical pollen assemblage data is input into the model, the model output count size does not fluctuate by more than ±13% from the average count size for Model 1 (Figure 5.2). This indicates that Model 1 count size estimates from a preliminary input of 100 pollen grains are equally as acceptable as those generated when 1000 pollen grains are input. Therefore, to save time, and minimise wasted pollen counting effort, we recommend only 100 grains need to be initially counted for input if the detection of major vegetation components is the goal (Model 1). The target pollen count size estimate produced by the model can then be used to acquire the remaining empirical pollen assemblage data.

The amount of additional pollen data required to detect the next not yet seen pollen taxa, is directly related to the size of the empirical pollen count input (Figure 5.2), i.e. when only 100 grains have been counted it is likely that you will come across a new taxa quicker than if you have counted 1000 grains (compare Figure 5.2A with 5.2J). Therefore, for the detection of next not yet seen pollen taxa Model 2 is required to be run iteratively through the counting process. At each step of the model, a decision can be made by the palynologist for the satisfactory completion of the sub-sample count. To ensure consistency between sub-samples, a threshold cut-off value could be set. For example, a sub-sample pollen assemblage count could be considered to have been completed when no further new taxa are anticipated to be discovered within the next 500 grains, based on the estimates of Model 2.

5.5.2. Assessment of model effectiveness

To assess the functioning of the model, 'dummy' pollen assemblage data were input to ascertain how different ecological characteristics (e.g. richness and evenness) affected the model target pollen count size output estimates. These checks ensure that the model is working intuitively and give confidence for the application of the statistical sub-sampling tool as a guide for empirical pollen counting (see Section 5.8 for details of the operation of the model).

Two hypothetical pollen assemblage data sets of ten samples each were input into the model; the amount of pollen data input for each sample was varied to maintain the desired richness and evenness characteristics. In the first data set (scenario 1) the evenness increased whilst the richness remained consistent (Figure 5.3). In the second dataset (scenario 2), the richness increased whilst the evenness remained consistent (Figure 5.4). By using the two test scenarios it was possible to see, under controlled conditions, whether the model is performing as anticipated.

5.5.2.1. Model 1

In scenario 1 it was expected that as evenness increased, the order of the major pollen assemblage components should become easier to predict, i.e. the Model 1 estimate target pollen count size should decrease proportionally with increased evenness of the pollen assemblage data (Figure 5.3).

In scenario 2 it was expected that as richness increases, the pollen assemblage should become increasingly harder to predict, i.e. the Model 1 estimate target pollen count size should increase proportionally with increased richness of the pollen assemblage data (Figure 5.4).

The two hypothetical pollen count data sets input into the statistical sub-sampling tool demonstrate that the model is performing intuitively, i.e. more data (higher pollen counts) are recommended for pollen assemblages with low evenness and high richness characteristics.

5.5.2.2. Model 2

As anticipated from investigation of the input count size data (Figure 5.2), in both scenarios 1 and 2 the outputs from Model 2 were closely related to the size of the pollen assemblage data input (Figures 5.3 and 5.4).

5.5.3. Model output pollen count size estimates for specific study sites

To further assess model performance, model target pollen count size outputs were generated for ten samples from five different tropical fossil pollen records (Section 5.4.1). Modelled target pollen count sizes for major taxa (biome) characterisation (Model 1) were highest for Mera Tigre East 1 (870 grains) and Pacucha (741 grains), and lowest for Bosumtwi (122 grains) and Challacaba (256 grains) (Figure 5.5). Modelled target pollen count sizes for rare taxa detection (Model 2) were highest for Mera Tigre East 5 (input data: count size = 2495, richness = 34, evenness = 0.83; output estimate of additional grains required to count to detect one new taxa =

8553) and Mera Tigre East 4 (input data: count size = 1449, richness = 32, evenness = 0.81; output estimate of additional grains required to count to detect one new taxa = 6116 grains), and lowest for Khomer Kotcha Upper (input data: count size = 1000, richness = 21, evenness = 0.59; output estimate of additional grains required to count to detect one new taxa = 1518 grains) and Challacaba (input data: count size = 860, richness = 26, evenness = 0.63; output estimate of additional grains required to count to detect one new taxa = 1667 grains) (Figure 5.5). Different consideration of evenness and richness characteristics of the pollen assemblage within the two models means that the highest (lowest) pollen count size estimates from one model do not necessarily correspond to the highest (lowest) pollen count size estimates from the other (Figure 5.5).

5.5.4. Example application of the statistical sub-sampling tool to a fossil pollen record

To assess if using the count size estimates produced by the model for major taxa detection (Model 1) made a difference to the reconstructed vegetation community from a fossil pollen record, two different pollen counts from each of the six Mera Tigre East samples were compared (Figure 5.6). The first pollen count comprises pollen assemblage data obtained from a 'standard' pollen count of 300 terrestrial pollen grains (black outline). The second pollen count comprises pollen assemblage data obtained from pollen count targets estimated by Model 1 (ranging from 370 to 870 grains per sample; grey silhouette). The pollen assemblage data acquired from the two sub-sampling techniques indicate that 10 of the 13 the major taxa present (>5% abundance) are the same for both the 'standard' and 'model' count size target pollen assemblage data; however, the relative abundance of some taxa alters, e.g. decrease in relative abundance of taxa 4 and 9, and increase in relative abundance of taxa 1 and 2. The consistent occurrence of most of the major components demonstrates that the count size of 300 was just about sufficient to identify the major elements of the vegetation community, but not to establish the relative proportions.

Although Model 1 was not specifically designed to improve the detection of pollen assemblage richness, by counting to the higher target count sizes new insight into the diversity of the samples has been revealed. Three previously unidentified taxa are now recorded at >5%. Using the pollen assemblage data from the counts achieved following the guidance from Model 1 as input, the model was run again and an estimate of the additional grains to be counted to detect one more taxa were obtained from Model 2 (Figure 5.6). Additional pollen counting of between 994 grains (sample 5) and 2598 grains (sample 1) were estimated by Model 2. Therefore, to detect the presence of any further taxa within the Mera Tigre East samples, significant additional investigator effort would have to be deployed.

5.6. Discussion

5.6.1. Application of statistical sub-sampling tool to study sites

To ensure that the maximum amount of information can be collected from a palynological investigation without counting an excess of pollen grains, it is recommended that each sample is treated individually. Individual pollen samples, regardless of whether or not they are from the same sedimentary sequence, or different study sites, are characterised by different richness and evenness values (Figure 5.5). The models both take into account the richness and evenness characteristics of individual samples to produce an estimate of the optimal pollen count size required to: i) determine the relative abundance of major taxa (Model 1), and ii) detect the next not yet seen pollen taxa (Model 2).

Pollen assemblages with high richness require a pollen count size higher than the often used 'standard' pollen count target of 300 grains to characterise the major components. For example the high richness Mera Tigre East sample 1 (richness = 30) has an estimated target pollen count size of 870 grains (Model 1; Figure 5.5). Application of the pollen count size recommended by Model 1 reveals a change in major taxa abundance and richness between counts of 300 and 870

grains (Figure 5.6), i.e. a count size of only 300 grains for Mera Tigre East 1 provided an inaccurate picture of the major taxa abundance and an under representation of richness in the pollen assemblage.

Pollen assemblages with high evenness require a relatively lower pollen count size, because, with the increase in evenness the sample will be easier to describe as all taxa are equally represented. The Bosumtwi study site has the highest evenness (and lowest richness) of all of the sites presented here (Figure 5.5). The combination of high evenness and low richness results in the statistical sub-sampling tool estimating an ideal pollen count size of only 122 grains (Figure 5.5). Therefore, if this Bosumtwi sample was counted to the 'standard' 300 terrestrial pollen grains then the palynologist would 'waste' effort on the sample.

As count sizes are predominantly driven by evenness and richness (and other factors mentioned in sections 1 and 2), it is imperative that these are calculated (from the initial input data) for each sample and taken into account when using the statistical sub-sampling tool to generate target pollen count sizes. Application of the statistical sub-sampling tool for acquiring a target count size for pollen assemblage data will help ensure that investigator effort is efficient, without compromising the statistical robustness of the pollen assemblage data produced. The application of Model 2 to a data set to assess how efficiently pollen assemblage richness has been sampled is best done iteratively due to the relationship between probability of detection and pollen assemblage count size (Figure 5.2).

The following steps are recommended for using the statistical sub-sampling tool as a guide for empirical pollen counting:

i) Count 100 pollen grains from sub-sample.

ii) Run model using count of 100 pollen grains as input data.

iii) Extract target pollen count size estimate from Model 1.

iv) Count sub-sample up to Model 1 pollen count size target.

v) Run model using data from Model 1 count size target as input data.

vi) Extract number of additional grains required to detect next not yet seen pollen taxa from Model 2.

vii) Evaluate if additional investigator effort is required/ possible. If "no", pollen count of this sub-sample is complete. If "yes", iterate steps v – vii until the answer is "no" using increased pollen count sizes as input data for each increment.

5.6.2. Detecting major vegetation community (biome) composition assemblage data

As anticipated, Model 1 predicts count sizes which are higher for pollen assemblages with high richness and low evenness, e.g. for the Pacucha sample, which has a high richness (28 taxa in a pollen count of 337 grains) and low evenness (0.608) characteristics, a pollen count size of 741 grains is estimated (Figure 5.5). In contrast, pollen assemblages which have lower richness and a higher evenness are estimated to require a relatively lower count size to detect major vegetation composition, e.g. for the Bosumtwi sample, which has low richness (18 taxa in a pollen count of 971 grains) and high evenness (0.9), a pollen count size of 122 grains is estimated. Estimates of pollen count sizes required to characterise the parent vegetation community in the Bosumtwi sample are much lower than the Pacucha sample, and much lower that the 'standard' 300 grain pollen count size that is widely used. Therefore, in the Bosumtwi example, the application of Model 1 to determine the pollen count size required during pollen counting would have reduced investigator effort into this sample, i.e. there was little point counting to >300 grains for the purpose of determining major vegetation components.

The six Mera Tigre East samples were analysed to both a 'standard' count size of 300 grains, and to the count size estimates produced by Model 1 (Figure 5.6). After the Model 1 count size targets had been achieved, the most noticeable difference to the pollen assemblage was that the

relative abundance of some major taxa changed (taxa 2, 4 and 9) and three new taxa were detected at >5% abundance (Figure 5.6). Although most of the major taxa within the pollen assemblage were ever present, the change in relative abundances and diversity could impact in the interpretation of the pollen assemblage data. In the Mera Tigre East example, counting to the Model 1 estimates indicates a more diverse parent vegetation community than would have been interpreted if only the 'standard' pollen counts of 300 grains had been achieved.

5.6.3. Detecting pollen assemblage richness and rare taxa

To provide statistical support for the detection, or otherwise, pollen count size estimates required to detect the next not yet seen pollen taxa are provided by Model 2. The probability of how quickly a 'new' pollen type will be detected by further counting is directly related to the number of pollen grains already counted and input into the model (Figures 5.2–5.5). Consequently, to use Model 2 as a guide for pollen counting we advocate an iterative application (Section 5.6.1). Given the probability of extra-regional pollen being transported into any study site amongst other reasons, it is unlikely that any pollen count can ever sample the total pollen richness of an assemblage. Therefore, the decision on when a pollen count is complete becomes a trade–off between investigator time available and importance of detecting rare taxa to the ecological question posed.

The Mera Tigre East example was counted up to the target pollen counts established using Model 1 (Figure 5.6, data in grey silhouette), and these data were then inputted into the model to obtain an estimate of how many more pollen grains would need to be counted for each sample to detect another pollen type (Model 2; Figure 5.6, black and crosses). In all instances to reach the Model 2 target the pollen count size would have to be more than doubled to detect one further pollen type (Figure 5.6). Therefore, in the Mera Tigre East example, it was decided that the high investigator effort required (more than doubling of time already invested), coupled with the low additional insight into the ecological characteristics projected (detection of one additional pollen

type in each sample) was insufficient to merit further pollen counting. The Mera Tigre East fossil pollen samples were, therefore, considered to be complete upon reaching the pollen count size estimates projected by Model 1.

5.7. Conclusions

The widely used 'standard' pollen count size of 300 terrestrial pollen grains has been shown to be sufficient to provide an overview of pollen assemblage major composition (Figure 5.1); (Birks and Birks, 1980). However, consideration of the ecological characteristics (richness and evenness) of individual pollen assemblages (sub-samples) can facilitate more effective and efficient pollen counting. The sub-sampling tools presented here offer an alternative methodology for pollen counting specifically designed to detect both vegetation community (biome) composition and richness.

We recommend that the statistical sub-sampling tool be applied to palynological investigations on a sample-by-sample basis to account for the variance in parent vegetation community (pollen assemblage) ecological characteristics through both time and space. We recommend that Model 1 be applied to palynological investigations interested in determining major components of vegetation communities. We recommend that Model 2 is only applied after target count sizes estimated by Model 1 have been achieved, and to palynological investigations where determining the diversity characteristics, and/or detection of rare taxa is particularly critical due to the high investigator effort required. The key advantages to the palynologist of using the statistical sub-sampling tool are:

- All pollen assemblage data have the same statistical confidence (not count size).
- Pollen count size targets are linked to the research question.
- Investigator effort can be deployed in a targeted manner.

Although designed with the specific application to investigate pollen assemblages, there is no reason why the statistical sub-sampling tool presented here could not be used to guide other types of ecological and palaeoecological investigations.

5.8. Statistical sub-sampling tool

README file for pollen counter python package.

This archive should contain six files:

- README: The current file.
- LICENSE: A copy of the LGPL v3.0 which governs the distribution of the program.
- pollen_counter.py: python executable for a single pollen counting run.
- pollen_counter_stats.py: python executable for a common pollen counting run with Spearman's rank statistics included.
- documentation.txt: Documentation of all available keywords for controlling the simulation.
- control.example.in: example simulation used for Figure 6 in the accompanying paper. Figure 5.7 represents the input file and output file for this file. Note: This example contains more than the recommended 100 input grains.

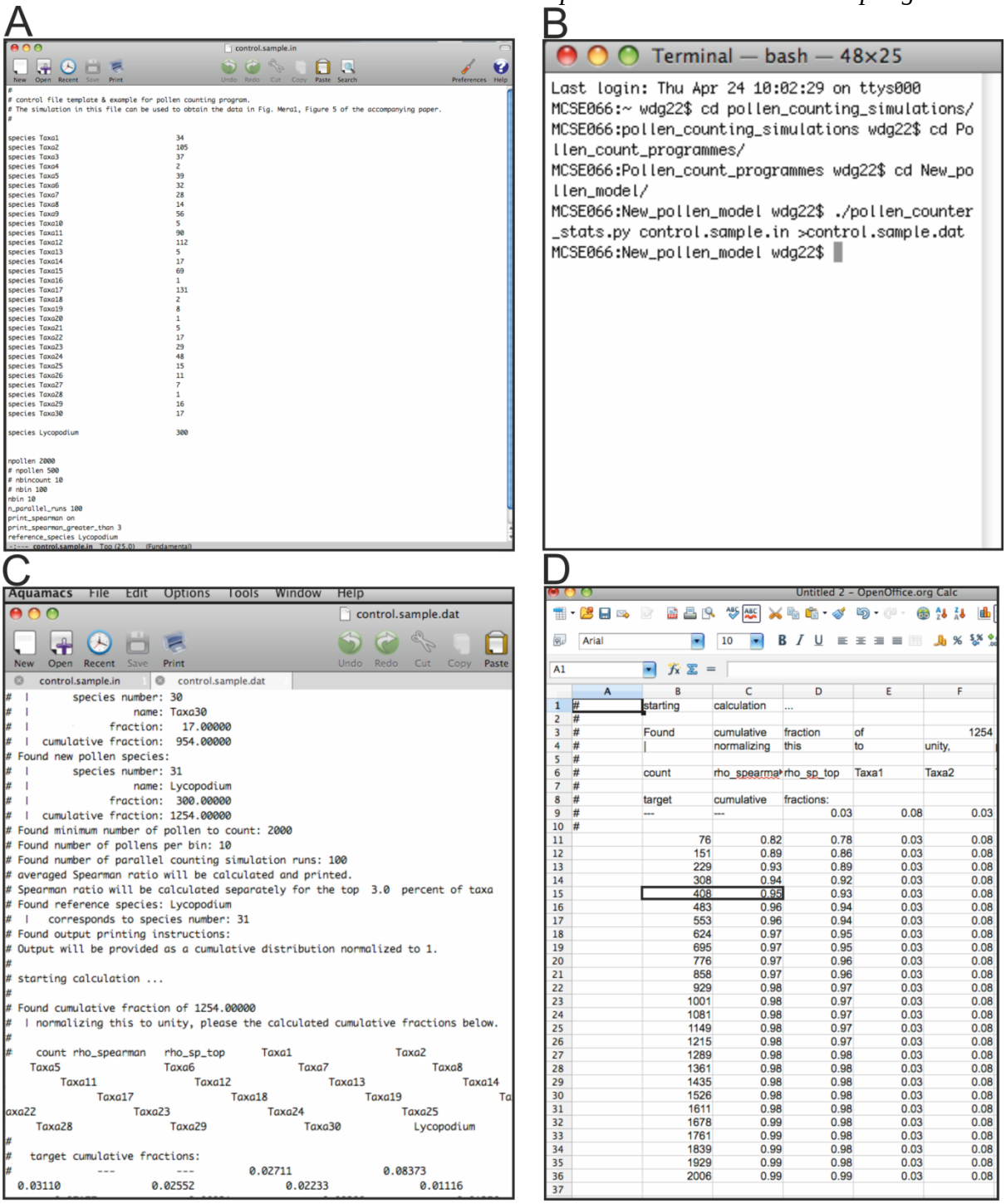

Figure 5.7: Model input file for 'control.example.in' shown in Aquamacs (www.aquamacs.org). A) represents the format for data input into the model. The input file is composed in Aquamacs. Data should be formatted in three columns, column one being species, two being the taxa name and three being the count of the taxa. The marker should be included as a reference (here *Lycopodium*). B) represents the code required to run the model (./pollen_counter_stats.py control.sample.in >control.sample.dat), this is simply the model file, the input file name and then the name you want to output the file to. C) shows the model output in the form of a .dat file (shown in Aquamacs). D) shows

the model output exported into Microsoft Excel. The count size is reached when column C (rho_spearmans) reaches 0.95; in this case the count size is 408.

NOTE: This package requires an implementation of the python programming language to be installed and needs to be run from a terminal prompt. Some operating systems (e.g. linux/ unix and OSX) provide these facilities by default, others may require the download of additional software available freely on the internet.

Acknowledgements

This research was undertaken as part of a PhD studentship (HFK) funded by NERC (NE/J500288/1) and The Open University. Two anonymous reviewers are also acknowledged for their helpful comments which much improve the manuscript. The following authors contributed to the manuscript: HFK collated the data, counted the Mera Tigre East samples and wrote a large proportion of the manuscript. WDG wrote and edited a large proportion of the manuscript. FH developed the statistical model and contributed to the manuscript. CSM contributed the data for Bosumtwi and commented on the manuscript. EM helped with the writing of the manuscript. BGV contributed the data for Pacucha and commented on the manuscript. JJW contributed the data for Khomer Kotcha Upper and Challacaba and commented on the manuscript.

Supplementary material

Six files comprising the statistical sub-sampling tool are found as supplementary material. This contains Model 1 and Model 2, one documentation file, the license, an example run file and an instruction document. It also contains information about all of the software required to run the model. The supplementary material is available online at DOI: 10.1016/j.palaeo.2014.05.001.

5.9. Summary

In this chapter a new statistical sub-sampling tool used to create individual pollen count sizes was introduced. The sub-sampling tool was applied to the pollen counting of all Mera Tigre samples (Chapters 7 and 8). The next chapter, Chapter 6, will discuss the process undertaken to obtain an independent age estimate for the Mera Tigre sediments.

References

BENNETT, K. D. & WILLIS, K. J. 2001. Pollen. *In:* SMOL, J. P., BIRKS, J. H. B. & LAST, W. M. (eds.) *Tracking environmental change using lake sediments. Volume 3: Terrestrial, Algal and Siliceous Indicators.* Dordrecht: Kluwer Academic Publishers.

BEUNING, K. R. M., TALBOT, M. R., LIVINGSTONE, D. A. & SCHMUKLER, G. 2003. Sensitivity of carbon isotopic proxies to paleoclimatic forcing: a case study from Lake Bosumtwi, Ghana, over the last 32,000 years. *Global Biogeochemical Cycles,* 17**,** 31 - 32.

BIRKS, H., H. & BIRKS, H. J. B. 2006. Multi-proxy studies in palaeolimnology. *Vegetation History and Archaeobotany,* 15**,** 235 - 251.

BIRKS, H. J. B. & BIRKS, H., H. 1980. *Quaternary Palaeoecology,* New Jersey, The Blackburn Press.

BIRKS, H. J. B. & LINE, J. M. 1992. The use of rarefaction analysis for estimating palynological richness from Quaternary pollen - analytical data. *The Holocene,* 2**,** 1 - 10.

BROOKS, D. & THOMAS, K. W. 1967. The distribution of pollen grains on microscopic slides. The non randomness of the distribution. . *Pollen et spores,* 9**,** 621 - 629.

BUSH, M. B. 1995. Neotropical plant reproductive strategies and fossil pollen representation. *American Society of Naturalists,* 145**,** 594 - 609.

BUSH, M. B. & COLINVAUX, P. A. 1988. A 7000-year pollen record from the Amazon lowlands, Ecuador. *Vegetatio,* 76**,** 141-154.

BUSH, M. B. & WENG, C. 2007. Introducing a new (freeware) tool for palynology. *Journal of Biogeography,* 34**,** 377-380.

COLINVAUX, P. A., DE OLIVEIRA, P. E. & PATIÑO, J. E. M. 1999. *Amazon pollen manual and atlas,* Amsterdam, Harwood Academic Publishers.

FERDON, E. N. J. 1950. *Studies in Ecuadorian Geography,* Santa Fe, New Mexico, School of American Research and University of Southern California.

FRÉCHETTE, B. & DE VERNAL, A. 2013. Evidence for large-amplitude biome and climate changes in Atlantic Canada during the last interglacial and mid-Wisconsinan periods. *Quaternary Research,* 79**,** 242-255.

GILL, H. E. 1969. A ground-water reconnaissence of the Republic of Ghana, with a description of geohydrologic provinces. *USGS water supply paper,* 1757 - K.

GORING, S., LACOURSE, T., PELLATT, M. G. & MATHEWES, R. W. 2013. Pollen assemblage richness does not reflect regional plant species richness: A cautionary tale. *Journal of Ecology,* 101**,** 1137-1145.

GOSLING, W. D. 2004. *Characterisation of amazonian forest and savannah ecosystems by their modern pollen spectra.* PhD, University of Leicester.

GOSLING, W. D., MAYLE, F. E., TATE, N. J. & KILLEEN, T. 2005. Modern pollen-rain characteristics of tall terra firme moist evergreen forest, southern Amazonia. *Quaternary Research,* 64**,** 284-297.

GOSLING, W. D., MAYLE, F. E., TATE, N. J. & KILLEEN, T. J. 2009. Differentiation between Neotropical rainforest, dry forest, and savannah ecosystems by their modern

pollen spectra and implications for the fossil pollen record. *Review of Palaeobotany and Palynology,* 153**,** 70-85.
GOSLING, W. D., MILLER, C. S. & LIVINGSTONE, D. A. 2013. Atlas of the tropical West African pollen flora. *Review of Palaeobotany and Palynology,* 199**,** 1 - 135.
HALL, J.B. & SWAINE, M. D. 1981. Distribution and ecology of vascular plants in a tripical rain forest. *In:* JUNK, W. (ed.) *Forest vegetation in Ghana.* The Hague.
HAVINGA, A. J. 1964. Investigation into the differential corrosion susceptibility of pollen and spores. *Pollen et Spore,* VI**,** 621-635.
HAVINGA, A. J. 1984. A 20-year experimental investigation into the differential corrosion susceptibility of pollen and spores in various soil types. *Pollen et Spore,* XXVI**,** 541-558.
HOLT, K., ALLEN, G., HODGSON, R., MARSLAND, S. & FLENLEY, J. 2011. Progress towards an automated trainable pollen location and classifier system for use in the palynology laboratory. *Review of Palaeobotany and Palynology,* 167**,** 175-183.
HOOGHIEMSTRA, H. 1984. Vegetational and climatic history of the high plain of Bogotá, Colombia: a continuous record of the last 3.5 million years. . *Dissertationes Botanicae,* 79**,** 1 - 138.
HOOGHIEMSTRA, H. & CLEEF, A. M. 1995. Pleistocene climatic change and environmental and generic dynamics in the north Andean montane forest and paramo. *In:* CHURCHILL, S. P., BALSLEV, H., FORERO, E. & LUYEYN, J. L. (eds.) *Biodiversity and conservation of Neotropical montane forests.* . New York Botanical Garden, 1993: Proc. symposium.
JACKSON, S. T. 2012. Representation of flora and vegetation in Quaternary fossil assemblages: known and unknown knowns and unknowns. *Quaternary Science Reviews,* 49**,** 1-15.
JANTZ, N., HOMEIER, J. & BEHLING, H. 2014. Representativeness of tree diversity in the modern pollen rain of Andean montane forests. *Journal of Vegetation Science,* 25**,** 481 - 490.
KOEBERL, C., MILKEREIT, B., OVERPECK, J. T., SCHOLZ, C. A., AMOAKO, P. Y. O., BOAMAH, D., DANUOR, S. K., KARP, T., KUECK, J., HECKY, R. E., KING, J. W. & PEACK, J. A. 2007. An international and multidisciplinary drilling project into a young complex impact structure: The 2004 ICDP Bosumtwi Crater Drilling Project - An overview. *Meteoritics and Planetary Science,* 42**,** 483-511.
KREBS, C. J. 2014. Chapter 13 - Species Diversity Measures. *Ecological Methodology.* 3rd ed. In prep.
LÉZINE, A.-M. 2005. African Pollen Database. http://medias.obs-mip.fr/apd/accueil.htm.
LIU, K.-B. & COLINVAUX, P. A. 1985. Forest changes in the Amazon Basin during the last glacial maximum. *Nature,* 318**,** 556 - 557.
MAHER, L. J. 1972. Nomograms for computing 0.95 confidence limits of pollen data. *Review of Palaeobotany and Palynology,* 13**,** 85-93.
MILLER, C. S. & GOSLING, W. D. 2014. Quaternary forest associations in lowland tropical West Africa. *Quaternary Science Reviews,* 84**,** 7 - 25.
MOORE, P. D., WEBB, J. A. & COLLINSON, M. E. 1991. *Pollen analysis,* Oxford, Blackwell Scientific.
ODGAARD, B. V. 1999. Fossil pollen as a record of past biodiversity. *Journal of Biogeography.,* 26**,** 7 - 17.
ODGAARD, B. V. 2001. Palaeoecological perspectives on pattern and process in plant diversity and distribution adjustments: A comment on recent developments. *Diversity and Distributions,* 7**,** 197-201.
REBELO, A. G. & SIEGFRIED, W. R. 1990. Protection of Fynbos vegetation: ideal and realworld options. *Biological Conservation,* 54**,** 15 - 31.
REILLE, M. 1995. Pollen et spores d'Europe et d'Afrique du Nord. *Laboratoire de Botanique Historique et Palynologie*.

ROUBIK, D. W. & MORENO, J. E. P. 1991. *Pollen and spores of Barro Colorado Island,* United States, Missouri Botanical Garden.

RULL, V. 1987. A note on pollen counting in palaeoecology. *Pollen et Spores,* XXIX**,** 471-480.

RULL, V., ABBOTT, M. B., POLISSAR, P. J., WOLFE, A. P., BEZADA, M. & BRADLEY, R. S. 2005. 15,000-yr pollen record of vegetation change in the high altitude tropical Andes at Laguna Verde Alta, Venezuela. *Quaternary Research,* 64**,** 308-317.

SHANAHAN, T. M., OVERPECK, J. T., BECK, J. W., WHEELER, C. W., PECK, J. A., KING, J. W. & SCHOLZ, C. A. 2008. The formation of biogeochemical laminations in Lake Bosumtwi, Ghana, and their usefulness as indicators of past environmental changes. *Journal of Paleolimnology,* 40**,** 339-355.

SMITH, B. & WILSON, J. B. 1996. A consumer's guide to evenness indices. *OIKOS,* 76**,** 70 - 82.

STOCKMARR, J. 1971. Tablets with spores used in absolute pollen analysis. *Pollen et spores,* 13**,** 615 - 621.

SUGITA, S. 1994. Pollen representation of vegetation in Quaternary sediments: Theory and method in patchy vegetation. *Journal of Ecology,* 82**,** 881-897.

VALENCIA, B. G., URREGO, D. H., SILMAN, M. R. & BUSH, M. B. 2010. From ice age to modern: a record of landscape change in an Andean cloud forest. *Journal of Biogeography,* 37**,** 1637-1647.

VAN DER KNAAP, W. O. 2009. Estimating pollen diversity from pollen accumulation rates: a method to assess taxonomic richness in the landscape. *The Holocene,* 19**,** 159-163.

VAN DER KNAAP, W. O., VAN LEEUWEN, J. F. N., FROYD, C. A. & WILLIS, K. J. 2012. Detecting the provenance of Galápagos non-native pollen: The role of humans and air currents as transport mechanisms. *The Holocene,* 22**,** 1373 - 1383.

WILLIAMS, J. J., GOSLING, W. D., BROOKS, S. J., COE, A. L. & XU, S. 2011a. Vegetation, climate and fire in the eastern Andes (Bolivia) during the last 18,000years. *Palaeogeography, Palaeoclimatology, Palaeoecology,* 312**,** 115-126.

WILLIAMS, J. J., GOSLING, W. D., COE, A. L., BROOKS, S. J. & GULLIVER, P. 2011b. Four thousand years of environmental change and human activity in the Cochabamba Basin, Bolivia. *Quaternary Research,* 76**,** 58-68.

Chapter 6: Dating techniques applied to Mera Tigre West and East

The previous chapter developed and tested a new statistical sub-sampling technique designed to create a statistically reliable count size for each individual pollen sample. In this chapter three dating techniques (Radiocarbon, $^{40}Ar/^{39}Ar$ and optically stimulated luminescence) are described and the process of their application to the sediments of Mera Tigre West (MTW) and Mera Tigre East (MTE) is explained. Full methodologies for all of the techniques covered here are detailed in Chapter 4 (radiocarbon; section 4.4.1, $^{40}Ar/^{39}Ar$; section 4.4.2 and optically stimulated luminescence; section 4.4.3). A conservative explanation for Mera Tigre sediments age is also provided, framed in a regional scale compared to previous studies.

6.1 Dating techniques

Dating is an integral part of palaeoecological studies, as it allows the temporal framework for determining key Earth events (e.g. glacial-interglacial cycles) to be established and related to different palaeoecological proxies (Walker, 2005). There are various dating techniques that can be used, including those based on isotopic decay (e.g. radiocarbon [Libby, 1955, Libby, 1960] or Argon-Argon [Merrihue and Turner, 1966]), methods based on radiation exposure (e.g. thermoluminescence [Aitken, 1985] or optically stimulated luminescence [Huntley et al., 1985]), techniques using annually banded records (e.g. dendrochronology [Douglass, 1919] and annual layers or varves) and relative dating methods (e.g. amino acid geochronology [Miller and Brigham-Grette, 1989] and pedogenesis (Walker, 2005)). This variety of dating techniques provides the palaeoecologist with the ability to date a range of different samples across a broad range of time scales, as each of these different techniques works best with a specific type of sample (e.g. dendrochronology only works on trees with tree rings present), and can often only work over a certain time period (e.g. radiocarbon dating is only useful up to c. 50,000 years before present; Walker, 2005).

Three dating techniques were applied to the Mera Tigre sections to try and establish an independent age estimate for the sequences, and ultimately a chronology. Preliminary observations from the field regarding the occurrence of several components (organic and inorganic layers, wood remains and fluvial deposits) suggested that the Mera Tigre sedimentary archives presented a great opportunity for testing a range of dating methods in palaeoenvironmental studies. Three techniques were chosen to be applied to the Mera Tigre sites; these were radiocarbon, optically stimulated luminescence (OSL) and Argon-Argon ($^{40}Ar/^{39}Ar$) dating. These three particular techniques were chosen due to their suitability across a wide range of time periods (Figure 6.1), and there suitability for use on a broad range of sedimentary deposits. The selection of these three dating techniques was also based around the debate regarding sediment age of the original Mera site, which has been estimated to be between c. 8,000 and 86,000 years old (Chapter 2; Heine, 1994, Liu and Colinvaux, 1985). Two dating techniques were applied to obtain the dates from the original Mera site, these were radiocarbon and Uranium-Thorium dating (Heine, 1994, Liu and Colinvaux, 1985), however, during this research debate, it was proposed that the Uranium-Thorium method was not suitable for determining the age range of these sediments due to the unsuitability of the weathered sediments and overlying lahar (Colinvaux et al., 1996). Therefore, for this project, alternative techniques were used that covered the time range included in the debate (Figure 6.1). The process of establishing an age control on the MTW and MTE sediments using these three techniques was developed throughout the entire project (Figure 6.2).

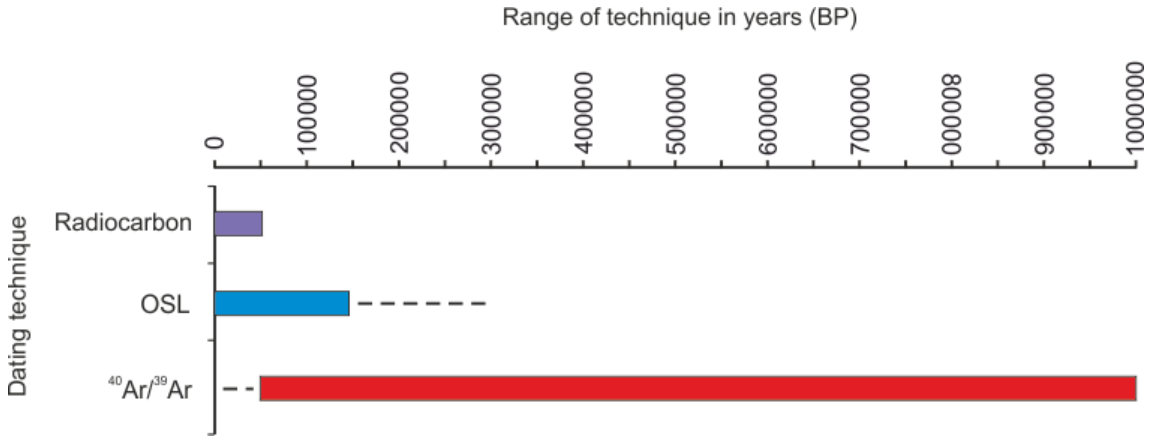

Figure 6.1: Age range of dating techniques applied in this thesis. Solid colours indicate proven applicability of each technique; dashed lines indicate a further tentative range of each technique. Radiocarbon analysis can be applied on organic samples, OSL on organic and inorganic samples, and $^{40}Ar/^{39}Ar$ on inorganic samples.

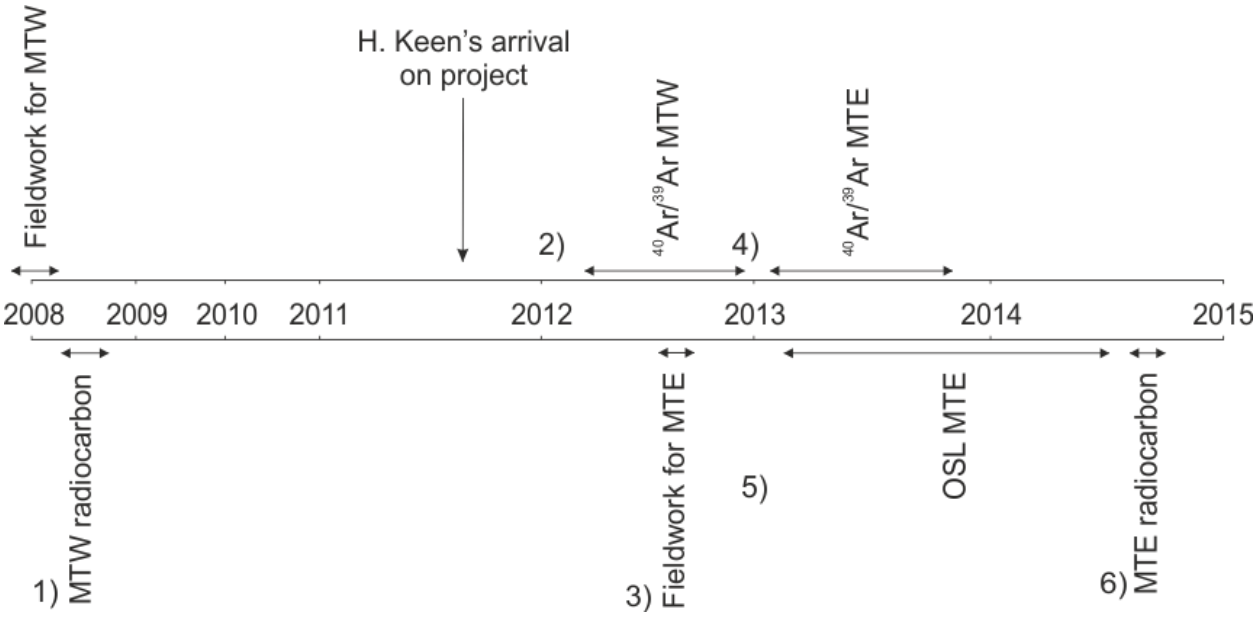

Figure 6.2: Development of the age control techniques throughout the PhD research. The arrival of H. Keen on the project is indicated, as is the fieldwork expedition to obtain the MTE samples. 1) Indicates the time radiocarbon dating was performed on MTW, pre H. Keen's arrival on the project. 2) $^{40}Ar/^{39}Ar$ was performed following H. Keen's arrival on the project due to this technique being useful over a longer time scale (Figure 6.1), also as it could be applied to the abundant inorganic layers. 3) Fieldwork was undertaken to increase the resolution of sites on the eastern Andean flank, also providing a comparative

site to MTW. 4) $^{40}Ar/^{39}Ar$ was performed following fieldwork to try and link the two sites using the abundant inorganic layers. 5) An opportunity was provided to apply OSL dating to the MTE sequence, providing a unique opportunity of testing an additional dating technique on MTE. 6) Radiocarbon dating was performed as OSL indicated that the samples were of a suitable age, and it also meant that radiocarbon was performed on both MTW and MTE.

Figure 6.3 shows the location of the dated samples within MTW and Figure 6.4 shows the location of dated samples within MTE. Table 6.1 summarises the samples analysed using the three different techniques.

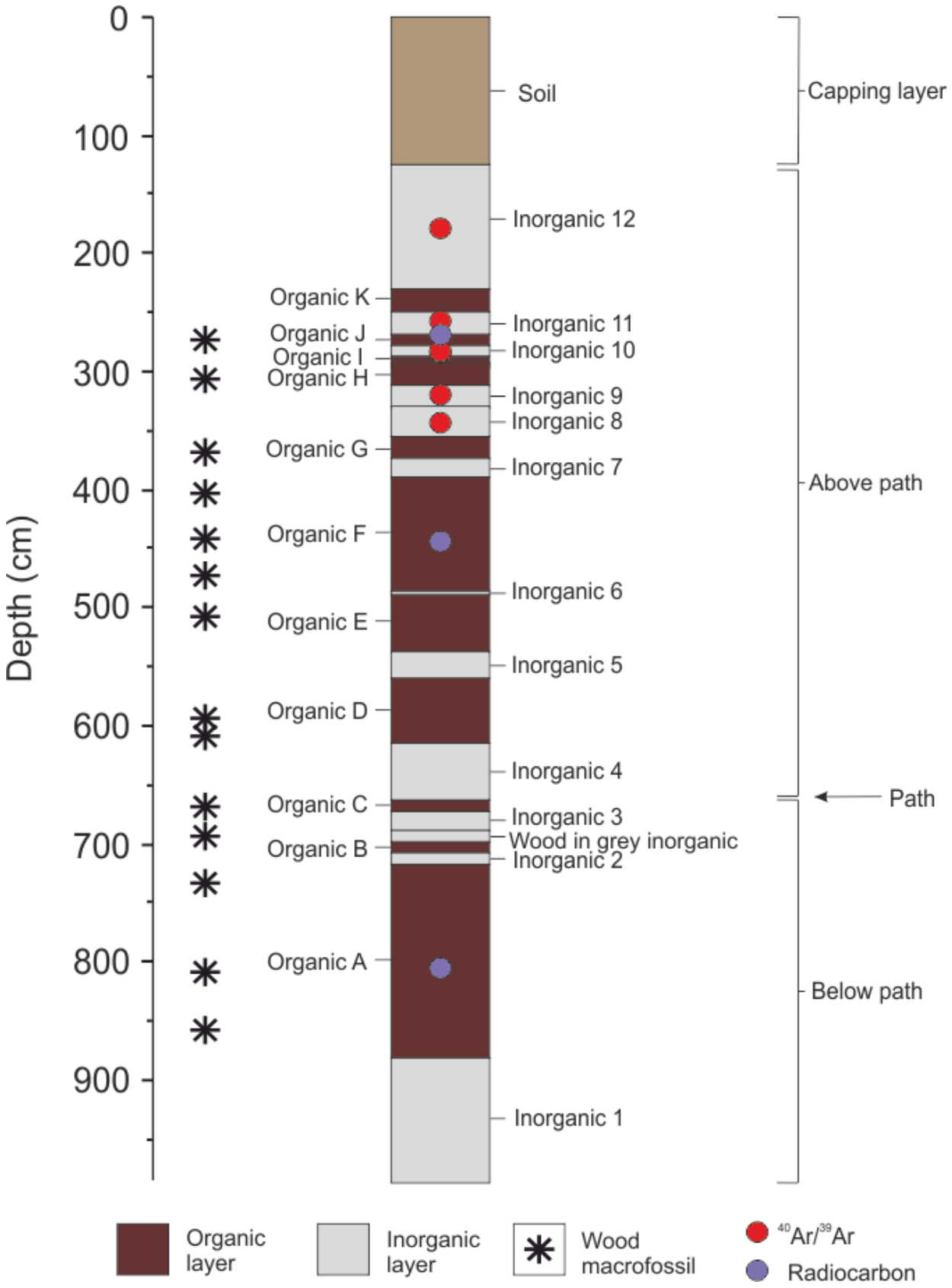

Figure 6.3: Stratigraphy for Mera Tigre West showing the position of samples for $^{40}Ar/^{39}Ar$ and radiocarbon dating.

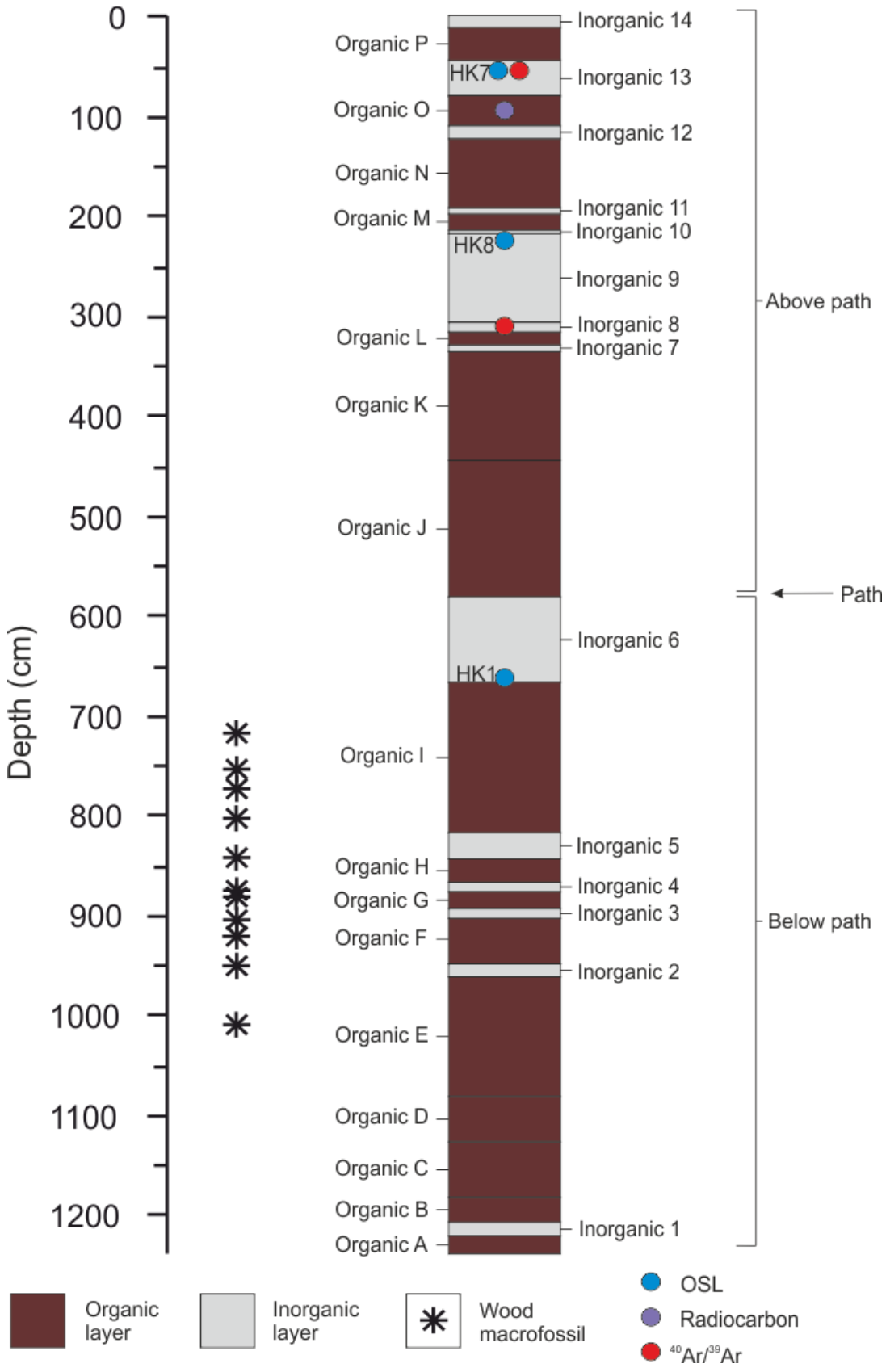

Figure 6.4: Stratigraphy for Mera Tigre East showing the position of samples for $^{40}Ar/^{39}Ar$, radiocarbon and OSL dating.

Table 6.1: Sample ID, section, depth (cm), nature of the sample and the dating technique are included to provide further clarification to Figures 6.3 and 6.4.

Sample ID	Section	Depth (cm)	Nature	Dating technique
H9	MTW	120	Inorganic	$^{40}Ar/^{39}Ar$
H7	MTW	236	Inorganic	$^{40}Ar/^{39}Ar$
Organic 7	MTW	262	Wood	Radiocarbon
H5	MTW	264	Inorganic	$^{40}Ar/^{39}Ar$
H3 and H13	MTW	279	Inorganic	$^{40}Ar/^{39}Ar$
H1 and H12	MTW	317	Inorganic	$^{40}Ar/^{39}Ar$
Organic 3	MTW	433	Wood	Radiocarbon
Organic A	MTW	741	Wood	Radiocarbon
HK7	MTE	46	Inorganic	OSL
Section Y, Inorganic 13	MTE	46	Inorganic	$^{40}Ar/^{39}Ar$
Mera2Y29091	MTE	101	Organic	Radiocarbon
HK8	MTE	220	Inorganic	OSL
Section Y, Inorganic 8	MTE	308	Inorganic	$^{40}Ar/^{39}Ar$
HK1	MTE	671	Inorganic	OSL

6.2. Radiocarbon dating

Radiocarbon dating is a radiometric dating technique based on the decay of ^{14}C to the stable ^{14}N (see Section 4.4.1). Living organisms incorporate ^{14}C whilst they are alive, and radiocarbon dating can date the time of their death and deposition because, once an organism is deceased, no more ^{14}C can be taken up, meaning decay starts at the point of death. This technique is only effective over a short period of geological time, presently up to 50,000 years (Birks and Birks, 1980, Lowe and Walker, 1997). Figure 6.1 shows the useful time frame of radiocarbon dating (up to 50,000 years). Beyond this current age limit, ages obtained lose precision and become uncertain; this is because it is beyond the limit of the half-lives (Walker, 2005). Even in the useful time period of radiocarbon dating, uncertainties are still associated with any age produced. These uncertainties are presented as age errors and in general they get larger as the sediments get older (Walker, 2005). Despite this short time scale, radiocarbon dating is one of the most widely used radiometric dating techniques in terrestrial and Late Quaternary palaeoecology (Lowe and Walker, 1997).

6.2.1. Results for Mera Tigre West and Mera Tigre East

Radiocarbon dating was applied to three wood macrofossils obtained in 2008 from the MTW study site (Figure 6.3). The three wood macrofossils were recovered independently from organic samples (for pollen analysis) and all three were over >1 cm^3 in size. Dating was undertaken at Lawrence Livermore National Laboratory (CAMS- Centre for Accelerator Mass Spectrometry) by Dr Tom Guilderson. Results from all three wood macrofossils indicate that the samples were radiocarbon infinite (reported as >48,000 years), meaning the sediments were older than the range available for radiocarbon dating (see Table 6.2 for results).

Table 6.2: Summary of results obtained from radiocarbon dating for MTW wood macrofossils. A full analytical table of results is available in Appendix B.

Lab ID	**Sample ID**	**Date**	**Type**	**d13C**	**Error**	**Age**	**d14C**
78165	Organic 3	24/3/10	Wood	-26.46	0.0002	> 48,000	-998.8
78166	Organic 7	24/3/10	Wood	-26.98	0.0004	> 48,000	-997.9
78167	Organic A	24/3/10	Wood	-27.68	0.0003	> 48,000	-998.7

Radiocarbon dating for MTE was applied to a 2 cm^3 pollen residue sample, obtained from an organic layer (Figure 6.4). Analysis was undertaken at the Beta Analytic radiocarbon facility in Miami, Florida. The result from the pollen residue sample is listed in Table 6.3.

Table 6.3: Summary of the result obtained from radiocarbon dating for the MTE pollen residue sample. A full analytical table of results is available in Appendix B.

Lab ID	**Sample ID**	**Date**	**Type**	**d13C**	**Conventional age**	**d14C**
397417	Mera2Y29091	18/12/14	Pollen	-29.0	16,690 ± 60	-874.8 ± 0.9

The reported conventional age for this sample is 16,690 ± 60 years BP. The two sigma calibrated age generated using the programme CALIB and the Southern hemisphere calibration for this

sample is 19,872-20,306 Cal BP, placing this sample in the Late Pleistocene epoch of the Quaternary (Reimer et al., 2013).

6.3. $^{40}Ar/^{39}Ar$ dating

$^{40}Ar/^{39}Ar$ is a radiometric dating technique based on the decay of ^{40}K to ^{40}Ar (see Chapter 4; Section 4.4.2). The ^{40}Ar content is measured directly from the sample using a mass spectrometer; however, the ^{40}K is measured indirectly. The sample is irradiated to convert the ^{39}K in the sample to ^{39}Ar. ^{39}Ar is directly proportional to ^{39}K and the ^{39}K is proportional to ^{40}K (assumed stable at 0.0001167), as such the $^{40}Ar/^{40}K$ ratio can be inferred and the age can be calculated (Walker, 2005). Similar to radiocarbon dating, the $^{40}Ar/^{39}Ar$ technique is prone to uncertainties, this is particular the case in sediments of a younger age, this is due to lower amounts of ^{39}K being present (see Section 4.4.2.1), leading to higher errors associated with any ages produced (Walker, 2005).

6.3.1. Results

$^{40}Ar/^{39}Ar$ radiometric dating was undertaken on nine samples, seven from MTW (Figure 6.3; five inorganic layers) and two from MTE (Figure 6.4; two inorganic layers). All samples were analysed using step heating. Step heating involves gradually increasing the laser power, meaning progressively more gas is released into the mass spectrometer, each step produces a different age. As such the results below have an age range associated with them and a number of steps. Results for MTW are represented in Table 6.4 and results for MTE are represented in Table 6.5.

Table 6.4: $^{40}Ar/^{39}Ar$ results for MTW. Age ranges are shown alongside the mineral type sampled, the steps performed in the step heat and the inorganic layer the sample was retrieved from. Negative ages are excluded from the age range. Full results generated for each step are included in Appendix B alongside all Argon age spectrum plots.

Sample name	**Inorganic layer**	**Steps**	**Mineral type**	**Age range (ma)**	**Plateau age (ma)**
H1	Above path, Inorganic 8	23	Feldspar	72.02 – 208.88	---
H3	Above path, Inorganic 9	19	Feldspar	44.75 – 322.51	---
H5	Above path, Inorganic 10	17	Feldspar	87.01 – 192.28	---
H7	Above path, Inorganic 11	13	Feldspar	74.82 – 391.34	---
H9	Above path, Inorganic 12	13	Feldspar	44.08 – 281.54	---
H12	Above path, Inorganic 8	3	Biotite	64.55 – 135.99	---
H13	Above path, Inorganic 9	18	Biotite	42.94 – 89.50	---

Table 6.5: $^{40}Ar/^{39}Ar$ results for MTE. Age ranges are shown alongside the mineral type sampled, the steps performed in the step heat and the inorganic layer the sample was retrieved from. Negative ages are excluded from the age range. Full results alongside all Argon age spectrum plots are included in Appendix B.

Sample name	**Inorganic layer**	**Steps**	**Mineral type**	**Age range (ma)**	**Plateau age (ma)**
H17	Section Y, Inorganic 13	27	Feldspar	10.88 – 1574.53	---
H20	Section Y, Inorganic 8	15	Feldspar	82.89 – 840.43	---

None of the nine samples dated using $^{40}Ar/^{39}Ar$ reached a plateau age (plateau age here is described as over a 50% agreement between the individual step heat stages) meaning that none of the samples provided a reliable age for either of the stratigraphic sections.

6.3.2. Reasons for lack of plateau ages

There are two possible explanations for the lack of plateau ages for the MTE and MTW samples; these are i) contamination with ancient material within the modern environment, and ii) contamination with ancient material at the time of deposition. In relation to reason 1, the Mera Tigre sites are currently situated in the catchment area of the modern day Río Alpayacu. MTW is found on the bank of the river, and MTE is 0.29 km away from the present river channel. The

catchment area for this river covers 5 % of Ecuador's land surface (see Section 3.1). This high level of fluvial activity occurring at the Mera Tigre sites means that fluvial erosion, transport and deposition is an important issue with the potential for ancient sediment to be reworked from within this wide catchment. However, during fieldwork, the front two centimetres (at least) were removed from the sections before sampling, meaning that the likelihood of modern contamination was greatly reduced (Chapter 4). As such this is not a likely reason for the lack of plateau ages at the Mera Tigre sites. Contamination at the time of deposition (reason ii) is the alternative explanation. The introduction of ancient sediments during deposition could be as a result of mixing of older sediments from the surrounding area through fluvial transport mechanisms (see Chapter 7 for further investigation into contamination from a fluvial influence). The ancient sediments contributing to the range of ages seen in the step heats could be from a variety of sources, including but not limited to, volcanic deposits created during the separation of South America and Africa (110 – 60 ma; Pletsch et al., 2001) or through contamination with volcanic deposits that erupted with crustal fragments, i.e. bringing up older age rocks from the Earth's mantle and crust during eruption (Deruelle, 1982). This contamination at the time of deposition created inorganic layers with a mixed sediment source meaning they are unsuitable for dating.

6.4. Optically stimulated luminescence dating

Unlike radiocarbon and $^{40}Ar/^{39}Ar$ dating, optically stimulated luminescence (OSL) dating dates the burial of the sediment (last exposure to light), by artificially exposing crystal lattices within feldspar/ quartz crystals of a sample and measuring the amount of electrons released (Walker, 2005). OSL is a relatively modern technique (dating back to 1985; Huntley et al., 1985); however, it has been widely used, especially within the field of environmental sciences (Rhodes, 2011). Figure 6.1 shows the age range that OSL is used for; however, at the end of this age scale, the ages become more uncertain. At the upper end of the scale (150,000 years before present)

ages become erroneous due to problems with fading of the signal (Walker, 2005). Ages older than this can be obtained (using quartz not feldspar), however, they become even more erroneous with high levels of associated uncertainty (Walker, 2005).

OSL dating for this project was undertaken at the University of Leicester by Dr Andrew Carr, a full report was written by Dr Carr for the samples analysed, this has been included in Appendix B. Sections 6.4.1. and 6.4.2. are based on the final report and also on conversations and meetings with Dr Carr.

6.4.1. Results

Optically stimulated luminescence dating was undertaken initially on three samples (HK1 [inorganic 6], HK7 [inorganic 13] and HK8 [inorganic 10]; Figure 6.2) from MTE to see if the methodology would work. This cautious approach was deemed appropriate because there have been problems using isolated grains for OSL dating on previous Andean samples taken from Peru (Steffen et al., 2009). This study found that ages generated using quartz were underestimates of the actual depositional age due to a weak fast component in the initial part of the signal generated from the sample alongside other unstable OSL signal components (Murray and Wintle, 2000, Steffen et al., 2009). HK1 consisted of entirely organic rich material <60μm so preparation was halted and only HK7 and HK8 went through the entire analytical procedure. In order to calculate the final age, dose rates needed to be calculated (Chapter 4). These were calculated using sediment taken from the tube ends taken from the short cores (Chapter 4, Section 4.1.5); these results are included in Table 6.6.

Table 6.6: Dose rate determinations for HK7 and HK8. The environmental dose rates assume no change in environmental conditions throughout the burial period – i.e. all components (e.g. water %) are representative of the whole burial period.

Sample name	Water (%)	Depth (m)	Lat	Long	m (asl)	U (ppm)	Th (ppm)	K (%)
HK7	40 ± 5	0.7	-1.5	78.1	1117	4.18 ± 0.42	14.6 ± 1.46	2.58 ± 0.13
HK8	22 ± 5	1.6	-1.5	78.1	1117	1.73 ± 0.17	6.05 ± 0.61	3.55 ± 0.18

Alpha (µGy a^{-1})	Total beta (µGy a^{-1})	Total gamma (µGy a^{-1})	Total cosmic (µGy a^{-1})	Total dose rate (Gy/ka)
10 ± 2.5	1663 ± 107	1245 ± 68	211 ± 11	3.13 ± 0.13
10 ± 2.5	2097 ± 171	1090 ± 65	186 ± 9	3.38 ± 0.18

The OSL dating results obtained indicate a significant age depth reversal (Table 6.7), i.e. in the stratigraphic context of the MTE site sample age for HK8 from inorganic 10 should be older than the HK7 sample from inorganic 13 as in a stratigraphic sense HK8 would have been deposited first as it is lower down in the stratigraphic sequence (Figure 6.4, Table 6.1).

Table 6.7: Age estimates for samples HK7 and HK8. De (Gy) represents the OSL count per unit dose, the dose rate (Gy ka^{-1}) was determined in Table 4 and the age was derived using a combination of them both.

Sample name	De (Gy)	Dose rate (Gy ka^{-1})	Age (ka)
HK7	151 ± 10	3.13 ± 0.13	48 ± 4
HK8	95 ± 7	3.38 ± 0.18	28 ± 3

6.4.2. Possible explanations for age reversal

There are three possible explanations for the age reversal observed in the MTE OSL samples; these are: i) elemental concentrations between HK7 and HK8 are very different, ii) water percentage content in the two samples is dissimilar and iii) problematic nature of the HK7 and HK8 samples. The first possible explanation as to why there is an age reversal is that the concentrations of uranium, thorium and potassium are very different for the two samples,

because of this, the environmental dose rate used in producing the ages is dissimilar between the samples (see Section 4.4.3). Similar to this, reason 2 also means there is further variation in the environmental dose rate between the two samples, as the water percentage content of the two samples is different. The higher water content associated with HK7 (18 % higher than HK8; Table 6.6) contributes to a lower environmental dose rate, and subsequently this leads to an older age. There is no evidence of an altered water percentage during the burial period. The high level of water content in HK7 is not unexpected due to the current water laden environment surrounding MTE (mean annual precipitation >4800 mm; Ferdon, 1950) and the possibility of a river incising the environment around the time of deposition for HK7 (see chapter 7). The low water content for HK8 could be due to the sample potentially drying out during transportation from the field site to The Open University cold store facilities. It could also be that HK8 dried out at a point in geological time following its deposition. However, these cannot be determined for sure, and as such, the water content for HK8 remains as listed in Table 6.5. Possible decreased water content could have contributed to the lower age, therefore, contributing to the age reversal for the samples. The other potential cause of the age reversal observed between HK8 and HK7 is the problematic nature of the samples, a factor observed in other Andean samples from Peru (Steffen et al., 2009). Both of the samples exhibit incomplete bleaching (see complete OSL report in Appendix B), meaning there was an insufficient length of exposure to sunlight, and that, therefore, the natural optical signal of the sediment was not entirely erased (estimations indicate that 90% is erased within a 10 second sunlight exposure; Godfrey-Smith et al., 1988). This incomplete bleaching is a common reason for age discrepancies (Steffen et al., 2009), and is another possible reason for the age reversal observed with HK7 and HK8. In order to assess this, further single grain work will be performed on HK8 (by Dr Carr) to try and establish whether incomplete bleaching could be responsible for the age reversal. It is expected that this work will lead to a future publication as it provides further knowledge into poorly

behaved quartz in the Andean setting. Despite this, with the current information, it is not clear which reason caused the age reversal, or whether all of these factors contributed to the observed age discrepancy.

6.4.3. Comparison of the dating techniques

The different dating techniques applied to the MTW and MTE samples provided the opportunity to assess the age of the deposits within a time frame of present day to >1 million years (Figure 6.1), and allowed both organic and inorganic samples to be examined. The $^{40}Ar/^{39}Ar$ method produced no age estimates for the MTW and MTE sites, however, the radiocarbon and OSL methods both produced age estimates for MTE.

Unfortunately the ages produced from OSL for samples HK7 and HK8 produced an age reversal. The intact stratigraphic context of the sediments (Figure 6.4) means that one of these ages is, for some reason, erroneous (see section 6.4.2). To assess which of the two OSL ages is likely to be more robust, performance against the Single Aliquot Regeneration (SAR) protocol was assessed (outlined in Murray and Wintle, 2003). Indications show that for HK7, fewer aliquots were rejected for the recycling ratio when compared to HK8. The better performance of HK7 suggests that the age estimate from this sample is more reliable. However, despite HK7 performing better in response to the SAR protocol, the radiocarbon date obtained from Organic O in between the two OSL samples provided a calibrated age of 19.872-20306 Cal yr BP, suggesting that the age provided by HK7 is unreliable and that the age provided by HK8 is more accurate. In order to assess which, if any of these OSL dates can be used to generate a chronology for MTE, further radiocarbon dates will be needed (application to be submitted to the NERC radiocarbon steering committee 2015). Additional single grain work on HK8 in relation to the age reversal will also help link the ages retrieved from the OSL and radiocarbon dating techniques.

6.4.4. Comparison of MTW and MTE results in relation to previous study

The dates produced for MTE from radiocarbon and OSL dating were similar to that of the 33,000 year old age produced for the original Mera site (1.32 km away from MTW and 1.12 km from MTE; Liu and Colinvaux, 1985). Due to this, it is highly likely that at least part of MTE was deposited at the same time as the original Mera site, a site of high palaeoecological importance (Liu and Colinvaux, 1985). This similar timeframe means that MTE has the potential to increase the accuracy of the original Mera site by improving the analytical resolution (the original Mera site was based on only six samples) (Bush et al., 1990, Liu and Colinvaux, 1985). The similarity in ages obtained for MTE and the original Mera site suggests that sediments obtained from the site were more likely to be 33,000 years in age as opposed to the 86,000 year age suggested by Heine, (1994). The pollen data generated from the MTE stratigraphic sequence (Chapter 8) will aid the understanding of this region, contributing to the important information from the original Mera site.

A further site situated close to the Mera Tigre sites (Erazo, 105 km away, see Section 2.4.2) had $^{40}Ar/^{39}Ar$ analysis performed upon inorganic layers similar to those at the Mera Tigre sites. The $^{40}Ar/^{39}Ar$ analysis performed at Erazo provided dates ranging from 193,000 to 324,000 years ago (Cárdenas et al., 2011a), providing evidence of a further radiocarbon infinite site (similar to MTW) from the eastern Andean flank. The research performed at Erazo did also report issues with the $^{40}Ar/^{39}Ar$ analysis (Cárdenas et al., 2011a) and questions were raised about sediment provenance (Cárdenas et al., 2011b, Punyasena et al., 2011), Chapter 7 discusses the importance of understanding the depositional environment of a site, so that the sediment provenance can be ascertained.

San Juan Bosco, another site situated close to Mera (187 km away) was also dated to an age similar to the ages obtained for Mera Tigre East. Two dates were obtained from wood fragments

recovered; these were 26,020 ± 300 and 30,990 ± 350 yr BP (Bush et al., 1990). Similar to the original Mera site, data obtained from San Juan Bosco was based on a small amount of samples (in this case 12 samples), meaning it was hard to identify vegetation response to drivers of change (Bush et al., 1990), the data presented in Chapters 7 and 8 will provide further evidence on the vegetation of the eastern Andean flanks response to drivers of change.

6.4.5. Mera Tigre chronology

Since early studies on the Mera region in 1985, dating the sequences obtained has proved challenging (Colinvaux et al., 1996, Espín, 2014, Heine, 1994, Liu and Colinvaux, 1985). The original Mera sequence was reported at two exposures. A radiocarbon date of 33,520 ± 1,010 yr BP was reported for the first exposure, and a date of 26,530 ±270 yr BP was reported for the second, placing them in the last glacial period (Liu and Colinvaux, 1985). These two ages were, however, refuted by Heine (1994) due to proposed issues regarding contamination from lahars and debris laden rivers (see Section 7.6.2.2). Using uranium-thorium dating, Heine produced ages ranging from c. 8,000 to 86,000 years BP (Heine, 1994), therefore, shedding uncertainty on the original dates. Following on from this, work performed by a student thesis from the Instituto Geofisico, Ecuador, produced a radiocarbon infinite age obtained from a piece of wood from the Mera debris flow (see Section 7.3.1) (Espín, 2014). This provided further uncertainty relating to the origin of the sediments in the Mera region. Additionally, work performed in 2003 provided two additional radiocarbon analyses for a site less than 0.5 km away (Bes de Berc, 2003). A radiocarbon analysis of a wood remain from the nearby site (between the two lahars) produced an age of 40,580 ± 1030 BP, providing further evidence towards the original Mera date (Bes de Berc, 2003, Liu and Colinvaux, 1985). A radiocarbon sample was also performed at a nearby Alpayacu profile, the date retrieved from this was 17.920 ± 100 yr BP (Bes de Berc, 2003). From photographs of the Alpayacu sequence reported in 2003 (Bes de Berc, 2003), it was thought that this section could be representative of the very upper part of the MTE sequence (upper organic

layer P; see Section 3.4.2 and the inorganic layer and soil above; see Unit 5, section 7.5.1.5). Additional dates from MTW and MTE (presented in this thesis) provided further confusion regarding the sediment age. MTW (see Section 6.2.1) was radiocarbon infinite (>48,000 years) whereas sediments from MTE produced a calibrated radiocarbon age of 19,872 – 20,306 Cal yr BP (see Section 6.2.1) and two OSL ages (with an age reversal, see section 6.4.1) of 48,000 ± 4000 and 28,000 ± 3000 years BP. The ages produced from the Mera Tigre sites did not clarify the age issues reported from original work.

Due to the high level of uncertainty relating to the age of the Mera sediments, the dates presented in this chapter are not going to be used in this thesis, as there is obvious uncertainty and difficulty relating to dating these sediments. Although the record could be of glacial age (MTE date and due to pollen assemblages; see Chapter 8) this interpretation is not going to be assumed. In order to be able to use these dates, further work needs to be done to resolve the uncertainty existing around the Mera sediment age.

6.5. Summary

In this chapter, results from three different dating techniques applied at the study sites were covered. This chapter discusses some of the difficulties in working with sediments older than 48,000 years (MTW) and for sediments preserved in fluvially active regions (MTW and MTE). Despite applying two different techniques to MTW, an age could not be generated. It is unfortunately not possible to try OSL dating on MTW as since sample collection in 2008 the sediments have been washed away by the Río Alpayacu. Unlike MTW, it was possible to obtain three ages for MTE, with both radiocarbon and OSL dating providing ages. The two OSL ages produced did have an age reversal, this is in line with previously reported issues in Andean samples (Steffen et al., 2009). The radiocarbon date produced for MTE placed the top part of the section in the Late Pleistocene (19,872 – 20,306 cal yr BP). The difficulties reported in this

chapter have prevented an age chronology being generated for either site (see Section 6.4.5), however, despite this; all aims outlined in Chapter 1 can still be investigated.

The next chapter, (Chapter 7), will look at the depositional environment of the study sites, and discuss what type of environment is required for the preservation of palaeoecological sediments on the eastern Andean flank. Chapter 7 will also further explore sediment provenance at the time of deposition (following on from Section 6.3.2, and why understanding the sediment source area is important in order to appropriately interpret palaeoecological data.

References

AITKEN, M. J. 1985. *Thermoluminescence Dating,* London, Academic Press.

BES DE BERC, S. 2003. *Tectonique de chevauchement, surrection et incision fluviatile (exemple de la Zone Subandine equatorienne, Haut Bassin Amazonien). [Overlapping tectonic uplift and fluvial incision (example of the Sub-Andean Zonem, Ecuadorian upper Amazon basin]*. PhD, Universite Toulouse III - Paul Sabatier.

BIRKS, H. J. B. & BIRKS, H., H. 1980. *Quaternary Palaeoecology,* New Jersey, The Blackburn Press.

BUSH, M. B., COLINVAUX, P. A., WIEMANN, M. C., PIPERNO, D. E. & LIU, K.-B. 1990. Late Pleistocene temperature depression and vegetation change in Ecuadorian Amazonia. *Quaternary Research,* 34**,** 330 - 345.

CÁRDENAS, M. L., GOSLING, W. D., SHERLOCK, S. C., POOLE, I., PENNINGTON, R. T. & MOTHES, P. 2011a. The Response of Vegetation on the Andean Flank in Western Amazonia to Pleistocene Climate Change. *Science,* 331**,** 1055-1058.

CÁRDENAS, M. L., GOSLING, W. D., SHERLOCK, S. C., POOLE, I., PENNINGTON, R. T. & MOTHES, P. 2011b. Response to comment on "The response of vegetation on the Andean flank in Western Amazonia to pleistocene climate change". *Science,* 333**,** 1825c.

COLINVAUX, P. A., LIU, K.-B., DE OLIVEIRA, P. E., BUSH, M. B., MILLER, M. C. & STEINITZ - KANNAN, M. 1996. Temperature depression in the lowland tropics in glacial times. *Climatic Change,* 32**,** 19 - 33.

DERUELLE, B. 1982. Petrology of the Plio-Quaternary volcanism of the south-central and meridional Andes. *Journal of Volcanology and Geothermal Research,* 14**,** 77-124.

DOUGLASS, A. E. 1919. *Climatic Cycles and Tree Growth: A study of the annual rings of trees in relation to climate and solar activity,* Washington, DC, Carnegie Institute Publication.

ESPÍN, B. P. A. 2014. *Caracterizacin geológica y litoógica de los depósitos laháricos de Mera, provincia de Pastaza (Geological and lithological characterisation of lahar deposits, Mera province of Pastaza).* Escuela Politécnica Nacional, Quito.

FERDON, E. N. J. 1950. *Studies in Ecuadorian Geography,* Santa Fe, New Mexico, School of American Research and University of Southern California.

GODFREY-SMITH, D. I., HUNTLEY, D. J. & CHEN, W.-H. 1988. Optical dating studies of quartz and feldspar sediment extracts. *Quaternary Science Reviews,* 7**,** 373-380.

HEINE, K. 1994. The Mera site revisited: Ice - age Amazon in the light of new evidence. *Quaternary International,* 21**,** 113 - 119.

HUNTLEY, D. J., GODFREY-SMITH, D. I. & THEWALT, M. L. W. 1985. Optical dating of sediments. *Nature,* 313**,** 105 - 107.

LIBBY, W. F. 1955. *Radiocarbon Dating,* Chicago, University of Chicago Press.

LIBBY, W. F. 1960. Radiocarbon Dating. *Nobel Lectures,* Chemistry 1942-1962**,** 593-610.

LIU, K.-B. & COLINVAUX, P. A. 1985. Forest changes in the Amazon Basin during the last glacial maximum. *Nature,* 318**,** 556 - 557.

LOWE, J. J. & WALKER, M. J. C. 1997. *Reconstructing Quaternary environments,* England, Addison Wesley Longman Limied.

MERRIHUE, C. & TURNER, G. 1966. Potassium-Argon Dating by activation with fast neutrons. *Journal of Geophysical Research,* 71**,** 2852-2857.

MURRAY, A. S. & WINTLE, A. G. 2000. Luminescence dating of quartz using an improved single-aliquot regenerative-dose protocol. *Radiation Measurements,* 32**,** 57 - 73.

MURRAY, A. S. & WINTLE, A. G. 2003. The single aliquot regenerative dose protocol: potential for improvements in reliability. *Radiation Measurements,* 37**,** 377 - 381.

PLETSCH, T., ERBACHER, J., HOLBOURN, A. E. L., KUHNT, W., MOULLADE, M., OBOH-IKUENOBEDE, F. E., SÖDING, E. & WAGNER, T. 2001. Cretaceous separation of Africa and South America: the view from the West African margin (ODP Leg 159). *Journal of South American Earth Sciences,* 14**,** 147-174.

PUNYASENA, S. W., DALLING, J. W., JARAMILLO, C. A. & TURNER, B. L. 2011. Comment on "The response of vegetation on the Andean flank in Western Amazonia to Pleistocene climate change". *Science,* 333**,** 1825b.

REIMER, P. J., BARD, E., BAYLISS, A., BECK, J. W., BLACKWELL, P. G., RAMSEY, C. B., BUCK, C. E., CHENG, H., EDWARDS, R. L., FRIEDRICH, M., GROTTES, P. M., GUILDERSON, T. P., HAFLIDASON, H., HAJDAS, I., HATTÉ, C., HEATON, T. J., HOFFMANN, D. L., HOGG, A. G., HUGHEN, K. A., KAISER, K. F., KROMER, B., MANNING, S. W., NIU, M., REIMER, R. W., RICHARDS, D. A., SCOTT, E. M., SOUTHON, J. R., STAFF, R. A., TURNEY, C. S. M. & VAN DER PLICHT, J. 2013. IntCal13 and Marine13 Radiocarbon Age Calibration Curves 0-50,000 Years cal BP. *Radiocarbon,* 55.

RHODES, E. J. 2011. Optically stimulated luminescence dating of sediments over the past 200,000 years. *Annual review of earth and planetary sciences,* 39**,** 461 - 488.

STEFFEN, D., PREUSSER, F. & SCHLUNEGGER, F. 2009. OSL quartz age underestimation due to unstable signal components. *Quaternary Geochronology,* 4**,** 353 - 362.

WALKER, M. J. C. 2005. *Quaternary Dating Methods,* Chichester, West Sussex, John Wiley & Sons.

Chapter 7: Effective sediment deposition and preservation and their suitability for palaeoecological research on the eastern Andean flank, Ecuador.

In this chapter the depositional environment for Mera Tigre East is established, providing an insight into the sediment source area for this stratigraphic sequence. The sequence is used to establish the depositional environment required to preserve sediments suitable for palaeoecological investigation; it also highlights the importance of taking the depositional environment into account so that palaeoecological data can be interpreted correctly. Only one stratigraphic sequence has been analysed in this chapter (Mera Tigre East). It was chosen not to also analyse Mera Tigre West due to Mera Tigre East having a more varied sediment type, a more varied pollen record and a longer record for study. Mera Tigre West had no evidence of fluvial disturbance in its sediment where as Mera Tigre East did. For these reasons only Mera Tigre East had been focused on.

This chapter has been written for publication in an international journal and it has been submitted to the *Journal of South American Earth Sciences*. It is currently under review following its submission on the 4th June 2015. The full reference is included below. The contribution of H. Keen to this manuscript was the collection and analysis of all data, interpretation of the data and writing the manuscript (co-authors contributed to the interpretation and manuscript editing).

Keen, H. F., Gosling, W.D., Montoya, E. and Mothes, P.A. (in review). Effective sediment deposition and preservation and their suitability for palaeoecological research on the eastern Andean flank, Ecuador. *Journal of South American Earth Sciences.*

Abstract

Sites suitable for palaeoecological study from the eastern Andean flank (EAF) are scarce, because the steep elevation gradient stretching from low (700 m asl) to high (4800 m asl) altitudes is not conducive to sediment accumulation and preservation. Consequently commonly used palaeoecological sedimentary archives (e.g. lakes and bogs) are scarce, and interpretation of alternative deposits is debated because of questions relating to signal provenance. To assist with the discovery and interpretation of palaeoecological study sites on the EAF, an improved understanding of the landscape scale processes that facilitate the deposition and preservation of sediments is required. Here, sedimentological and palynological techniques are combined to investigate the depositional environment which resulted in the accumulation of 12.83 vertical metres of sediment near Mera, Ecuador. By reconstructing change in depositional environments through time, volcanic and fluvial processes have been identified as the main drivers of landscape scale change. Large, infrequent volcanic events were found to: (i) create depositional environments suitable for sediment accumulation, (ii) assist preservation of sediments, and (iii) impact vegetation community composition. While smaller, more frequent volcanic events were found not to modify the depositional environment or greatly perturb the local vegetation community. Two scales of landscape and vegetation reorganisation were identified related to volcanic processes, which suggests a threshold relationship between eruptive events and landscape/ vegetation dynamics at a regional scale, i.e. larger events have a major ecological impact, but smaller events have little or no discernible impact. The critical role of large volcanic events in the deposition and preservation of sediments suitable for palaeoecological analysis indicates that the search for new sites could be guided by the location of major volcanic deposits.

Keywords

Palaeoecology, Stratigraphy, Fluvial erosion, Andean flank, Source area, Volcanic material

7.1. Introduction

Tropical ecosystems are important to the functioning of the Earth's systems due to their: role in the global climate system (Malhi et al., 2008), contribution to the carbon cycle (Denman et al., 2007), and high levels of biodiversity (Barlow et al., 2007). Modern tropical ecosystems have been observed to vary in response to climate change, and to human impact, over annual and decadal timescales (Feeley et al., 2012, Lewis et al., 2009). However, tropical ecosystems are also known to be dynamic on longer timescales with the generation time for some species of large tropical tree being >1000 years (e.g. *Cariniana micrantha,* Chambers et al., 1998), and modern vegetation communities assembling over the last c. 10,000 years (Bush et al., 1992, Francisquini et al., 2014). It is, therefore, important for the effective management of these complex ecosystems that a good understanding of their origins, trends and drivers of change are obtained over long (>1000 year) timescales and large (>10 km^2) spatial scales.

To gain further insight into the long-term ecology of the South American tropics (Neotropics), studies have been conducted to reconstruct past ecological dynamics (palaeoecology) from swamp/lake sedimentary archives at high (e.g. van der Hammen, 1974, Hooghiemstra, 1984, Hanselman et al., 2011) and low elevations (e.g. Mayle et al., 2006, Colinvaux et al., 1996) . However, the steep elevation range of the Ecuadorian eastern Andean flank (EAF; ~700m - ~4800m) means few sites suitable for palaeoecological study have so far been located (Figure 7.1) . Of the three sites published to date (Figure 7.1), two are from the last glacial (Mera, San Juan Bosco, c. 26-33 thousands years ago [ka]; Bush, 1990, Liu and Colinvaux, 1985), and one was deposited earlier in the Pleistocene, (Erazo, c. 600-200 ka; Cárdenas et al., 2011a, Cárdenas et al., 2014). Therefore, study of additional sites in order to improve understanding of the EAF's ecological and palaeoecological complexities are required. Furthermore, the few palaeoecological studies that have been published from the EAF have been debated in the scientific literature with regard to whether the signal obtained could be interpreted as coming

from local, regional or extra regional sources (Cárdenas et al., 2011a, Cárdenas et al., 2011b, Heine, 1994, Liu and Colinvaux, 1985, Punyasena et al., 2011).

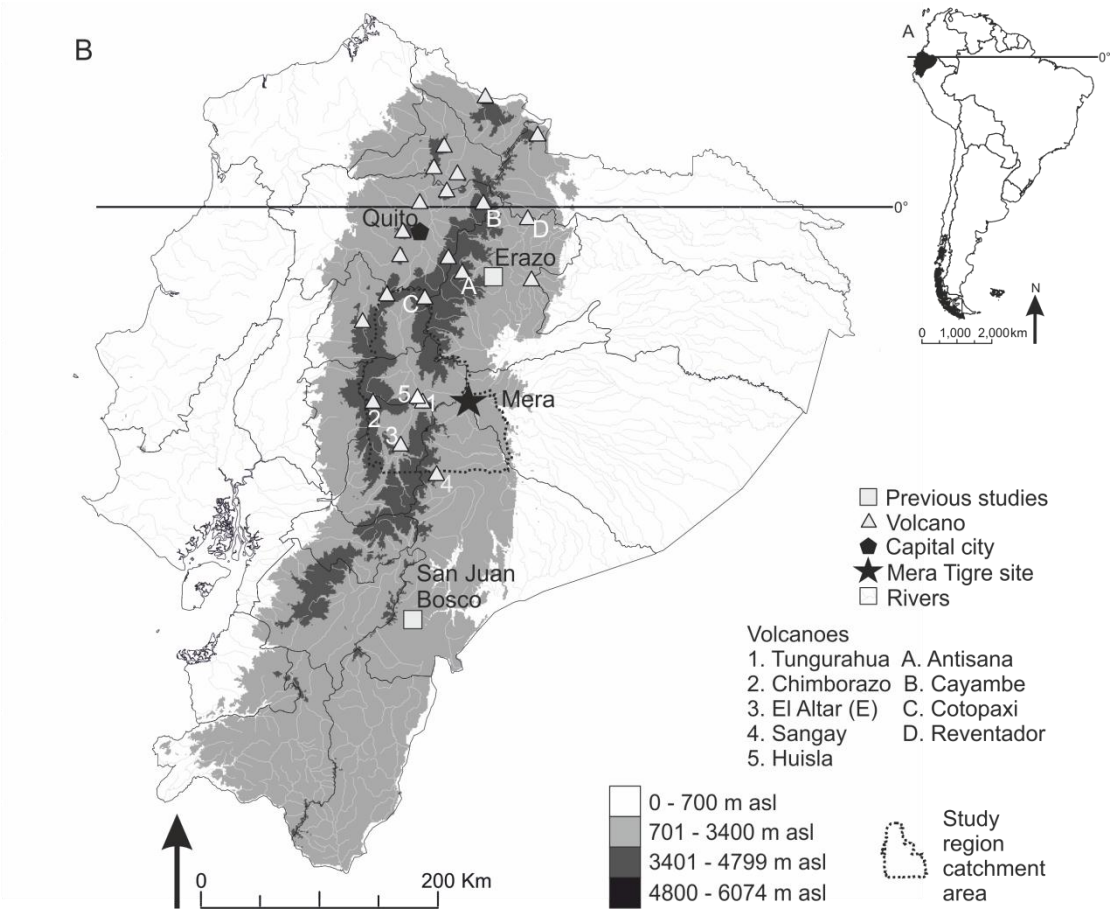

Figure 7.1: Map showing the location of the stratigraphic section (Mera Tigre East). (A) the location of Ecuador in South America. (B) the location of the stratigraphic section in relation to previous palaeoecological sites Erazo (Cárdenas et al., 2014), Mera (Liu and Colinvaux, 1985) and San Juan Bosco (Bush et al., 1990). Fluvial and volcanic sources are included on the map as a reference of nearby modern disturbances. Volcanoes labelled with numbers represent local volcanoes (1-5), those labelled with letters (A-D) represent major volcanoes. The study region was defined as the catchment area for the modern day fluvial system at the stratigraphic section. The catchment area was defined using tools available in ArcGIS 10.1 and ArcHydro tools version 2.0 using a digital elevation model (DEM) and river data (Hijmans et al., 2004, webGIS, 2009). The DEM for Ecuador is shown with the eastern Andean flank spanning 701-4799 m asl (light and medium grey).

The low number of palaeoecological studies from the EAF is, in part, due to steep slopes and volcanic activity limiting the deposition and preservation of suitable sedimentary archives. Steep slopes mean that few swamps/lakes exist, and deposits that do accumulate are prone to perturbation by slumping (Rodbell, 1993) and high rates of fluvial incision mean subsequent erosion of any deposits is likely. Volcanic activity can result in increased erosion, mixing and deposition (Kuenzi et al., 1979); the latter of which can significantly reduce the effectiveness of palaeoecological work through the examination of fossil pollen due to a dilution effect. Conversely, volcanic activity that overwhelms the drainage system can lead to the formation of small lakes that can trap sediment over decades to tens of thousands of years (Manville et al., 2010).

The research presented here introduces a new Pleistocene sedimentary archive (>19 ka, to <1 Ma), from near the town of Mera on the EAF (Ecuador). The new sedimentary archive is a 12.83 m thick section. Discussion focuses on the landscape dynamics that allowed such a substantial sequence of sediments to be deposited and preserved, the implications for palaeoenvironmental interpretations (in particular the new site presented here and previously published Mera and Erazo sites), and the discovery of new palaeoecological archives elsewhere on the EAF.

7.2. Study region: Eastern Andean flank (Ecuador)

The EAF in Ecuador is roughly 50 km wide, with a steep elevation gradient which separates the lowland rain forest (<700 m asl) from the snowline c. 4800 m asl (Bush et al., 2005, Niemann and Behling, 2008)

7.2.1.1. Underlying geology

The underlying geology of the EAF is composed of metamorphic rocks of Palaeozoic to Jurassic age (Bès de Berc et al., 2005). The rocks were metamorphosed during the late Cretaceous and the Paleocene, and subsequently were overlain by volcanic/volcaniclastic formations of late Miocene to Quaternary origin (Bernal et al., 2011, Bernal et al., 2012).

7.2.1.2. Tectonic processes

The modern topography of the EAF was formed when the Andes uplifted c. 25 Ma, as a result of convergence between the Nazca and South American plates (Insel et al., 2009, Montgomery et al., 2001). It is estimated that the Andes reached their modern elevation around 2.7 Ma (Gregory-Wodzicki, 2000).

7.2.1.3. Volcanic processes

The EAF of Ecuador is located within the currently active Northern Volcanic Zone (Garrison et al., 2006), and it has experienced a high level of volcanic activity in the recent geological past; containing 20 major Quaternary volcanic edifices (Figure 7.1; Hall et al., 1999) . Details of the four largest volcanoes within the study site river catchment and five nearby volcanoes (<90 km) with explosive eruptions within the last 300 years are included in Table 7.1.

Table 7.1: Details about the local (less than 90 km away from Mera Tigre East) and recent major (explosive eruption less than 300 years ago) volcanoes surrounding Mera Tigre East located on the volcanic arc of Ecuador.

Name and codes from Figure 7.1	Coordi -nates	Height (m asl)	Distance from Mera (km)	Type of volcano	Last known eruption (AD)	Eruptive features	Local or major	Source
Altar (El) (3)	01°41'S, 78°24'W	5319	47.3	Andesitic	Unknown (extinct)	Unknown	Local	(Rosqvist, 1995)
Antisana (A)	00°28'S, 78°09'W	5758	104.7	Mafic andesite to dacite	1801	Lava flows, pyroclastic flow	Major	(Bourdon et al., 2002)
Cayambe (B)	00°01'N, 77° 59'W	5790	161.4	Andesitic	1786	Lava flows, debris flows, ash fall, pyroclastic flow	Major	(Guillier and Chatelain, 2006, Samaniego et al., 2005)
Chimborazo (2)	01°30'S, 78°27'W	6268	80.2	Andesitic	~550 (dormant)	Lava flows, pyroclastic flows, ash falls, debris flows	Local	(Barba et al., 2008, Samaniego et al., 2012)
Cotopaxi (C)	01°15'S, 78°25'W	5897	92.3	Basaltic - andesite	1940	Lava flows, pyroclastic flows, ash falls, debris flows	Major	(Garrison et al., 2011)
Huisla (5)	01°23'S, 78°33' W	3763	50.3	Andesitic to dacitic	Unknown	Debris flow	Local	(Obando, 2012)
Reventador (D)	00°40'S, 77°40'W	3560	156.1	Andesitic	2009	Lava flows, pyroclastic flows	Major	(Lees et al., 2008)
Sangay (4)	02°00'S, 78°34'W	5230	71.1	Andesitic	2007	Lava flows, pyroclastic flows, ash fall	Local	(Monzier et al., 1999)
Tungurahua (1)	01°30'S, 78°36'W	5023	37.8	Andesitic	2014	Lava flows, pyroclastic flows,	Local	(Arequipa , 2008, Biggs et al., 2010, Hall et al., 1999)

7.2.1.4. Fluvial processes

The EAF is a highly fluvial area (Figure 7.1) and the dynamics of the rivers found on the EAF impact both sediment accumulation and nearby vegetation (Restrepo et al., 2009, Toivonen et al.,

2007). Rivers are also associated with increased erosion, the potential of which is driven by factors such as precipitation, drainage area and slope (Montgomery et al., 2001).

7.2.2. Modern climate

Two main climate systems influence the climate on the EAF: i) the Inter Tropical Convergence Zone, and ii) the South Atlantic Convergence Zone (Cook, 2009), with precipitation on the EAF also being caused by moisture transport from the Atlantic Ocean and the Amazon basin by the South American low-level jet (Bookhagen and Strecker, 2008). Warm, moist air is transported to the Andes from the Amazon rainforest, contributing to high levels of rainfall (in general, altitudes greater than 1000 m receive >4000 mm of rain, less than 1000 m of relief receives <2000 mm of rain a year) on the EAF (Bookhagen and Strecker, 2010, Garreaud and Aceituno, 2007).

7.2.3. Modern vegetation

The EAF contains three major vegetation types: lower montane rainforest (700-2500 m asl), upper montane rainforest (2500-3400 m asl) and páramo (3400- 4800 m asl; Harling, 1979) . The lower montane rainforest is composed of a mix of families common in the lowlands (<700 m asl) such as Myristicaceae and Lecythidaceae and also families typically associated with higher elevations (>2500 m asl) including Ericaceae and Betulaceae. The upper montane rainforest is dominated by families including Melastomataceae, Rubiaceae and Ericaceae (Harling, 1979). The páramo is segregated further into three sub types, grass páramo (3400-4000 m asl; comprised predominantly of Poaceae interspersed with a range of herbs and small shrubs), shrub and cushion páramo (4000-4500 m asl; families include Asteraceae and Apiaceae) and desert páramos (4500- c. 4800 m asl; sparse vegetation present with the prime components being xerophytic grasses, mosses and lichens; Harling, 1979).

7.3. Study site: Mera Tigre East

On the EAF, approximately 1 km away from the town of Mera, and close to the confluence of the Tigre and Alpayacu rivers, a 12.83 m high sedimentary section, exposed by recent fluvial activity was sampled for palaeoecological and sedimentological analysis during fieldwork in September 2012 (01°27.546S, 78°06.199W; 1117 m asl; Figure 7.1). The Mera Tigre East study site is within a region of high fluvial activity with the two local rivers feeding into the larger Río Pastaza within c. 1.55 km. The area immediately adjacent to the study site today is a swampy floodplain area on the bank of the Río Alpayacu (river is c. 0.29 km from the site). The sedimentary section is split into two by a path, 584 cm up from the base (Figure 7.2).

The climate station at Mera indicates a mean annual temperature of 20.8 °C and a mean annual precipitation of >4800 mm (Ferdon, 1950). The vegetation at Mera is classified as lower montane rainforest following Harling (1979). Taxa noted as growing close to the stratigraphic section during fieldwork were Apiaceae, *Asplenium* spp. (Aspleniaceae), Asteraceae, Bromeliaceae, *Cecropia* spp. (Urticaceae), Cyperaceae, Fabaceae, *Lycopodium* spp. (Lycopodiaceae), Melastomataceae, Orchidaceae, Poaceae, *Polypodium* spp. (Polypodiaceae), Sapindaceae, and Urticaceae.

7.3.1. Sediments

The town of Mera is underlain by a variety of types of diamicton deposits composed of pebbles, sands and silts, these are most likely associated with debris flows from volcanic events (Bès de Berc et al., 2005). One of the main debris flow units is the "Mera lahar" which has a thickness of 30-70 m (Espín, 2014). The Mera lahar unit is thought to have been deposited following an eruption of the Huisla volcano (Tungurahua province; Table 7.1) during the Pleistocene (Espín, 2014).

Samples collected from the Mera Tigre East study site were from inorganic and organic deposits, additionally 11 wood macrofossil samples were recovered from the sediments (>1cm^3; Figure 7.2). Each stratigraphic layer was designated a letter (organic A-P) or number (inorganic 1-15) code (Figure 7.2). Radiocarbon analysis performed on pollen residue from organic layer O (Figure 7.2 and Table 7.2) provided a 2 sigma calibrated age using the Southern hemisphere calibration of 19,872-20,306 cal yr BP (Reimer et al., 2013).

Table 7.2: Results obtained from radiocarbon dating for the Mera Tigre East pollen residue sample taken from organic layer O (Figure 7.2).

Lab ID	Sample ID	Date	Type	d13C (‰)	Conventional age	d14C (‰)
397417	Mera2Y29091	18/12/14	Pollen	-29.0	16,690 ± 60	-874.8 ± 0.9

Biochronological markers within the section indicate the Mera Tigre East sediments are younger than one million years; specifically based on the presence of pollen from *Alnus* spp. (Betulaceae), which did not enter South America until c. 1 Ma (Hooghiemstra, 1984).

7.4. Methodology

Three analytical techniques were used on the Mera Tigre East sediments to help understand sediment deposition and preservation: (i) X-ray fluorescence analysis (to determine major element composition of inorganic sediments), (ii) loss-on-ignition (to characterise the physical properties of organic sediments), and (iii) pollen analysis (to investigate the vegetation composition and assess the pollen source area). Other analytical techniques introduced in Chapter 4 (including charcoal analysis) will be discussed in Chapter 8 and are not included here.

7.4.1. X-ray fluorescence analysis

To determine the major element composition (SiO_2, TiO_2, Al_2O_3, Fe_2O_3, MnO, Cao, Na_2O, K_2O and P_2O_5) glass discs were produced for X-ray fluorescence (XRF) analysis from 10 inorganic samples and the diamicton layer collected from Mera Tigre East. Glass discs were created

following standard procedure by combining 0.7 g of dry powdered sample with 3.5 g of lithium metaborate flux (Thomas and Haukka, 1978). The samples were stirred and then fused for 20 minutes at 1100 °C in a muffle furnace to create the discs (Enzweiler and Webb, 1996). Glass disc analysis occurred on an ARL 8420+ dual goniometer wavelength dispersive XRF spectrometer. Two standards of known composition were run alongside the inorganic and diamicton samples from Mera Tigre East.

7.4.2. Loss-on-ignition

Loss-on-ignition (LOI) was used to characterise the sediments physical properties (organic and carbonate abundance). Sub-samples (1 cm^3) were taken from all organic layers (179 sub-samples). Each sub-sample was prepared following standard procedures, i.e. they were dried at 105 °C for 12 hours and ignited at 550 °C and 925 °C in a muffle furnace for two and four hours respectively (Dean, 1974, Heiri, 2001).

7.4.3. Pollen analysis

Sub-samples (0.5 cm^3) were taken from organic layers (67 sub-samples) at a 10 cm resolution. Sub-samples were prepared following standard procedure including acetolysis and Hydrochloric acid, Potassium hydroxide and Hydrofluoric acid digestions (Moore et al., 1991). *Lycopodium* spores (batch 124961, Lund University) were added to the samples as an exotic marker to allow pollen concentrations to be calculated (Stockmarr, 1971). Resulting sub-samples were mounted on slides using glycerol and the pollen grains were identified using published pollen reference material (Bush and Weng, 2007, Colinvaux et al., 1999, Roubik and Moreno, 1991) and modern reference material held at The Open University. Total terrestrial pollen counts varied from 289 to 982; target count sizes were calculated on a sample by sample basis to ensure the major elements of the pollen assemblage were robustly characterised in each sample, following Model 1 of Keen et al. (2014).

7.5. Results

7.5.1. Sedimentary units

Five sedimentary units have been determined at Mera Tigre East based upon the sedimentary characteristics (Figure 7.2). Unit 1 was defined by the presence of cobble and boulder size material. Unit 2 was defined as a diamicton and a sample was taken. Unit 3 (12.39-4.48 m) was identified by the high organic composition of the sediment (>50 % organic LOI) and the presence of interbedded inorganic layers. Sedimentary layers were identified in the field by colour: organic layers (dark black/brown), inorganic layers (grey/yellow). Unit 4 (4.49-0 m) was defined by low organic composition (<50 % LOI) and the presence of inorganic sand, gravel and pebble size material in the deposits. Unit 5 was identified in the field as inorganic due to its colour (grey/yellow).

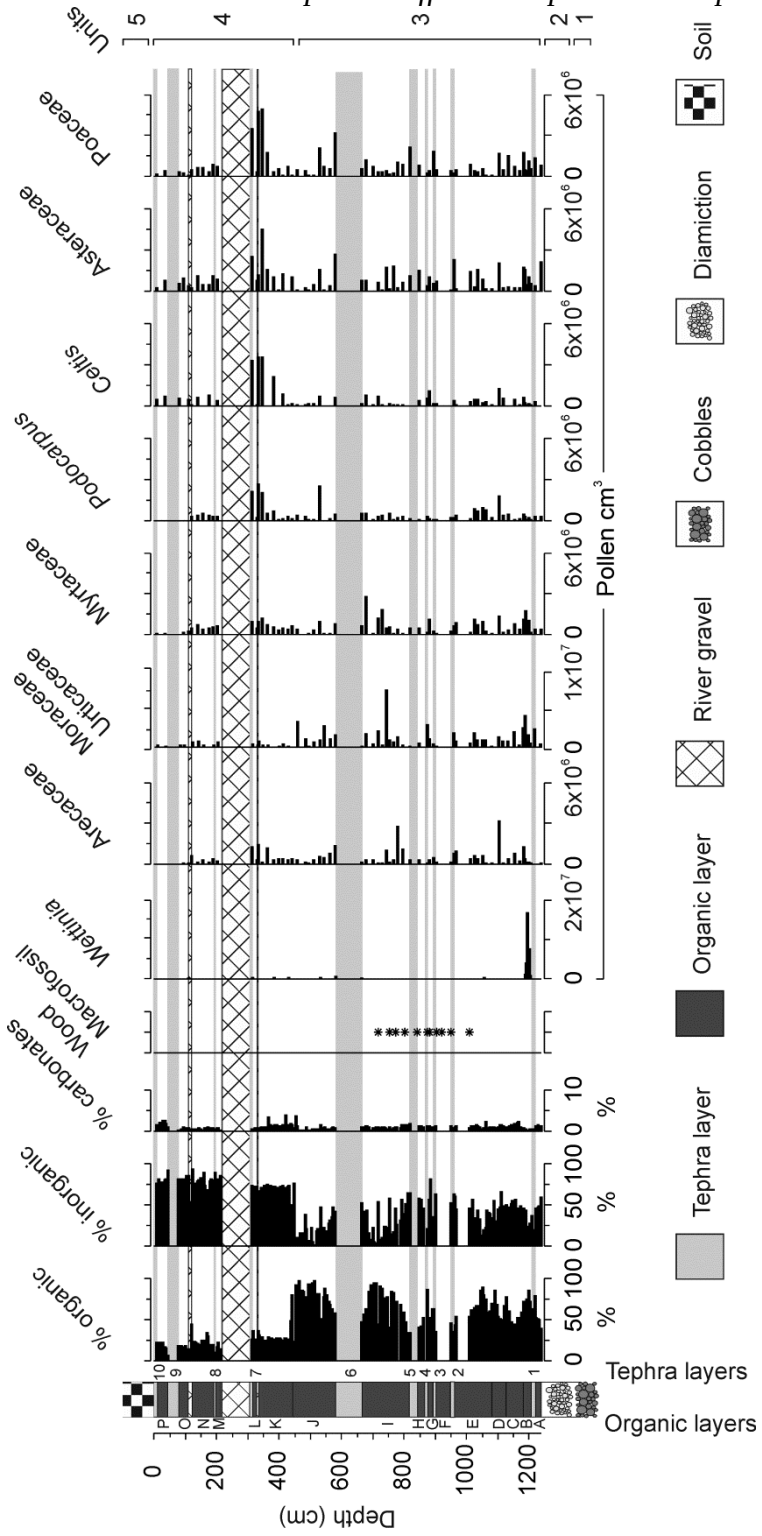

Figure 7.2: Summary diagram including a stratigraphic column, non-biological evidence (loss-on-ignition) and biological evidence (pollen and wood macrofossils). The stratigraphic section is split into two by a path; this is found above layer 6 at a depth of 584 cm. Pollen concentrations are represented in standard mathematical notation (e.g. $6x10^6$ = 6,000,000). Pollen sub units discussed in Section 5 are included as dashed lines.

7.5.1.1. Unit 1 (no samples taken)

Unit 1 is defined by a layer of cobbles and boulders (~100-500 mm) at the base of the stratigraphic section. Unit 1 was recorded in the field but no samples were taken.

7.5.1.2. Unit 2 (one diamicton layer)

Unit 2 is a layer of diamicton, it is poorly sorted and geochemical analysis indicates that the deposits were basaltic in nature (Figure 7.3).

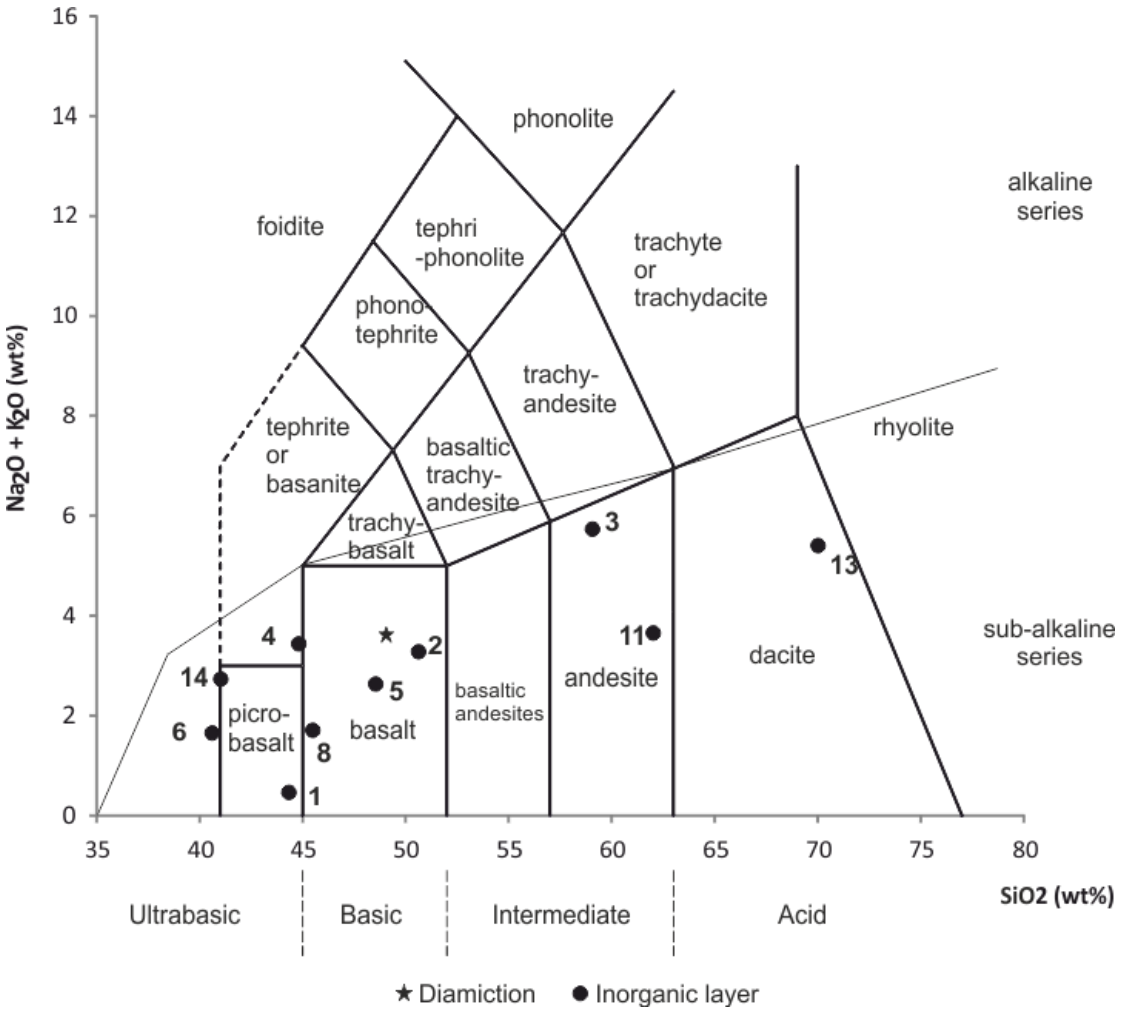

Figure 7.3: Total alkali-silica (TAS) diagram representing the X-ray fluorescence (XRF) silica (Silicon dioxide) and alkali (Sodium oxide and Potassium oxide) content for ten inorganic layers (represented by circles) and one diamicton layer (represented by a star) from the stratigraphic section. The numbers related to tephra layers on Figure 7.2.

7.5.1.3. Unit 3 (12.39-4.48 m, ten organic and six inorganic layers)

Unit 3 is subdivided into ten organic layers (labelled A-J) and six interbedded inorganic layers (labelled 1-6); stratigraphy is shown in Figure 7.2. Subdivisions were determined in the field based on changes in sediment colour and texture. Organic layers A-J are characterised by a high organic component of the sediment determined by LOI (54, 71, 50, 60, 61, 42, 56, 47, 66 and 77% respectively). Biological indicators suggest that Unit 3 can be divided into three nested sub-units; two distinct pollen assemblages (pollen zone I and II), and a period of high wood macrofossil abundance included within the second pollen assemblage sub-unit (layers E-I). Pollen zone I (layers A-B) contain a high concentration of Asteraceae, Poaceae and Moraceae/Urticaceae pollen. Immediately following inorganic layer 1 (organic layer B), there is a high concentration of pollen grains (>$1x10^7 cm^3$) of the palm *Wettinia* (Arecaceae undiff). Synchronous with the increase in *Wettinia* is an increase in other palms (Arecaceae) and also Myrtaceae. Pollen zone II (layers C-J) forms the second vegetation assemblage of Unit 3, throughout these layers Asteraceae, Poaceae, Moraceae/Urticaceae, Arecaceae and Myrtaceae are present in high concentrations. Geochemical analysis of inorganic layers found within Unit 3 indicates the layers as picro-basaltic (inorganics 1 and 6), andesitic (inorganic 3) and basaltic (inorganics 2, 4 and 5) in nature (Figure 7.3).

7.5.1.4. Unit 4 (4.49-0 m, six organic, eight inorganic layers).

Unit 4 is subdivided into six organic layers (K-P) and eight inorganic layers (labelled 7-14), Figure 7.2. Organic layers K-P are characterised by a low proportion of organic sediment as determined by LOI (31, 30, 14, 23, 18 and 20% respectively). Two distinctive pollen assemblages are represented in Unit 4 (Pollen zones III and IV). Pollen zone III (layers K-L) contain high (>$2x10^6$) pollen grain concentrations of *Podocarpus* (Podocarpaceae), *Celtis* (Ulmaceae), Asteraceae and Poaceae. While pollen zone IV (layers M-P) sees a concentration decrease for all taxa present on Figure 7.2. Geochemical analysis was undertaken on inorganic

layers 8, 10, 13 and 14. These were defined as andesitic (8 and 10), dacitic (13) and picro-basaltic (10) in nature (Figure 7.3).

7.5.1.5. Unit 5 (no samples taken)

Unit 5 caps the sedimentary sequence and is composed of a thick inorganic layer (>1.5 m) on top of which is thin soil (c. 20 cm) supporting modern vegetation. Significant mixing of inorganic layer 15 by root penetration was observed in the field. No samples were taken of this layer.

7.6. Discussion

First we present a potential scenario for the landscape evolution interpreted from the Mera Tigre East deposits (Figure 7.4). Second, we assess how sediment deposition and preservation is impacted by volcanoes and fluvial systems on the EAF.

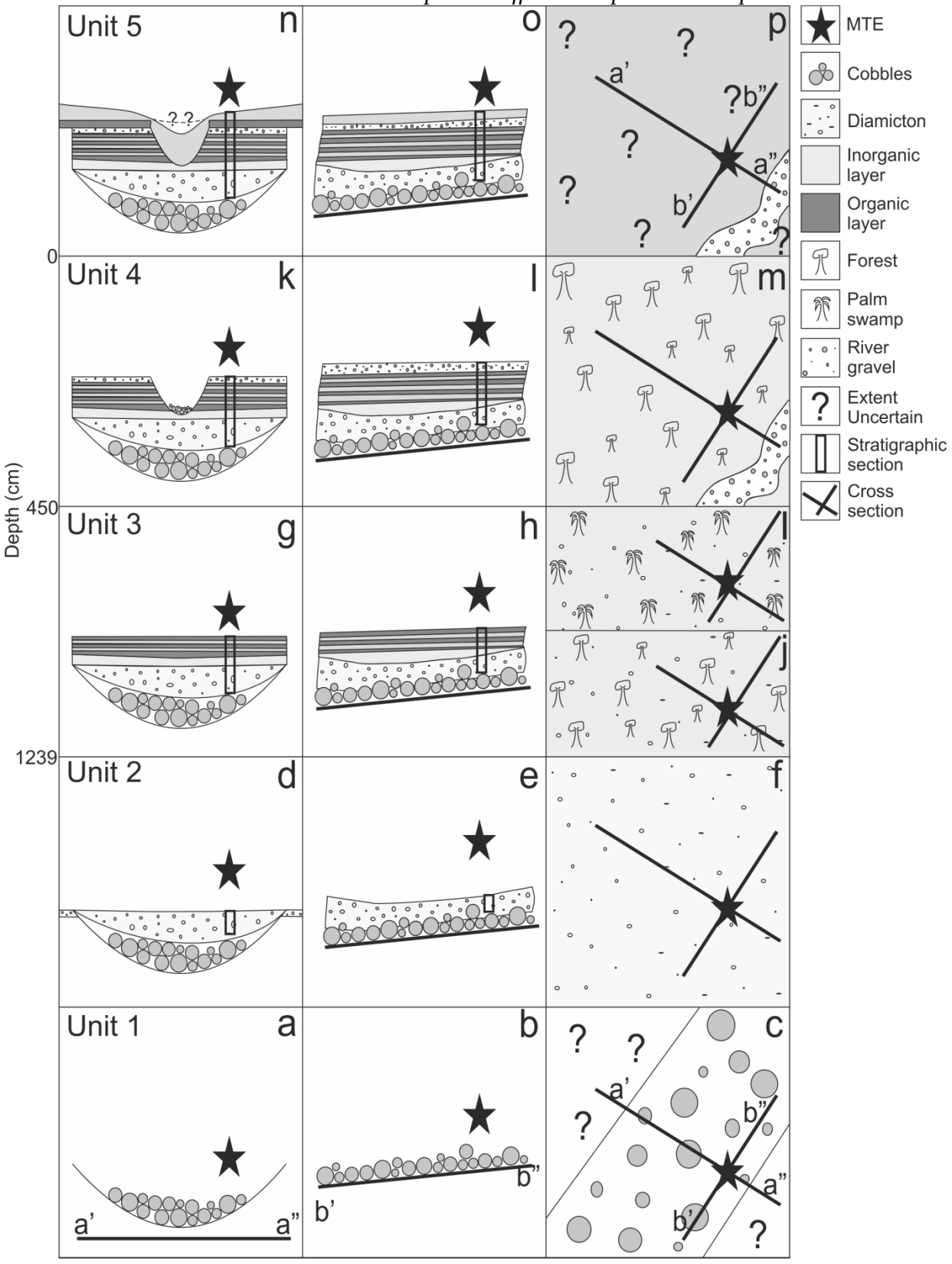

Figure 7.4: An interpretation of the depositional environment at Mera Tigre East, this diagram is not to scale and represents a potential scenario, based on interpretation of sediments from the Mera Tigre East stratigraphy. An approximate depth scale is included to show where each unit begins in relation to Figure 7.2 (i.e. Unit 4 youngest, Unit 2 oldest). In all cases the star represents the location of the Mera Tigre East

stratigraphic section. Inorganic fluvial layers are represented as white with cobbles or gravels in them; the debris flow is represented as light grey with small debris embedded within it. The shallow water area (swamp) is represented as light grey. Organic layers are represented in dark grey and inorganic volcanic layers as medium grey. Question marks indicate uncertainty as to the extent of coverage or vegetation type. a' to a" of the cross section represents the view seen in the first column, b' to b" of the cross section represents the view of the river seen in the second column. The letters a-p are referred to in the text following this diagram.

7.6.1. Landscape evolution

7.6.1.1. Unit 1

The nature of Unit 1 sediments implies fluvial erosive processes and suggests a large river was present in the region, causing the deposition of cobbles and boulders (Figure 7.4 a-c). To transport and deposit the cobbles and boulders (~100-500 mm) that comprise Unit 1 would have required a river with an entrainment velocity of >1 m/s (Novak, 1972). Cobble and boulder size material is today found on the bed of the nearby Pastaza (annual average discharge 121 $m^3s^{—1}$; Bernal et al., 2012; 1.34 km from Mera Tigre East), suggesting the potential for this river to have a flow rate suitable for transporting cobbles and boulders, therefore, providing a good analogue for the depositional environment of Unit 1.

7.6.1.2. Unit 2

Unit 2 is a diamicton composed of poorly sorted sediment (including sand, gravel and cobble size material). The poorly sorted sediment composition suggests that it is a debris flow deposit. It is likely that this deposit is the Mera lahar, the debris flow which originated from an avalanche from the Huisla volcano, situated upstream of Mera Tigre East (Espín, 2014). Espín (2014) suggested that the Mera lahar caused the Río Pastaza to alter its course and, consequently flow rates (deposition and erosion) along its reach, in the Pleistocene (Espín, 2014). Figure 7.4 (d-f) illustrates the potential impact of the debris flow/Mera lahar on the local environment at Mera

Tigre East, i.e. the river channel (Unit 1) was filled and the gradient of the slope was reduced, thus creating a surface suitable for sediment deposition and preservation. It is likely that the debris flow prevented the river of Unit 1 from running its course at Mera Tigre East creating a suitable area for a swamp to develop; this swamp provided the area suitable for deposition and preservation. As well as altering the depositional environment, debris flows have been shown to alter vegetation communities (see Iverson, 1997, May and Gresswell, 2004). Historically, volcanic events have been recorded as having a similar, but smaller scale, impact on river valley landscapes on the EAF; for example an eruption by Tungurahua dammed the Pastaza river in AD 1773 (Harden, 2006, Le Pennec et al., 2008).

7.6.1.3. Unit 3

The low gradient of the debris flow deposit (Unit 2) allowed swampy and/or shallow water conditions to develop, accumulate and preserve a thick sequence of organic and inorganic deposits (Unit 3, Figure 7.4g-j). Unit 3's pollen assemblage obtained from the preserved organic layers was split into two distinct lower (Figure 7.2; layers A-B, Figure 7.4i) and upper (Figure 7.2; layers C-J, Figure 7.4j) sub-units.

In terms of vegetation the lower part of Unit 3 (Figure 7.2; layers A-B) was dominated by the palm *Wettinia* spp. indicating the presence of a palm swamp. The increase in *Wettinia* is immediately above layer 1. *Wettinia* spp. is known to colonise readily on forest edges or cleared (but not deforested) landscapes (Henderson et al., 1995). This suggests that the volcanic eruption could have cleared vegetation present in the landscape, allowing *Wettinia* spp. to dominate the flat shallow water which formed post Unit 2 (Figure 7.4i). It is likely that the volcanic eruption and debris flow preserved in Unit 2 would have largely cleared vegetation in its path, leaving behind a layer with a concrete like consistency composed of a lithic sandy mixture. In contrast to layers A-B, vegetation in the upper part of Unit 3 (Figure 7.2; layers C-J) was interpreted as lower montane forest vegetation (Figure 7.4). Pollen taxa such as Moraceae/Urticaceae,

Myrtaceae, Asteraceae and Poaceae were present in high concentrations, alongside the presence of preserved macrofossils (Figure 7.2). Five inorganic layers (Figure 7.2; layers 2-6) are present within the upper part of Unit 3, and these have been interpreted as indicative of volcanic eruptions, preserved as tephra layers, due to the nature of the sediment in geochemical analysis (Figure 7.3), alongside their appearance in the field (grey with the presence of visible minerals such as feldspar and biotite) and the presence of plagioclase and biotite when observed using optical microscopy. Interestingly, the volcanic events (tephra deposits up to 0.81 m thick) do not appear to greatly perturb the vegetation composition, i.e. pollen assemblages before and after deposition are similar. This could be due to the fine-grained nature of the ash layers and the high levels of precipitation allowing the dilution of the ash layers. It is also likely that the tephra did not fall as one continuous layer and that it fell in multiple layers during a main eruptive episode.

Sediment composition throughout Unit 3 remained organic (Figure 7.2), suggesting that the depositional environment remained the same. The volcanic eruptions preserved throughout Unit 3 were associated with a range of difference volcanic source types (basalt, andesitic and picro-basalt); suggesting tephra deposits were from a range of different volcanoes implying a wide volcanic source area or a mixing of samples occurring at the time of deposition (through crustal contamination during eruption or mixing with sediment already on the surface).

7.6.1.4. Unit 4

Inorganic layers 7, 9 and 12 (Figure 7.2) are composed of moderately sorted sands and gravels, and this combined with their appearance in the field were interpreted as of fluvial origin. These layers occur concurrently with a decrease in the proportion of organic content within the organic layers (compare Unit 3, layers A-J with Unit 4, layers K-P; Figure 7.2). The fluvial deposits are interpreted as overbank (flood) deposits associated with a nearby incising river (Figure 7.4 k-m). The high siliciclastic input from the river explains the reduction in the organic component of the sediment (Figure 7.4). The nearby fluvial activity might have altered the depositional

environment from a forested swamp to a floodplain (Figure 7.4). Inorganic layers 8, 10, 13 and 14 are interpreted as volcanic tephras due to their appearance in the field alongside the geochemical analysis and the presence of biotite and plagioclase under an optical microscope. Geochemical analysis was not performed on the remaining inorganic layers due to the presence of moderately sorted sands and gravels in them indicating they were different to the other inorganic layers, this was noted in the field. The compositional variability of these volcanic layers suggests a large source area for volcanic sediment deposition.

Alongside the physical proxy evidence for a shift to a more fluvial influenced depositional environment, the pollen assemblage altered from taxa typical of lower montane forest (Myrtaceae, Asteraceae and Moraceae/Urticaceae) to taxa today found at higher elevations (*Podocarpus*, *Celtis*, Asteraceae and Poaceae). The concomitant change in sediment type and pollen taxa is interpreted as indicative of a change in pollen source area, i.e. a switch from local/regional pollen signal input into a swamp or shallow lake (Unit 3), to a floodplain environment with a higher proportion of pollen arriving via fluvial transport along the course of the river. The Alpayacu river, adjacent to the study site today, has a catchment of ~15,000 km^2 (c. 5% of Ecuador's land surface) before it reaches Mera Tigre East today (Figure 7.1). If the catchment of the ancient river responsible for the floodplain deposits in Unit 4 were of a similar scale to the Alpayacu, then it could easily have transported pollen grains from high elevation taxa and deposited it in the Mera area.

7.6.1.5. Unit 5

Unit 5 comprises a thick inorganic layer (layer 15; >1.5 m) which covers the stratigraphic section. Layer 15 was also interpreted as a volcanic tephra due to its appearance in the field. The tephra is overlain by a thin soil which supports modern vegetation. The tephra and the soil reduce the risk of the stratigraphic section being eroded away by processes such as weathering,

bioturbation and fluvial activity. The spatial extent of Unit 5 is unknown; however, the layer definitely covers the whole of the preserved sediments at Mera Tigre East (Figure 7.4 n-p).

7.6.2. Sediment deposition on the eastern Andean flank

7.6.2.1. Volcanic influence

Debris flows from volcanic sources are widespread across the Ecuadorian Andes (Hall et al., 2008, Mothes et al., 2004). A comparable size debris flow to the one found at Mera Tigre East (Unit 2) originating from Cotopaxi volcano (c. 4500 cal yr BP) covered 440 km^2 with c. 2-3 m of material (Mothes et al., 1998). Another debris flow from Cotopaxi volcano (2400 cal yr BP) caused a nearby valley (Latacunga) to be overlain by c. 8 m of volcanic deposit in a single event (Mothes et al., 2015). Furthermore, a recent (AD 1987) debris flow in Ecuador has been observed to alter the direction and channel form of rivers (Schuster et al., 1996), similar to our hypothesis of what happened to the river represented by Unit 1 of the stratigraphic sequence (Figure 7.4).

Volcanic eruptions in Ecuador have been shown to disrupt the sedimentation, alter the type of sediment being deposited and have an impact on the depositional environment. The debris flow at Mera Tigre East (Unit 2) is an example of the impact an extremely large debris flow can have at a landscape scale, i.e. it changed the elevation profile of the EAF regionally to create a flat shallow basin suitable for sedimentary deposition (compare Figure 7.4 a-c with d-f). Without the debris flow, the organic and tephra sediments (Units 3 and 4) would most likely not have accumulated at Mera Tigre East. As such, the debris flow was a landscape defining event essential in the deposition of the sedimentary sequence.

It is interesting to compare, based on sediments nature (shallow water swamp/ bog), time interval spanned (Pleistocene) and distance between sites (102 km), the pollen assemblage fluctuation at

Mera Tigre East (Figure 7.2) with those found at Erazo (Cárdenas et al., 2011a, Cárdenas et al., 2011b). Erazo is preserved as an open stratigraphic sequence and it was also impacted by volcanic activity in the recent geological past. At Mera Tigre East the pollen assemblage shift in the upper portion of the sequence is related to a change in depositional environment (swamp/shallow lake to floodplain), whilst at Erazo no change in the depositional environment is concurrent with the pollen assemblage shift (Cárdenas et al., 2011b). The Mera Tigre East pollen assemblage shift, is, therefore, attributed to a change in the proportion of local/regional vs. extra-regional pollen, whereas the Erazo signal is thought to be climatic (Cárdenas et al., 2011b). However, the radiocarbon age in layer O of Mera Tigre East places this part of the sequence in the last glacial, it cannot, therefore, be discounted that at least part of this upper pollen signal could also be as a result of cooler than modern temperatures leading to downslope taxa migration, similar to that observed Erazo (Cárdenas et al., 2011a).

7.6.2.2. Fluvial influence

Across the EAF fluvial activity is high (Harden, 2006), with many tributaries contributing to the massive outflow from the Amazon River (annual discharge: 6.6×10^{12} m^3 of water and 800×10^6 t of sediment; Laraque et al., 2009) . The high fluvial activity means that fluvial erosion, transport and deposition is dynamic (Lal, 1995), and is likely to result in variation in the proportion of local, regional and extra-regional signal contained within the palaeoecological record derived from indicators such as pollen.

A previous eastern Andean flank study site, Mera, was heavily debated in regards to whether or not the published age for the site was as a result of contamination from material transported in lahars and/or nearby debris laden rivers (Heine, 1994, Liu and Colinvaux, 1985). The debate was as a result of research performed by Heine (1994) and this study highlighted the importance of fully understanding the depositional environment of an open stratigraphic sequence such as Mera or Mera Tigre East. In Mera Tigre East it was very evident that a fluvial system existed at the

time of deposition in the upper part of the sequence (Unit 4; see Figures 7.2 and 7.4). In contrast, at the original Mera site, the wood sample in question (dated to 33,520 ± 1010 yr BP, using Calib 7.1, the 2 sigma calibrated age using the Southern Hemisphere calibration curve is 35,408-40,022 Cal yr BP, Reimer et al., 2013) was extracted from marsh/ soil deposits containing wood macrofossils up to 10 cm in size (Liu and Colinvaux, 1985). The sedimentary evidence from Liu and Colinvaux suggested that the sediments they examined from near Mera were not fluvially influenced, consequently, unlike Unit 4 of Mera Tigre East, the ecological signal contained within the sediments can be considered as a local signal. This means that the wood remain dated by Liu and Colinvaux is likely to be indicative of the actual age of deposition and that the theory of fluvial contamination causing a lower age seems unlikely (Heine, 1994, Liu and Colinvaux, 1985).

7.6.3. Sedimentary preservation of the eastern Andean flank

7.6.3.1. Volcanic influence

The Mera Tigre East (Figure 7.2) and Erazo (Cárdenas et al., 2014, Cárdenas et al., 2011a) sedimentary sequences both have significant (>0.5 m thick) "capping" volcanic deposits. It is hypothesised that these thick deposits of volcanic origin played a key role in protecting the underlying sedimentary layers from subsequent fluvial erosion. At both Mera Tigre East and Erazo, the exposure is on the edge of a modern river valley, so fluvial incision through these "capping" deposits is obviously possible; however, maybe a locally thicker deposit contributed to the preservation. Within both the Mera Tigre East and Erazo sections there are also thinner (<0.10 m thick) tephra deposits. In the field, it was noted that macrofossil deposits were often found immediately below these tephra deposits (Figure 7.2; layers 2-5). The close relationship between macrofossils and tephra is interpreted as the crushing of living woody plants by the volcanic fallout. The presence of these wood remains are highly valuable for their subsequent use in radiocarbon analysis and their ecological value as additional taxa identification. It,

therefore, appears that both large (capping) and small tephra deposits play a significant positive role in preserving sedimentary deposits suitable for palaeoecological investigations on the EAF.

7.6.3.2. Fluvial influence

Fluvial activity on the EAF is high and constantly mobilising, transporting, and depositing sediments. The impact of rivers on sediment preservation is, therefore, largely negative (reworking and erosion) from the perspective of palaeoecological investigations. Despite the negative connotations associated with fluvial influence, without this influence the Mera Tigre East site would not have been exposed, meaning that it can occasionally play a positive role.

7.7. Conclusions

The sequence preserved at Mera Tigre East has been impacted by both fluvial and volcanic drivers of change. However, despite these drivers sediments were preserved during the Pleistocene, and influence from long distance sources (regional and extra regional) was minimal (restricted to Unit 4). The capping deposit found in Unit 5 ensured the sediments were preserved to the present day and that erosive processes acting upon the site were minimal. The debris flow present in Unit 2 allowed sediment deposition, by creating a flat swamp/shallow water environment. Volcanic events, including the debris flow of Unit 2, are, therefore, integral in the formation and subsequent preservation of potential palaeoecological archives on the EAF.

Fluvial events also have wide implications for the preservation, and interpretation of sedimentary archives. The debris flow Unit preserved in Unit 2 most likely prevented the river represented in Unit 1 from running its course through the Mera Tigre East site (Espín, 2014), providing a suitable area for a swamp environment to develop (this in turn allowed the deposition and preservation of sediments). The deposition of the debris flow would have caused the river to incise a new course through the environment. Fluvial activity can also alter the depositional source area, the source area being driven by the size of a catchment area. Long distance transport

due to a large catchment has implications for the interpretation of a sedimentary archive. In Mera Tigre East long distance fluvial transport was restricted to Unit 4, with the sediments in this Unit having a large source area from within the catchment, based on the presence of fluvial sediments implying the incision of a river near to the stratigraphic section. In order for Unit 4 to be interpreted correctly the source area of the sediments needs to be taken into account to discount regional influence. For Mera Tigre East, Unit 4, the deposit should be interpreted as having a strong regional and extra-regional component. The depositional environment of records with fluvial influence should be carefully interpreted (as in this interpretation of Mera Tigre East) before/ if they are used to interpret local climatic change, as the source area could be more representative of a regional signal (such as in Unit 4 of Mera Tigre East). Understanding the depositional environment of palaeoecological sites is critical if data from them can be relied upon to help reconstruct the environment, and, therefore, be used to help protect the EAF conservation hotspot in the future. Therefore, before inferences about palaeoenvironmental change are made, the depositional environment of a site should be thoroughly investigated to ensure that conclusions are based on the correct source area, be it local or regional. By doing this, it can be certain that the palaeoenvironment and palaeoclimate has been correctly interpreted so that future environmental change can be contextualised.

Acknowledgments

This work was undertaken as part of a PhD studentship (HFK) funded by NERC (NE/J500288/1) and The Open University. The analysis for the radiocarbon sample was performed at the Beta Analytic Radiocarbon facility in Florida. Thanks are provided to the late John Watson at The Open University for assistance with the XRF sample processing.

7.8. Summary

In this chapter the depositional environment of Mera Tigre East was explored, investigating in particular how fluvial and volcanic processes influenced upon the deposition and preservation of sediments sampled. The source area for the Mera Tigre East sediments was analysed with Unit 4 having a regional source area and Unit 3 a local source area. The impact of these fluvial and volcanic processes on sediment preservation for a wider context was then discussed. The next chapter (Chapter 8) discusses the vegetation history preserved at the Mera Tigre sites, taking into consideration the pollen source area for Mera Tigre East. The chapter also looks at how fire (preserved as charcoal) impacted upon the vegetation.

References

AREQUIPA, J. E. B. 2008. *Las Avalanchas de Escombros en el sector del volcán Tungurahua (Debris avalanche in the field of Tungurahua volcano).* Escuela Politecnica Nacional.

BARBA, D., ROBIN, C., SAMANIEGO, P. & EISSEN, J.-P. 2008. Holocene recurrent explosive activity at Chimborazo volcano (Ecuador). *Journal of Volcanology and Geothermal Research,* 176**,** 27 - 35.

BARLOW, J., GARDNER, T. A., ARAUJO, I. S., ÁVILA-PIRES, T. C., BONALDO, A. B., COSTA, J. E., ESPOSITO, M. C., FERREIRA, L. V., HAWES, J., HERNANDEZ, M. I. M., HOOGMOED, M. S., LEITE, R. N., LO-MAN-HUNG, N. F., MALCOLM, J. R., MARTINS, M. B., MESTRE, L. A. M., MIRANDA-SANTOS, R., NUNES-GUTJAHR, A. L., OVERAL, W. L., PARRY, L., PETERS, S. L., RIVEIRO-JUNIOR, M. A., DA SILVA, M. N. F., DA SILVA, C. & PERES, C. A. 2007. Quantifying the biodiversity value of tropical primary, secondary, and plantation forests. *Proceedings of the National Academy of Sciences,* 104**,** 18555-18560.

BEHLING, H., BERRIO, J. C. & HOOGHIEMSTRA, H. 1999. Late Quaternary pollen records from the middle Caquetá river basin in central Colombian Amazon. *Palaeogeography, Palaeoclimatology, Palaeoecology,* 145**,** 193 - 213.

BERNAL, C., CHRISTOPHOUL, F., DARROZES, J., SOULA, J.-C., BABY, P. & BURGOS, J. 2011. Late Glacial and Holocene avulsions of the Rio Pastaza Megafan (Ecuador–Peru): Frequency and controlling factors. *International Journal of Earth Sciences,* 100**,** 1759-1782.

BERNAL, C., CHRISTOPHOUL, F., SOULA, J. C., DARROZES, J., BOURREL, L., LARAQUE, A., BURGONS, J., BÈS DE BERC, S. & BABY, P. 2012. Gradual diversions of the Rio Pastaza in the Ecuadorian piedmont of the Andes from 1906 to 2008: Role of tectonics, alluvial fan aggradation, and ENSO events. *International Journal of Earth Sciences,* 101**,** 1913 - 1928.

BÈS DE BERC, S., SOULA, J. C., BABY, P., SOURIS, M., CHRISTOPHOUL, F. & ROSERO, J. 2005. Geomorphic evidence of active deformation and uplift in a modern continental wedge-top–foredeep transition: Example of the eastern Ecuadorian Andes. *Tectonophysics,* 399**,** 351-380.

BIGGS, J., MOTHES, P., RUIZ, M., AMELUNG, F., DIXON, T. H., BAKER, S. & HONG, S.-H. 2010. Stratovolcano growth by co-eruptive intrusion: The 2008 eruption of Tungurahua Ecuador. *Geophysical Research Letters,* 37**,** 1 - 5.

BOOKHAGEN, B. & STRECKER, M. R. 2008. Orographic barriers, high-resolution TRMM rainfall, and relief variations along the eastern Andes. *Geophysical Research Letters,* 35**,** 1 - 6.

BOOKHAGEN, B. & STRECKER, M. R. 2010. Modern Andean rainfall variation during ENSO cycles and its impact on the Amazon drainage basin. *In:* HOORN, C. & WESSELINGH, F. P. (eds.) *Amazonia, landscape and species evolution: A look into the Past.* Chichester, UK: Wiley-Blackwell.

BOURDON, E., EISSEN, J.-P., MONZIER, M., ROBIN, C., MARTIN, H., COTTEN, J. & HALL, M. L. 2002. Adakite-like lavas from Antisana volcano (Ecuador): Evidence for slab melt metasomatism beneath the Andean Northern Volcanic Zone. *Journal of Petrology,* 43**,** 199 - 217.

BURN, M. J., MAYLE, F. E. & KILLEEN, T. J. 2010. Pollen - based differentiation of Amazonian rainforest communities and implications for lowland palaeoecology in tropical South America. *Palaeogeography, Palaeoclimatology, Palaeoecology,* 295**,** 1 - 18.

BUSH, M. B. 2002. Distributional change and conservation on the Andean flank: A palaeoecological perspective. *Global Ecology and Biogeography,* 11**,** 463 - 473.

BUSH, M. B., COLINVAUX, P. A., WIEMANN, M. C., PIPERNO, D. E. & LIU, K.-B. 1990. Late Pleistocene temperature depression and vegetation change in Ecuadorian Amazonia. *Quaternary Research,* 34**,** 330 - 345.

BUSH, M. B., HANSEN, B. C. S., RODBELL, D. T., SELTZER, G. O., YOUNG, K. R., LEÓN, B., ABBOTT, M., SILMAN, M. R. & GOSLING, W. D. 2005. A 17 000-year history of Andean climate and vegetation change from Laguna de Chochos, Peru. *Journal of Quaternary Science,* 20**,** 703-714.

BUSH, M. B., PIPERNO, D. R., COLINVAUX, P. A., DE OLIVEIRA, P. E., KRISSEK, L. A., MILLER, M. C. & ROWE, W. E. 1992. A 14 300-YR paleoecological profile of a lowland tropical lake in Panama. *Ecological Monographs,* 62**,** 251 - 275.

BUSH, M. B. & WENG, C. 2007. Introducing a new (freeware) tool for palynology. *Journal of Biogeography,* 34**,** 377-380.

BUSH, M. B. C., P.A. 1990. A pollen record of a complete glacial cycle from lowland Panama. *Journal of Vegetation Science***,** 105 - 118.

CÁRDENAS, M. L., GOSLING, W. D., PENNINGTON, R. T., POOLE, I., SHERLOCK, S. C. & MOTHES, P. 2014. Forests of the tropical eastern Andean flank during the middle Pleistocene. *Palaeogeography, Palaeoclimatology, Palaeoecology,* 393**,** 76 - 89.

CÁRDENAS, M. L., GOSLING, W. D., SHERLOCK, S. C., POOLE, I., PENNINGTON, R. T. & MOTHES, P. 2011a. The response of vegetation on the Andean flank in Western Amazonia to Pleistocene climate change. *Science,* 331**,** 1055-1058.

CÁRDENAS, M. L., GOSLING, W. D., SHERLOCK, S. C., POOLE, I., PENNINGTON, R. T. & MOTHES, P. 2011b. Response to comment on "The response of vegetation on the Andean flank in Western Amazonia to Pleistocene climate change". *Science,* 333**,** 1825c.

CHAMBERS, J. Q., HIGUCHI, N. & SCHIMEL, J. P. 1998. Ancient trees in Amazonia. *Nature,* 391**,** 135 - 136.

COLINVAUX, P. A., DE OLIVEIRA, P. E., MORENO, J. E., MILLER, M. C. & BUSH, M. B. 1996. A long pollen record from lowland Amazonia: Forest and cooling in glacial times. *Science,* 274**,** 85 - 88.

COLINVAUX, P. A., DE OLIVEIRA, P. E. & PATIÑO, J. E. M. 1999. *Amazon pollen manual and atlas,* Amsterdam, Harwood Academic Publishers.

COOK, K. H. 2009. South American climate variability and change: remote and regional forcing processes. *In:* VIMEAUX, F. S., F. & KHODRI, M. (eds.) *South American climate variability and change: Remote and regional forcing processes.* Paris: Springer.

DEAN, W. E. 1974. Determination of carbonate and organic matter in calcaerous sediments and sedimentary rocks by loss on ignition: Comparison with other methods. *Journal of Sedimentary Research (SEPM),* 44**,** 242 - 248.

DENMAN, K. L., BRASSEUR, G., CHIDTHAISONG, A., CIAIS, P., COX, P. M., DICKINSON, R. E., HAUGLUSTAINE, D., HEINZE, C., HOLLAND, E., JACOB, D., LOHMANN, U., S., R., DA SILVA DIAS, P. L., WOFSY, S. C. & ZHANG, X. 2007. Couplings between changes in the climate system and biogeochemistry. *In:* SOLOMON, S., QIN, D., MANNING, M., CHEN, Z., MARQUIS, M., AVERYT, K. B., TIGNOR, M. & MILLER, H. L. (eds.) *Climate change 2007.* Cambridge, United Kingdom: Cambridge University Press.

ENZWEILER, J. & WEBB, P. C. 1996. Determination of trace elements in silicate rocks by X-ray fluorescence spectrometry on 1:5 glass discs: Comparison of accuracy and precision with pressed powder pellet analysis. *Chemical Geology,* 1996**,** 195 - 202.

ESPÍN, B. P. A. 2014. *Caracterizacin geológica y litoógica de los depósitos laháricos de Mera, provincia de Pastaza (Geological and lithological characterisation of lahar deposits, Mera province of Pastaza).* Escuela Politécnica Nacional, Quito.

FEELEY, K. J., MALHI, Y., ZELAZOWSKI, P. & SILMAN, M. R. 2012. The relative importance of deforestation, precipitation change, and temperature sensitivity in determining the future distributions and diversity of Amazonian plant species. *Global Change Biology,* 18**,** 2636 - 2647.

FERDON, E. N. J. 1950. *Studies in Ecuadorian Geography,* Santa Fe, New Mexico, School of American Research and University of Southern California.

FRANCISQUINI, M. I., LIMA, C. M., PESSENDA, L. C. R., ROSSETTI, D. F., FRANÇA, M. C. & COHEN, M. C. L. 2014. Relation between carbon isotopes of plants and soils on Marajó Island, a large tropical island: Implications for interpretation of modern and past vegetation dynamics in the Amazon region. *Palaeogeography, Palaeoclimatology, Palaeoecology*.

GARREAUD, R. D. & ACEITUNO, P. 2007. Atmospheric circulation over South America: Mean features and variability. *In:* VEBLEN, T., YOUNG, K. & ORME, A. (eds.) *The Physical Geography of South America.* Oxford: Oxford University Press.

GARRISON, J., DAVIDSON, J., REID, M. & TURNER, S. 2006. Source versus differentiation controls on U-series disequilibria: Insights from Cotopaxi Volcano, Ecuador. *Earth and Planetary Science Letters,* 244**,** 548-565.

GARRISON, J. M., DAVIDSON, J. P., HALL, M. L. & MOTHES, P. 2011. Geochemistry and petrology of the most recent deposits from Cotopaxi volcano, Northern Volcanic Zone, Ecuador. *Journal of Petrology,* 52**,** 1641 - 1678.

GREGORY-WODZICKI, K. M. 2000. Uplift history of the Central and Northern Andes: A review. *GSA Bulletin,* 112**,** 1091 - 1105.

GUILLIER, B. & CHATELAIN, J.-L. 2006. Evidence for a seismic activity mainly constituted of hybrid events at Cayambe volcano, Ecuador. Interpretation in a iced-domes volcano context. *Comptes Rendus Geoscience,* 338**,** 499 - 506.

HALL, M. L., ROBIN, C., BEATE, B., MOTHES, P. & MONZIER, M. 1999. Tungurahua Volcano, Ecuador: Structure, eruptive history and hazards. *Journal of Volcanology and Geothermal Research,* 91**,** 1 - 21.

HALL, M. L., SAMANIEGO, P., LE PENNEC, J. L. & JOHNSON, J. B. 2008. Ecuadorian Andes volcanism: A review of Late Pliocene to present activity. *Journal of Volcanology and Geothermal Research,* 176**,** 1 - 6.

HANSELMAN, J. A., BUSH, M. B., GOSLING, W. D., COLLINS, A., KNOX, C., BAKER, P. A. & FRITZ, S. C. 2011. A 370.000-year record of vegetation and fire history around

Lake Titicaca (Bolivia/ Peru). *Palaeogeography, Palaeoclimatology, Palaeoecology,* 305**,** 201 - 214.
HARDEN, C. P. 2006. Human impacts on headwater fluvial systems in northern and central Andes. *Geomorphology,* 79**,** 249-263.
HARLING, G. 1979. The vegetation types of Ecuador - A brief survey. *In:* LARSEN, K. & HOLM-NIELSEN, L. B. (eds.) *Tropical botany.* London: Academic press.
HEINE, K. 1994. The Mera site revisited: Ice - age Amazon in the light of new evidence. *Quaternary International,* 21**,** 113 - 119.
HEIRI, O., LOTTER, A.F. AND LEMCKE, G 2001. Loss on ignition as a method for estimating organic and carbonate content in sediments: reproducibility and comparability of results. *Journal of Paleolimnology,* 25**,** 101 - 110.
HENDERSON, A., GALEANO, G. & BERNAL, R. 1995. *Field guide to the Palms of the Americas.,* Princeton, New Jersey, Princeton University Press.
HESSLER, I., DUPONT, L., BONNEFILLE, R., BEHLING, H., GONZÁLEZ, C., HELMENS, K. F., HOOGHIEMSTRA, H., LEBAMBA, J., LEDRU, M.-P., LÉZINE, A.-M., MALEY, J., MARRET, F. & VINCENS, A. 2010. Millennial-scale changes in vegetation records from tropical Africa and South America during the last glacial. *Quaternary Science Reviews,* 29**,** 2882 - 2899.
HIJMANS, R. J., GUARINO, L., BUSSINK, C., MATHUR, P., CRUZ, M., BARRENTES, I. & ROJAS, E. 2004. *DIVA-GIS. Vsn. 5.0. A geographic information system for the analysis of species distribution data.* [Online]. Available: http://www.diva-gis.org.
HOOGHIEMSTRA, H. 1984. *Vegetational and climatic history of the high plain of Bogotá, Colombia: A continuous record of the last 3.5 million years.* . PhD, UVA.
INSEL, N., POULSEN, C. J. & EHLERS, T. A. 2009. Influence of the Andes Mountains on South American moisture transport, convection, and precipitation. *Climate Dynamics,* 35**,** 1477 - 1492.
IVERSON, R. M. 1997. The physics of debris flows. *Review of Geophysics,* 35**,** 245 - 296.
KEEN, H. F., GOSLING, W. D., HANKE, F., MILLER, C. S., MONTOYA, E., VALENCIA, B. G. & WILLIAMS, J. J. 2014. A statistical sub-sampling tool for extracting vegetation community and diversity information from pollen assemblage data. *Palaeogeography, Palaeoclimatology, Palaeoecology,* 408**,** 48 - 59.
KUENZI, D. W., HORST, O. H. & MCGEHEE, R. V. 1979. Effect of volcanic activity on fluvial-deltaic sedimentation in a modern arc-trench gap, southwestern Guatemala. *Geological Society of America Bulletin.,* 90**,** 827-838.
LAL, R. 1995. Global soil erosion by water and carbon dynamics. *In:* LAL, R., KIMBLE, J. M., LEVINE, E. R. & STEWART, B. A. (eds.) *Soils and global change.* Florida: CRC Press.
LARAQUE, A., BERNAL, C., BOURREL, L., DARROZES, J., CHRISTOPHOUL, F., ARMIJOS, E., FRAIZY, P., POMBOSA, R. & GUYOT, J. L. 2009. Sediment budget of the Napo River, Amazon basin, Ecuador and Peru. *Hydrological Processes,* 23**,** 3509 - 3524.
LE PENNEC, J. L., JAYA, D., SAMANIEGO, P., RAMÓN, P., YÁNEZ, S. M., EGRED, J. & VAN DER PLICHT, J. 2008. The AD 1300-1700 eruptive periods at Tungurahua volcano, Ecuador, revelaed by historical narratives, stratigraphy and radiocarbon dating. *Journal of Volcanology and Geothermal Research,* 176**,** 70-81.
LEES, J. M., JOHNSON, J. B., RUIZ, M., TRONCOSO, L. & WELSH, M. 2008. Reventador volcano 2005: Eruptive activity inferred from seismo-acoustic observation. *Journal of Volcanology and Geothermal Research,* 176**,** 179 - 190.
LEWIS, S. L., LLOYD, J., SITCH, S., MITCHARD, E. T. A. & LAURANCE, W. F. 2009. Changing ecology of tropical forests: evidence and drivers. *Annual Review of Ecology, Evolution and Systematics,* 40**,** 529 - 549.
LIU, K.-B. & COLINVAUX, P. A. 1985. Forest changes in the Amazon Basin during the last glacial maximum. *Nature,* 318**,** 556 - 557.

MALHI, Y., ROBERTS, J. T., BETTS, R. A., KILLEEN, T. J., LI, W. & NOBRE, C. A. 2008. Climate change, deforestation, and the fate of the Amazon. *Science,* 319**,** 169-172.

MANVILLE, V., HODGSON, K. A. & NAIRN, I. A. 2010. A review of break-out floods from volcanogenic lakes in New Zealand. *New Zealand Journal of Geology and Geophysics,* 50**,** 131-150.

MAY, C. L. & GRESSWELL, R. E. 2004. Spatial and temporal patterns of debris-flow deposition in the Oregon Coast Range, USA. *Geomorphology,* 57**,** 135 - 149.

MAYLE, F. E., LANGSTROTH, R. P., FISHER, R. & MEIR, P. 2006. Long-term forest-savannah dynamics in the Bolivian Amazon: Implications for conservation. *Philosophical Transactions of the Royal Society B: Biological Sciences,* 367**,** 291-301.

MONTGOMERY, D. R., BALCO, G. & WILLETT, S. D. 2001. Climate, tectonics, and the morphology of the Andes. *Geology,* 29**,** 579 - 582.

MONZIER, M., ROBIN, C., SAMANIEGO, P., HALL, M. L., COTTEN, J., MOTHES, P. & ARNAUD, N. 1999. Sangay volcano, Ecuador: Structural development, present activity and petrology. *Journal of Volcanology and Geothermal Research,* 90**,** 49 - 79.

MOORE, P. D., WEBB, J. A. & COLLINSON, M. E. 1991. *Pollen analysis,* Oxford, Blackwell Scientific.

MOTHES, P., HALL, M. L., ANDRADE, D., SAMANIEGO, P., PIERSON, T. C., RUIZ, A. G. & YEPES, H. 2004. Character, stratigraphy and magnitude of historical lahars of Cotopaxi volcano (Ecuador). *Acta Vulcanologica,* 16**,** 1-23.

MOTHES, P., HALL, M. L. & JANDA, R. J. 1998. The enormous Chillos Valley Lahar: an ash-flow-generated debris flow from Cotopaxi Volcano, Ecuador. *Bulletin of Volcanology,* 59**,** 233 - 244.

MOTHES, P., VALLANCE, J. W., HALL, M. L. & GARRISON, J. M. 2015. Cotopaxi's most recent rhyolitic eruption, 2400 yBP. *International union of Geodesy and Geophysics (IUGG).* Prague, Czech Republic.

NIEMANN, H. & BEHLING, H. 2008. Late Quaternary vegetation, climate and fire dynamics inferred from the El Tiro record in the southeastern Ecuadorian Andes. *Journal of Quaternary Science,* 23**,** 203-212.

NOVAK, I. D. 1972. Swash-zone competency of gravel-size sediment. *Marine Geology,* 13**,** 335-345.

OBANDO, J. P. O. 2012. *Depósitos volcánicos del Pleistoceno Tardío en la cuenca de Ambato: caracterización, distribución y origen.* Escuela Politécnica nacional.

PUNYASENA, S. W., DALLING, J. W., JARAMILLO, C. A. & TURNER, B. L. 2011. Comment on "The response of vegetation on the Andean flank in Western Amazonia to Pleistocene climate change". *Science,* 333**,** 1825b.

REIMER, P. J., BARD, E., BAYLISS, A., BECK, J. W., BLACKWELL, P. G., RAMSEY, C. B., BUCK, C. E., CHENG, H., EDWARDS, R. L., FRIEDRICH, M., GROTTES, P. M., GUILDERSON, T. P., HAFLIDASON, H., HAJDAS, I., HATTÉ, C., HEATON, T. J., HOFFMANN, D. L., HOGG, A. G., HUGHEN, K. A., KAISER, K. F., KROMER, B., MANNING, S. W., NIU, M., REIMER, R. W., RICHARDS, D. A., SCOTT, E. M., SOUTHON, J. R., STAFF, R. A., TURNEY, C. S. M. & VAN DER PLICHT, J. 2013. IntCal13 and Marine13 Radiocarbon Age Calibration Curves 0-50,000 Years cal BP. *Radiocarbon,* 55.

RESTREPO, J. D., LÓPEZ, S. A. & RESTREPO, J. C. 2009. The effects of geomorphic controls on sediment yield in the Andean rivers of Colombia. *Latin American Journal of Sedimentology and Basin Analysis,* 16**,** 79-92.

RODBELL, D. T. 1993. The timing of the last deglaciation in Cordillera Oriental, northern Peru, based on glacial geology and lake sedimentology. *Geological Society of America Bulletin.,* 105**,** 923 - 934.

ROSQVIST, G. C. 1995. Proglacial lacustrine sediments from El Altar, Ecuador: Evidence for late - Holocene climatic change. *The Holocene,* 5**,** 111-117.

ROUBIK, D. W. & MORENO, J. E. P. 1991. *Pollen and spores of Barro Colorado Island,* United States, Missouri Botanical Garden.

SAMANIEGO, P., BARBA, D., ROBIN, C., FORNARI, M. & BERNARD, B. 2012. Eruptive history of Chimborazo volcano (Ecuador): A large, ice - capped and hazardous compound volcano in the Northern Andes. *Journal of Volcanology and Geothermal Research,* 221 - 222**,** 33 - 51

SAMANIEGO, P., MARTIN, H., MONZIER, M., ROBIN, C., FORNARI, M., EISSEN, J.-P. & COTTEN, J. 2005. Temporal evolution of magmatism in the Northern Volcanic Zone of the Andes: The geology and petrology of Cayambe Volcanic complex (Ecuador). *Journal of Petrology,* 46**,** 2225 - 2252.

SCHUSTER, R. L., NIETO, A. S., O'ROURKE, T. D., CRESPO, E. & PLAZA-NIETO, G. 1996. Mass wasting triggered by the 5 March 1987 Ecuador earthquakes. *Engineering Geology,* 42**,** 1 - 23.

STOCKMARR, J. 1971. Tablets with spores used in absolute pollen analysis. *Pollen et Spores,* 13**,** 615 - 621.

THOMAS, I. L. & HAUKKA, M. T. 1978. XRF determination of trace and major elements using a single - fused disc. *Chemical Geology,* 1978**,** 39 - 50.

TOIVONEN, T., MÄKI, S. & KALLIOLA, R. 2007. The riverscape of Western Amazonia - a quantitative approach to the fluvial biogeography of the region. *Journal of Biogeography,* 34**,** 1374 - 1387.

TOVAR, C., ARNILLAS, C. A., CUESTA, F. & BUYTAERT, W. 2013. Diverging responses of tropical Andean biomes under future climate conditions. *PLoS ONE,* 8**,** e63634.

VAN DER HAMMEN, T. 1974. The Pleistocene changes of vegetation and climate in tropical South America. *Journal of Biogeography,* 1**,** 3 - 26.

VAN DER HAMMEN, T. 1994. Amazonia during the last glacial. *Palaeogeography, Palaeoclimatology, Palaeoecology,* 109**,** 247 - 261.

VELÁSQUEZ-TIBATÁ, J., SALAMAN, P. & GRAHAM, C. H. 2013. Effects of climate change on species distribution, community structure, and conservation of birds in protected areas in Colombia. *Regional Environmental Change,* 13**,** 235 - 248.

WEBGIS. 2009. *Terrain Data* [Online]. Lakes Environmental Software. Available: http://www.webgis.com/srtm3.html [Accessed 25/02/2013 2013].

Chapter 8: Vegetation and fire dynamics on the eastern Andean flank, Ecuador.

In the previous chapter the depositional environment of the Mera Tigre East study site was analysed, in order to gain an understanding about how sediments suitable for palaeoecological analysis are preserved. It was found that both fluvial and volcanic events were important in the deposition and preservation of sediments at the site, and that the distribution of volcanic deposits could be a useful guide to find further palaeoecological sites on the eastern Andean flank.

This chapter investigates the diverse fossil pollen (vegetation) record preserved in sedimentary layers at the Mera Tigre West and East sections. It also looks at the complex relationship between fire (charcoal) and the composition of the floristically diverse montane forest on the eastern Andean flank. Fossil pollen, spore and charcoal data are presented in this chapter to explain the relationship between the vegetation assemblage and fire activity.

8.1. Introduction

Tropical forests cover just 7 % of the Earth's land surface, however, they are recognised as globally important because they contain the highest biodiversity of all of Earth's terrestrial ecosystems, they store 25 % of global terrestrial carbon, and they play a key role in global climate patterns (Barlow et al., 2007, Denman et al., 2007, Malhi et al., 2008, Zuidema et al., 2013). Current projections indicate that future environmental change could have dire consequences for tropical forests, with high levels of species (biodiversity) loss occurring (Huntingford et al., 2013). Current anthropogenic activities are also impacting biodiversity found within tropical ecosystems, with disturbances such as deforestation and fires causing rapid forest loss (Cardoso et al., 2009).

Despite the global importance of tropical forests, many of these fragile ecosystems are still relatively unknown entities in terms of species composition and vegetation history. This means that the development of robust conservation strategies is challenging; especially when compared to the very well-studied temperate regions (Malhi et al., 2010). The tropical forests on the eastern flank of the Andes mountain range are some of the least understood forests on the globe, despite being recognised as important for biodiversity, and as being threatened by projected climate change and anthropogenic activities (Myers et al., 2000). The lower montane rain forest (LMRF; 700-2500m asl; Harling, 1979, see Section 2.3.2.1) of the eastern Andean flank is one of the endangered ecosystems currently listed as a biodiversity hotspot (Myers et al., 2000). The LMRF contains high levels of flora, including many endemic species (>191 endemics; Borchsenius, 1997). The high biodiversity and many endemics of the LMRF are, however, restricted to a narrow altitudinal distribution found on steep topography, meaning it is highly sensitive to environmental change (Bush, 2004). Therefore, in order to develop effective conservation strategies for the LMRF, an understanding of its likely response to environmental change is required.

Some future climate scenarios suggest that the Amazon could receive less rainfall over the next 100 years, meaning fire occurrence will likely become more of a threat (Barlow and Peres, 2008, Bush et al., 2008), i.e. as the vegetation and soils will receive less moisture, they will be increasingly vulnerable to ignition (natural ignition sources being lightning and volcanic activity). Today the LMRF of the eastern Andean flank receives large amounts of rain (up to >4000 mm a year) (Harling, 1979). High precipitation on the LMRF means that today, fire is not seen as an important ecological control due to the fires not being able to easily take hold in this wet ecosystem (Bush et al., 2008, Cárdenas et al., 2014). However, when present, fire can have an immediate impact on an ecosystem by potentially causing rapid biodiversity changes, i.e. fires

cause a reduction in taxa present in diverse communities, with these taxa being replaced by a limited number of taxa that are able to colonise rapidly, therefore, reducing overall diversity (Bush et al., 2008). Consequently, it is important to investigate what impact a future increase in fire regime would have on the LMRF. As fires do not often occur naturally in the present day (hard to tell their frequency due to dense forest cover masking fire occurrence), it is not easy to look at the present day ecosystem to see how the vegetation responds naturally to burning. However, it has been noted that the vegetation on the eastern Andean flank did burn more frequently prior to human arrival (>12,000 years BP) on the continent, with lightning and volcanic eruptions being probable ignition sources (Baied and Wheeler, 1993, Barnosky and Lindsey, 2010, Belcher et al., 2010, Cárdenas et al., 2014). Therefore, by looking at palaeoecological studies recording vegetation dynamics before 12,000 years ago, an understanding can be gained as to how the projected increase in fire events could impact the LMRF in the future. The Mera Tigre West (MTW) and the Mera Tigre East (MTE) study sites have both been determined to contain sediments deposited prior to 12,000 years ago; MTW samples were radiocarbon infinite (older than 50,000 years; Chapter 6) and the upper part of MTE was radiocarbon dated to 19,965-20,215 cal yr BP (Chapter 6).

Fossil pollen, spores and charcoal from these two stratigraphic sequences deposited prior to human arrival on the eastern flank of the Andes, allow two important palaeoecological questions to be addressed (research aims 4 and 5 of this thesis, see Chapter 1, Section 1.3):

i) In the absence of humans, what was the magnitude of vegetation change on the eastern Andean flank?

ii) Did pre-human natural fires impact vegetation associations on the eastern Andean flank?

8.2. Study site

Two fluvially exposed stratigraphic sections (MTW, 01°27.546 S, 78°06.791 W and MTE, 01°27.546 S, 78°06.199 W, both 1117m asl) were sampled, from within the LMRF on the eastern Andean flank of Ecuador. The sections are c. 0.38 km apart from each other, c. 1 km away from the town of Mera and c. 144 km south east of Ecuador's capital city, Quito (see Chapter 3; Figures 3.1 and 3.2).

8.2.1. Mera Tigre West

MTW is an 8.49 m stratigraphic section, exposed by incision of the present day Río Alpayacu (Section 3.4.1, Figure 3.6). Eleven organic and thirteen inorganic layers were sampled throughout the section (Chapter 4, Section 4.1.3). A capping layer of soil and a further inorganic layer lie on the top of the MTW section; neither deposit was sampled. Fourteen wood macrofossils were also extracted from the MTW stratigraphic section.

8.2.2. Mera Tigre East

MTE is a 12.83 m stratigraphic section exposed by fluvial processes (Section 3.4.2, Figure 3.8). The section is currently 0.29 km away from the nearby Río Alpayacu and the lower portion of the section goes into swampy grassland (pantano; Chapter 3, Figure 3.2). Samples were extracted in the field from sixteen organic layers, fourteen inorganic layers; ten tephra layers and four fluvial layers (Chapter 4, Section 4.1.3), inorganic layers as defined in Chapter 7. Eleven wood macrofossils were also recovered.

8.2.3. Relationship of the MTW and MTE sequences

The MTW and MTE stratigraphic sequences both feature the "Mera lahar" which was deposited during the Pleistocene (see section 7.3.1). However, unfortunately no further stratigraphic or chronological control points have established a link between the two sections (see section 8.5.3).

Further details about both stratigraphic sequences, including detailed information about modern vegetation and climate have been covered in Chapters 2 and 3 (Sections 2.2.3, 2.3.3, 3.1).

8.3. Methodology

In order to obtain the data presented in this chapter, two methodologies were used (analysis of fossil pollen/spores and charcoal particle analysis). These methods have been explained in detail in Chapter 4 (Sections 4.3.1 and 4.3.2), they will be summarised briefly here. Statistical analysis and the zonation of pollen zones are also described below (Sections 4.3.3. and 4.3.4).

Sub-samples of 0.5 cm^3 were taken from all 97 sampled organic layers from both MTW and MTE at a 10 cm resolution for both pollen and macro charcoal analysis (particle size >100 μm).

8.3.1. Fossil pollen and spore analysis

Following standard procedure, organic sediment sub-samples of 0.5 cm^3 taken for pollen analysis underwent acetolysis and Hydrochloric acid, Potassium hydroxide and Hydrofluoric acid digestions (Moore et al., 1991). An exotic marker (*Lycopodium* spores, batch 124961, Lund University) was added to the samples allowing pollen concentrations to be calculated (Maher, 1972, Stockmarr, 1971). Once processed, sub-samples were mounted on slides using glycerol and pollen grains were identified using modern reference material held at The Open University, alongside published reference material (Bush and Weng, 2007, Colinvaux et al., 1999, Hooghiemstra, 1984, Roubik and Moreno, 1991). Total terrestrial pollen grain count sizes were generated using Model 1 of a statistical approach developed in this thesis (see Chapter 5), and count sizes for individual samples varied from 196 to 982. Fossil pollen and spores presented in this chapter occurred in at least one sample, with a value of over 10 % abundance of the total terrestrial pollen grain count.

8.3.1.1. Interpreting palynological records

Due to their small size, fossil pollen and spores can be easily transported long distances by aeolian and fluvial transport mechanisms (Birks and Birks, 1980), care must, therefore, be taken when interpreting fossil pollen and spore records. Chapter 7 discussed specific issues relating to how pollen may have been transported into the Mera Tigre sequences, and how this impacts the interpretation of palaeoecological records.

8.3.2. Macro charcoal (>100 µm) particle analysis

Organic sediment sub-samples of 0.5 cm^3 were processed for charcoal analysis; sub-samples were deflocculated through the addition of 8-10 ml of Potassium hydroxide (KOH); they were left in the KOH for 24 hours. Sub-samples were sieved through 100 µm sieves and washed using deionised water. All charcoal particles within the sediment were then counted and represented as a charcoal particle concentration per cm^3. Charcoal particles were identified due to their angular structure and their high reflectivity (Clark and Royall, 1995).

8.3.2.1 Interpreting charcoal records

As briefly covered in Chapter 4, caution must be taken when interpreting charcoal records, as charcoal particles can be transported long distances (fluvial or aeolian transport) and as such do not necessarily relate simply to a local fire record. Using macro charcoal particles (>100 µm) instead of micro charcoal particles (<100 µm) reduces the risk of long distance transportation (Whitlock and Larsen, 2001); however, this does not completely negate the risk of having a noisy regional/local fire signal. In order to reduce regional noise, only abundant levels of charcoal (charcoal peaks) within the stratigraphic levels are interpreted as local fire events, abundances of charcoal below the 'peak' cut off value get classified as noise only (Whitlock and Larsen, 2001). Interpreting when charcoal concentrations represent a fire peak requires a sediment accumulation rate (derived from a chronology; Higuera et al., 2005); however, as there is no chronology for either MTW or MTE, a different method of determining fire events was

used. In this study, a fire event is defined as a sample in the stratigraphic layer that had a greater number of charcoal particles than the average number of particles calculated from all samples. For MTW the average number of charcoal particles was 596 per cm^3 (rounded to zero decimal points), therefore, any samples with a charcoal particle number greater than this will be described as a fire event. In MTE the average number of charcoal particles per cm^3 is 811 (rounded to zero decimal points); samples with a particle number greater than this will be classified as a fire event.

8.3.3. Statistical analysis

Four statistical techniques were applied to MTW and MTE pollen and charcoal data: i) Correspondence analysis ii) Detrended Correspondence Analysis, iii) Cluster analysis and iv) Correlation analysis. Both a canonical correspondence analysis (CCA) and a non-metric multi-dimensional scaling (NMDS) were also applied, however, as DCA's are more commonly used in palaeoecology it was decided to use these as the CCA and NMDS showed nothing different to the DCA (Appendix 2).

Correspondence analysis (CA) is a multivariate statistical technique that can be used to summarise and display multivariate data, including pollen data (Hill, 1974), it has been applied to MTW and MTE to provide the percentage variance explained by the data. CA analysis was performed on all taxa occurring above 10 % abundance (10 % abundance provides an overview of the major taxa in the sample and is a standard level used in palaeoecological studies when looking at the variation in important taxa) in any one sample using the Vegan package in R (Oksanen et al., 2013). MTW and MTE were run individually as separate analyses and axes scores and percent variability explained were extracted using the command 'summary(variablename)'.

Detrended Correspondence Analysis (DCA) is a statistical technique used to identify the axes of variance in a multivariate data set. DCA analysis was chosen over a NMDS as it is a technique more often used in palaeoecology, as it provides a method of determining the similarity and correlation amongst a set of samples or species data (De Toledo et al., 2009). A DCA was applied alongside a CA as a DCA improves on two problems associated with a CA through two modifications, these are: i) detrending which removes the arch effect associated with the CA, the arch effect being where all axes proceeding the first axis only appear as functions of the first axes, ii) rescaling the axes which provides consistent and interpretable units of length, and it also removes compression at the end of the axes (Peet et al., 1988). DCA analysis of all taxa occurring above 10 % abundance in any one sample was performed using the Vegan package in R (Oksanen et al., 2013). DCA analyses were run for both sites individually and also the two sites were plotted passively together. The DCA axes produced were also extracted for comparison against charcoal particle concentration (cm^3) data.

Cluster analysis was performed on MTW and MTE pollen data to investigate any similarities between individual samples and the two sites. A complete cluster analysis was performed using the Vegan package in R, providing one entire cluster for all of the samples for MTW and MTE.

Correlation analysis was performed using the CORREL function in Microsoft Excel 2010. Correlation analysis was applied to the MTW and MTE sites as a means of analysing the similarity between data sets, in this case, to measure the association between Charcoal and the MTW and MTE DCA axes. This correlation coefficient provides the linear association between two variables. A correlation coefficient of +1 indicates a positive correlation, 0 indicates no correlation and a value of -1 shows a negative correlation. Within this thesis, correlation coefficients greater than 0.6 or less than -0.6 are defined as “strong” relationships, coefficients

between 0.4 and 0.2 and -0.4 and -0.2 are defined as weak, coefficients between 0.2 and -0.2 are defined as no correlation.

8.3.4. Zonation

Pollen zones presented in this research were defined visually. Boundaries of the zones were placed at areas of significant pollen change (pollen taxa used to define the zones are discussed in Section 8.4.1 and 8.4.3). This method of visually zoning a pollen diagram was based on its successful application in other palaeoecological research, for example Litwin et al., 1997, Moreno et al., 2012 and Ngomanda et al., 2005. For the purpose of this research, visual segregation of the pollen zones was adequate, and statistical analysis (normally CONISS cluster analysis; Cárdenas et al., 2014) was not required as the zones were only needed to provide a structure for the results section.

8.4. Results

The results from MTW and MTE are now presented in turn. For each site the pollen zones are defined (Sections 8.4.1 and 8.4.3) and then descriptions of pollen and charcoal within the zones are presented (Sections 8.4.1.1 to 8.4.1.5 and 8.4.3.1 to 8.4.3.6). Finally, DCA analyses for each site are presented.

8.4.1. Description of MTW pollen zones

Pollen zone 1 was defined by the high abundance of *Hedyosmum* (>20 %); zone 2 was distinguished from zone 1 as the abundance of *Hedyosmum* fell to <15 %. Pollen zone 3 was defined due to low abundances of *Ilex* (<5 % for most of the samples). Pollen zone 4 had low percentage abundances of *Hedyosmum* (<10 %) and zone 5 was defined due to a rise in *Hedyosmum* to values greater than 15 %.

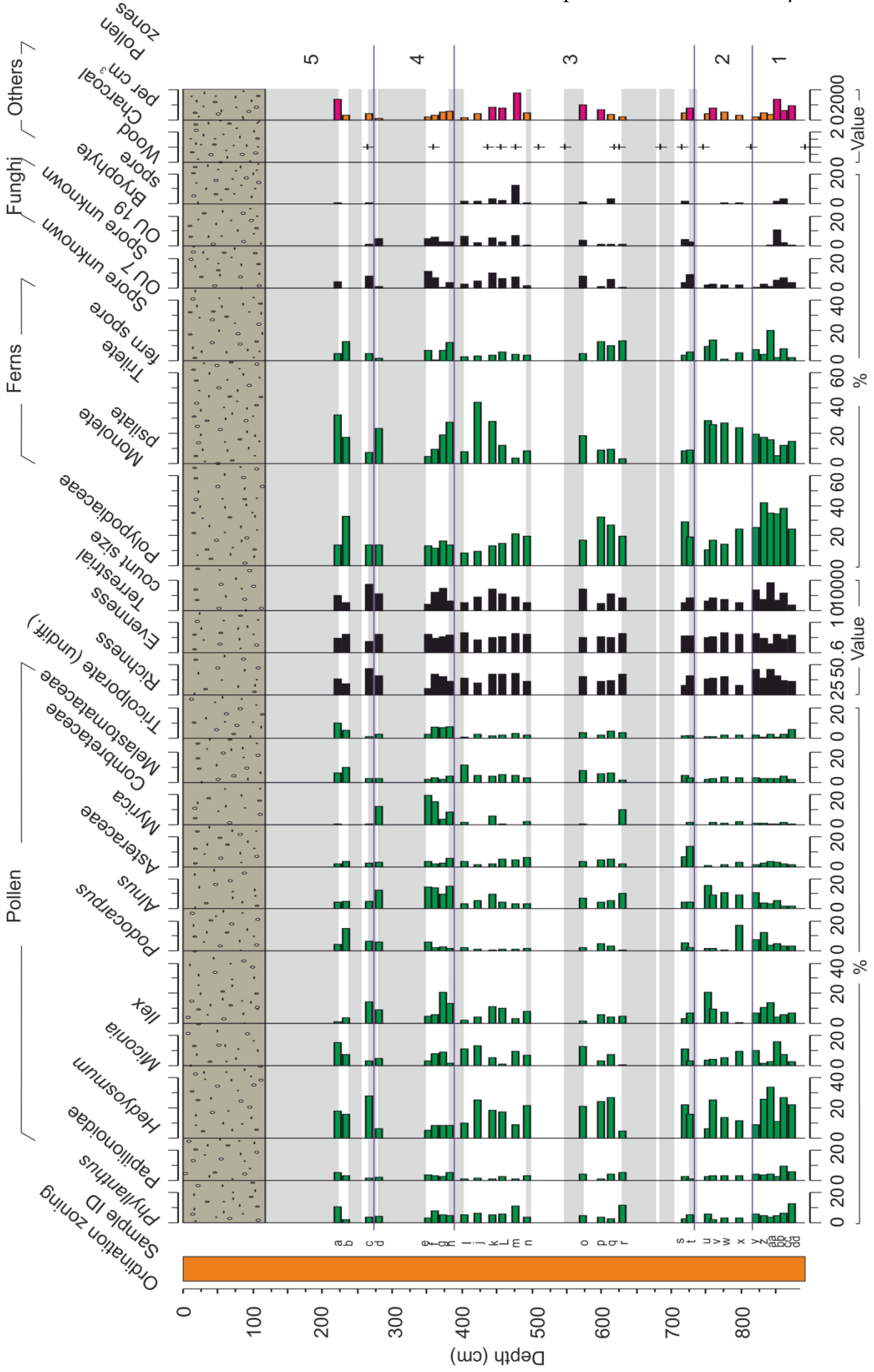
Ordination zoning
Sample ID
Phylianthus
Papilionoidae
Hedyosmum
Miconia
Ilex
Podocarpus
Alnus
Asteraceae
Myrica
Combretaceae
Melastomataceae
Tricolporate (undiff.)
Richness
Evenness
Terrestrial count size
Polypodiaceae
Monolete psilate
Trilete fern spore
Spore unknown
OU 7
Spore unknown
OU 19
Bryophyte spore
Wood
Charcoal per cm3
Pollen zones
Pollen
Ferns
Funghi
Others
Depth (cm)
Value
%
Value
%

Figure 8.1: Proxy diagram for Mera Tigre West. All pollen taxa and non-pollen-palynomorphs over 10 % abundance are included. Charcoal concentration per cm^3 is included; pink charcoal samples represent fire events (over 596 particles per cm^3). The pollen richness, evenness and count size values are shown. The proxy diagram has been zoned into five sections which are also shown. The orange column on the left hand side corresponds to the ordination analyses of Figure 8.6 and 8.7. Samples ID's are represented by letters and included on the left hand side; this sample coding has been used in Figures 8.6 and 8.7.

8.4.1.1. MTW pollen zone 1 (six samples, 866-815 cm)

In MTW pollen zone 1 (Figure 8.1), *Hedyosmum* (Chloranthaceae) is an important component; it is within this zone that this taxa reaches its highest percentage abundance for the whole stratigraphic sequence (33.44 %). *Hedyosmum* decreases in abundance to 9.05 % for the last sample of this zone. *Podocarpus* (Podocarpaceae), *Alnus* (Betulaceae) and *Ilex* (Aquifoliaceae) all increase in abundance during this vegetation zone (3.06-12.16 %, 1.53-10.83 % and 7.14-13.74 % respectively). Concomitantly with the increase of these taxa, monolete psilate and trilete fern spores both increase in abundance (14.49-19.49 % and 2.17-20.06 % correspondingly). However, whilst these taxa are increasing, *Phyllanthus* (Phyllanthaceae) decreases from 12.76 % to 5.79 % and tricolporate undif. decreases from 5.80 % to 2.17 %. During this zone *Miconia* (Melastomataceae) and Papilionoideae fluctuate in abundance, Combretaceae/Melastomataceae and *Myrica* (Myricaceae), however, remain stable throughout. Polypodiaceae reaches its highest abundance of the entire stratigraphic sequence during this zone (peaks up to 42.07 %), Spore unknown OU 7 reached abundances of 7.03 % and Spore unknown OU 19 increases to 10.81 % for one sample. Total pollen richness also increased throughout this zone, with values increasing from 36 to 46. The pollen evenness remained stable throughout this zone with values averaging 0.8 (see Chapter 5 Sections 5.3.1 and 5.3.2 for explanations on pollen richness and evenness). During this high level of pollen richness and evenness, the total terrestrial count size reached the highest value at 924 pollen grains. This zone contains a wood macrofossil.

Charcoal particle concentration in zone 1 varied from 222 to 1344 particles per cm^3, in general, decreasing from the beginning of the zone to the end (Figure 8.1). Three samples at the beginning of this zone saw a charcoal particle concentration over 596, defining these as fire events (shown in pink). These samples saw concentrations of 966, 656 and 1344 particles per cm^3.

8.4.1.2. MTW pollen zone 2 (four samples, 791-746 cm)

Following a decrease in abundance in the last sample of pollen zone 1, *Hedyosmum* increases up to 25.95 %, to once more account for the most important taxa in this zone. Abundances of *Alnus* and *Ilex* remained high throughout this vegetation zone, with abundances increasing to 15.85 % and 20.73 % respectively. The beginning sample in this zone did, however, see *Ilex* decrease to its lowest percentage abundance (0.75 %) for the entire stratigraphic sequence. *Miconia* and *Podocarpus* both decreased in abundance during this zone, with abundances falling to 3.66 % and 0.79 % respectively. During this zone Papilionoideae, Asteraceae, *Myrica,* Combretaceae/Melastomataceae and tricolporate undif. all remain stable. Monolete psilate and trilete fern spores increase in abundance throughout this zone, whereas Polypodiaceae decreases from 24.64 % to 10.86 %. Richness is low at the beginning of this zone at 33 total taxa; however, for the remaining three samples, richness remains stable at an average of 39. Evenness is stable during this zone (Figure 8.1). This zone contains two wood macrofossils.

The concentration of charcoal particles (cm^3) present in zone 2 remained relatively steady (Figure 8.1). One sample in this zone contained 774 particles, counting this as a fire event (represented in pink).

8.4.1.3. MTW pollen zone 3 (twelve samples, 720-400 cm)

Taxa present during pollen zone 3 (Figure 8.1) remain steady throughout, with only minor fluctuations of taxa present. This zone contains an organic layer which was not sampled for

pollen due to the layer being dominated by the presence of a large wood macrofossil; this layer is in the middle of this zone. *Hedyosmum*, *Ilex*, Combretaceae/ Melastomataceae, *Phyllanthus* and tricolporate undif. are constant taxa throughout this vegetation zone. *Myrica* sees an increase to 9.77 % in one sample of this vegetation zone, however, for the remaining part of the zone percentage abundances are low (average percentage abundance of 1.10 %). Similar to all taxa (aside from *Myrica*) present on Figure 8.1, pollen richness and evenness values remain stable throughout the entirety of zone 3. Bryophyte spores peak to an abundance of 12.38 %. Towards the upper samples of this zone, Spore unknown OU 7 and OU 19 also increase in value, with abundances reaching 10.33 % and 7.19 % respectively. Polypodiaceae abundances remain high during this zone (average 19.24 % abundance) and monolete psilate increases towards the end of the zone, reaching 40.27 % abundance. Trilete fern spores, however, decrease in abundance towards the end of this zone, with percentages falling from 13.08 % to 2.46 %. This zone contains nine wood macrofossils.

Charcoal particle concentration (cm^3) varies greatly in this zone (Figure 8.1), with the charcoal particles varying from 180 through to 1784 (the highest concentration of charcoal particles in this stratigraphic sequence). Six samples in this stratigraphic sequence fall above the threshold of determining fire events (detailed in pink). Charcoal particle concentrations increase in the lower part of this section, they then reach a peak in charcoal particle concentration and then they decrease in concentration in the upper part of this zone.

8.4.1.4. MTW pollen zone 4 (five samples, 379-279 cm)

During pollen zone 4 (Figure 8.1) *Myrica* increases to 19.70 %, *Ilex* increases to 20.65 % and *Alnus* increases to 15.18 %. *Hedyosmum*, *Miconia*, *Phyllanthus*, Asteraceae, Papilionoideae and Combretaceae/Melastomataceae remain stable throughout this pollen zone. Richness fluctuates during zone 4, with values ranging from 30 to 42. Pollen evenness remains stable. Monolete psilate fern spores decrease in abundance from 27.5 to 4.72 %. There are no bryophyte spores

present during zone 4. Spore unknown OU 7 and OU 19 are both present in stable concentrations, with average abundances of 4.78 % and 4.17 % respectively. This zone has one wood macrofossil present.

Charcoal particle concentration has a decreasing trend in zone 4, with the lowest concentration of particles (120 particles per cm^3) present during this zone (Figure 8.1). Charcoal particle concentration ranges from 120 to 594, meaning that no samples in this zone are above the threshold for fire events.

8.4.1.5. MTW pollen zone 5 (three samples, 264-220 cm)

Pollen taxa present during this zone vary greatly in abundance (Figure 8.1). *Hedyosmum*, *Miconia*, *Podocarpus* and *Phyllanthus* are all present in greater abundances than the previous zone 4. *Myrica* sees very low abundances during this zone, with the maximum percentage abundance in zone 5 being 0.61 %. Tricolporate undif., however, increases in abundance with values increasing from 0.88 % to 10.10 % during this zone; Combretaceae/Melastomataceae also increases, with values rising from 2.64 % to 6.31 %. Total pollen richness of samples fluctuates between 34 and 47, and evenness alters from 0.75 to 0.84. Monolete psilate increases in abundance, whilst trilete fern spores decrease in abundance. Spore unknown OU 19 is not present in the top two samples of this zone, and is only present at a low abundance (1.32 %) in the first sample of this zone. Spore unknown OU 7 is present in two of the three samples. Bryophyte spores are present in this zone, however, abundances are low (0.78 %). One wood macrofossil is present in this zone.

The first two samples in this zone see low levels of charcoal particle concentration (402 and 330 particles per cm^3; Figure 8.1). The remaining sample sees a rise in charcoal particles, with the concentration increasing to 1370 particles per cm^3, meaning this sample is representative of a fire event (fire event shown in pink).

8.4.2. MTW pollen assemblage and charcoal concentration data

8.4.2.1. Variance within the MTW pollen dataset

To characterise the main variance between the pollen assemblage, a CA and a DCA were performed on all taxa with abundances >10 % in at least one sample. A CCA and a NMDS were also performed, these, however, showed nothing more than the DCA and as such are only shown in Appendix 2. Due to the two methodological issues explained in Section 8.3.3, only the DCA analysis is used in helping to analyse this data, however, the CA values of percentage variance are included in Table 8.1 for completeness.

The DCA shows that 28.05 % of variance was captured in the first four DCA axes (12.41 %, 7.27 %, 5.55 % and 2.82 % respectively; Table 8.1 and Figure 8.2). As the percentage variance captured in each axis was reducing rapidly (i.e. the percentage variability explained by axis 4 was 77 % less than axis 1) only the first four axes are presented in the results, as the variance explained in further axes would be minor.

Table 8.1: Percentage variability data produced from the CA and DCA performed for MTW. Number of axes produced is also included.

Analysis type	Axes produced	Percentage variability explained (%)			
		Axis 1	Axis 2	Axis 3	Axis 4
CA	18	14.96	8.39	6.29	5.46
DCA	4	12.41	7.27	5.55	2.82

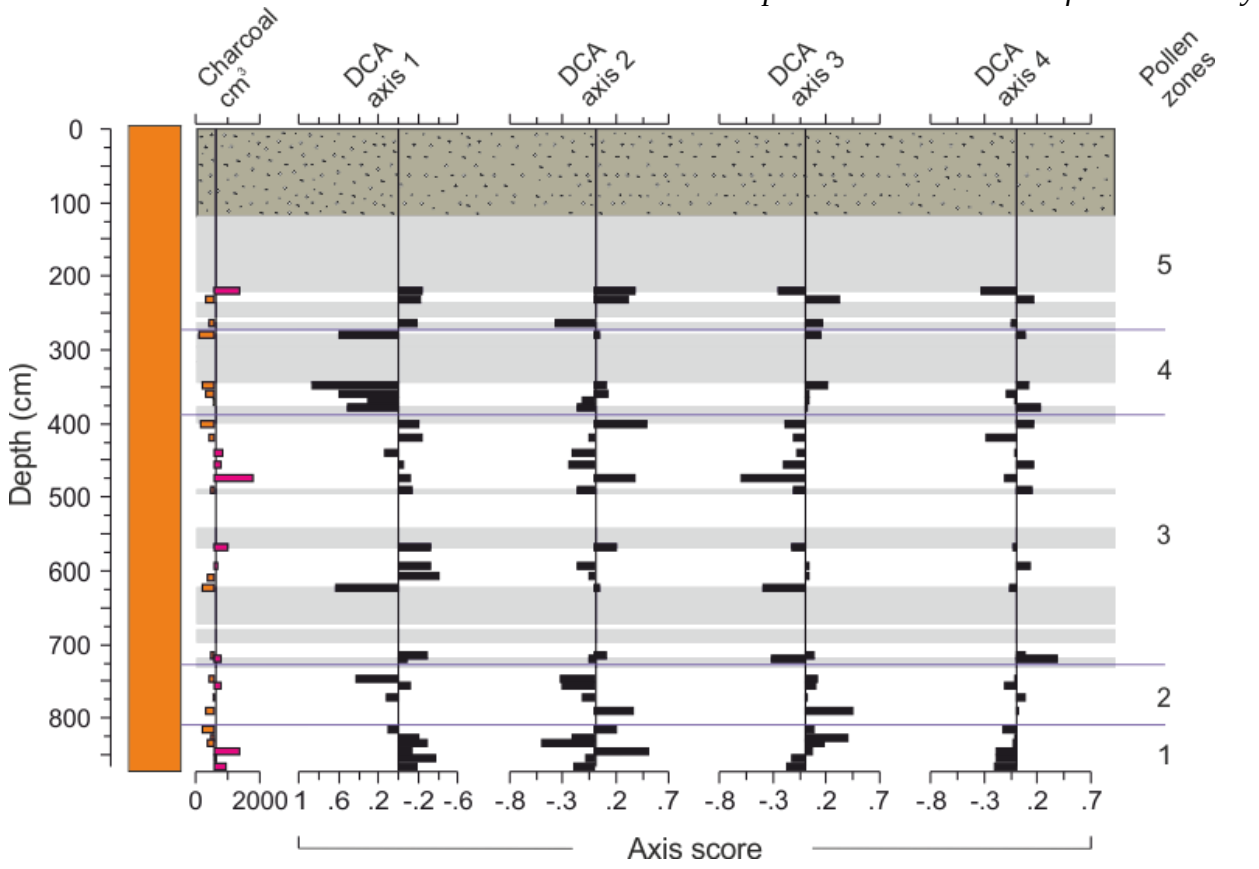

Figure 8.2: MTW charcoal concentration per cm^3 is represented alongside DCA axis scores for axis 1-4 (DCA scores produced using pollen taxa above 10 %). DCA axis 1 has been reversed to show a clearer relationship with Charcoal cm^3. Charcoal peaks are represented in pink; a vertical line is shown representing the fire event cut off point on the charcoal particle per cm^3 graph. Pollen zones 1-5 have been included. A vertical line has been included on the DCA axes representing zero to be used as a reference point. The orange column corresponds to the ordination analyses used in Figures 8.6 and 8.7.

Figure 8.2 represents the four DCA axes obtained for MTW, all of the axes are variable throughout the stratigraphic sequence, and axis 1, as expected, shows the highest variance throughout the sequence. DCA axis 1 has the highest values (>0.5) in zone 4, at this time the percentage abundance of *Hedyosmum* is low (average 7.31 %) and *Myrica, Ilex* and *Alnus* become more important components of the vegetation assemblage (Figures 8.1 and 8.2). Pollen zone 2, and the lower part of zone 3 also see higher DCA values (>0.4), at this time *Hedyosmum* decreases in importance and *Ilex, Alnus* and *Phyllanthus* increase in abundance (Figures 8.1 and 8.2). DCA axis 2 has its highest values (>0.4) during zone 1 and in the upper part of zone 3. At the time of high values in pollen zone 1, *Miconia* is an important assemblage component. During

zone 3 *Hedyosmum* decreases in abundance and the values of Combretaceae/Melastomataceae increased to their highest abundances of the sequence (11.76 %). DCA axis 3 sees low values (<-0.3) during zone 3 (Figure 8.2), at this time *Myrica* increased in abundance to 9.77 % and *Phyllanthus* increased in abundance to 11.40 %. DCA axis 4 remains fairly stable, with the largest change occurring at the boundary of pollen zone 2 and 3, when the axis score increased to >0.2 (Figure 8.2). At this time Asteraceae increased in importance to 13.57 %, *Miconia* abundance increased and *Ilex* decreased (Figure 8.3).

8.4.2.2. Correlation of pollen and charcoal data

To explore the relationship between variance in the pollen assemblage (vegetation) and charcoal (fire), DCA axis 1 and the charcoal concentration data were compared (Figures 8.2 and 8.3). In general, DCA axis 1 has lower values at times of high charcoal concentration, with the greater DCA values occurring at times of low charcoal particle concentration. The only exclusion to this is during zone 3, when DCA axis 1 increases following the peak in charcoal concentration in the upper part of the zone.

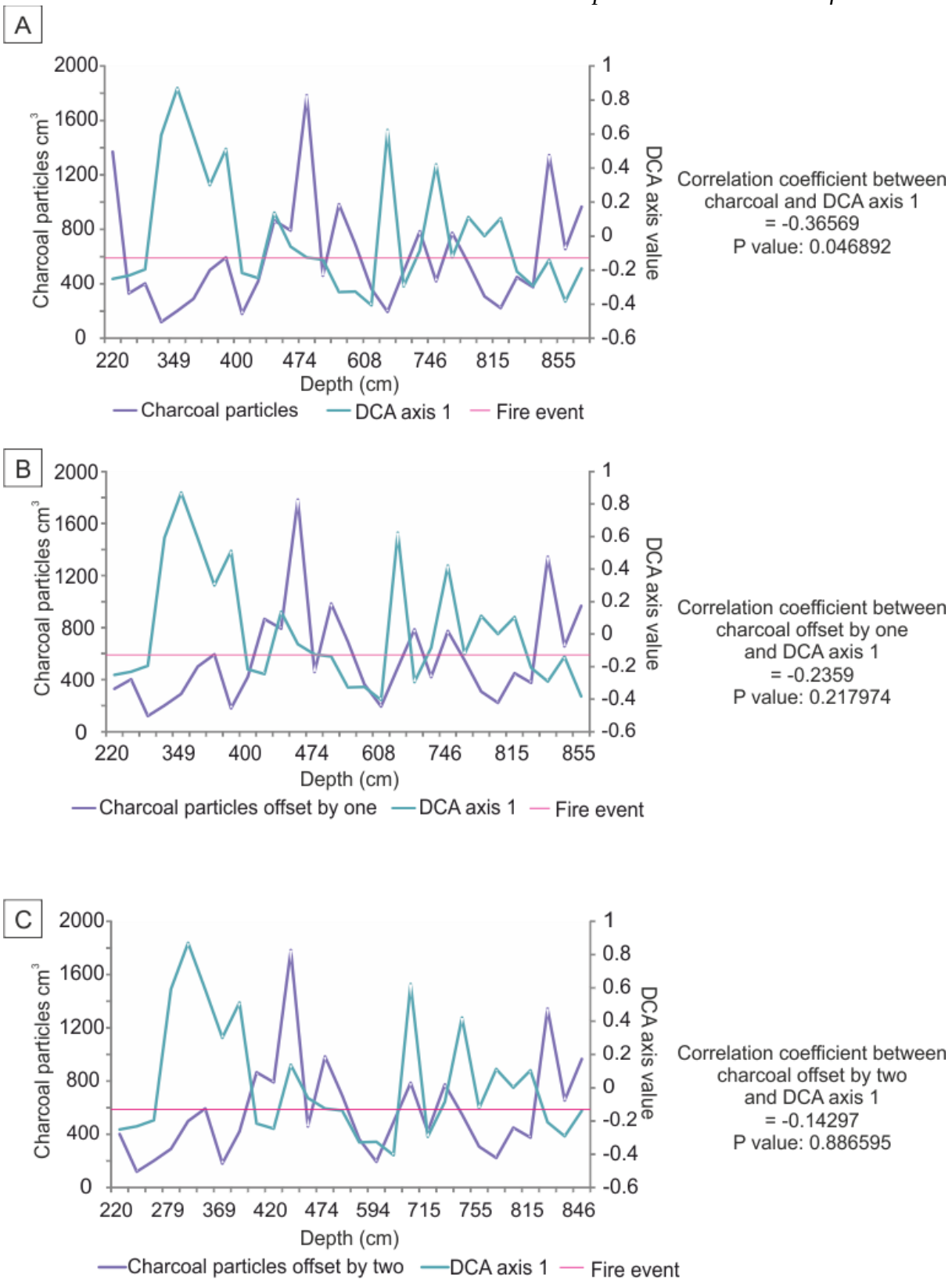

Figure 8.3: Correlation between charcoal particles and DCA axis 1 for MTW. Correlation coefficient values are also shown. A) shows all charcoal particle samples plotted against the DCA axis 1 (S_i). B) shows charcoal particles which are offset by one sample (S_i+1). C) shows charcoal particles which are offset by two sample (S_i+2).

To assess if there was a time lag between charcoal (fire events) and pollen (vegetation change) like that observed in upper zone 3, a correlation of data sets was performed to compare pollen with charcoal in the same sample and each of the two following samples (situated above; i.e. S_i, S_i+1 and S_i+2; Figure 8.3), i.e. the charcoal particle concentrations were moved up the stratigraphic sequence by one (S_i+1) and two (S_i+2) samples. Linear correlation of pollen assemblage (DCA axis 1; Figure 8.3) change and charcoal data showed from all three scenarios there was a weak negative correlation (S_i=-0.37; Figure 8.3A, S_i+1 = -0.24; Figure 8.3B and S_i+2=-0.14; Figure 8.3C). Figure 8.3 part A shows a weak correlation, as the concentration of charcoal particles increase, the axis score for DCA 1 decreased, however, in other parts of the sequence the two variables had no relationship (Figure 8.3). Figure 8.3 part B had a weaker correlation than observed in part A. On Figure 8.3 part B it can be seen that the two variables had no relationship with each other. Part C of Figure 8.3 (S_i+2) showed no correlation between the two variables, this is evident on the graph as the two curves vary completely independently of each other.

To establish if there was a correlation between charcoal (fire) and the abundance of individual taxa (as opposed to the overall assemblage), the same analysis was performed against six pollen types. The six types selected were *Alnus, Hedyosmum, Ilex, Podocarpus,* monolete psilate and trilete fern spores. These taxa were selected from those on Figure 8.1, due to their high abundances throughout the stratigraphic sequence, and also as they vary visually during times of high charcoal concentration (Figure 8.1). There was found to be no correlation or a very weak correlation between these variables, even at S_i+1 and S_i+2, as such these graphs are only included in Appendix 2.

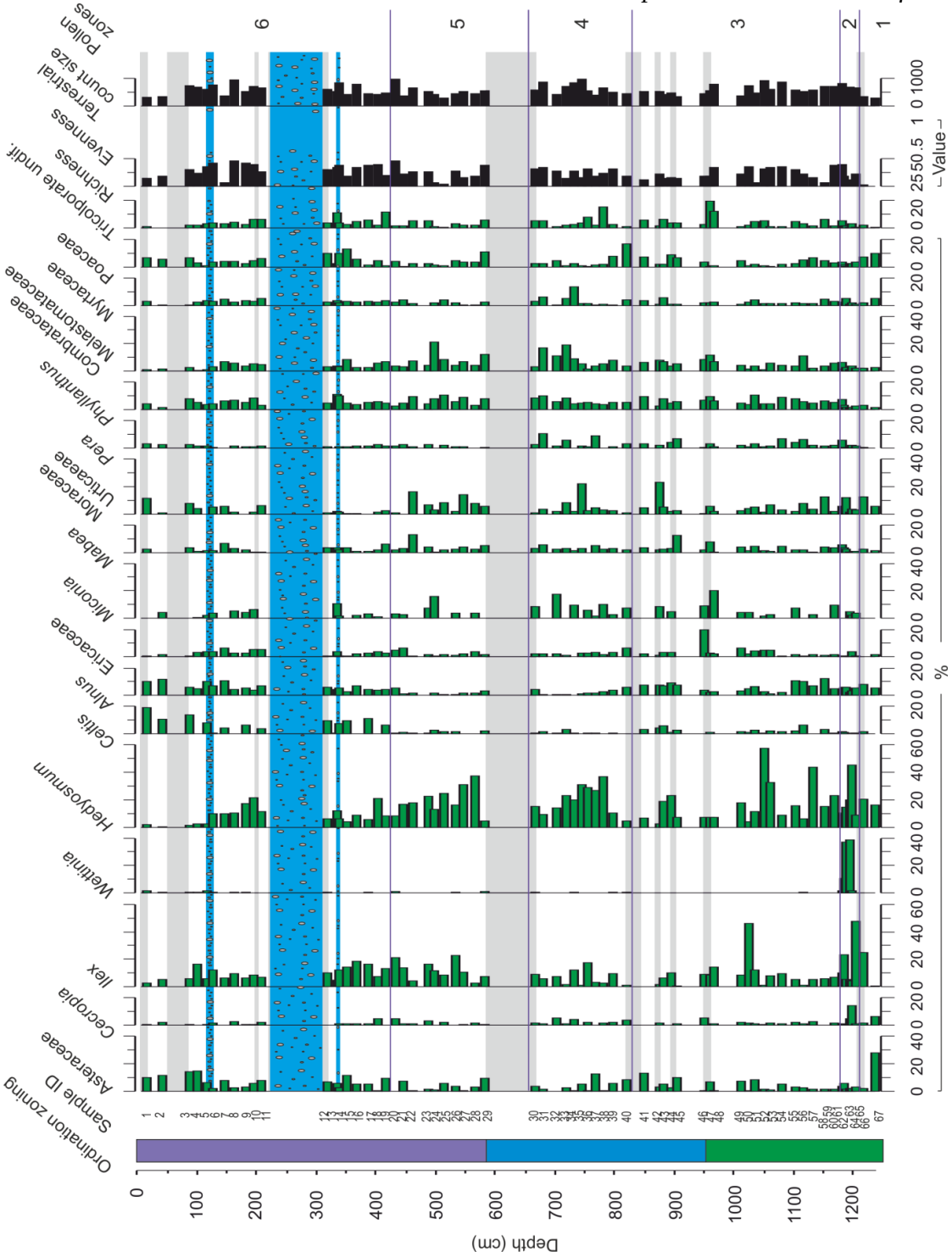

Figure 8.4: Proxy diagram for Mera Tigre East. All pollen taxa and non-pollen-palynomorphs over 10 % abundance are included. Charcoal concentration per cm^3 are included; pink charcoal samples represent fire events (over 811 particles per cm^3). The pollen richness, evenness and count size values are shown. The proxy diagram has been zoned into six sections which are also shown. The green, blue and purple column on the left hand side corresponds to the ordination analyses of Figures 8.6 and 8.7, the colours used are based on interpretations of Chapter 7. Sample ID's are represented by letters and included on the left hand side; this sample coding has been used in Figures 8.6 and 8.7.

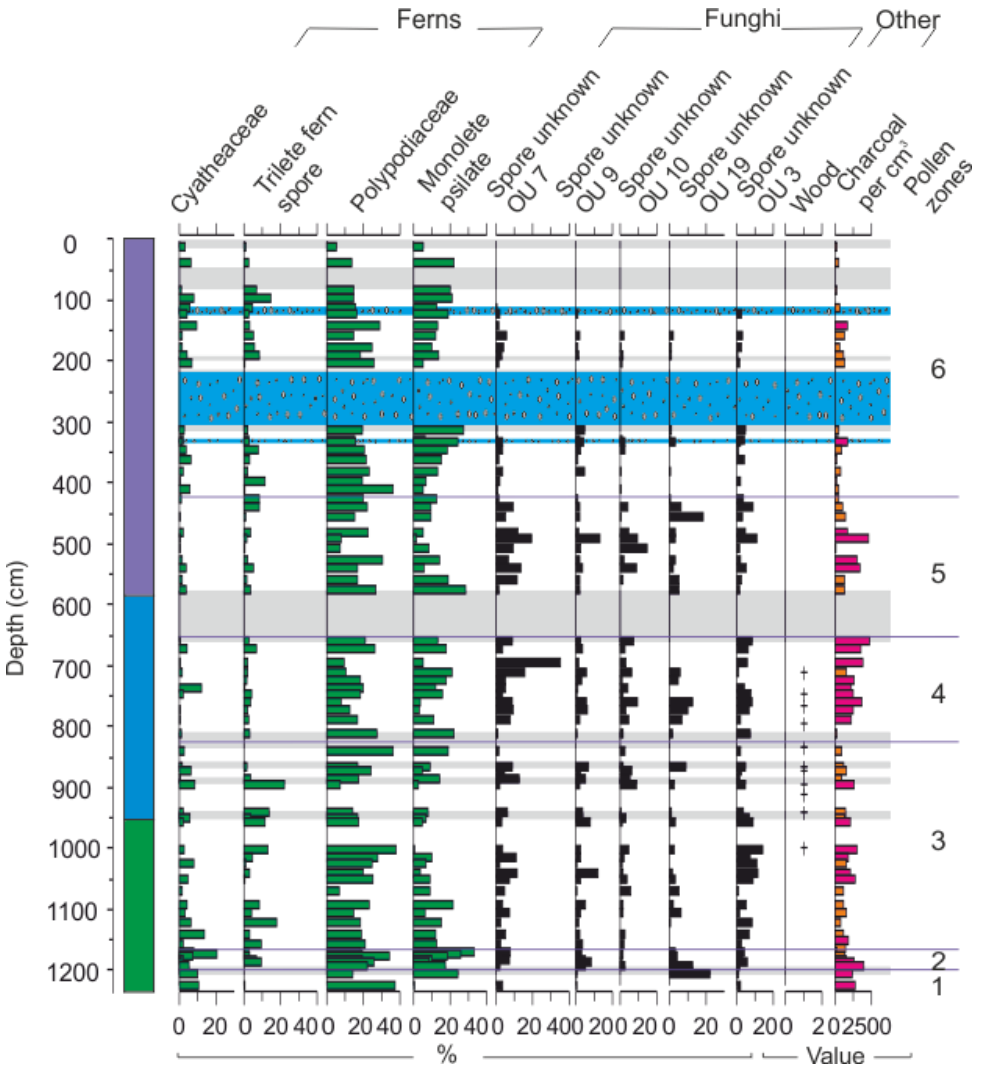

Figure 8.4 (continued).

8.4.3. Description of MTE pollen zones

Pollen zone 1 was defined due to a high percentage abundance of Asteraceae (>25 %). Pollen zone 2 was depicted due to a high abundance of *Ilex* (>45 %) and *Wettinia* (Arecaceae; >35 %) pollen. Pollen zone 3 was demarcated due to a decrease in *Ilex* (<15 %) and *Wettinia* (<2 %). Pollen zone 4 was separated from zone 3 due to an increase in *Hedyosmum* abundance (> 30 %). Pollen zone 5 was demarcated due to an increase in *Hedyosmum* following a decrease at the end of Zone 4. Pollen zone 6 was separated from the rest of the section due to an increase in *Celtis* and *Alnus* (both >10 %) and a decrease in *Hedyosmum* (<10 %; Figure 8.4).

8.4.3.1. MTE pollen zone 1 (two samples, 1239-1220 cm)

This zone sees stable values of diversity indices, with richness remaining low, but stable at 24 and 26, and evenness values being 0.77 and 0.74. The pollen abundances shown on Figure 8.4 do, however, show changes in abundance. Asteraceae is the most important taxa in this zone with the percentage abundance reaching 27.93 % within the first sample; however, the second sample sees a decrease to 1.97 % (Figure 8.4). *Hedyosmum* also has high abundances during this pollen zone, with percentage abundances of 16.21 and 20.56 %. Two taxa (*Miconia* and *Wettinia*) are not present in either sample in this zone. Other taxa including Combretaceae/Melastomataceae, *Phyllanthus, Pera* (Euphorbiaceae) and *Celtis* (Cannabaceae) are present in low abundances in this zone. Polypodiaceae is present in high abundances during this zone, reaching 37.5 % abundance. Monolete psilate increases during this zone, with abundances rising from 0.71 % to 24.45 %. Trilete fern spore, however, has a low abundance during this zone, and is only present in this first sample with an abundance of 0.71 %. Spore unknown OU 19 reaches its highest abundance in this zone, increasing to an abundance of 22.27 %. Spore unknown OU 3, 7, 9 and 10 are present in low abundances during this zone.

The charcoal particle concentration (cm^3) in zone 1 saw values of 1350 and 1176 for the two samples (Figure 8.4). Both of these samples are above the threshold of 811, defining both of these concentrations as indicative of fire events (shown in pink).

8.4.3.2. MTE pollen zone 2 (five samples, 1205-1185 cm)

Pollen zone 2 sees three shifts in taxa abundance (Figure 8.4). In the first sample, *Ilex* is a major component with an abundance of 47.72 %. *Cecropia* (Urticaceae) and *Hedyosmum* become important palynological components in the second sample. *Hedyosmum* remains a main component during the remainder of zone 2, however, following its peak, *Cecropia* decreases in abundance and is replaced by *Wettinia* which reaches an abundance of 38.67 %. This zone also sees taxa stability, with *Alnus,* Ericaceae, *Pera*, Myrtaceae and Asteraceae remaining stable

throughout. Pollen richness varies from 27 to 36, rising slightly from zone 1. Evenness decreases following zone 1, with values decreasing down to 0.63. Polypodiaceae, monolete psilate and Cyatheaceae are important components of zone 2. Spore unknown OU 19 has a high percentage abundance in the first sample (22.27 %) but it then decreases in abundance, and in two of the five samples it is not present at all.

Zone 2 sees a decreasing trend in the concentration of charcoal particles present (Figure 8.4). The first two samples see high charcoal concentrations (1986 and 1292 per cm^3); the concentration then falls to 150. The first two samples in this zone see concentrations above the threshold (shown in pink), therefore, defining them as fire events. The remainder of the samples in this zone see low particle concentrations, and they are not defined as fire events.

8.4.3.3. MTE pollen zone 3 (twenty samples, 1184-850 cm)

Hedyosmum is an important component of pollen zone 3 (values over 40 %, Figure 8.4). Although it is the taxa with the highest abundance, its percentage abundance does fluctuate throughout this zone, with percentages varying from 2.85 % to 57.14 %, the abundance of *Hedyosmum* does decrease towards the upper part of this zone. Following the peak in *Hedyosmum*, *Ilex* peaks to 46.06 %. Aside from this peak, *Ilex* abundance remains below 12.01 % for the rest of pollen zone 3. Ericaceae and *Miconia* both increase towards the middle of this pollen zone, with peaks reaching 19.74 and 20.26 % abundance respectively. Moraceae/Urticaceae increases at the end of this zone, with values rising to 23.34 %. Despite these taxa altering in abundance, Poaceae, Myrtaceae, *Mabea* (Euphorbiaceae) and *Cecropia* remain stable throughout. Pollen richness varies with the bottom and top part of zone 3 having lower values than the rest of the section (28-34), in comparison to values up to 45 in the middle of the section. Pollen evenness remains stable at around 0.83, aside from two samples in the lower part of the zone where the evenness dropped to 0.54 and 0.66. Trilete fern spores, Polypodiaceae and monolete psilate fluctuate throughout this zone. Spore unknown OU 3 and

OU 7 remain stable, Spore unknown OU 9, 10 and 19 see a slight increase towards the end of zone 3. Seven wood macrofossils are present in this zone.

Charcoal concentrations present in zone 3 vary throughout, with a few peaks being reached (Figure 8.4). This zone sees seven samples with charcoal particle concentrations per cm^3 above 811, defining them as fire events (in pink). The remainder of the samples fall below this value, therefore, being interpreted as regional noise.

8.4.3.4. MTE pollen zone 4 (eleven samples, 819-666 cm)

Pollen zone 4 sees taxa reassortment (Figure 8.4). Combretaceae/Melastomataceae increases in abundance during zone 4, with values rising from 3.98 % to a peak of 19.02 %. *Cecropia* and *Pera* both reach higher abundances than in zone 3, with an average value of 2.08 % and 3.34 % compared to 1.25 % and 2.92 % respectively. Myrtaceae increases in abundance towards the upper half of this zone, with abundances rising to 13.51 %. *Miconia* also increases in abundance throughout this zone. Conversely, *Hedyosmum* decreases in abundance with values falling from peaks of 36.94 % to 9.61 %, it does, however, remain a principal component of pollen zone 4. Moraceae/Urticaceae peaks to 22.10 % for one sample, remaining well below 10 % for the remainder of the samples. Abundances of *Ilex,* Asteraceae and Poaceae have a decreasing trend throughout this zone. Richness and evenness values remain stable throughout the zone, with only minor fluctuations present. Cyatheaceae has low values during this zone, aside from a peak to 12.28 % in the middle of the zone. Trilete fern spores, Polypodiaceae and monolete psilate remain stable during this zone. Spore unknown OU 7 sees an increase in abundance, leading to a peak of 15.70 %. Spore unknown OU 19 decreases in abundance with values falling from a peak of 12.39 % to absent by the end of the zone. Spore unknown OU 9, OU 10 and OU 3 remain stable during this zone. Four wood macrofossils are also present in this zone.

Zone 4 sees an increase in charcoal concentrations throughout the zone (Figure 8.4). Charcoal particle concentrations per cm^3 begin the zone at only 100 particles; however, this rises to 2356 particles, the highest concentration in the stratigraphic section. Nine samples in this zone are above the threshold level for fire events (in pink), with only two samples falling below this level.

8.4.3.5. MTE Pollen zone 5 (ten samples, 580-429 cm)

Similar to the pattern observed in pollen zone 4 and the upper part of pollen zone 3, there is a decrease in *Hedyosmum* abundance throughout the zone, falling from 37.33 % to 8.16 % (Figure 8.4). Poaceae also decreases through this zone, with values falling from 11.13 % to 4.34 %. *Mabea* reaches a peak of 12.97 % during this zone, despite remaining below 5 % for the remainder of the zone. *Ilex*, *Miconia* and Moraceae/Urticaceae varied in abundance throughout the zone. The abundances of Moraceae/Urticaceae decreased towards the end of the zone. The abundance of *Pera* is low in this zone compared to zone 4. Richness sees a drop to 27 during the middle of this zone; pollen evenness remains stable at an average value of 0.78. Cyatheaceae, trilete fern spore and Polypodiaceae remain stable throughout zone 5, whereas monolete psilate decreases towards the middle of this section. Spore unknown OU 9, 10 and 19 all see peaks in abundance during this zone, with values reaching 12.99, 14.80 and 18.28 % respectively. Spore unknown OU 7 oscillated in value throughout.

Charcoal particle concentration (cm^3) in zone 5 greatly fluctuates, with values ranging from 76 to 2288 (Figure 8.4). Four samples in this zone are above the threshold of 811 particles meaning they are recognised as fire events, these fire events are highlighted in pink.

8.4.3.6. MTE Pollen zone 6 (nineteen samples, 414-11 cm)

In pollen zone 6 there is an increase in abundance of *Celtis*, *Alnus* and Asteraceae (Figure 8.4), to values of 18.83, 12.16 and 14.83 % respectively. *Hedyosmum* decreases in abundance throughout the section, mimicking the trend seen in previous zones (4 and 5), with values falling

from 20.86 % to the lowest value in the stratigraphic sequence (0.30 %). Combretaceae/Melastomataceae, Myrtaceae and *Ilex* all see drops in values towards the top of this zone, in parallel to the drop in *Hedyosmum*. Pollen richness also falls towards the top of the zone with values decreasing to 32. Evenness remains stable throughout the whole zone. Towards the upper half of this zone, Cyatheaceae and trilete fern spores have an increased average abundance in comparison to zone 5. Polypodiaceae and monolete psilate remain stable throughout this zone. Corresponding with the declines in pollen taxa, Spore unknown OU 3, 7, 9, 10 and 19 all decrease dramatically with abundances mainly disappearing apart from a few low percentage abundances.

In comparison to the rest of the stratigraphic section, charcoal particle concentrations are low (Figure 8.4), reaching the lowest value of the entire stratigraphic sequence, at only 16 particles per cm^3. Only two samples in zone 6 go above the threshold required to register them as fire events (highlighted in pink), the charcoal particle concentrations for these two events are 836 and 884, meaning they are only just above the cut off of 811 to register them as fire events. The remaining 17 samples fall below this level.

8.4.4. MTE pollen assemblage and charcoal concentration data

8.4.4.1. Variance within the MTE pollen dataset

To characterise the main variance between the MTE pollen assemblage, a CA and a DCA were performed on all taxa with abundances >10 % in at least one sample. A CCA and a NMDS were also performed, however, the results did not show anything and as such they are confined to Appendix 2. Due to the methodological problems for the CA explained in Section 8.3.3, only the DCA analysis is used in helping to analyse the MTE data. The CA values of percentage variance are, however, included in Table 8.2 for completeness.

The DCA showed that 43.25 % of variance was captured in the first four DCA axes (16.78 %, 11.97 %, 7.87 % and 6.63 % respectively; Table 8.2 and Figure 8.5). As the percentage variance explained by each axes was reducing (the variability explained by axis 4 was 60.49 % less than axis 1), only the first four axes are included, as variance explained in further axes is minor.

Table 8.2: Percentage variability data produced from the CA and DCA performed for MTE. Number of axes produced is also included.

Analysis type	Axes produced	Percentage variability explained (%)			
		Axis 1	Axis 2	Axis 3	Axis 4
CA	18	21.25	16.26	10.51	8.87
DCA	4	16.78	11.97	7.87	6.63

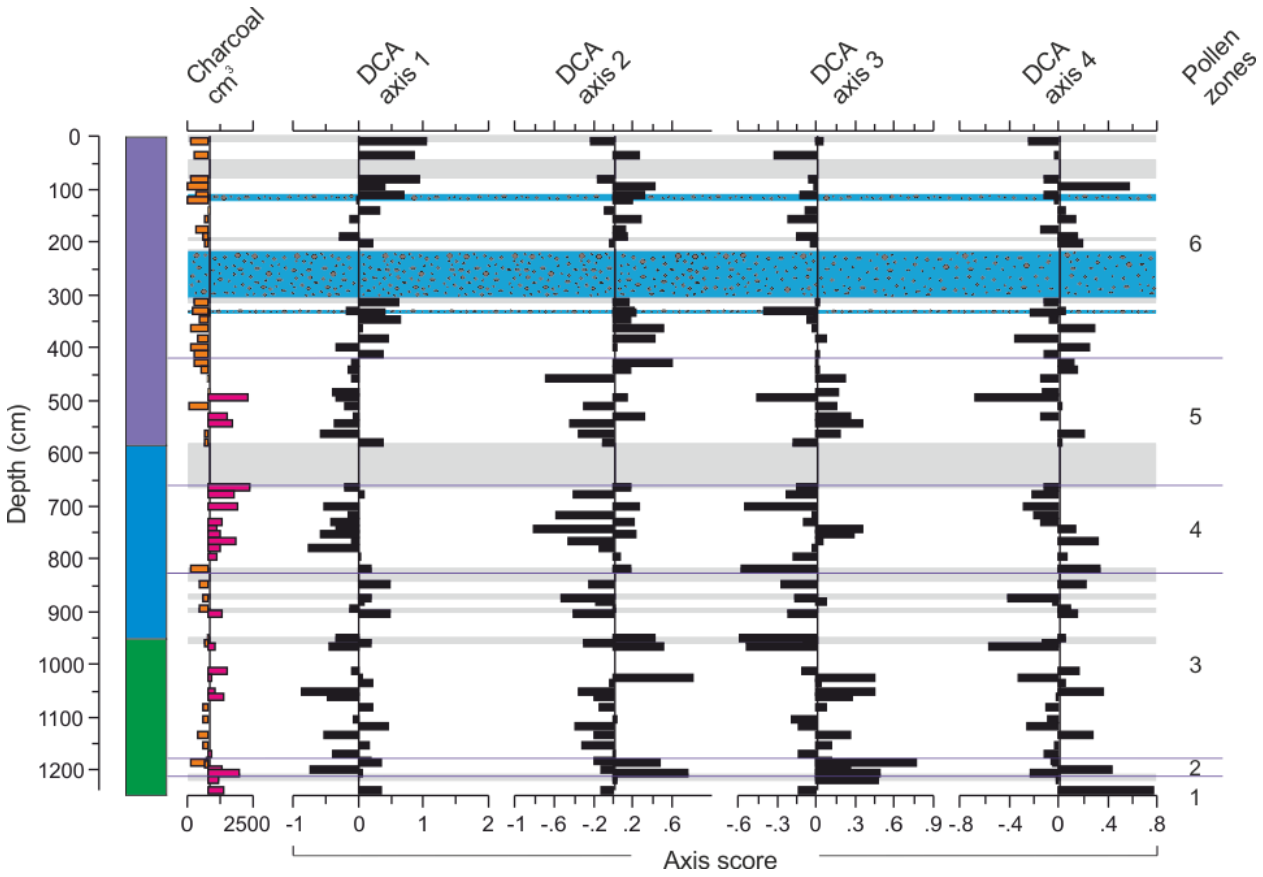

Figure 8.5: Charcoal concentration per cm^3 for MTE represented alongside DCA axis scores for axes 1-4 (DCA scores generated from pollen taxa data over 10 % abundance). Charcoal peaks are represented in pink. Pollen zones 1-6 have been included. A line indicating zero has been included as a reference on the DCA axes. A line indicating charcoal samples above and below the fire event cut-off point is also included.

Figure 8.5 represents the four DCA axes for MTE; all axes are variable throughout the stratigraphic sequence. Samples 62 and 63 were excluded from the DCA analysis as a high abundance of one taxa, (*Wettinia* > 35 %), in just these two samples, was causing these two samples to behave differently from the rest of the stratigraphic sequence. Figure 8.6a and Figure 8.7 show the obvious difference in these samples that led to their exclusion from the DCA used to produce Figure 8.5. These two samples are isolated from the remaining cluster of samples and cause the variability in the data to be reduced and unclear, by removing these samples the variance in the dataset is more prominent (Figure 8.6b).

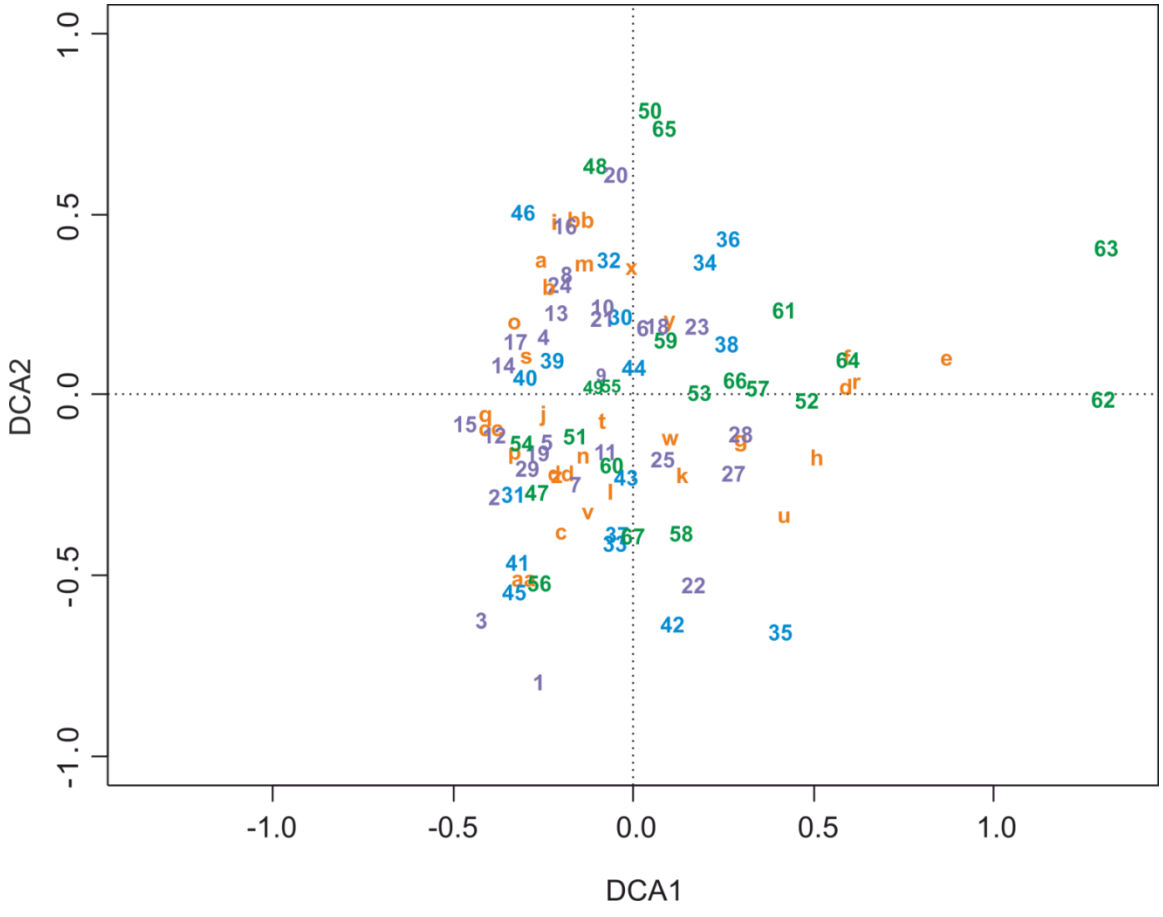

Figure 8.6a: Detrended correspondence analysis (DCA) for all samples from MTE and MTW, DCA produced using all pollen taxa over 10 %. MTE is plotted passively over MTW. The orange letters represent MTW samples and the purple, blue and green numbers represent the MTE samples with the colours relating to those included on the MTE proxy diagram (Figure 8.4). The letters (MTW) and numbers (MTE) shown here are shown in situ on Figures 8.1 and 8.4.

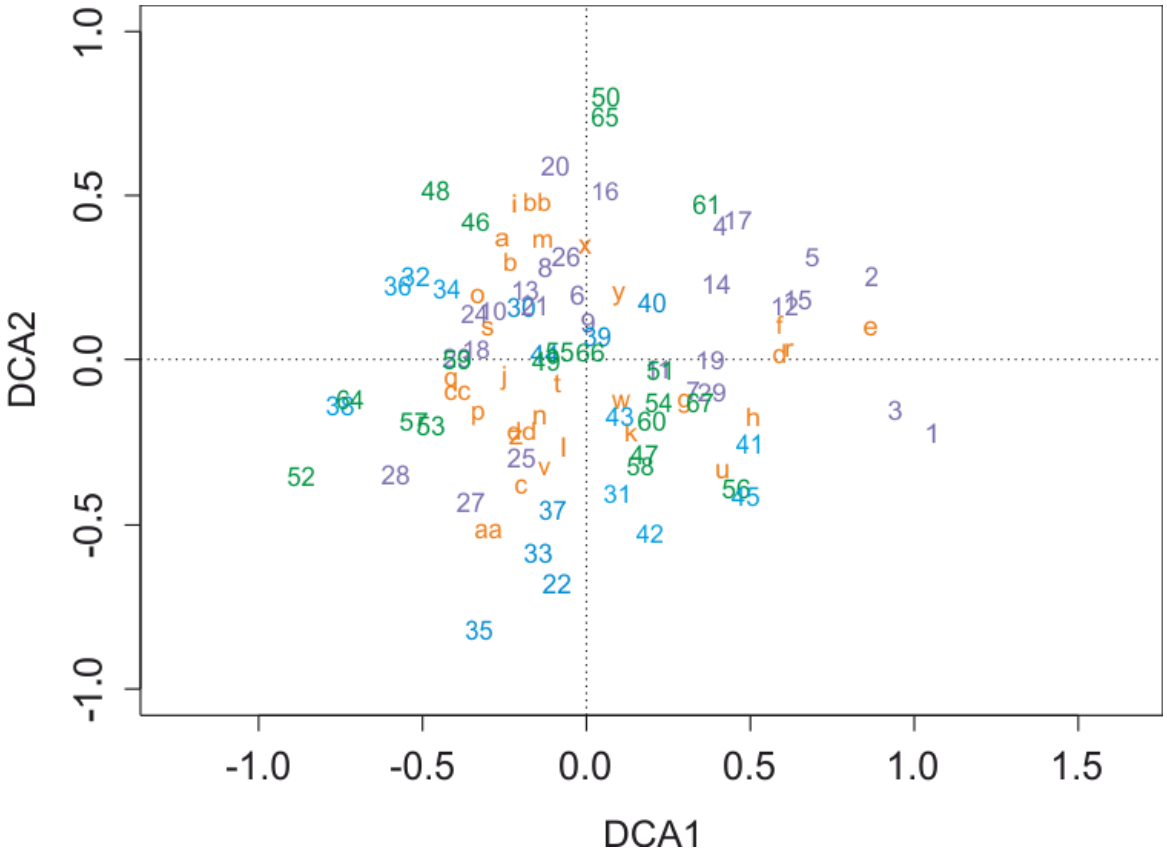

Figure 8.6b: Detrended correspondence analysis (DCA) for samples from MTE and MTW, DCA produced using all pollen taxa over 10 %, however, it excludes samples 62 and 63 (see text). MTE is plotted passively over MTW. The orange letters represent MTW samples and the purple, blue and green numbers represent the MTE samples with the colours relating to those included on the MTE proxy diagram (Figure 8.4). The letters (MTW) and numbers (MTE) representing samples are shown in situ on Figures 8.1 and 8.4.

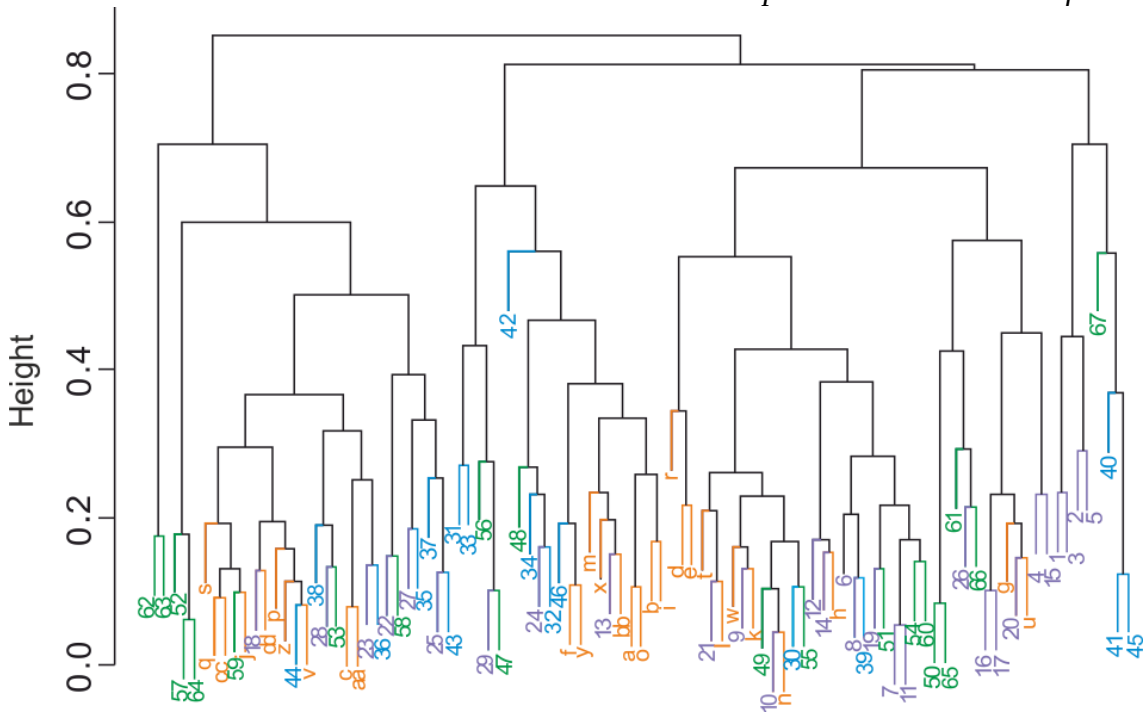

Figure 8.7: Cluster analysis for all MTW and MTE samples. All pollen taxa occuring in any one sample at an abundance of >10 % are included in the cluster analysis. Orange letters represent MTW samples, purple, blue and green numbers represent the MTE samples (the colours correspond to the MTE proxy diagram; Figure 8.4). Letter (MTW) and number (MTE) codes representing samples are included on Figure 8.1 and Figure 8.4 in situ.

DCA axis 1 has the highest values (>1.0) in the stratigraphic sequence, particularly in zone 6 (Figure 8.5). At the time of the high DCA values in zone 6, the abundances of *Celtis*, *Alnus* and Asteraceae all increased and the abundance of *Hedyosmum* and *Ilex* decreased correspondingly (Figures 8.4 and 8.5). Low DCA axis scores (<-0.5) were also present in DCA axis 1, particularly in zone 4 and the lower part of zone 3, corresponding to these low DCA axis scores, concentrations of *Miconia* and *Hedyosmum* fluctuated (Figures 8.4 and 8.5). DCA axis 2 saw a high level of variation, particularly in zones 3 and 4; this is in line with the fluctuations of *Hedyosmum*, *Ilex* and Moraceae/Urticaceae. DCA axis 2 sees high axis scores (>0.5) during zone 1 and 2, this occurs at the same time as an increase in Asteraceae, *Cecropia*, *Ilex* and *Hedyosmum* (Figures 8.4 and 8.5). The axis scores for DCA axes 3 are also high during zone 1 and 2, again occurring at the same time as the increase in Asteraceae, *Cecropia*, *Ilex* and

Hedyosmum. DCA axis 3 sees low axis scores during the upper part of zone 3 and zone 4, this occurs in correlation with an increase in Ericaceae, Moraceae/Urticaceae and changing abundances of *Miconia* (Figures 8.4 and 8.5). DCA axis 4 has high axis scores (>0.5) in zone 1, in line with the increase in Asteraceae and also in the upper part of zone 6, this correlates with an increase in *Celtis, Alnus* and Asteraceae (Figures 8.4 and 8.5). Low DCA axis scores (<-0.5) are observed in zone 5, this correlates with an increase in *Miconia*, *Mabea* and Moraceae/Urticaceae and a decrease in *Hedyosmum* (Figures 8.4 and 8.5).

8.4.4.2. Correlation of pollen and charcoal data

To explore the relationship between variance in the pollen assemblage (vegetation) and charcoal (fire), DCA axis 1 and the charcoal concentration data were compared (Figures 8.5 and Figure 8.8). DCA axis 1 has a varied relationship with the concentration of charcoal particles. During the upper part of the section, (zone 6), the DCA axis scores are mostly high (>0.5), whereas the charcoal concentrations are low (Figure 8.5). The lower part of the section sees a very varied relationship between the two separate variables.

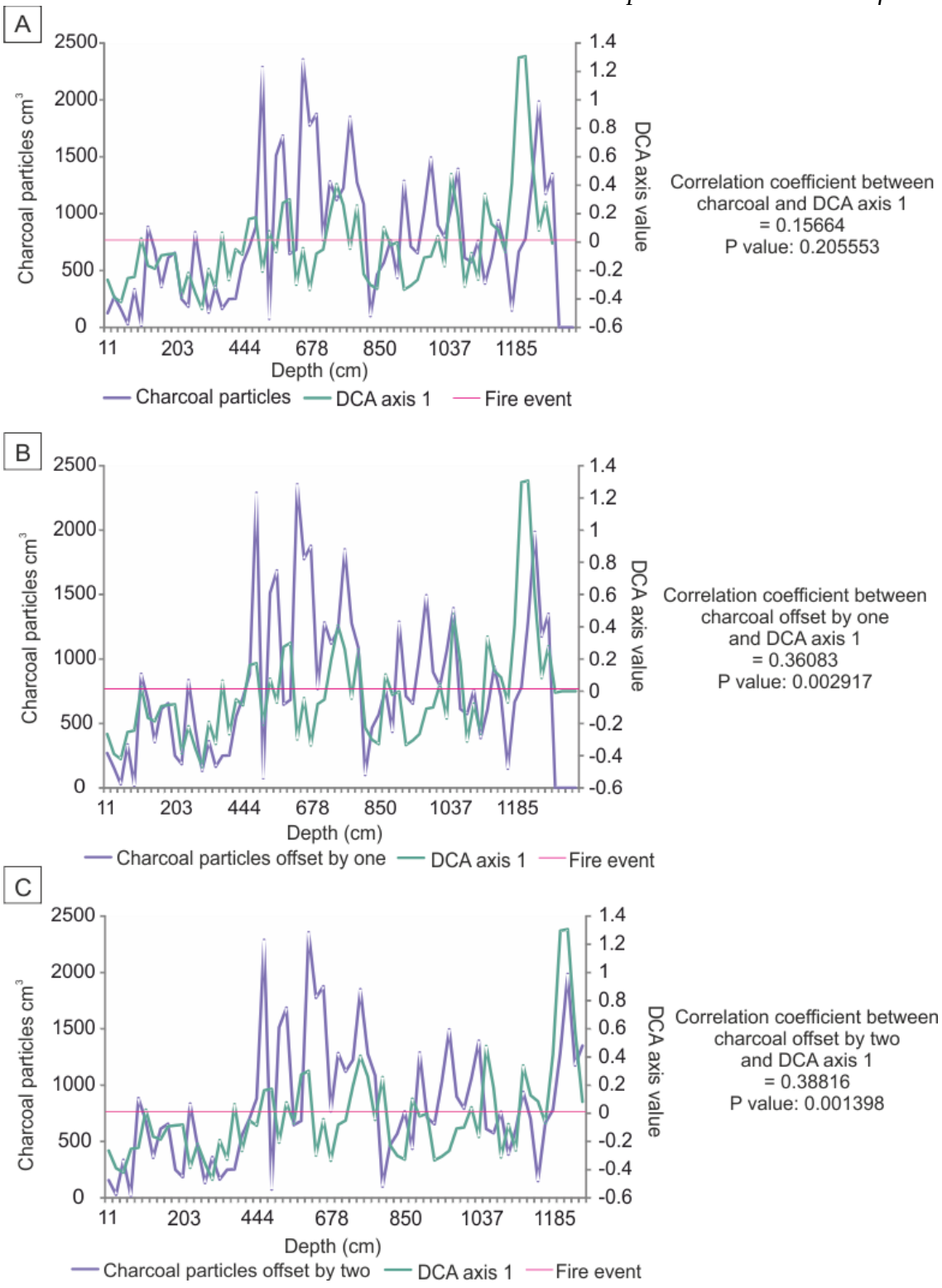

Figure 8.8: Correlation between charcoal particles and DCA axis 1 for MTE. Correlation values are also shown. A) shows all charcoal particle samples plotted against the DCA axis 1 (S_i). B) shows charcoal particles which are offset by one sample (S_i+1). C) shows charcoal particles which are offset by two samples (S_i+2).

In order to assess whether there was a time lag between the charcoal (fire events) and pollen (vegetation change) a correlation of data sets to test a response to offset was performed (S_i, S_i+1, S_i+2; see Section 8.4.2.2). The linear correlation of the pollen assemblage represented in DCA axis 1 (Figure 8.3) and charcoal data showed that S_i had a very weak/ no correlation (S_i=0.16) and S_i+1 and S_i+2 had a weak correlation (0.36 and 0.39 respectively; Figure 8.8). Figure 8.8 part B (correlation of S_i+1) shows a weak positive correlation. In particular the lower part of this section sees a strong relationship between the two variables, this relationship is less pronounced in the middle and upper part of the graph. Figure 8.8 part C (correlation of S_i+2) also has a weak positive correlation, for this data set, though, the correlation between charcoal and DCA axis 1 is stronger in the upper part of the sequence and weaker at the bottom of the sequence.

To establish if there was a correlation between charcoal (fire) and the abundance of individual palynological taxa (as opposed to the overall assemblage) the same analysis was performed against eight pollen types. The eight types selected were *Celtis*, *Hedyosmum*, *Wettinia*, *Ilex*, *Cecropia*, Poaceae, monolete psilate and trilete fern spores. These types were selected from those on Figure 8.4 due to their high abundances throughout the stratigraphic sequence and also as they vary visually during times of high charcoal concentration (Figure 8.4). There was found to be no correlation or a very weak correlation between *Ilex*, *Cecropia*, Poaceae, monolete psilate, trilete fern spores and charcoal particles, even at S_i+1 and S_i+2, as such these graphs are only included in Appendix 2. The correlation between *Celtis*, *Hedyosmum* and *Wettinia* was also shown on a CCA, as the correlation graphs represented in Figures 8.9-11 showed the correlation/ lack of correlation in more detail it was decided to only include these here. As such the CCA is only included in Appendix 2.

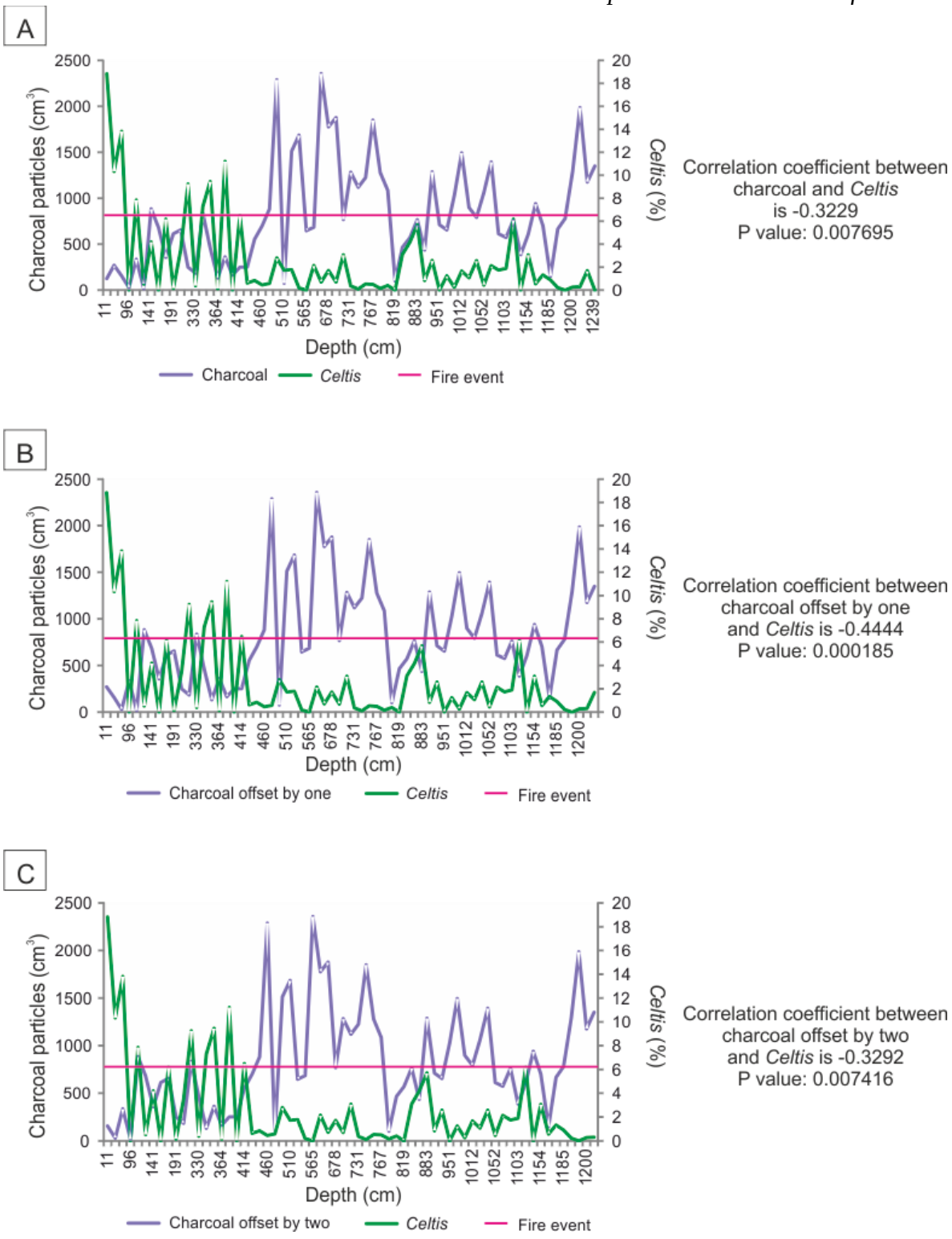

Figure 8.9: Correlation between *Celtis* (percentage abundance) and charcoal particle concentration (cm^3) for MTE. The correlation coefficient is included for all three scenarios (S_i, S_i+1 and S_i+2).

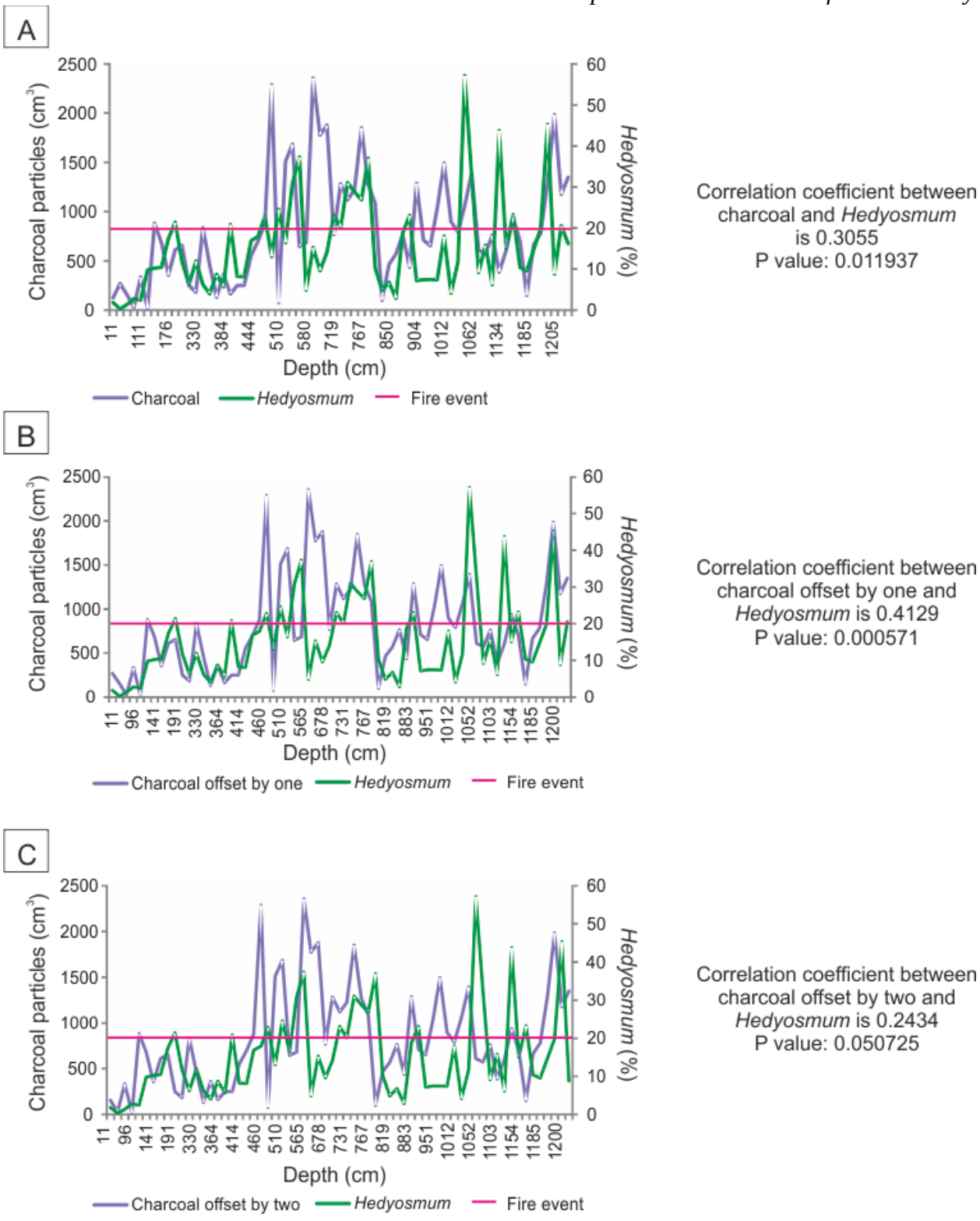

Figure 8.10: Correlation between *Hedyosmum* (percentage abundance) and charcoal particle concentration (cm^3) for MTE. Correlation coefficients have been included for all three scenarios (S_i, S_i+1 and S_i+2).

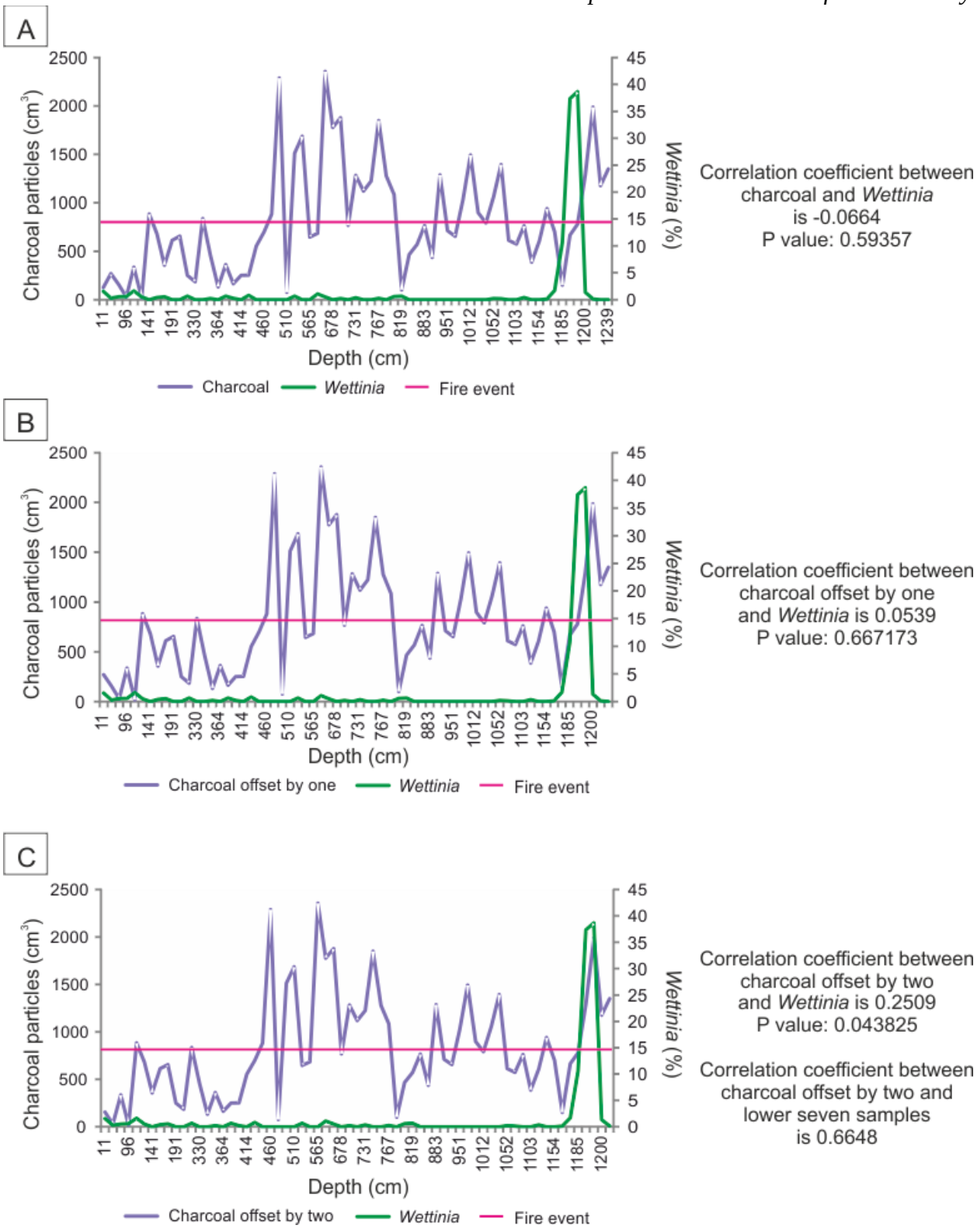

Figure 8.11: Correlation between *Wettinia* (percentage abundance) and charcoal particle concentration (cm^3) for MTE. Correlation coefficients have been included for all three scenarios (S_i, S_i+1 and S_i+2).

Figure 8.9 shows the correlation between charcoal particle concentration and *Celtis*. For all three scenarios tested, a weak correlation was recorded. The highest correlation was represented in

Figure 8.9 part B (at -0.4444). Figure 8.10 shows the correlation between *Hedyosmum* and charcoal particle concentration. *Hedyosmum* has a weak correlation with charcoal particle concentration, highest at a delay of one sample (part B, correlation coefficient 0.4129). Figure 8.11 shows the correlation between *Wettinia* and charcoal particle concentration. Figure 8.11 A and B show no relationship, with part C showing a weak relationship when the samples were offset by two, however, when taking into consideration only the seven lowest samples (zones 1 and 2; chosen as this was the time of the high levels of *Wettinia* pollen) of the stratigraphic sequence, the correlation between *Wettinia* and charcoal was a strong correlation of 0.6648 (graph shown in Appendix 2).

8.4.5. Comparison of pollen data from MTW and MTE

8.4.5.1. Shared pollen taxa in MTW and MTE
The MTW and MTE stratigraphic sequences contain ten pollen types above 10 % abundance that are present in both sites (*Phyllanthus*, *Hedyosmum*, *Miconia*, *Ilex*, *Alnus*, Asteraceae, Combretaceae/Melastomataceae, Polypodiaceae, monolete psilate and trilete fern spores). This means that out of the 34 pollen taxa included for both sites (>10 %), 29.41 % are shared. For MTW these ten pollen types account for between 34.65 and 62.99 % of the total pollen sum, for MTE they explain between 29.94 and 76.01 % of the pollen sum. Two non-pollen-palynomorphs are also similar features between the two stratigraphic sequences (Spore unknown OU 7 and Spore unknown OU 19).

8.4.5.2. Similarity of pollen assemblage data in MTW and MTE
The cluster analysis depicted on Figure 8.7 shows the relationship between the MTW and MTE stratigraphic sequences. The MTW samples (orange) form two main clusters, one on the left and one in the middle of the analysis. The MTE samples form no specific groups on the analysis; the samples are predominantly spread out. The lower samples of MTE (green) form a small group on

the far left and also on the right. The middle samples (blue) form a small cluster in between the two clusters of the orange MTW samples (Figure 8.7). The upper samples (purple) are intermixed with all of the samples.

8.4.5.3. Similarity in observed variance for the MTW and MTE pollen dataset

The DCA shown in Figure 8.6a shows that the variance in the pollen assemblage data from MTW is a sub-set of the variance found at MTE, i.e. the MTW samples (orange) are nested within the MTE points (purple, blue, green; Figures 8.6a and 8.7).

8.5. Discussion

8.5.1. Environmental change at MTW

8.5.1.1. Pollen and vegetation

The pollen preserved at MTW shows that the vegetation present during deposition was diverse (average pollen richness 39; Figure 8.1). Major taxa (>15 %, Hedyosmum, *Alnus* and *Ilex*; Figure 8.1) remained the same throughout the time of deposition, however, some minor taxa (e.g. *Myrica*, Papilionoideae; Figure 8.1) varied. The consistency of the major taxa implies that, despite some taxa reassortment, the vegetation present remained mostly stable through the period of deposition (stable vegetation being defined as a period in which major taxa have the highest abundances throughout). The major taxa present, as well as the taxon *Podocarpus,* suggest the pollen grains preserved within the sediments at MTW, were sourced from vegetation similar to modern upper montane forest (2500-3400 m asl; Harling, 1979). MTW is today at 1117 m asl so the pollen assemblage does not match the vegetation currently found at the site. The presence of higher elevation taxa in the MTW sediment is likely to be due to one of, or a mixture of the following reasons: i) occurrence of climate different than current values, ii) an extra regional source for the pollen, or (iii) presence of equivalent taxa found growing in other lowland locations today. Each of these reasons is now discussed in turn.

A decrease in temperature (compared to present day) could be responsible for the occurrence of upper montane forest at MTW. In two previous studies on the eastern Andean flank (970 m asl and 1914 m asl), the presence of *Podocarpus* along with taxa such as *Alnus* and *Hedyosmum* have been associated with a glacial cooling of 5-7.5 °C (Bush et al., 1990, Cárdenas et al., 2014). The presence of *Podocarpus*, *Alnus* and *Hedyosmum* within the MTW pollen assemblage could be indicative of local vegetation growing under cooler than modern conditions; however, due to the absence of independent dating (Chapter 6; Section 6.4.5), it is not possible to confirm that these samples were deposited during glacial conditions. Without independent dating, it was also not possible to relate this vegetation assemblage with any other data that would provide an idea about the temperature at the time of deposition (e.g. marine isotope stages). In order to avoid circular reasoning (Chapter 1), taxa typically associated with cooler temperatures should not be used to infer cooler temperatures, without a comparison with another proxy. As it cannot be ascertained whether a lower temperature than today is the cause of this change in taxa assemblage, other reasons were investigated. One other potential cause is that the signal preserved at MTW represents a mixed sediment source.

Today, there is high fluvial activity close to the MTW site (on the bank of the Río Alpayacu). The catchment area for the Río Alpayacu above MTW covers a 5622 m elevation range (Chapter 3). The large catchment means that the potential for pollen reaching the site (along water courses) from higher elevations in the modern day is large (see Chapter 7). It could, therefore, be that case that in the geological past, there was a level of fluvial activity impacting the deposition of sediments to MTW, bringing in pollen grains from higher elevation taxa. However, the presence of taxa typically associated with higher elevations (*Hedyosmum* and *Alnus*) is present in abundances >15 %, suggesting that at least part of this signal was as a result of the local growth of this genus. Also, in the sediment record for MTW (see stratigraphy on Figure 8.1), there is no

evidence of fluvial sediments; this can be taken as evident of no large fluvial inputs during deposition, meaning the pollen signal at MTW was likely to be representative of local taxa.

Aside from potential contamination issues, the fact that these pollen taxa could only be identified to genus level also proposes a problem, as within a genus, species can be extremely varied and grow at various altitudes. Species of both *Hedyosmum* and *Podocarpus* genera do grow at the elevation of MTW, for example *Hedyosmum cuatrecazanum* (Todzia) grows between 1000-1500 m asl, and *Podocarpus ingensis* (de Laub) which is the sole species which can grow at the elevation of MTW, growing between 1000 and 3000 m asl (Jørgensen and León-Yánez, 1999). It is, therefore, possible that the abundances of *Hedyosmum* and *Podocarpus* preserved in the pollen taxa could be related to these lower montane species *(Hedyosmum cuatrecazanum* (Occhioni) and *Podocarpus ingensis* (de Laub)). Current locations indicate that *Podocarpus ingensis* (de Laub) is only found in the South of Ecuador, at locations ~100 km south of Mera, and *Hedyosmum cuatreacazanum* (Occhioni) is only found in provinces surrounding Mera, with its nearest locale being c. 30 km away (Jørgensen and León-Yánez, 1999). *Alnus*, however, is only found nowadays growing at elevations higher than MTW in the Andes (1500-4000 m asl; *Alnus acuminata* (Kunth); Jørgensen and León-Yánez). A vegetation distribution map including *Alnus* shows that this taxon is not currently growing near MTW (Punyasena et al., 2011).

Two modern pollen samples (retrieved from surface cores; see Section 4.1.4; see Appendix B for data) contained small abundances of *Podocarpus* (1.34 % and 0.67 %), *Alnus* (4.35 % and 3.13 %) and larger abundances of *Hedyosmum* (8.03 % and 15.44 %), suggesting that these taxa could grow locally (hypothesis iii). The presence of this pollen could, however, be as a result of fluvial transportation from the nearby Alpayacu River (hypothesis ii). Presently there are no local (<30 km) populations of these taxa, however, this does not mean that at the time of deposition there were no local populations existing. It is uncertain as to which of these three

reasons caused the upper montane forest taxa to be so prevalent in the MTW stratigraphic sequence; they could all be contributing factors. Based on the presented evidence, it is suggested that such occurrence is most likely due to a combination of cooler than today's temperatures (due to the presence of *Podocarpus, Alnus* and *Hedyosmum* which have in previous studies been interpreted as a cooling; Bush et al., 1990, Cárdenas et al., 2014) and the presence of species which today survive at similar elevations.

8.5.1.2. Vegetation and fire

Despite the stability of the major taxa (>15 %) preserved at MTW, minor pollen taxa did see some instability, however, this was not necessarily as a result of fire, there was little visual correlation observed (Figure 8.1). Alongside this taxa reassortment, fire events were prevalent (eleven out of thirty samples classified as fire events) and as fire is a known ecological control (Bush et al., 2008), the relationship between fire and vegetation change was tested (Figures 8.2 and 8.3).

Figure 8.2 shows that DCA axes 1-4 are all varying independently of each other, suggesting that they are all corresponding to different variables acting upon the vegetation (for example precipitation, temperature and landscape scale change). Despite their differences, none of the four DCA axes closely follow the fire event occurrence. DCA axis 1 shows a small correlation to fire events; the relationship is a negative correlation (correlation coefficient -0.37; Figure 8.3). When the DCA axis is reversed (as on Figure 8.2), there is a good visual correlation. The weak correlation shown on Figure 8.3 (S_i) suggests that fire occurrence alone was not the sole control on taxa reassortment at MTW. The visual correlation observed in Figure 8.2 does, however, suggest it does play a role in the taxa reassortment, but it is likely that other drivers of change (such as precipitation, temperature, plant competition) also contributed in different degrees to the reassortment of the minor taxa and that fire alone was not the sole issue.

The vegetation preserved at MTW shows that at the time of deposition, the major taxa present did not respond directly to fire events, whereas minor taxa saw some reassortment. As only evidence of upper montane forest was found at MTW, it cannot be determined as to how the lower montane forest found today at MTW would respond to fire events. However, the information obtained for the response of the upper montane forest is important to help understand the impact fire has on other ecosystems of the ecologically important eastern Andean flank.

8.5.2. Environmental change at MTE

8.5.2.1. Pollen and vegetation

The pollen preserved at MTE shows that the vegetation present during the time of deposition was diverse (total pollen richness varied from 24 to 48; Figure 8.4). However, major taxa (*Hedyosmum, Ilex* and Asteraceae) in MTE varied in abundance throughout six defined vegetation zones (Figure 8.4).

MTE zones 1 and 2 in particular saw great changes in the abundant taxa, during these zones Asteraceae, *Ilex, Cecropia, Wettinia* and *Hedyosmum* were all, separately, major components (>15 %, Figure 8.4). The presence of *Cecropia* as a dominant taxon suggests that the vegetation assemblage has been disturbed, as *Cecropia* is often used in palaeoecological studies as potentially indicative of perturbations in the environment (Guariguata and Ostertag, 2001). In Chapter 7 it was hypothesised that the inorganic layer preserved at the beginning of zone 2 altered the landscape to a flat swamp environment. This disturbance could have cleared the previous vegetation, allowing *Cecropia* to rapidly colonise (Guariguata and Ostertag, 2001, Hartshorn, 1980). Following the increase in abundance of *Cecropia*, the palm *Wettinia* increased in abundance. *Wettinia* colonises readily on forest edges and on cleared, but not deforested, landscapes (Henderson et al., 1995), allowing its growth in this disturbed environment. The

growth of both *Cecropia* and *Wettinia* suggest that the environment saw some disturbance, possibly through either landscape change, increased fire occurrence (observed in zone 1 and 2, Figure 8.4) or a combination of them both. *Hedyosmum* increases in abundance following this, and it remains an important component of the vegetation assemblage until zone 6, when it sees a decrease in abundance, replaced by *Alnus*, *Celtis* and Asteraceae. The shift in taxa abundance in zone 6 is interpreted in Chapter 7 as a change in source area, with fluvial influence contributing to a more regional pollen source area leading to the arrival of taxa associated with higher elevation upper montane forest.

The vegetation assemblage at MTE is representative of two vegetation types, with the presence of *Alnus*, Ericaceae and Myrtaceae being indicative of the upper elevation range of the lower montane rainforest (~1500-2500 m asl), and the presence of *Ilex* and *Hedyosmum* suggesting the presence of upper montane forest (2500-3400 m asl). The combination of these two vegetation types suggests that this was a non-analogous community (Bush et al., 2011b), with high vegetation reassortment. Non-analogous communities are not uncommon in the past and are often formed due to some species having different tolerance ranges and/or sensitivity to environmental changes (e.g. temperature change during a deglaciation), and as such a mixture of species forms, leading to these non-analogous communities which no longer exist, or are rare combinations (Bush et al., 2011b, Williams and Jackson, 2007).

8.5.2.2. Vegetation and fire

Fire was a natural component of the landscape at MTE during the period of deposition, with twenty six out of sixty seven samples being recognised as fire events (Figure 8.4). All of the DCA axes relating pollen abundances to charcoal particle concentration are highly variable, and all of them bare little relationship to each other, suggesting they are each related to different drivers (Figure 8.5).

Figure 8.8A shows that there was no correlation observed between fire events and DCA axis 1 (correlation coefficient of 0.16). However, when the samples were offset against charcoal concentration (S_i+1 and S_i+2), there was a weak correlation (Figures 8.8B and C). The weak correlation observed in Figure 8.8B (S_i+1) shows that the lower part of the section had a good correlation between DCA axis 1 and charcoal. Figure 8.8C (S_i+2) shows that the upper part of the section has a better correlation between charcoal particles and DCA axis 1. This possibly implies that, in case the vegetation shift is being driven by fire occurrence, the lower part of the stratigraphic sequence responded faster to fire events than the upper half of the sequence. It could also be the case that the lower part of the sequence had a slower sedimentation rate than the upper part of the sequence, meaning more sediment accumulated in less time in the lower part, leading to a blurred (quicker) signal being preserved.

The highest occurrence of fire events is in zone 4 and zone 5, with a total of 13 samples out of 21 being classified as fire events. This zone sees low values in DCA axis 1, with values only rising above zero when the charcoal particle concentration was reduced (Figure 8.5). The pollen preserved in MTE responds to the increase in fire, in particular the taxon *Hedyosmum* (Figure 8.3). At the beginning of zones 4 and 5, abundances of *Hedyosmum* are high (>35 %), however, correlating with the high occurrence of fire events, the levels of *Hedyosmum* decrease throughout the zones (Figure 8.4). Levels of Ericaceae also drop during zones 4 and 5, falling from a high of 19.74 % in zone 3 to an average of 2.52 % in zones 4 and 5. Conversely, levels of Combretaceae/Melastomataceae rise (average of 7.81 % across the zones compared to an average of 5.62 %) coeval to increased levels of fire events.

The lowest occurrence of fire events was in zone 6, where only 2 samples reached the minimum values recognised as fire events here. This decrease in fire events could be due to: i) increased moisture availability, or ii) decreased fuel load. During the time of decreased fire levels it was

hypothesised that a river incised through the environment (Chapter 7, Section 7.6.1.4). The incision of a river would have caused higher water levels at MTE meaning the moisture availability would increase; this would make it harder for the fuel load to burn (consequently a decrease in fire events). Secondly, in zone 6 it was hypothesised that the pollen here was representative of a more regional signal (Chapter 7; section 7.6.1.4). It could be the case that at this time the vegetation at MTE became less dense (supported by an increase in Poaceae; Figure 8.4; Gosling et al., 2009), and consequently there was a drop in the availability of fuel at MTE during zone 6. It cannot, however, be determined whether that was the case from this data. A possible decrease in fuel load combined with an increase in moisture could have contributed to the decrease in fire events during this zone, both reasons are acknowledged in the literature as common causes for reduced fire occurrence (Gosling et al., 2009, Kitzberger et al., 1997).

During zone 6, DCA axis 1 saw its highest values (>0.5) synchronous to decreasing fire levels, suggesting that DCA axis 1 had a correlation with the charcoal particle concentration, regardless of the reasons for a reduction in fire events. Zone 6 also saw a distinct change in the pollen assemblage (increased abundances of *Alnus*, *Celtis* and Asteraceae; see 7.6.1.4), parallel to a decrease in charcoal. During the decreased fire events of zone 6, *Celtis* increased in abundance from an average of 1.32 % in zones 1-5 to 5.77 % in zone 6. Due to this rise, the correlation of *Celtis* was tested against charcoal particles (Figure 8.9). However, *Celtis* had a weak correlation with charcoal (correlation coefficient: -0.32), suggesting that another variable is mainly driving this change in taxon abundance, as hypothesised in Chapter 7 (section 7.6.1.4: this increase in taxa abundance could be due to a change in pollen source area).

Wettinia was an important taxon at the beginning of the section (zone 2; Figure 8.4). It was hypothesised that *Wettinia* may respond at a delay of one sample to increasing charcoal concentrations (Figure 8.10). *Wettinia* had no correlation at a delay of one sample, but a positive

correlation to charcoal concentration was observed at a delay of two samples, and when only the samples with high concentrations of *Wettinia* were tested, the correlation was high (correlation coefficient =0.6648). This implies that *Wettinia* most likely responded to the occurrence of fires within the environment, possibly due to its readiness to grow in the cleared environments that exist following a fire. Chapter 7 hypothesises a cleared environment at the bottom of the section, and the increase in fire would have also contributed to the growth of *Wettinia*, following the establishment of the pioneer taxon *Cecropia*.

Aside from the potential relationship between *Wettinia* and fire, the overall relationship between charcoal and DCA axis 1 was a weak correlation. This suggests that fire events were only a minor component in the vegetation reassortment that was occurring, with other variables also causing the vegetation change.

8.5.3. Comparison of vegetation at MTW and MTE

The pollen preserved at MTW and MTE was varied, with only a 29.41 % similarity between the pollen taxa present (10 out of 34 taxa over 10 % were the same; Figures 8.1 and 8.4). However, even though the two sites are close (c. 0.38 km away from each other), the dissimilarity in the pollen assemblage between the two sites is not unexpected when modern vegetation studies on mega diverse locations are considered (Condit et al., 2002). A study of modern vegetation was performed in 2002 to identify beta diversity in lowland Amazonia (in Ecuador's Yasuní National Park and Peru's Manu Biosphere Reserve), and it stated that adjacent 1 Ha plots shared only 55% of species, and that at greater distances between plots (>1 km), the similarity in diversity between the two plots decreased even further (Condit et al., 2002). The high floristic diversity observed at MTW (Figure 8.1) and MTE (Figure 8.4) suggests that a difference between the two sites can be expected, as a large range of taxa are present. Despite major taxa being shared between the two sites (*Hedyosmum, Ilex* and *Alnus*), different minor taxa were present, a factor that is not unexpected when considering the study by Condit (2002). Furthermore, it has not been

clarified whether the MTW and MTE sites cover the exact same time period (Chapter 6). Based on the preliminary dating attempts (Chapter 6), it is likely that at least part, or all of the section was deposited at different time periods, meaning that a high dissimilarity in taxa presence would not be unusual. If these two sections were deposited at different times, the climate could also have been different, meaning a dissimilar type of plant species would flourish, and the source of the pollen signal could also be different, leading to a different input of regional pollen at both sites. The dissimilar spatial and/or temporal deposition of the MTW and MTE stratigraphic sections is the likely reason for the different pollen types and taxa found.

8.5.4. Response to fire, similarities between MTW and MTE

The response of MTW and MTE to fire events is also different, with MTW having a weak/no correlation between DCA axis 1 and charcoal particle concentration, and MTE having a weak correlation (Figures 8.3 and 8.11). Both of the sites see a stronger correlation when the charcoal particle concentration and DCA axis 1 are offset by one (S_i+1), or two (S_i+2) samples, suggesting a potential delay in vegetation response, possibly indicative of a post fire succession occurring. However, due to the sampling resolution (every 10 cm), and lack of age-depth model, it is not possible to say whether these samples would capture a post fire succession, or if the gap between samples was too large to see any response in the vegetation system. As an example, Lake Consuelo (13°57.1'S, 68°59,45'W; 1360 m asl) situated on the Peruvian eastern Andean flank, had a sedimentation rate varying from 0.01 to 0.06 cm/year (Urrego et al., 2010). If this was the case for the Mera Tigre sites then 10 cm of sediment could represent between 1000 and 166.67 years. The sedimentation rate for MTW and MTE could, however, be vastly different than the rate estimated for that of Lake Consuelo. If the sedimentation rate of MTW and MTE was similar to Lake Consuelo, it is unlikely that a full post fire succession would be captured. A palaeoecological study performed in Lake La Cocha, Colombia (01°06'N, 77°09W, 2780 m asl) reported that forest stability only lasted for a maximum of 200 to 600 years (González-Carranza

et al., 2012), suggesting constant reassortment in a time period that would not necessarily be covered by a 10 cm resolution.

In the present day, fire is not an important driver on vegetation dynamics in the Mera Tigre region due to the high level of precipitation (Ferdon, 1950, Liu and Colinvaux, 1985). The area does not burn naturally, it only burns through human intervention (Cárdenas et al., 2014); however, pre-human fire did play a role in vegetation ecosystems, as MTE in particular, shows. The impact of fire on the vegetation at MTW is less obvious, however, it is likely that it did still play a role in shaping the vegetation community, but it was not the dominant driver impacting vegetation dynamism, meaning that its impact could have been masked by additional environmental drivers. For both MTW and MTE, fire was not the dominant driver, other drivers of change were likely to be responsible for the vegetation change observed, however, in order to observe those drivers further proxies are required.

Other palaeoecological studies have also found mixed responses of vegetation to fire as a driver. In 2014, Cárdenas hypothesised that fires (ignition source of volcanoes) had a significant impact on the vegetation of the eastern Andean flank of Ecuador during the Pleistocene (Cárdenas et al., 2014). Although they noted differences in the vegetation following increased charcoal particle abundance, similar to the Mera Tigre sections, they stated there was insignificant resolution to detect the impact of a specific event to an individual ecosystem (Cárdenas et al., 2014). A palaeoecological study performed in Noel Kempff Mercado National Park in the Bolivian Amazon discovered that, similar to the Mera Tigre sites, fire was only one of many drivers of change acting upon vegetation (Burbridge et al., 2004). It was discovered that in this case, alteration in the precipitation levels was also responsible for vegetation change, as was temperature (Burbridge et al., 2004).

8.6. Palaeoecology of MTW and MTE compared to other South American records

The pollen and charcoal data presented in this chapter, combined with the dating results included in Chapter 6, and the physical data in Chapter 7 (LOI, XRF), represent the introduction of two additional multi proxy sites to the understudied montane forests of the eastern Andean flank (Bush et al., 2011a, Bush et al., 2011b). In order to place these sites in regional context, the results obtained from the proxies presented in this thesis will be compared briefly against previously published sites on the eastern Andean flank.

An obvious comparison to the Mera Tigre sequences (due to proximity; <1.5 km from Mera Tigre sites) is the original Mera site (Bush et al., 1990, Colinvaux et al., 1996, Heine, 1994, Liu and Colinvaux, 1985). A comparison between the dating obtained at the Mera site and the Mera Tigre sites was covered in section 6.4.4. Pollen data for MTW, MTE and Mera, show that two taxa above 10 % at the Mera Tigre sites were also present in abundances >10 % in Mera, these taxa were Combretaceae/Melastomataceae and *Alnus* (Bush et al., 1990). High percentages of *Hedyosmum* were also present at the original Mera site; however, percentage abundances only reached ~9.5 % (Bush et al., 1990); in MTW and MTE *Hedyosmum* reached abundances of over 15 %. Minor taxa (see Appendix B for pollen taxa <10 %) were also shared between the two sites. No charcoal record was produced for the original Mera site. Compared to the original Mera site, the two stratigraphic sequences presented in this thesis have: i) improved the resolution of palaeoecological data from the Mera region (from 6 in the original Mera site to 107 samples for MTW and MTE, all of which were counted to a statistically significant level following Chapter 5; Keen et al., 2014), and ii) applied a multi proxy approach by introducing the charcoal and physical proxy records (LOI and XRF). The depositional environment of MTE was also analysed, providing information about sediment provenance.

Other sites on the eastern Andean flank of Ecuador (San Juan Bosco and Erazo) also share similarities with the Mera Tigre sites presented in this thesis. San Juan Bosco (03° 03.45’S, 78°

27.20'W; 970 m asl) was dated to 26,020 ± years BP, similar to the Mera site, there was no charcoal record presented, meaning it was not possible to compare the response of vegetation and fire to that of the Mera Tigre sites (Bush et al., 1990). The pollen record (vegetation) at San Juan Bosco was comprised of mainly swampland taxa, with a shift to high *Weinmannia* (>20 %) in the upper part of the sequence. San Juan Bosco only shared one taxon above 10 % (Combretaceae/Melastomataceae) with the two Mera Tigre sequences. The major taxon present at San Juan Bosco (and the original Mera site) was *Weinmannia* (Cunoniaceae) (Bush et al., 1990). *Weinmannia* is a montane taxa and it was not present in either Mera Tigre site at greater than 4 % abundance (see Appendix B). The pollen assemblages of San Juan Bosco and Mera were interpreted as indicative of a glacial cooling of up to 7.4 °C (Bush et al., 1990, Liu and Colinvaux, 1985), despite sharing a similar taxa assemblage, the same cannot be inferred from the MTW and MTE sequences due a lack of age constraint (see 6.4.5).

The palaeoecological site of Erazo (0°33.42' S, 77°52.43' W; 1914 m asl), also located on the eastern Andean flank, observed a glacial cooling of c. 5 °C compared to modern temperatures during glacial periods (between 192,000 and 620,000 years BP), similar to Mera and San Juan Bosco this was inferred from the presence of *Podocarpus* (Cárdenas et al., 2014, Cárdenas et al., 2011). Glacial flora inferred from Erazo was comprised of *Podocarpus,* Hedyosmum and Poaceae, interglacial flora was comprised of Arecaceae, Cyperaceae, ferns and aquatics (Cárdenas et al., 2014). Palaeoecological data obtained from Erazo (spanning c. 192,000 to c. 620,000 years BP), showed that fires had a significant impact on vegetation reassortment (Cárdenas et al., 2014). At the Mera Tigre sites, there was no strong correlation relating reassortment of vegetation and fire (see Sections 8.5.1.2 and 8.5.2.2). Interestingly, Erazo also saw parts of the stratigraphic sequence with high inorganic levels similar to MTE (see Figure 7.2). In MTE, this was interpreted as an influx of inorganic fluvial sediments, however, in Erazo there was no interpretation. Despite the production of Argon ages for Erazo, a chronology could

not be constructed for the sequence, similar to the Mera Tigre dates (radiocarbon and OSL) there was analytical uncertainty in the ages (Cárdenas et al., 2014).

In Colombia, a record (Piagua; 2°30'N, 76°30'W) taken from a small swamp at 1700 m elevation was dated to represent the time period between 650 and >14,500 years BP (Wille et al., 2001). Similar to both MTW and MTE, Piagua contained high percentages of *Miconia* (>10 %), *Alnus* (20 %) and Melastomataceae (>15 %; Wille et al., 2001). Unlike in MTW and MTE, however, the percentages of these taxa were only high sporadically during the sequence, where as in MTW and MTE they were consistently high (Wille et al., 2001; Figures 8.1 and 8.4). The occurrence of *Miconia* (combined with *Weinmannia*), was interpreted as a period of cooling (4-5 °C cooler than today), similar to that observed in Mera and San Juan Bosco (Bush et al., 1990, Wille et al., 2001). From the evidence presented at Piagua, Mera and San Juan Bosco, the presence of *Hedyosmum*, *Miconia*, *Ilex*, *Alnus* in MTE and also *Podocarpus* in MTW and MTE could be indicative of cooler temperatures. This is based on a combination of the taxa and dates used to infer cooler temperatures at other palaeoecological sites on the eastern Andean flank. However, due to issues constraining the age of the Mera Tigre sections (Section 6.4.5) this cannot be said for certain.

Changes in pollen taxa were also recorded during the last 46,300 years at Lake Consuelo, Peru (13°57.1'S, 68°59.45'W; 1360 m asl; Bush et al., 2004, Urrego et al., 2010). Similar to both MTW and MTE, Lake Consuelo recorded the reassortment of minor taxa during the depositional period, it also saw the reassortment of major taxa, similar to MTE (Urrego et al., 2010 and Figure 8.4). In MTE the major taxa included Asteraceae, *Cecropia*, *Ilex*, *Wettinia* and *Hedyosmum*, in Consuelo the major taxa included Melastomataceae-Combretaceae, Moraceae-Urticaceae, Poaceae and *Cecropia* (Bush et al., 2004, Urrego et al., 2010). In Consuelo, the reassortment of major taxa was interpreted as a response to temperature and moisture change; in

MTE these changes were associated with burning (*Wettinia*), landscape change and regional pollen influx. No micro charcoal was observed in the analysed pollen slides for Consuelo and no macro charcoal analysis was undertaken, meaning the fire record of MTE and MTW cannot be compared with Consuelo.

Other palaeoecological sites discussed in this section show the wide variety of drivers impacting upon the vegetation of the eastern Andean flank, these include: i) fire –MTW, MTE, Erazo, ii) temperature – Mera, San Juan Bosco, Erazo, Piagua and Consuelo, iii) moisture availability – Consuelo and finally iv) landscape change – MTW and MTE (Bush et al., 1990, Cárdenas et al., 2014, Cárdenas et al., 2011, Liu and Colinvaux, 1985, Urrego et al., 2010, Wille et al., 2001). This wide variety of drivers indicates the complexity surrounding the interpretation of eastern Andean vegetation records. In this thesis, the impacts of landscape change (Chapter 7) and fire (this Chapter) on eastern Andean flank vegetation were analysed, greatly improving the data currently available for the Mera region. The complexity of dating outcrop sediments from the Mera region was also covered (Chapter 6).

8.7. Conclusions

The vegetation present during the period of deposition for both MTW and MTE was diverse and dynamic. The most abundant taxa (*Hedyosmum*) at both sites was the same, however, overall the sites only shared 34.48 % of taxa over 10 %. This is likely due to the diverse nature of the vegetation of the eastern Andean flank, and possible differences in the time of deposition. MTW saw high levels of taxa representative of the upper montane forest, and despite taxa reassortment throughout the time of deposition, the ecosystem represented was stable throughout (meaning the major taxa, namely *Hedyosmum* did not alter). The occurrence of this higher elevation vegetation type at MTW could be attributed to a: i) lower temperature than the modern day, ii) a high proportion of pollen from regional sources brought in by rivers, or iii) the presence of species from these taxa that can survive at this elevation. Due to a lack of age constraint, or other

supporting data from MTW, it is difficult to determine which mechanism was likely to have caused the presence of these higher elevation taxa; however, it was proposed that it was most likely due to lower temperatures and the local growth of taxa that can survive at low elevations. The pollen taxa present at MTE were more dynamic, with major taxa reassortment present at the beginning and end of the stratigraphic sequence (Figure 8.4). The diverse mixture of taxa present indicated the presence of a non-analogous mixture of lower montane forest (taxa associated with the upper portion) and the upper montane forest. The presence of the taxa forming this non-analogous vegetation type was likely due to a mixture of regional contamination (from fluvial influence) and fire and landscape changes in the lower part of the MTE section, (pollen zones 1 and 2; Figure 8.4) allowing a cleared environment for taxa such as *Cecropia* and *Wettinia* to grow.

As well as having different pollen assemblages, both sites reacted in different ways to fire events. MTW saw a weak/no correlation between fire events and the vegetation dynamics represented in DCA axis 1, suggesting that other drivers of change (temperature, precipitation, regional pollen source, landscape change) were attributing to the taxa reassortment observed in Figure 8.1. MTE, however, saw a weak correlation between fire events and vegetation change, the value increasing when the fire events were related to the DCA value in the sample after, suggesting the vegetation had a delayed reaction to the fire events. This delayed response to fire could be related to a post fire succession occurring in the environment, but it could also be due to the length of time taken for plants to produce pollen following a disturbance. Age constraints are required to test the likelihood of these potential explanations in a high resolution analysis.

In this chapter, the MTW and MTE sequences were also compared with other palaeoecological work from the eastern Andean flank (Ecuador, Colombia and Peru). Vegetation preserved at MTW and MTE was partially similar to some assemblages found at other sites, that were

interpreted as a cooling in the magnitude of ~5 °C (from modern day temperatures), therefore, suggesting a potential cooling at the Mera Tigre sites during the time of the palynomorphs deposition (Bush et al., 1990, Urrego et al., 2010, Wille et al., 2001). Due to a lack of age constraints, this could not be proven for the Mera Tigre sites. Previous fire records from the eastern Andean flank (Erazo), showed a greater relationship with fire, than that observed at the Mera Tigre sites (Cárdenas et al., 2014, Cárdenas et al., 2011). At Erazo, fire was deemed to be an important driver of vegetation change, in the Mera Tigre sites presented in this thesis, other drivers (e.g. landscape change) played an important role.

In order to further understand the impact fire has on vegetation, in light of a potential future impact of an increased fire regime (as a result of decreased precipitation and anthropogenic impact) on the forests of the eastern Andean flank, it is essential that further palaeoecological sites are studied, particularly those with a higher resolution. The higher resolution (tens of years between samples) will allow any post fire succession that is occurring to be identified, allowing a greater understanding of how this region will respond to future fire events. Although this study has not uncovered the relationship between fire events and vegetation change, it has provided two further studies which have highlighted the fact that fire has impacted the forests of the eastern Andean flank previously, alongside other drivers of change. It has also shown the complexity of vegetation-fire dynamics on the eastern Andean flank, providing further information towards understanding this intricate relationship.

8.8. Summary

This chapter investigated the vegetation preserved as pollen at MTW and MTE and how it responded to fire events (preserved as charcoal particles). It also compared MTW and MTE with relevant palaeoecological sites from the eastern Andean flank of Ecuador, Colombia and Peru. The next chapter, Chapter 9, presents the conclusions of the thesis in relation to the aims outlined in Chapter 1. Limitations of the research and future work are also highlighted.

References

BAIED, C. A. & WHEELER, J. C. 1993. Evolution of High Andean Puna Ecosystems: Environment, Climate, and Culture Change over the Last 12,000 years in the Central Andes. *Mountain Research and Development,* 13**,** 145 - 156.

BARLOW, J., GARDNER, T. A., ARAUJO, I. S., ÁVILA-PIRES, T. C., BONALDO, A. B., COSTA, J. E., ESPOSITO, M. C., FERREIRA, L. V., HAWES, J., HERNANDEZ, M. I. M., HOOGMOED, M. S., LEITE, R. N., LO-MAN-HUNG, N. F., MALCOLM, J. R., MARTINS, M. B., MESTRE, L. A. M., MIRANDA-SANTOS, R., NUNES-GUTJAHR, A. L., OVERAL, W. L., PARRY, L., PETERS, S. L., RIVEIRO-JUNIOR, M. A., DA SILVA, M. N. F., DA SILVA, C. & PERES, C. A. 2007. Quantifying the biodiversity value of tropical primary, secondary, and plantation forests. *Proceedings of the National Academy of Sciences,* 104**,** 18555-18560.

BARLOW, J. & PERES, C. A. 2008. Fire-mediated dieback and compositional cascade in an Amazonian forest. *Philosophical Transactions of the Royal Society B: Biological Sciences,* 363**,** 1787-1794.

BARNOSKY, A. D. & LINDSEY, E. L. 2010. Timing of Quaternary megafaunal extinction in South America in relation to human arrival and climate change. *Quaternary International,* 217**,** 10 - 29.

BELCHER, C., MANDER, L., REIN, G., JERVIS, F. X., HAWORTH, M., HESSELBO, S. P., I.J., G. & MCELWAIN, J. C. 2010. Increased fire activity at the Triassic/ Jurassic boundary in greenland due to climate-driven floral change. *Nature Geoscience,* 3**,** 429-429.

BIRKS, H. J. B. & BIRKS, H., H. 1980. *Quaternary Palaeoecology,* New Jersey, The Blackburn Press.

BORCHSENIUS, F. 1997. Patterns of plant species endemism in Ecuador. *Biodiversity & Conservation,* 6**,** 329-399.

BURBRIDGE, R., MAYLE, F. E. & KILLEEN, T. J. 2004. Fifty-thousand-year vegetation and climate history of Noel Kempff Mercado National Park, Bolivian Amazon. *Quaternary Research,* 61**,** 215-230.

BUSH, M. B. 2004. 48,000 Years of Climate and Forest Change in a Biodiversity Hot Spot. *Science,* 303**,** 827-829.

BUSH, M. B., COLINVAUX, P. A., WIEMANN, M. C., PIPERNO, D. E. & LIU, K.-B. 1990. Late Pleistocene temperature depression and vegetation change in Ecuadorian Amazonia. *Quaternary Research,* 34**,** 330 - 345.

BUSH, M. B., GOSLING, W. D. & COLINVAUX, P. A. 2011a. Climate and vegetation change in the lowlands of the Amazon Basin. *In:* BUSH, M. B., FLENLEY, J. R. & GOSLING, W. D. (eds.) *Tropical rainforest responses to climatic change.* 2nd ed. Berlin Heidelberg: Springer- Verlag.

BUSH, M. B., HANSELMAN, J. A. & HOOGHIEMSTRA, H. 2011b. Andean montane forests and climate change. *In:* BUSH, M. B., FLENLEY, J. R. & GOSLING, W. D. (eds.) *Tropical rainforest responses to climatic change.* 2nd ed. Berlin Heidelberg: Springer - Verlag.

BUSH, M. B., SILMAN, M. R., MCMICHAEL, C. H. & SAATCHI, S. 2008. Fire, climate change and biodiversity in Amazonia: a Late-Holocene perspective. *Philosophical Transactions of the Royal Society B: Biological Sciences,* 363**,** 1795-1802.

BUSH, M. B., SILMAN, M. R. & URREGO, D. H. 2004. 48,000 Years of Climate and Forest Change in a Biodiversity Hot Spot. *Science,* 303**,** 827-829.

BUSH, M. B. & WENG, C. 2007. Introducing a new (freeware) tool for palynology. *Journal of Biogeography,* 34**,** 377-380.

CÁRDENAS, M. L., GOSLING, W. D., PENNINGTON, R. T., POOLE, I., SHERLOCK, S. C. & MOTHES, P. 2014. Forests of the tropical eastern Andean flank during the middle Pleistocene. *Palaeogeography, Palaeoclimatology, Palaeoecology,* 393**,** 76 - 89.

CÁRDENAS, M. L., GOSLING, W. D., SHERLOCK, S. C., POOLE, I., PENNINGTON, R. T. & MOTHES, P. 2011. The Response of Vegetation on the Andean Flank in Western Amazonia to Pleistocene Climate Change. *Science,* 331**,** 1055-1058.

CARDOSO, M., NOBRE, C. A., SAMPAIO, G., HIROTA, M., VALERIANO, D. & CÂMARA, G. 2009. Long-term potential for tropical-forest degradation due to deforestation and fires in the Brazilian Amazon. *Biologia,* 64**,** 433-437.

CLARK, J. S. & ROYALL, P. D. 1995. Particle-Size evidence for source areas of charcoal accumulation in Late Holocene sediments of Eastern North American Lakes. *Quaternary Research,* 43**,** 80 - 89.

COLINVAUX, P. A., DE OLIVEIRA, P. E. & PATIÑO, J. E. M. 1999. *Amazon pollen manual and atlas,* Amsterdam, Harwood Academic Publishers.

COLINVAUX, P. A., LIU, K.-B., DE OLIVEIRA, P. E., BUSH, M. B., MILLER, M. C. & STEINITZ - KANNAN, M. 1996. Temperature depression in the lowland tropics in glacial times. *Climatic Change,* 32**,** 19 - 33.

CONDIT, R., PITMAN, N., LEIGH JR, E. G., CHAVE, J., TERBORGH, J., FOSTER, R. B., NÚÑEZ, P., AGUILAR, S., VALENCIA, R., VILLA, G., MULLER-LANDAU, H. C., LOSOS, E. C. & HUBBELL, S. P. 2002. Beta-diversity in tropical forest trees. *Science,* 295**,** 666-669.

DE TOLEDO, M. B., BARTH, O. M., SILVA, C. G. & BARROS, M. A. 2009. Testing multivariate analysis in paleoenvironmental reconstructions using pollen records from Lagoa Salgada, NE Rio de Janeiro State, Brazil. *Anais de Academia Brasileira de Ciências,* 81**,** 757-768.

DENMAN, K. L., BRASSEUR, G., CHIDTHAISONG, A., CIAIS, P., COX, P. M., DICKINSON, R. E., HAUGLUSTAINE, D., HEINZE, C., HOLLAND, E., JACOB, D., LOHMANN, U., S., R., DA SILVA DIAS, P. L., WOFSY, S. C. & ZHANG, X. 2007. Couplings between changes in the climate system and biogeochemistry. *In:* SOLOMON, S., QIN, D., MANNING, M., CHEN, Z., MARQUIS, M., AVERYT, K. B., TIGNOR, M. & MILLER, H. L. (eds.) *Climate Change 2007.* Cambridge, United Kingdom: Cambridge University Press.

FERDON, E. N. J. 1950. *Studies in Ecuadorian Geography,* Santa Fe, New Mexico, School of American Research and University of Southern California.

GONZÁLEZ-CARRANZA, Z., HOOGHIEMSTRA, H. & VÉLEZ, M. I. 2012. Major altitudinal shifts in Andean vegetation on the Amazonian flank show temporary loss of biota in the Holocene. *The Holocene,* 22**,** 1227-1241.

GOSLING, W. D., MAYLE, F. E., TATE, N. J. & KILLEEN, T. J. 2009. Differentiation between Neotropical rainforest, dry forest, and savannah ecosystems by their modern pollen spectra and implications for the fossil pollen record. *Review of Palaeobotany and Palynology,* 153**,** 70-85.

GUARIGUATA, M. R. & OSTERTAG, R. 2001. Neotropical secondary forest succession: changes in structural and functional characteristics. *Forest ecology and management,* 148**,** 185-206.

HARLING, G. 1979. The vegetation types of Ecuador - A brief survey. *In:* LARSEN, K. & HOLM-NIELSEN, L. B. (eds.) *Tropical Botany.* London: Academic press.

HARTSHORN, G. S. 1980. Neotropical forest dynamics. *Biotropica,* 12**,** 23-30.

HEINE, K. 1994. The Mera site revisited: Ice - age Amazon in the light of new evidence. *Quaternary International,* 21**,** 113 - 119.

HENDERSON, A., GALEANO, G. & BERNAL, R. 1995. *Field Guide to the Palms of the Americas.,* Princeton, New Jersey, Princeton University Press.

HIGUERA, P. E., SPRUGEL, D. G. & BRUBAKER, L. B. 2005. Reconstructing fire regimes with charcoal from small-hollow sediments: a calibration with tree-ring records of fire. *The Holocene,* 15**,** 238-251.

HILL, M. O. 1974. Correspondence analysis: A neglected multivariate method. *Journal of the royal statistical society. Series C (Applied Statistics),* 23**,** 340-354.

HOOGHIEMSTRA, H. 1984. Vegetational and climatic history of the high plain of Bogotá, Colombia: a continuous record of the last 3.5 million years. . *Dissertationes Botanicae,* 79**,** 1 - 138.

HUNTINGFORD, C., ZELAZOWSKI, P., GALBRAITH, D., MERCADO, L. M., SITCH, S., FISHER, R., LOMAS, M., WALKER, A. P., JONES, C. D., BOOTH, B. B. B., MALHI, Y., HEMMING, D., KAY, G., GOOD, P., LEWIS, S. L., PHILLIPS, O. L., ATKIN, O. K., LLOYD, J., GLOOR, E., ZARAGOZA-CASTELLS, J., MEIR, P., BETTS, R., HARRIS, P. P., NOBRE, C. A., MARENGO, J. & COX, P. M. 2013. Simulated resilience of tropical rainforests to CO_2-induced climate change. *Nature Geoscience,* 6**,** 268 - 273.

JØRGENSEN, P. M. & LEÓN-YÁNEZ, S. 1999. *Catalogue of the vascular plants of Ecuador,* St Louis, Missouri, Missouri Botanical Garden Press.

KEEN, H. F., GOSLING, W. D., HANKE, F., MILLER, C. S., MONTOYA, E., VALENCIA, B. G. & WILLIAMS, J. J. 2014. A statistical sub-sampling tool for extracting vegetation community and diversity information from pollen assemblage data. *Palaeogeography, Palaeoclimatology, Palaeoecology,* 408**,** 48 - 59.

KITZBERGER, T., VEBLEN, T. T. & VILLALBA, R. 1997. Climatic influences on fire regimes along a rain forest-to-xeric woodland gradient in northern Patagonia, Argentina. *Journal of Biogeography,* 24**,** 35-47.

LITWIN, R. J., ADAM, D. P., FREDERIKSEN, N. O. & WOOLFENDEN, W. B. 1997. An 800,000-year pollen record from Owens Lake, California: Preliminary analyses. *In:* SMITH, G. L. & BISCHOFF, J. L. (eds.) *An 800,000-Year paleoclimatic record from Core OL-92, Owens Lake, Southeast California.* Colorado: Geological Society of America Special Paper 317.

LIU, K.-B. & COLINVAUX, P. A. 1985. Forest changes in the Amazon Basin during the last glacial maximum. *Nature,* 318**,** 556 - 557.

MAHER, L. J. 1972. Nomograms for computing 0.95 confidence limits of pollen data. *Review of Palaeobotany and Palynology,* 13**,** 85-93.

MALHI, Y., ROBERTS, J. T., BETTS, R. A., KILLEEN, T. J., LI, W. & NOBRE, C. A. 2008. Climate Change, Deforestation, and the Fate of the Amazon. *Science,* 319**,** 169-172.

MALHI, Y., SILMAN, M. R., SALINAS, N., BUSH, M., MEIR, P. & SAATCHI, S. 2010. Introduction: Elevation gradients in the tropics: laboratories for ecosystem ecology and global change research. *Global Change Biology,* 16**,** 3171-3175.

MOORE, P. D., WEBB, J. A. & COLLINSON, M. E. 1991. *Pollen analysis,* Oxford, Blackwell Scientific.

MORENO, P. I., VILLA-MARTÍNEZ, R., CÁRDENAS, M. L. & SAGREDO, E. A. 2012. Deglacial changes of the southern margin of the southern westerly winds revealed by terrestrial records from SW Patagonia (52°S). *Quaternary Science Reviews,* 41**,** 1-21.

MYERS, N., MITTERMELER, R. A., MITTERMELER, C. G., DA FONSECA, G. A. B. & KENT, J. 2000. Biodiversity hotspots for conservation priorities. *Nature,* 403**,** 853 - 858.

NGOMANDA, A., CHEPSTOW-LUSTY, A. J., MAKAYA, M., SCHEVIN, P., MALEY, J., FONTUGNE, M., OSLISLY, R., RABENKOGO, N. & JOLLY, D. 2005. Vegetation changes during the past 1300 years in western equatorial Africa: a high-resolution pollen record from Lake Kamalété, Lopé Reserve, Central Gabon. *The Holocene,* 15**,** 1021-1031.

OKSANEN, J., BLANCHET, F. G., KINDT, R., LE GENDRE, P., MINCHIN, P. R., O'HARA, R. B., SIMPSON, G. L., SOLYMOS, P., STEVENS, M. H. H. & WAGNER, H. 2013.

Vegan: Community Ecology Package [Online]. Available: http://CRAN.R-project.org/package=vegan [Accessed 09/03/2015.

PEET, R. K., KNOX, R. G., CASE, J. S. & ALLEN, R. B. 1988. Putting things in order: The advantages of detrended correspondence analysis. *American Society of Naturalists,* 131**,** 924-934.

PUNYASENA, S. W., DALLING, J. W., JARAMILLO, C. A. & TURNER, B. L. 2011. Comment on "The response of vegetation on the Andean flank in Western Amazonia to Pleistocene climate change". *Science,* 333**,** 1825b.

ROUBIK, D. W. & MORENO, J. E. P. 1991. *Pollen and spores of Barro Colorado Island,* United States, Missouri Botanical Garden.

STOCKMARR, J. 1971. Tablets with spores used in absolute pollen analysis. *Pollen et spores,* 13**,** 615 - 621.

URREGO, D. H., BUSH, M. B. & SILMAN, M. R. 2010. A long history of cloud and forest migration from Lake Consuelo, Peru. *Quaternary Research,* 73**,** 364-373.

WHITLOCK, C. & LARSEN, C. 2001. Charcoal as a fire proxy. *In:* SMOL, J. P., BIRKS, H. J. B. & LAST, W. M. (eds.) *Tracking environmental change using lake sediments: Volume 3: terrestrial, algal, and siliceous indicators.* Dordrecht: Kluwer academic publishers.

WILLE, M., HOOGHIEMSTRA, H., BEHLING, H., VAN DER BORG, K. & NEGRET, A. J. 2001. Environmental change in the Colombian subandean forest belt from 8 pollen records: the last 50 Kyr. *Vegetation History and Archaeobotany,* 10**,** 61-77.

WILLIAMS, J. W. & JACKSON, S. T. 2007. Novel climates, no-analog communities, and ecological surprises. *Frontiers in Ecology and the Environment,* 5**,** 475-482.

ZUIDEMA, P. A., BAKER, P. J., GROENENDIJK, P., SCHIPPERS, P., VAN DER SLEEN, P., VLAM, M. & STERCK, F. 2013. Tropical forests and global change: filling knowledge gaps. *Trends in Plant Science,* 18**,** 413 - 419.

Chapter 9: Conclusions

This chapter summarises the main findings of this thesis, placing them in a regional context. The conclusions from the five research aims set out in Chapter 1 will be identified, as will the wider implications of the research. The limitations of the thesis will be discussed, and future work will be proposed.

9.1. Introduction

The palaeoecological research presented in this thesis provided an additional two sites that investigated the past vegetation history of the eastern Andean flank, contributing to the previously sparse nature of study sites for this region. The multi-proxy datasets developed for the two sites presented (MTW and MTE) helped to determine the nature of the vegetation at this location in the past, and how it responded to various disturbances (landscape change and fire events; Chapter 8). To get to the endpoint of an improved understanding of past vegetation change on the eastern Andean flank, a number of key steps were undertaken, i) a new methodology for sub-sampling diverse systems was developed (Chapter 5), ii) multiple methods were employed to develop an age estimate for the sediment deposition (Chapter 6) and iii) the mechanisms leading to the deposition and preservation of the sediments was explored (Chapter 7).

The research in this thesis was presented in four different types (literature review, scene setting, methodological and palaeoecological investigation), all of which helped to answer the aims outlined in Chapter 1. Chapters 1 and 2 were presented as a literature review, introducing the current state of palaeoecological research on the eastern Andean flank and areas of research to be improved. Chapters 2 and 3 were scene setting chapters, introducing the study region and the study site used to approach the aims listed in Chapter 1. Chapters 4, 5 and 6 had a methodological component, using sediments obtained from the study sites described in Chapter

3, to provide answers to two aims from Chapter 1. Chapters 5, 6, 7 and 8 were presented as palaeoecological investigation chapters, answering the remaining three aims outlined in Chapter 1. The chapters in this thesis each used a combination of methodologies outlined in Chapter 4. Chapter 5 used pollen analysis and statistical techniques. Chapter 6 used the three dating techniques (radiocarbon [^{14}C], Argon-Argon [$^{40}Ar/^{39}Ar$] and optically stimulated luminescence [OSL]). Chapter 7 used pollen analysis, Loss-on-ignition (LOI) and X-ray fluorescence (XRF - major elemental analysis). Chapter 8 used pollen analysis, non-pollen-palynomorph (NPP's) analysis, charcoal analysis and statistical techniques.

9.2. Research aims

Five research aims were outlined in Chapter 1; the overriding conclusions of these aims are discussed here.

9.2.1. Research aim 1

Research aim 1 was to create a statistical sub-sampling tool, capable of producing a sample specific count size for each individual pollen sample. This aim was met in Chapter 5 and the results were published in the international journal *Palaeogeography, Palaeoclimatology, Palaeoecology* (Keen et al., 2014). The statistical sub-sampling tool used an input of 100 counted pollen grains to produce a count size, based on the individual sample's richness and evenness (richness and evenness calculated from the initial 100 grains). The statistical sub-sampling tool enabled the production of robust count sizes; these were then applied to the MTW and MTE study sites. Following Model 1 of the sub-sampling tool, the two stratigraphic sequences required pollen count sizes between 196 and 982 in order to capture the major vegetation components preserved within them. This work demonstrated the variability in count sizes needed for highly diverse studies and the need for using these different count sizes, both in sequences closely located and within the same record, opposing the general approach of using fixed number counts. Aside from its uses in palynology, the statistical sub-sampling tool

presented in Chapter 5, is also applicable to other palaeoecological proxies requiring a count size (providing a reference marker is used; e.g. chironomids, foraminifera). This model has widespread uses in palaeoecology, and its use in this thesis has meant that the pollen results included in Chapters 7 and 8 are statistically robust.

9.2.2. Research aim 2

Research aim 2 was to apply dating methodologies to MTW and MTE, in order to understand the depositional age of the sequences. The results relating to this aim are presented in Chapter 6. Despite the use of two dating techniques for MTW (radiocarbon and $^{40}Ar/^{39}Ar$), and three techniques for MTE (radiocarbon, $^{40}Ar/^{39}Ar$ and OSL), this aim was not met in its entirety.

The dating techniques applied to MTW yielded no reliable age estimates for the stratigraphic sequence. The three radiocarbon samples for MTW were radiocarbon infinite (>48,000 years BP), meaning they were beyond the capabilities of the technique. The $^{40}Ar/^{39}Ar$ dating provided no reliable dates due to detrital nature of the inorganic samples. The MTW stratigraphic sequence is today located in a highly fluvial region, and the site has a catchment area covering 5 % of Ecuador's land surface. Two reasons were proposed for the unreliable age estimates (Chapter 6, Section 6.3.2), the most likely of these reasons was a contamination from ancient material at the time of deposition. Despite this, it is known that these samples were deposited between >48,000 years (radiocarbon infinite) and 1 million years (presence of the biochronological marker, *Alnus* pollen). Without an independent age estimate or chronology for MTW, the palaeoecological results still remain useful because they provide new insight into the vegetation history of the eastern Andean flank.

$^{40}Ar/^{39}Ar$ was also applied to two inorganic layers from MTE; it provided no reliable age estimates. This is most likely due to contamination of ancient sediments at the time of deposition. The part of the section the two samples for $^{40}Ar/^{39}Ar$ were taken from was

hypothesised to be influenced by fluvial sources, suggesting contamination was likely (Chapter 7). From its application to these two stratigraphic sequences it is recommended that $^{40}Ar/^{39}Ar$ is not suitable for use on stratigraphic sequences from the eastern Andean flank, which have been influenced by fluvial dynamics in the past, especially if other dating techniques are available. This recommendation is due to the potential issue of contamination of ancient sediments at the time of deposition causing complications; this was found to be the case in MTW and MTE. If, at the time of deposition, sediments mix with sediments of older origin (e.g. through fluvial or volcanic process), the age signal produced will be of a mixed origin, causing the production of unreliable ages, as produced for these two stratigraphic sequences.

Alternative dating techniques applied to MTE produced three ages, one from radiocarbon and two from OSL. Radiocarbon dating provided a calibrated (2 sigma, using Southern Hemisphere calibration curve; Stuiver., et al, 1998) age of 19,872-20,306 cal years BP for Organic O, (1 m depth), in the upper part of the stratigraphic sequence. OSL dating provided two ages either side of this, an age of 48,000 ± 4000 in inorganic layer 13 (0.46 m depth) and an age of 28,000 ± 3000 in inorganic layer 9 (2.20 m depth, Chapter 6, Section 6.4.1). The age reversal produced from the OSL dating technique was hypothesised to be due to either a changing water content of the samples, between deposition and analysis, or due to reported issues with dating samples in the region (Chapter 6, Section 6.4.2) (Steffen et al., 2009). Further work is being performed with the aim of reducing this age reversal (see Sections 6.4.5 and 9.5). Due to the time constraints of the project, further radiocarbon analysis has yet to be undertaken on MTE; but see section 9.5 for future plans to further develop the chronology. Due to previous complexity and uncertainty when dating sediments from the Mera region (Bes de Berc, 2003, Colinvaux et al., 1996, Espín, 2014, Heine, 1994, Liu and Colinvaux, 1985), and the lack of certainty regarding the three ages obtained from MTE (age reversal and lack of complete chronology), these dates were not used in the remainder of the thesis (see Section 6.4.5).

9.2.3. Research aim 3

Research aim 3 was to characterise the depositional environment required to preserve sedimentary archives such as MTW and MTE. Research aim 3 was answered in Chapter 7 using analysis undertaken on sediments from MTE. Five different depositional environments (Figure 7.4) were identified from the sediments at MTE, environments which enabled the sediments to be deposited and preserved. A debris flow preserved at the beginning of the stratigraphic sequence is thought to have created a flat swamp which allowed sediments deposited to be preserved. However, fluvial influence in the upper half of the stratigraphic sequence caused the sediments preserved to be representative of a regional, not local, source, due to long distance transport of sediment from the river catchment (Chapter 7). From this research on MTE sediments, it was concluded that volcanic events can aid the deposition and preservation of sediments, particularly large events such as the debris flow preserved at the bottom of MTE (Chapter 7). Fluvial influence, however, is largely negative, causing erosion and mixing of the sediments, creating difficulties when interpreting sediments due to a change in source area (local to regional). This was observed in the upper part of MTE (Chapter 7).

The research performed at MTE clarifies the importance of understanding the depositional environment when interpreting a palaeoecological record, this is due to two reasons: i) large scale environmental events (e.g. a debris flow; see unit 2, Figure 7.4) causing landscape defining change and, ii) knowledge of sediment provenance, allowing shifts in sediment source area to be detected. If the depositional environment is not considered, misinterpretations could be made when interpreting palaeoecological data.

By interpreting the depositional environment from the sediments preserved at MTE it was determined that flat, wet environments are highly suitable for the preservation of sediments, and

that big events such as the debris flow at the base of MTE often attributed to the creation of environments suitable for sediment deposition and preservation.

9.2.4. Research aim 4

Research aim 4 was to increase the spatial coverage of past vegetation sites, particularly those using a multi proxy approach. This aim was met throughout the entire thesis, however, Chapter 8 in particular focused on the ancient vegetation preserved at both MTW and MTE. Other proxies used alongside pollen analysis were covered in Chapters 4, 6, 7 and 8. The statistical model generated for research aim 1 (Chapter 5), was applied to both MTW and MTE, meaning that the pollen data captured the major components of the pollen rain (taking into consideration the regional pollen source area discussed in Chapter 7). In total, 159 pollen taxa were identified from the Mera Tigre sites, demonstrating the floristic diversity of the montane forests, contained within the eastern Andean flank.

The vegetation signal preserved in the fossil pollen at MTW was interpreted as representative of the upper montane forest, an ecosystem today found at higher elevations. Key taxa leading to this interpretation were *Hedyosmum*, *Ilex* and *Podocarpus*, these were present consistently throughout the stratigraphic sequence at abundances greater than 10 %. The vegetation found at MTE was dynamic, with reassortment of five abundant taxa occurring (Asteraceae, *Cecropia*, *Ilex*, *Wettinia* and *Hedyosmum*). During the period of deposition, the vegetation community preserved at MTE had no modern analogue. A mixture of the upper elevation (~1500-2500 m asl) lower montane forest (*Alnus*, Ericaceae and Myrtaceae) and upper montane forest (*Ilex* and *Hedyosmum*) taxa were present for this interpretation to be made.

MTW and MTE shared ten pollen types over 10 %, these were *Phyllanthus*, *Hedyosmum*, *Miconia*, *Ilex*, *Alnus*, Asteraceae, Combretaceae-Melastomataceae, Polypodiaceae, monolete psilate and trilete fern spores. These shared taxa meant that there was a 29.41 % similarity

between the pollen taxa (>10 %) in both sites. Despite the dissimilarity in the pollen assemblage, these taxa did contribute to a major proportion of the pollen sum for each site, suggesting they were of significance to each individual pollen assemblage. These taxa contributed to 34.65-62.99 % of the pollen sum for MTW and 29.94-74.01 % for MTE, meaning the taxa they shared were major contributors to both of the stratigraphic sequences. The two sites were not linked together temporally due to a lack of chronological constraint and different pollen assemblages.

9.2.5. Research aim 5

Research aim 5 was to investigate charcoal and pollen records preserved at MTW and MTE, with the aim of discovering how the vegetation responds to natural fires. This research aim was met in Chapter 8. The two sites responded differently to fire occurrence, with neither site having a strong correlation between charcoal and the palynological trends included in DCA axis 1 (MTW = -0.37 and MTE = 0.16). MTE had a stronger correlation when the charcoal was related to subsequent samples (S_i+1 = 0.36 and S_i+2 = 0.39). This improvement, when related to subsequent samples, could be as a result a post fire succession occurring, meaning the vegetation has a time-lag in response to the fire event. In order to fully understand the potential of post fire successions in this ecosystem, and, therefore, how this region may respond to a projected increased fire regime, further studies, in particular high resolution studies (sample resolution of decades), need to be obtained.

The lack of strong correlation between charcoal and the variance in the pollen record (DCA axis 1) at the two sites indicate that the abundant elements of these two stratigraphic sequences could be resilient to fire events. It also suggests that other drivers of change (e.g. temperature, precipitation and landscape change) were likely to be more important in the potential reassortment of minor taxa.

9.3. Wider implications of this thesis

9.3.1. Technical advances

The research undertaken in this thesis, in particular, that presented in Chapters 5, 6, 7 and 8, has wide implications for the scientific community. This thesis has contributed to the improvement of palaeoecological techniques through the generation of the statistical sub-sampling tool presented in Chapter 5. Aside from being of use to palynologists, this sub-sampling tool can be applied to other proxies within palaeoecology, and will, therefore, contribute to the production of statistically robust data throughout the discipline of palaeoecology. A statistical sub-sampling tool was required to help modify the calculation of count sizes, ensuring that inferences made from pollen counts are statistically robust. Previously there were limitations relating to investigator effort and effective sampling, i.e. obtaining meaningful pollen counts from diverse tropical pollen assemblages. The production of the sub-sampling tool presented in Chapter 5, ensured that these limitations can be reduced, as the tool provides a count size adequate enough to capture the pollen assemblage, whilst reducing the issue of potential under or over sampling. The publication of this work in an international journal means that the entire research community can use this new methodology to help further their own research.

9.3.2. Improvements in understanding past environmental change

9.3.2.1. Mera region

The research presented in Chapter 6 has provided further supporting evidence to the debate regarding the age of the original Mera sequence (Bes de Berc, 2003, Colinvaux et al., 1996, Espín, 2014, Heine, 1994, Liu and Colinvaux, 1985). Although the dating of the Mera region still remains a contentious issue (see Chapter 6), further advances have been made due to the three additional ages produced from the MTE sediments (see Chapter 6). Chapter 7 highlighted the importance in understanding the depositional environment, as it can provide evidence as to how the sediments may have preserved, what the source area for the sediments is (regional/local) and

whether or not the depositional environment was likely to contribute to unreliable dates. In Section 7.6.2.2. it was emphasised that it was unlikely that the dates produced for the original Mera site were as a result of fluvial contamination (Liu and Colinvaux, 1985). This was stated due to the lack of fluvial evidence at the location of the wood fragments extraction, suggesting that fluvial contamination was not an issue at the time of deposition, and that the contamination hypothesis by Heine (1994) could be rejected. However, as dating does still remain a contentious issue, the ages for MTE were not used throughout this thesis (see Section 6.4.5).

9.3.2.2. Eastern Andean flank, Ecuador

The research presented in Chapter 7 will help further palaeoecological research, as it develops a new framework for finding new study sites on the eastern Andean flank. The data and discussion presented in Chapter 7, will help to improve the resolution of study sites sampled across the eastern Andean flank, by encouraging the research community to investigate sedimentary archives currently undervalued (namely open stratigraphic sequences due to potential issues with sediment provenance). This chapter states the importance of these sites, and reduces the uncertainty associated with them. It does this by discussing the importance of considering the depositional environment, so that the origin of sediments at the site can be ascertained; this was demonstrated using sediments obtained from MTE. By taking the deposition into account, palaeoecological interpretations obtained from these currently underutilised sedimentary archives will be able to make a novel contribution to the study of the eastern Andean flank.

The addition of two multi proxy stratigraphic sequences into the palaeoecological literature of the eastern Andean flank also has wide reaching implications. The two sequences of this thesis (MTW and MTE) will help contribute to the understanding of how this region will respond to projected environmental change. The research presented in Chapter 8 is of particular importance as it will help scientists and policy makers understand how the projected increase of fire events may impact the biodiversity of this region. It provides information as to how specific taxa react

to fires, and will provide further evidence as to how this region may respond to future disturbance events.

9.4. Problems and limitations

9.4.1. Obtaining reliable age estimates

One of the primary problems with this research was the lack of ages that could be obtained for the stratigraphic sequences, with none being reported for MTW and only three tentative dates for MTE (Chapter 6). This lack of reliable age estimates occurred despite the use of three different dating techniques (radiocarbon, $^{40}Ar/^{39}Ar$ and OSL). Previous work from the Mera region also reported difficulty in dating sediments (Section 6.4.5). Due to the uncertainties surrounding the MTE (OSL age reversal), the lack of dates for MTW and analytical uncertainty surrounding ages obtained for sediments from the Mera region, it was decided not to use the dates from MTE in the remainder of the thesis, until further clarification can be obtained (see Sections 6.4.5 and 9.5). This, however, was out of the range of the current thesis, as trying to disentangle the dating issues would have prevented the introduction of two new multi-proxy palaeoecological sites for this understudied region.

Part of the reason dates could not be achieved for MTW and MTE was the high complexity of the samples, especially in relation to sediment provenance, and sediment contamination (at the time of deposition). The current fluvial location of both MTW and MTE could suggest that during the period of deposition, fluvial contamination from ancient sources was a possibility. This would certainly contribute to the unreliable $^{40}Ar/^{39}Ar$ ages produced for both sites. In this sense, the depositional environment of MTE was analysed (Chapter 7) and it was found that the upper part of the stratigraphic sequence was likely subject to fluvial influence. No fluvial evidence was found in the MTW sediments, however, this does not mean that this site was never influenced by fluvial processes; it could simply be the case that no fluvial sediments preserved.

Despite analytical uncertainty regarding dates for MTE, and the lack of dates for MTW, the data presented in this thesis has greatly improved the resolution of palaeoecological sites on the Ecuadorian eastern Andean flank.

9.4.2. Time constraints

Time constraints of the PhD were also a limitation. Due to the multi-proxy approach (eight analytical techniques) and the amount of samples taken from the two stratigraphic sequences (65 organic samples for MTW and 207 organic samples for MTE), the analyses were performed at a 10 cm resolution.

For the MTW and MTE stratigraphic sequences a total of 107 sub-samples were processed for pollen and macro charcoal analysis (Chapter 8). This dramatically improves the resolution of the original Mera site, in which only six samples were analysed (Liu and Colinvaux, 1985). As well as improving the resolution, these pollen samples were also counted using the statistical sub sampling tool (following model 1, Chapter 5), meaning that palaeoecological inferences from this site were statistically robust. A multi-proxy approach was also undertaken on the sequences meaning as much data as possible could be obtained from the samples. Loss-on-ignition was undertaken on all 272 samples and XRF (major elemental analysis) was performed on all inorganic (volcanic origin) layers, these analyses provided evidence about the depositional environment (Chapter 7). Three dating techniques were also applied to try and provide the best possible chance of obtaining a chronology for this sequence (Chapter 6). The multi-proxy approach ensured that the two stratigraphic sequences provided a novel contribution to the palaeoecological research of the eastern Andean flank, Ecuador.

9.5. Future work

The research undertaken in this thesis has outlined some future directions of work that could be performed on not only these sediments, but also in palaeoecology on the eastern Andean flank.

9.5.1. Future work on dating

In the case of the Mera Tigre sites, performing additional radiocarbon sampling on MTE is the first priority, particularly at the top of the stratigraphic sequence to corroborate with current ages. The radiocarbon dating for MTE should provide a chronology for at least the upper part of the sequence. In order to further understand the age of the MTE sequence, additional work is being undertaken on the OSL dating for the site by Dr Andy Carr at the University of Leicester. Dr Carr is performing single grain analysis on the two OSL samples to try and reduce potential analytical uncertainty associated with single aliquots. This work is hoped to improve on the potential age reversal reported in section 6.4.1, by providing a number of ages based on single individual grains, as opposed to a group of grains (aliquot).

As of the 26th March 2015, further work by Dr Carr had generated a new age estimate for HK7 (the upper OSL sample, previously dated at 48 ± 4 Ka (see Section 6.4.1)). Based on the analysis of 1300 single grain analyses for this sample, 37 of these tentatively indicated that the appropriate age for the sample was 17.3 ± 3.9 Ka (results included in Appendix B). The remaining 1263 grains were rejected due to a lack of signal or abhorrent OSL properties (e.g. incomplete bleaching; see Section 6.4.2). This age is not yet finalised as Dr Carr needs to refine the minimum age to check uncertainties before it can be used in any interpretation/ publication. This will require a few more analyses. The same process will then be undertaken on the HK8 sample (lower OSL sample) with the likelihood that this age will also alter. Table 9.1 indicates the new OSL age in relation to the other two reported MTE ages.

Table 9.1: Age estimates for the three MTE samples, also including information about the sample ID, depth of the sample, nature of the sample and the dating technique applied.

Sample ID	Depth (cm)	Nature	Dating technique	Age (Ka)
HK7	46	Inorganic	OSL	17.3 ± 3.9
Mera2Y29091	101	Organic	Radiocarbon	19.9 to 20.3
Hk8	220	Inorganic	OSL	28 ± 3

The preliminary alteration to the HK7 OSL age opens the possibility of no longer having an age reversal for the MTE sequence. Future work will involve clarifying the age produced for HK7 so it is suitable for use in interpretation and publication, applying single grain analysis on HK8 and obtaining additional radiocarbon ages. The additional work on the chronology will allow the MTE site to have a higher impact in the scientific community when published, as these dates show the sediments could go back into the last glacial (providing further work does not alter the dates). Multi-proxy palaeoecological studies covering the last glacial maximum on the eastern Andean flank of Ecuador are limited, and little is still known about how this region responded to changes in temperature (see Section 2.4). Future work with MTE will mean it should hopefully provide additional information relating to this uncertainty.

As of the 12th June 2015 (post viva), three additional radiocarbon dates were obtained for MTE from the Beta Analytic radiocarbon facility. Table 9.2 indicates the new results in relation to the ages reported in Table 9.1.

Table 9.2: Age estimates for the six MTE samples, also including information about the sample ID, depth of the sample, nature of the sample and the dating technique applied.

Sample ID	Depth (cm)	Nature	Dating technique	Age (Ka)
HK7	46	Inorganic	OSL	17.3 ± 3.9
Mera2Y29091	101	Organic	Radiocarbon	19.9 to 20.3
411028	185	Wood	Radiocarbon	31.8 to 33.1
Hk8	220	Inorganic	OSL	28 ± 3
411029	520	Wood	Radiocarbon	>43,500
411030	665	Organic	Radiocarbon	42.7 to 43.7

The three new age reversals have provided the depth at which the stratigraphic sequence becomes radiocarbon infinite (the path separating the sequence, Figure 3.8). There are discrepancies present in the sequence, with slight disagreement between the OSL age HK8 and the radiocarbon age 411028 and the two radiocarbon samples 411029 and 411030, these discrepancies are all within error of each other. Despite the uncertainties still remaining with the chronology of MTE, Figure 9.1 shows the age depth model produced for MTE using five of the six ages shown in Table 9.2 (sample 411029 was excluded due to the infinite nature of the date).

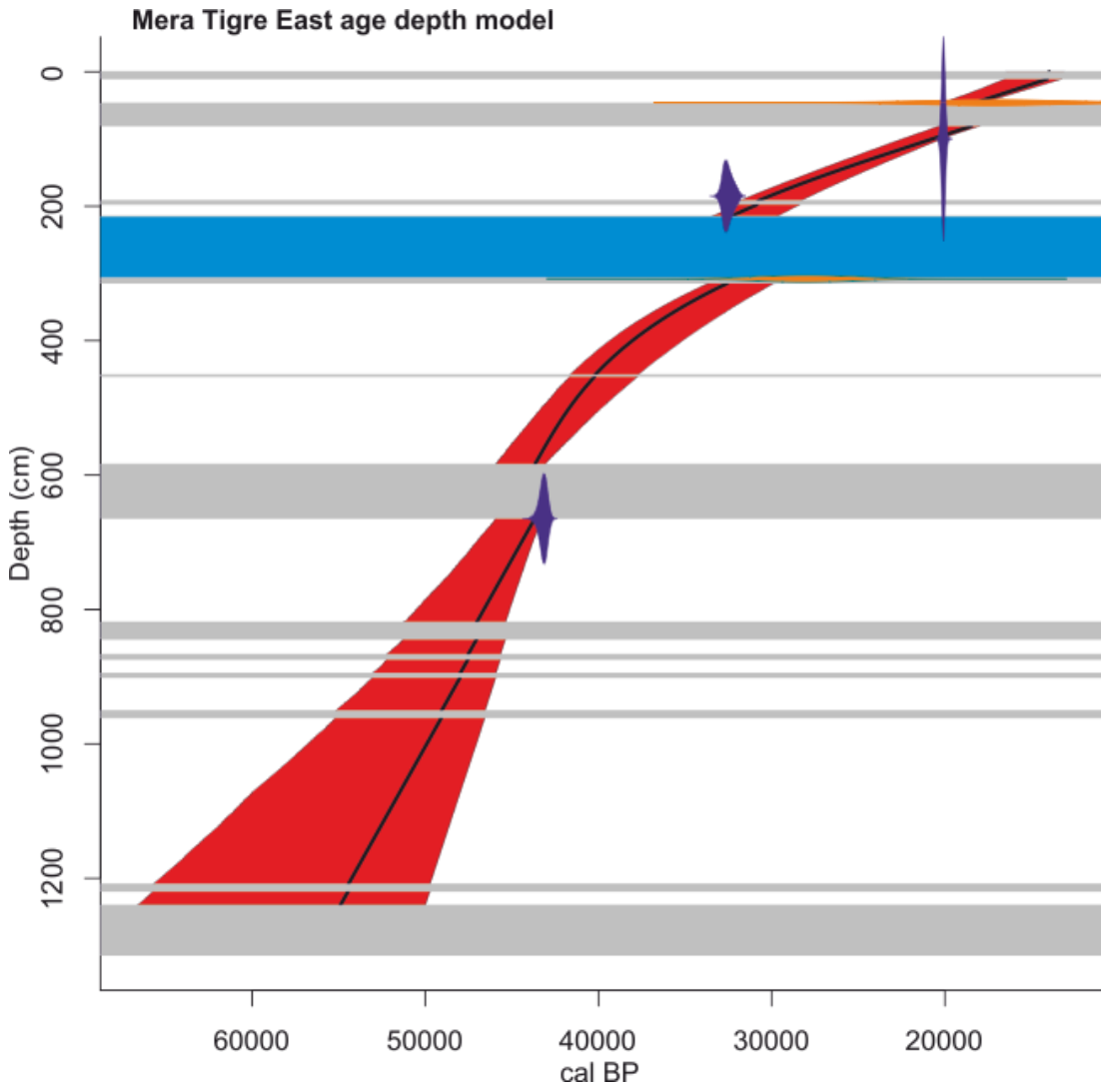

Figure 9.1: Age depth model produced for MTE using three radiocarbon ages and two OSL ages (see Table 9.2). The age depth model is a smooth spline and it was produced using the R package CLAM (Blaauw, 2010). The orange lines represent the age error associated with the OSL ages, the dark purple shows the error associated with the radiocarbon ages. The red represents the error associated with the

age depth curve in general. The grey and blue blocks represent the tephra layers and the fluvial layers in MTE respectively.

Due to the error associated with the dates in this age depth model, work will continue to provide a suitable chronology for MTE. This will involve further OSL work and further radiocarbon work. This will be completed before this work is published anywhere other than this thesis.

9.5.2. Future work on the depositional environment

In order to obtain further information on the depositional environment, and the likelihood of ancient contamination of inorganic sediments at MTW and MTE; high resolution analysis of these sediments is recommended as future work.

ICP-MS analysis and XRF minor element analysis would provide further information about the samples and their potential source (volcanic, fluvial or a contaminated mixture). Detailed analysis will be undertaken on these sediments as part of a master's student project, undertaken at the Instituto Geofísico, Quito, Ecuador during the summer/ autumn of 2015.

It is also recommended that particle size analysis is undertaken on the two stratigraphic sequences. Particle size will provide further information about changes in depositional environment and sediment provenance.

9.5.3. Additional future work

In relation to wider research on the eastern Andean flank, it is essential that the spatial resolution of study sites in this region is continually improved, in particular, in the montane rain forests of the eastern Andean flank. The research presented in Chapter 7 could help identify areas in which further sites could be located. By identifying and analysing further sites in this region with a multi proxy approach and a high sample resolution, it will be possible to further investigate the impact future environmental change will have on these ecosystems (for example a post fire succession following increased fire occurrence in projected drought conditions).

9.6. Summary

This chapter has provided a synthesis for the research presented in this thesis, as well as identifying limitations with the research, and further areas of interest which have stemmed from this work. The overriding outcomes from this thesis are as follows:

- Production of a statistical sub-sampling tool which provides individual sample specific count sizes, taking into consideration the richness and evenness of each sample. Following either model 1 or model 2, the count sizes generated are optimised to help detect major vegetation components, and to predict the amount of pollen grains that need to be counted to find the next not yet seen pollen taxa.
- Dating sediments deposited on the eastern Andean flank requires the use of a range of dating techniques, and in fluvial locations such as the Mera Tigre sites, it is not always possible to obtain a chronology. No dates were obtained for MTW; however, three dates were obtained for MTE following the use of three separate dating techniques.
- The consideration of depositional environments is essential when interpreting sedimentary archives on the eastern Andean flank. Without a full understanding of depositional environment, it cannot be determined whether a proxy signal is representative of a local or regional source area. Having a suitable depositional environment is also essential to preserving sedimentary archives, however, certain environmental features (e.g. fluvial influence) can be detrimental to the preservation of sediments (through erosion, transportation and contamination issues).
- Vegetation preserved at MTW was diverse, and representative of the modern day upper montane forest. This vegetation community had no strong correlation with fire events. The vegetation preserved at MTE was indicative of a vegetation community with no modern analogue, with a mixture of the modern day upper part of the lower montane

forest and the upper montane forest. The vegetation had a weak correlation to fire at a delayed response, suggesting a potential post fire succession or alternatively it changed as a response to landscape change or as a combination of both factors.

- Further work for the Mera Tigre sites includes dating the MTE sediments, including additional radiocarbon dating for MTE and clarification on the OSL analyses. In order to further understand the deposition of the sites, a high resolution analysis of the two sites inorganic layers is suggested.

References

BES DE BERC, S. 2003. *Tectonique de chevauchement, surrection et incision fluviatile (exemple de la Zone Subandine equatorienne, Haut Bassin Amazonien). [Overlapping tectonic uplift and fluvial incision (example of the Sub-Andean Zonem, Ecuadorian upper Amazon basin]*. PhD, Universite Toulouse III - Paul Sabatier.

BBLAAUW, M. 2010. Methods and code for 'classical' age-modelling of radiocarbon sequences. *Quaternary Geochronology*.5, 1047-1059.

COLINVAUX, P. A., LIU, K.-B., DE OLIVEIRA, P. E., BUSH, M. B., MILLER, M. C. & STEINITZ - KANNAN, M. 1996. Temperature depression in the lowland tropics in glacial times. *Climatic Change,* 32**,** 19 - 33.

ESPÍN, B. P. A. 2014. *Caracterizacin geológica y litoógica de los depósitos laháricos de Mera, provincia de Pastaza (Geological and lithological characterisation of lahar deposits, Mera province of Pastaza).* Escuela Politécnica Nacional, Quito.

HEINE, K. 1994. The Mera site revisited: Ice - age Amazon in the light of new evidence. *Quaternary International,* 21**,** 113 - 119.

KEEN, H. F., GOSLING, W. D., HANKE, F., MILLER, C. S., MONTOYA, E., VALENCIA, B. G. & WILLIAMS, J. J. 2014. A statistical sub-sampling tool for extracting vegetation community and diversity information from pollen assemblage data. *Palaeogeography, Palaeoclimatology, Palaeoecology,* 408**,** 48 - 59.

LIU, K.-B. & COLINVAUX, P. A. 1985. Forest changes in the Amazon Basin during the last glacial maximum. *Nature,* 318**,** 556 - 557.

STEFFEN, D., PREUSSER, F. & SCHLUNEGGER, F. 2009. OSL quartz age underestimation due to unstable signal components. *Quaternary Geochronology,* 4**,** 353 - 362.

STUIVER, M., REIMER, P. J., BARD, E., BECK, J. W., BURR, G. S., HUGHEN, K. A., KROMER, B., MCCORMAC, G., VAN DER PLICHT, J. & SPURK, M. 1998. INTCAL98 Radiocarbon age calibration, 24,000-0 cal BP. *Radiocarbon,* 40**,** 1041-1083.

Appendix 1: Methodologies

This Appendix contains detailed methodologies for the methods described in Chapter 4 of this thesis.

Appendix 1.1: Pollen preparation method

A1.1.1. Initial sampling

To ensure an equal amount of sample is taken from each site a 0.5cm^3 sample is measured using the water displacement method into appropriately labelled 15 ml plastic centrifuge tubes. The tubes are balanced (ensuring the same amount of liquid is in each tube) and then centrifuged for 3 minutes at 3000 rpm, ensuring all the sample is mobilised. The supernatant is decanted in one swift movement, leaving the solid residue at the bottom of the tube. This method of water washing and centrifuging remains the same throughout the pollen preparation procedure. 5 ml of 10% Hydrochloric acid (HCL) is added to each sample, any reactions should be noted.

An exotic marker grain, *Lycopodium,* is used to spike each sample. *Lycopodium* is not expected as part of the natural occurring taxa, meaning it is an acceptable exotic marker as it will not affect actual count sizes. A ratio of 1:1 or 1:2 is desirable between the exotic marker and the fossil pollen. One tablet is added to each sample and the batch number is noted for concentration purposes.

A1.1.2. Hydrochloric acid treatment

To remove carbonates from the sample, a solution of 10% HCL is added. 5ml of 10% HCL is added to each sample and reactions are noted. The solution is stirred using a wooden stirrer, ensuring the entire sample is exposed to the HCL. The tubes are then placed in a water bath (pre heated to 90ºC) for 20 minutes. The samples should be stirred after ten minutes using a wooden stirrer. The water bath should be within the fume cupboard and throughout this process the fan

should be on. After 20 minutes the tubes are removed from the water bath, balanced, centrifuged and then decanted into the sink inside the fume cupboard.

The sample is then 'whirlimixed' using the TopMix FB15024 until the entire sample is mobilised. 5ml of deionised water is then added. The sample is then balanced, centrifuged and decanted.

A.1.1.3. Potassium hydroxide treatment

To remove the humic acids from the samples, 6ml of 10% potassium hydroxide (KOH) is added to each sample. The samples are first 'whirlimixed' to mobilise all of the sediment and then the KOH is added. The samples are then placed into a hot water bath (90ºC) for 4 minutes. On removal from the water bath the samples are not 'whirlimixed' or decanted.

Whilst the samples are in the water bath, a second batch of 15ml plastic centrifuge are prepared and placed into a test tube rack with funnels and prepared 180µm sieves. Sieves should be prepared by placing in an ultrasonic bath for 3 minutes. Using a small amount of deionised water, each sample should be washed through an individual sieve into the new, corresponding tube. All sample should be washed through, taking care to wash all pollen grains through. A restricting nozzle on the deionising water can be used for this. Once all pollen grains have been washed through, the sample should be balanced, centrifuged and decanted.

A.1.1.4. Water washes

To ensure there are no remaining humic acids or clays in the sample it is important to wash the samples thoroughly. The samples should be washed until the decanted liquid is clear, the previously described washing procedure should be used. To ensure the decanted liquid is clear, between 5 and 16 washes might be needed, depending on the clay and humic acid composition of the sample.

A.1.1.5. Hydrofluoric acid treatment

To remove all carbonates and to acidify the samples before the Hydrofluoric acid (HF) treatment can begin, the samples should be washed in 10% HCL as per normal H_2O washing procedure (using 10% HCL in place of H_2O).

The HF treatment removes silicates from the samples. Samples are 'whirlimixed' and then, inside a fume cupboard with the fan and backwash on, 5ml of HF is added to each tube. The samples should be stirred with a wooden stirrer, neutralised by dipping in saturated Sodium Carbonate solution and then placed in a hot water bath (90ºC) for 3 hours. Once removed from the water bath, the samples are balanced, centrifuged and the waste is decanted into the fume cupboard sink (marble traps within the sink). Copious amounts of saturated Sodium Carbonate solution should be poured down the sink with the waste and the sink should be flushed with water throughout.

A.1.1.6. Hydrochloric acid treatment

To remove silicate residues and fluorosilicates, 5 ml of 10% HCL should be added to each sample. The samples should be placed in a hot water bath (90ºC) for 20 minutes. Once removed they should be balanced, centrifuged and decanted. The samples should then be mobilised using the whirlimix and then washed in H_2O.

A.1.1.7. Acetolysis

Acetolysis is performed in order to remove some of the remaining organics (cellulose and polysaccharides). However, before acetolysis can begin, it is essential to remove any water in the sample. This is achieved by washing in concentrated (glacial) Acetic acid (CH_3COOH). The normal washing procedure is followed; however, samples are washed in CH_3COOH instead of H_2O.

The acetolysis mixture should be made up using 9 parts of acetic anhydride and 1 part concentrated Sulphuric acid (H_2SO_4). The mixture should be made up in a measuring cylinder inside the fume cupboard with the fan on. The Sulphuric acid should be added after the acetic anhydride and care should be taken to add it slowly. Once mixed, 5ml of the mixture should be added to each sample, the sample should be stirred ensuring the entire sample interacts with the mixture. The sample should then be placed in a hot water bath (90ºC) for precisely 3 minutes.

As soon as the samples are removed from the water bath 5ml of Acetic acid should be added to stop the reaction. The samples should then be balanced, centrifuged and decanted as per normal procedure. The samples should be washed in H_2O as per normal procedure.

A.1.1.8. Slide preparation and mounting

To prepare samples for counting, 1ml of deionised water should be added to each sample, the samples should then be fully mobilised using the 'whirlimix'. The sample should then be transferred into labelled 3ml vials. The process should be repeated until the entire sample is in the vial. Equal quantities of glycerol to sample residue should be added to each sample and then stirred thoroughly using a wooden stirrer. The vials are then placed into a preheated oven (40ºC) with the lids off to dry overnight. Once the water has been evaporated a small amount can be mounted onto a slide and covered with a cover slip.

A.1.1.9. Pollen counting protocol

Standard procedure is that 300 terrestrial pollen grains are counted, by making regular traverses across the slide. For this thesis, a new technique for pollen count sizes was produced (see Chapter 5) and applied to all samples. For the purpose of generating a statistically significant pollen count size a two part statistical model was created. Model 1 produces a count size which would characterise the major components of the vegetation community. Model 2 produces a count size based on how many more pollen grains would need to be counted (following

application of the Model 1 count size) to find the next, not yet seen pollen taxa. Model 1 only was applied in this thesis.

To generate a count size using Model 1, a preliminary count of 100 terrestrial pollen grains counted for each sample needs to be entered into the statistical model. The preliminary 100 grains is then extrapolated through the use of a simple Monte Carlo simulation method (a method involving running a simulation multiple times) one hundred times in succession. By running the model multiple times, the pollen count required to determine the ecological characteristics (richness and evenness of a sample), can be estimated. By running the model multiple times, an individual sample specific count size is produced. The count size has a 95% confidence level attached to it. Count sizes produced for samples in this thesis range from 196 to 982.

Appendix 1.2: Mera Pollen count sheet (v. 5.0)

Location:	Analyst: Hayley Keen
Depth:	Date:

Podocarpus:	Arecaceae:
Trema:	Caesalpiniaceae:
Celtis:	Asteraceae:
Cecropia:	A.Eupatorium group:
Ficus:	A.form 1:
Alnus :	A.form 2:
Dalbergia:	Ericaceae:
Betula:	E.form 2:
Polylepis:	Piperaceae:
Euterpe:	Mor/ urt:
Genoma:	Mor/ urt 2pores:
Iriartea:	Comb/ Mel:
Mauritia (c/f):	Myrtaceae:
Moraceae – Symphonia:	Apocynaceae:
Hedyosmum:	Salicaceae:
Humiria:	Cyperaceae:
Ilex:	Poaceae:
Alchornea:	Fabaceae:
Aparisthmium:	Mimosoideae:
Weinmannia:	Caesalpiniodeae:
Astronium:	Papilinodieae:
Borreria:	Faboideae:
Tapirira:	Rubiaceae:
Copaifera:	Euphorbiaceae:
Machaeorium:	Apiaceae:
Acalypha:	Piperaceae:
Phyllanthus:	Bignoniaceae:
Hyeronima:	Anacardiaceae:
Croton:	Polypoidaceae:
Pera:	Sapindaceae:
Sapium:	Solanaceae:
Mabea:	Loranthaceae:
Charcoal <50µm:	Flacartiaceae:
Charcoal >50µm:	Polygalaceae:
Mandible:	
Sporomiella:	Tricolporate:
Damaged:	Monolete psilate:
Broken:	Trilete fern spore:
Crumpled:	Cyatheacea:
Corroded:	Unknown:
Obscured:	Bryophyte spore:
Degraded:	**Lycopodium:**

Appendix 1.3: Loss on ignition sample preparation

A1.3.1. Sample pre-preparation

A.1.3.1.1. Drying of crucibles

To ensure no excess moisture enters the process, porcelain crucibles needed for the process must be dried before they can be used. 25 porcelain crucibles were placed into an oven, heated to 105°C and dried for 12 hours. The crucibles should not be handled after this to avoid transfer of moisture from the skin to the crucible surface. The crucibles were then picked up using platinum tipped tongs and placed to cool for five minutes in a desiccator. Once cooled, the crucibles were weighed to an accuracy of four decimal places. If the crucibles are weighed pre cooling the weight will fluctuate, meaning an inaccurate weight is obtained.

A.1.3.1.2. Drying of samples

One cm^3 of wet organic sample (all 245 organic samples retrieved in the field were sampled) was taken and placed into the pre dried crucibles. The crucible and wet sample were weighed. The wet samples were then placed into an oven heated to 105°C and dried for 12 hours. Once dry the samples were then taken and placed into the desiccator to cool for five minutes. The samples were then weighed to four decimal places. Equation A1.3.1 was used to calculate the percentage water loss for each sample.

$$\%\, water = \frac{Crucible + wet\ sample - crucible + dry\ sample}{wet\ weight\ of\ sample} \times 100 \qquad \text{Equation A1.3.1}$$

A1.3.2. Loss-on-ignition sample process

For the following processes the extractor fan should be turned on. When placing and removing samples from a heated muffle furnace a lab coat, a face visor and heat resistant gloves should be worn. Samples should be handled using long handled, platinum tipped, tongs.

A1.3.2.1. First burning process

To determine percentage organic in each sample, the dried samples were placed into a muffle furnace heated to 550°C. The samples were left in the furnace for two hours. The samples were taken out of the furnace and placed on a heat resistant mat for five minutes to cool down, before being cooled for a further five minutes in the desiccator. Once cool the samples were weighed. To calculate the organic percentage of the samples, Equation A1.3.2 was used.

$$\%\ organic = \frac{Crucible + dry\ sample - Crucible + 550°C\ ash}{dry\ weight\ of\ sample} \times 100 \qquad \text{Equation A1.3.2}$$

A1.3.2.2. Second burning process

To determine the carbonate content in each sample, the pre-ignited samples were placed into a muffle furnace heated to 925°C. The samples were ignited for four hours. The samples were then removed from the furnace and placed onto a heat resistant mat to cool for five minutes. They were then placed in a desiccator for a further five minutes to cool completely. The samples were weighed to four decimal places once cool. To calculate the percentage carbonate, Equation A1.3.3 was used.

$$\%\ carbonate = \frac{Crucible + 550°C\ ash - crucible + 925°C\ ash}{dry\ weight\ sample} \times 100 \qquad \text{Equation A1.3.3}$$

To calculate the percentage inorganic for the sample, Equation A1.3.4 was applied.

$$\%\ inorganic = 100 - \%\ organic - \%\ organic \qquad \text{Equation A1.3.4}$$

Appendix 1.4: X-ray fluorescence sample preparation method

A1.4.1. Sample pre-preparation

A1.4.1.1. Drying of samples

Ten grams of wet tephra sample were taken and dried for 12 hours in an oven heated to 110°C. Removing water from the tephra samples is essential in order to avoid fluctuations in samples weights, to make sample crushing easier and as the results for major element calibrations are reported on a dried sample basis.

A1.4.1.2. Crushing of samples

Tephra samples were pre crushed using a pestle and mortar – this meant the samples were small grained, however, for XRF it is required that the particles can pass through a 250μm mesh. The extractor fan within the lab should be turned on to prevent inhalation of dust particles. The sample was then ground to a fine powder in an agate mill; the sample was in this for three minutes.

In between sample crushing, all parts of the agate mill were washed and dried to ensure cross contamination was kept at a minimum. Each sample, once crushed, was placed into a labelled sample bag.

A1.4.2. Glass disc preparation

A1.4.2.1. Weighing

To ensure samples are completely dry, three grams of the pre-dried tephra sample were placed into clean, numbered porcelain crucibles. The samples were dried for 12 hours in an oven over 110°C.

0.7000 grams of the dried rock powder was weighed accurately into a platinum crucible. The remaining sample powder was returned to the oven to ensure it remained dry. The scales were then tared and 3.5000 grams of lithium metaborate flux was accurately weighed into each crucible, along with the sample. The flux and sample mixture were then stirred with a clean re-usable polythene stirring rod until well mixed.

A1.4.2.2. Fusion

Once weighed out, the samples need to be fused together in a muffle furnace, heated to 1100°C. The platinum crucibles are picked up with platinum tipped tongs and placed into the furnace (two at a time) for 15 to 20 minutes. Each sample was swirled every 5 minutes, ensuring the sample and flux were mixed properly and that all air bubbles were removed. Once completely homogenised (meaning when swirled no mixture adhered to the side of the crucible) the melt was poured into the centre of a heated glass mould and a pre-heated plunger pressed down to form a glass disc. The plunger was pressed down steadily and kept in contact with the melt for three seconds leading to a flat, slightly rippled, glass disc. The glass disc (remaining inside its mould) was placed onto a heat resistant mat and covered with a glass evaporating basin in case of shattering. The glass disc was then labelled on the side in contact with the mould and placed into a sealed, labelled bag. It was important that during the process the glass disc was not touched on the surface to be analysed as this could increase the Sodium content, affecting the analysis.

A1.4.3. Loss-on-ignition

To quantify the volatile contents (H_2O and CO_2) of the tephra samples which are lost on fusion and cannot be analysed by XRF, the loss on ignition measures these volatiles. 1.2 grams of the dried tephra samples was accurately weighed into a pre-ignited alumina crucible. The weight of the tephra sample was recorded so that the loss on ignition could be calculated. The weighed

tephra samples were then ignited for 30 minutes in a muffle furnace heated to 1000°C. Once ignited, the crucibles were removed from the furnace and allowed to cool for ten minutes. The crucibles were then weighed and the following formula (Equation A1.4.1) was used to calculate the percentage loss on ignition.

$$\% \, LOI = \frac{loss \; or \; gain \; of \; rock \; powder}{original \; weight \; of \; rock \; powder} \; x100 \qquad \text{Equation A1.4.1}$$

A1.4.4. Major element analysis

The glass discs were analysed using an ARK 8420+ dual goniometer wavelength dispersive x-ray fluorescence spectrometer, equipped with a 3 kW Rh anode end-window X-ray tube. The major elements measured included SiO_2, TiO_2, Al_2O_3, Fe_2O_3, MnO, Cao, Na_2O, K_2O and P_2O_5. Two standards of known elemental composition were run alongside the tephra samples and the elements were corrected for background and known peak overlap interferences.

Appendix 1.5: $^{40}Ar/^{39}Ar$ radiometric dating method

A1.5.1. Sample preparation

Tephra samples should be prepared for initial sampling. One hundred grams of the sample should be weighed out and crushed using a pestle and mortar until the sediment is fine grained. The crushing ensures the sample is in small enough particles to be sieved. Sieving should ensure the largest possible fraction is sampled as this will ensure a large enough amount of sample can be obtained. 250μm size fraction and 125 - 250μm size fraction are the suggested sizes, grains smaller than this will be harder to pick due to static causing the grains to 'ping'. Sieving into the same size fraction means that when picked, all grains will be the same size, therefore, when melted using the laser, melt times will be nearly the same for all grains.

A1.5.2. Mineral grain picking

Due to the projected young age of the tephra samples (radiocarbon infinite >48,000 and less than 1 million [presence of *Alnus* sp]), a large amount of grains will need to be picked to ensure a suitable level of ^{39}K present. Based on previous Ar – Ar work on similar samples (Cárdenas et al., 2011), an overall grain weight of 0.2 – 0.25g has been suggested to ensure a large enough amount of ^{39}K will be present. The type of grain to be picked will be sample dependent, however, it is important that the mineral is known to contain ^{39}K as this is what is irradiated, allowing the decay ratio of ^{40}K to ^{40}Ar to be used to work out a radiometric date. In these tephra samples, feldspars and biotites were picked. The feldspars chosen were clear, white and well-rounded, with no disconformities present. The biotites should be dark in colour, occasionally white to grey streaks are present on the surface, and all disconformities should be avoided.

Part of the sieved fraction of the tephra sample should be poured into a clean petri dish and placed under a stereomicroscope. Mineral grains should be selected and carefully picked from the petri dish using fine pointed tweezers and placed into a 7ml vial. The vial should be weighed pre picking so it is possible to work out the total weight of grains picked. The sample should also be weighed at the end of picking to ensure an appropriate weight of sample has been picked.

If the sample is dusty, meaning hard to identify grains, it is suggested that the sample is washed before picking resumes. To wash the sample it must first be poured into a 250ml beaker. Deionised water should be poured into the beaker, covering the sample by $1cm^3$. The beaker containing the sample should then be placed into an ultrasonic bath. The sample should be agitated for fifteen minutes and then the supernatant containing dust particles should be poured off in one swift movement leaving only the clean sample behind. The sample should then be dried on a hot plate set at 40ºC. Once washed and dried the sample should then be picked as before.

A1.5.3. Pre irradiation preparation

Once the mineral grains have been picked they need to be washed and packed before being sent for irradiation. The picked sample should be poured into a 100ml beaker and washed in acetone. 1cm^3 of acetone should be poured into the beaker containing the sample; completely immersing the sample. The beaker should then be placed into an ultrasonic bath and agitated for fifteen minutes. By washing in acetone all grease is removed from the sample, meaning the samples are suitable to enter the mass spectrometer later in the process. The supernatant is then decanted and the sample washed twice in deionised water using the same method. The sample is then left to dry on the hot plate. Drying times is sample dependent; however, it is expected to be about an hour.

Once washed and dried the samples need to be packed. To remove the possibility of grease coming into contact with the samples, vinyl gloves should be worn throughout the packing process. First a large piece of foil (30cm x20cm) should be laid out onto the working surface; this ensures a clean surface so if any grains are dropped they can be picked up. This should be replaced and the surface wiped down between each sample. Next 3cm x 2cm foil pieces should be cut from another piece of foil; these are what the grains will be packed into. It is recommended to cut two per sample too be packed, plus one extra per sample, in case the foil rips. Taking one 3cm x 2cm foil, it should be carefully folded in half using tweezers, and then one other edge should be folded over leaving a pocket. The sample name should be written onto the foil at this stage. The foil should then be weighed. The following should take place over the large piece of foil. Once the foil has been weighed it should be opened out into a pocket and the grains carefully poured into the opening. Using tweezers, all edges around the foil should be folded securely over, taking care not to rip the foil with any potentially pointed grains. This process should leave a 1cm x 1cm foil parcel, this should then be weighed. The process should be repeated for all samples. For each sample, data about the weight of sample, the sample name, ‘rock’ type and the country of origin should be recorded in the irradiation book.

A.1.5.4. Irradiation

Once packed the sample is sent to the McMaster medium flux nuclear fission reactor in Canada. The samples are irradiated by bombarding them with neutrons. The neutrons transform the ^{39}K to ^{39}Ar, meaning their decay can be measured later. The irradiation occurs alongside a standard of known age. This provides a comparable standard which can be used to help produce an error on the ages later in the process.

Due to their young age the samples (<1 million years due to the presence of *Alnus* sp pollen grains; Hooghiemstra, 1984) were only in the nuclear reactor for one hour. This is because they only contained a small amount of ^{39}K to become radioactive. This time allows the maximum amount of 30Ar to be produced, whilst the amount of isotopes from interfering reactions is minimised. The length of time required within the reactor is based on the samples approximate age range and the K/Ca ratio. When returned, the samples should be monitored using a radiation dosimeter by a trained radiation supervisor, until they are at a suitable radiation level. At a low (suitable for young samples) irradiation the samples will be ready to use soon after their return. By checking the radiation dose, the samples are known to be at a safe level to work with, meaning exposure to radioactive materials is limited.

A.1.5.5. Sample analysis

Samples were loaded into the port of the Map 215 – 50 noble gas mass spectrometer. Sample analysis, both sample and standard, was performed on the Map 215 – 50 noble gas mass spectrometer (MAP 2) using a SPI 25W Infra – Red fibre laser (Dilbert). Map 2 consists of a high vacuum extraction system with three getters, one is kept cold at room temperature, and the other two are maintained hot at 450ºC. The different getters are used to separate different gaseous elements by trapping them at different temperatures. Map 2 has facilities to also add a

liquid nitrogen trap which traps gases at -196ºC. Analysis of samples using Map 2 is facilitated by the automated inlet software, LabVIEW.

Before sample analysis can begin, gas levels in the mass spectrometer and the air must be checked, this is done by running blanks. Blanks are run until they stabilise. Only once these are stabilised can sample analysis begin, this ensures that the final results can be calibrated with regards to the level of each gas previously in the machine and air. In every analysis (both blank and sample) the mass spectrometer scanned peaks at masses 35, 36, 37, 38, 39, 40 and 41. Peaks were measured ten times during one analysis.

Samples are step heated; this involves increasing the laser power a fraction each time, aiming to keep the output of the machine at a manageable level (around 0.3v of ^{40}Ar). This allows the gas to be released at manageable levels meaning the machine will be able to cope, anything higher than about 10v will cause the machine to saturate, meaning a loss in sample analysis time. If the machine is saturated, the inlet valve should be set to manual and the mass spectrometer should be left alone for 20 minutes to allow the blanks to stabilise again. To step heat, the laser is first turned on to its lowest power and then traverses are made across the sample port, making sure all sample comes in contact with the laser, this process takes about seven minutes. On the next step the laser power is increased and the same process repeated. This process is repeated until all sample grain has melted. This process is interspersed with a blank every two runs, however, the amount of blanks will need to be increased if blanks begin to destabilise.

Alongside running the samples it is also important to run standards of known age. The standards are irradiated at the same time as the samples and they provide a comparable sample which can help with the production of the J value, important for age calculation. The standards are run using single grain fusion. The laser is aimed at one grain of known age and the laser power is

slowly increased until the grain completely melts, this process should be completed for 12 grains per standard.

A.1.5.6. Age calculation

Age calculation is facilitated by the programme ArMaDiLo v.1.0.1. To calculate the age it is important to understand the principles behind the technique. The $^{40}Ar/^{39}Ar$ dating technique is based on the decay of the radiogenic 'parent' ^{40}K. ^{40}K has a half-life of 1250Ma, 10.5% of it decays to ^{40}Ar, the remaining 89.5% decays to ^{40}Ca. Within the samples ^{39}K is transformed to ^{39}Ar by fast neutron bombardment during irradiation in a nuclear reactor. Due to K isotopes undergoing very little fractionation, the $^{39}K/^{40}K$ ratio can be assumed as stable at 0.0001167 (Steiger and Jäger, 1977), therefore, the $^{40}Ar/^{39}Ar$ ratio is proportional to the $^{40}Ar/^{40}K$ and can be used to calculate the age. Corrections are applied for any decay for the time between sample irradiation and sample analysis

The amount of ^{39}Ar produced from ^{39}K during irradiation is a function of ^{39}K in the sample, proportional to an irradiation parameter 'J'. The J value is calculated using standards of known age which are distributed evenly throughout the irradiation, ensuring they receive a similar neutron bombardment. With the J value the age of the sample can be calculated with Equation A.1.5.1.

$$age = \frac{1}{\lambda} ln\left\{\left(\frac{40Ar^*}{39Ar}\right)J + 1\right\} \qquad \text{Equation A1.5.1}$$

λ represents the combined decay constant for ^{40}K, including the decay of ^{40}Ar to ^{40}Ca by beta emissions, the decay of ^{40}K to ^{40}Ar by electron capture and gamma emission, and finally the decay of ^{40}K to ^{40}Ar by electron capture (value of $5.543 \times 10^{-10} yr^{-1}$). * Denotes the ^{40}Ar which

purely resulted from the radiogenic decay. J is an irradiation parameter derived from standards of known age.

As with many analytical procedures errors need to be calculated, in the case of $^{40}Ar/^{39}Ar$ analysis, age precision is dependent on the amount of argon extracted from the sample. The error can be calculated using Equation A1.5.2.

$$\sigma_t^2 = \frac{J^2\sigma_R^2 + R^2\sigma_J^2}{\lambda^2(1+RJ)^2}$$ Equation A1.5.2

σ_t is the final error on the age, J is the irradiation parameter produced from standards of known age, R is the $^{40}Ar^*/^{39}Ar$ ratio, λ is the combined decay constant of ^{40}K, σ_R is the error on the $^{40}Ar^*/^{39}Ar$ ratio as measured and σ_J is the error on the J value.

Appendix 1.6: Optically stimulated luminescence (OSL) method

All sample preparation took place in a laboratory under red light conditions. This was to ensure no light influenced the sample, therefore, changing the results of the procedure. The OSL methodology was performed by Dr Andrew Carr at the University of Leicester.

A1.6.1. Sample pre-preparation

The outer three to five cm of each tube was removed to prevent any potential light contamination affecting the results. This material was retained and was used to calculate the percentage water content of the samples; it was also used to calculate the K, U and Th values of the samples (see environmental dose rate section of the method). The remaining sample was treated with 0.1M Hydrochloric acid to remove carbonates. The sample was treated with 32% Hydrogen peroxide to remove organic matter. The sample was then wet sieved into size fractions between 250μm and 90μm. Fine sediments below 90μm were lost at this stage as they do not contain any material

of use. The remaining sample was density separated, using heavy liquid, to isolate two fractions (<2.58g cm^{-3} and 2.58-2.70g cm^{-3}). Less than 2.58g cm^{-3} was primarily composed of feldspar and aggregated clay material. The 2.58 – 2.70g cm^{-3} fraction was composed of quartz. Material over 2.7g cm^{-3} was discarded, containing only heavy minerals with no use for this process.

Following separation, the quartz fraction was etched in 48% Hydrofluoric acid for one hour. Following the hydrofluoric acid etching, the samples were washed in Hydrochloric acid to remove residue fluorides. The samples were then washed in water to remove further fluoride traces. The samples were then dried. The quartz fraction that underwent processing was then re-sieved to remove any non-quartz minerals that had been etched by the Hydrofluoric acid and quartz grains that had been severely etched, meaning they were a smaller particle size.

A1.6.2. Sample measurement

Sample measurement took place on a Risø TL-DA 20TL/OSL reader. Small aliquots of samples (approximately a 2mm diameter of sample) were mounted into the centre of 9mm stainless steel disks using silicone spray. Such small aliquots of the sample were mounted due to the low yield of isolated quartz from the samples. The total grains mounted onto the disks were estimated to be between 150 and 250 grains.

OSL was detected using an EMI 9235QA photomultiplier tube and a U-340 filter in the UV range. To ensure the OSL signal was not contaminated by a signal from non-quartz minerals which survived the pre-processing, the samples were stimulated with IR diodes (40 second at 50°C). Following this, samples were stimulated using blue LEDs (40 second at 125°C, stimulation wavelength 470nm and power 90%).

Estimates of the equivalent dose (D_E) were made using the single aliquot regeneration (SAR) protocol, outlined by Murray and Wintle (2000). This measures the natural OSL on each aliquot

and calibrates this natural OSL signal against a series of laboratory doses. Throughout the protocol, a test dose is administered after each OSL measurement to monitor for sensitivity changes (amount of OSL per unit of administered dose, i.e. how "bright" a sample is) that occur through cycles of heating and stimulation. From the ratio Lx/Tx (i.e. natural/ regenerated OSL divided by the test dose OSL signal) a sensitivity correlated calibration curve is generated (Figure A1.6.1 presents an example from one sample).

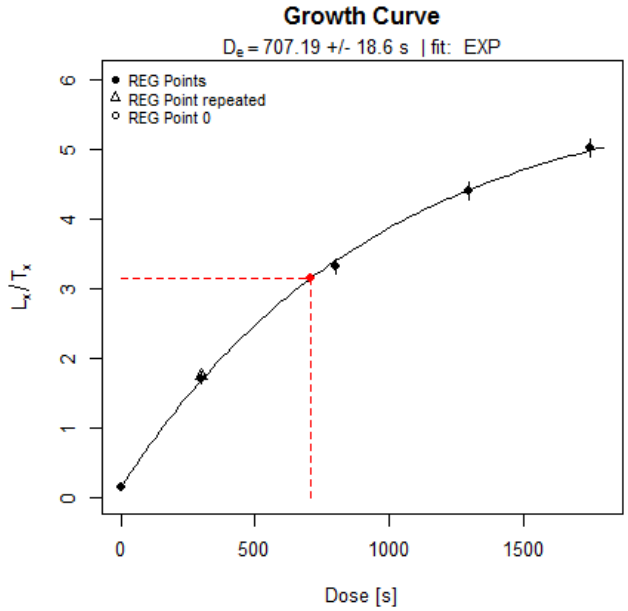

Figure A 1.6.1: Example growth curve, from which an equivalent dose can be interpolated. The plot is fitted with a saturating exponential equation. This example is from an aliquot of HK7. The doses are reported in seconds of exposure to irradiation. For the interpolated D_e this is equivalent to an equivalent dose of 103 Gy.

Prior to all OSL measurements (i.e. after irradiation), the samples are preheated to remove unstable charge that accumulates when the samples are irradiated artificially. When irradiated naturally, such charge is not usually present, but with the much higher rates of irradiation in laboratory conditions, preheating is necessary to remove these. By preheating the samples, unstable charges are removed and it also simulates the effects of geological burial. Selecting the appropriate preheat temperature is important and an experimental preheat plateau test is

undertaken. Temperatures used in the preheat test ranged from 160°C to 260°C. The former (160°C) is the minimum temperature that can be used as it is crucial in removing the 100°C thermoluminescence peak present particularly in quartz which interferes with the OSL signal. Above 280°C the preheat starts to thermally erode the OSL signals, which are the main target for OSL dating.

In order to calculate an estimated age for the sample, the OSL dose rate measured needs to be combined with an environmental dose rate. The environmental dose rate is a measure of the radiation received by the mineral since the last exposure to light (Walker, 2005). The procedure for calculating the environmental dose rate is outlined below. The environmental dose rate also includes the latitude and longitude of the samples, altitude and water content.

A.1.6.3. Environmental dose rate

From the retained tube ends sample, 20g of dried sample was ground to a fine powder using a tema ball mill. The following process was applied to 0.5mg of this dry powder.

A.1.6.3.1. ICP-MS

Dose rates were determined using inductively coupled plasma mass spectrometry (ICP-MS), undertaken at the Open University by Dr Samantha Hammond. Concentrations of Potassium, Thorium and Uranium were determined by following the process below:

All of the acids used in this process were subject to a two stage purification procedure, ensuring no additional trace elements were introduced to the samples. The acids were quartz distilled (QD; acid is produced by sub-boiling acid in a quartz still) and Teflon ® distilled (TD; acids were produced by thermal distillation of the QD grade acids in a Teflon still). Hydrochloric acid used in the process was thermally distilled in a cupola system (system used to produce ultra-pure

acids at temperatures far below the boiling point). Water used in the process was deionised, purified using the Milli-Q filtration system.

Teflon beakers used in the dissolution process were cleaned following a five stage process:

1. Rinse beakers three times with deionised water and leave to dry.
2. Add 1ml of QD Nitric acid and 1ml of QD Hydrofluoric acid seal with a lid and leave overnight on a hotplate at 130°C.
3. Discard the acid, and then rinse three times with deionised water and leave to dry.
4. Add 1ml of TD Nitric acid and 1ml of TD Hydrofluoric acid seal with a lid and leave overnight on a hotplate at 130°C.
5. Discard the acid, rinse three times with deionised water and leave to dry.

After all beakers have been cleaned to the above process the dissolution of the samples pre analysis can occur, following the process below.

1. Weigh out 0.1g of the powdered sample into a clean Teflon beaker.
2. Add 0.5ml of TD Nitric acid and 2ml of TF Hydrofluoric acid, seal with a lid and leave overnight on a hotplate at 120°C.
3. During dissolution, place in a sonic bath for twenty minutes. Repeat twice. This ensures all sample has been in contact with the acids.
4. Remove the lid and allow the solution to evaporate till dry.
5. Add 2ml of Hydrochloric acid (used to remove fluorides), seal with a lid and leave overnight on a hot plate at 120°C.
6. Remove the lid and allow the solution to evaporate till dry.
7. Add 2ml of TD Nitric acid and 4ml deionised water, seal with a lid and leave overnight on a hotplate at 120°C.

8. Place into a sonic bath for twenty minutes before removing the lid. Following this, remove the lid and allow the solution to evaporate till dry.
9. Add 3ml of TD Nitric acid, seal with a lid and leave overnight on a hotplate at 120°C.
10. Transfer sample to a Nalgene bottle and dilute using deionised water to 1000x dissolution.

Following the above process, the sample can then be measured on an Agilent 7500a ICP-MS fitted with a standard quartz spray chamber and a Babington nebuliser. The analytical procedure for the samples was undertaken alongside five standards of known values, providing analytical errors for the samples.

A.1.6.4. Calculation of the environmental dose rate

Concentrations of Uranium, Thorium and Potassium obtained by ICP-MS analysis were converted to annual dose rates following the process outlined in Guérin et al., 2011. These were then adjusted based on the grain size (Mejdahl, 1979), water content (Aitken, 1985) and impacts of Hydrofluoric acid etching (Bell, 1979). Cosmic dotes rates (based on altitude, latitude and longitude) were calculated with a 5% uncertainty included (Prescott and Hutton, 1994).

A.1.6.5. Age estimate calculation

Once the equivalent dose (process described in sample measurement) and the environmental dose rate have been ascertained then the estimated age of the sample can be calculated using Equation A1.6.1 below.

$$OSL\ age = \frac{equivalent\ dose}{environmental\ dose\ rate}$$ Equation A1.6.1

References

AITKEN, M. J. 1985. *Thermoluminescence Dating,* London, Academic Press.

BELL, W. T. 1979. Thermoluminescence dating: radiation dose rate data. *Archaeometry,* 21**,** 243 - 246.

CÁRDENAS, M. L., GOSLING, W. D., SHERLOCK, S. C., POOLE, I., PENNINGTON, R. T. & MOTHES, P. 2011. The Response of Vegetation on the Andean Flank in Western Amazonia to Pleistocene Climate Change. *Science,* 331**,** 1055-1058.

GUÉRIN, G., MERCIER, N. & ADAMIEC, G. 2011. Dose-rate conversion factors: update. *Ancient TL,* 29**,** 5-8.

HOOGHIEMSTRA, H. 1984. Vegetational and climatic history of the high plain of Bogotá, Colombia: a continuous record of the last 3.5 million years. . *Dissertationes Botanicae,* 79**,** 1 - 138.

MEJDAHL, V. 1979. Thermoluminescence dating - Beta-dose attenuation in quartz grains. *Archaeometry,* 21**,** 67 - 72.

MURRAY, A. S. & WINTLE, A. G. 2000. Luminescence dating of quartz using an improved single-aliquot regenerative-dose protocol. *Radiation Measurements,* 32**,** 57 - 73.

PRESCOTT, J. R. & HUTTON, J. T. 1994. Cosmic ray contributions to dose rates for luminescence and ESR dating: large depths and long-term variations. *Radiation Measurements,* 23**,** 497 - 500.

STEIGER, R. H. & JÄGER, E. 1977. Subcomission on geochronology: convention on the use of decay constants in geo- and cosmochronology. *Earth and Planetary Science Letters,* 36**,** 359 - 362.

WALKER, M. J. C. 2005. *Quaternary Dating Methods,* Chichester, West Sussex, John Wiley & Sons.

Appendix 2: Additional graphs from Chapter 8

This Appendix contains graphs that were produced for Chapter 8, but were not used in the thesis text.

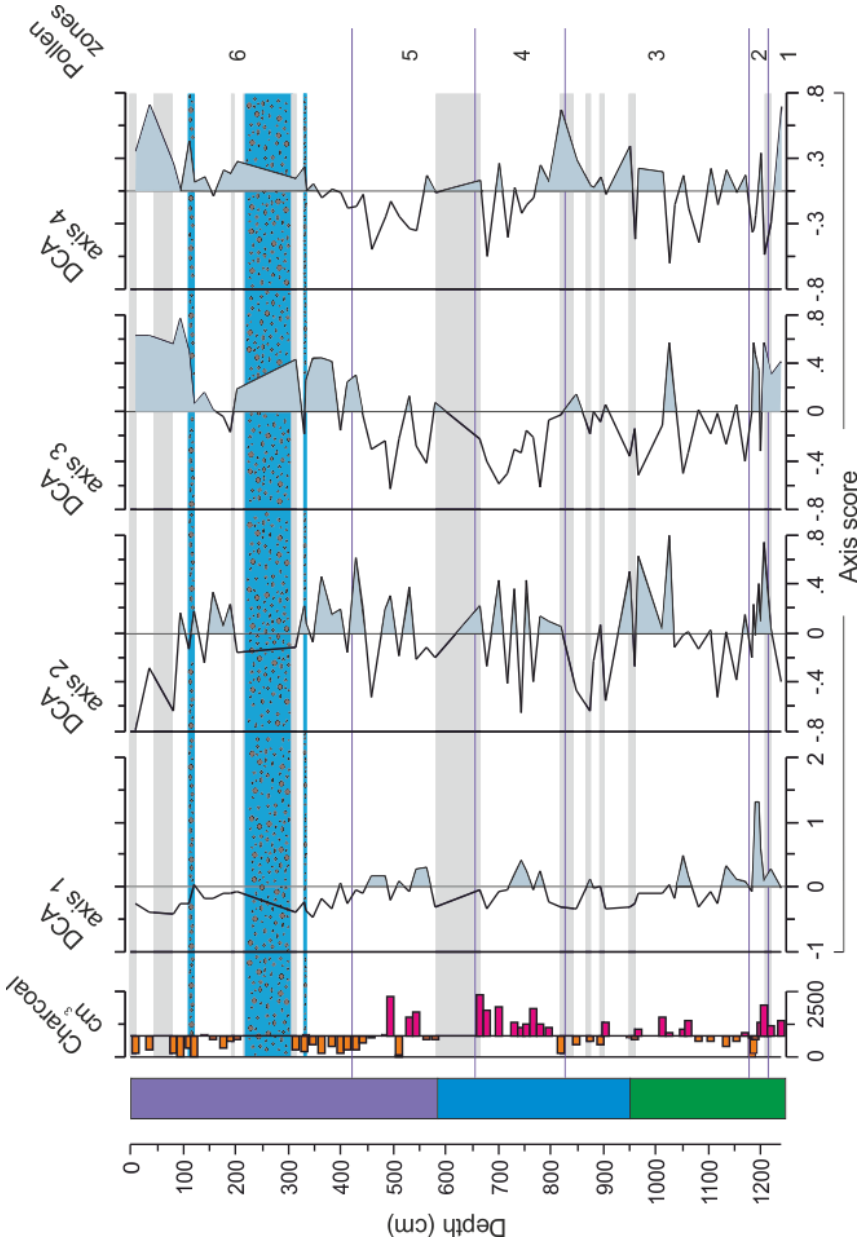

Figure A2.1: Charcoal and DCA for MTE above 10%, all samples are shown. This DCA includes samples 62 and 63 which were excluded from Figure 8.5.

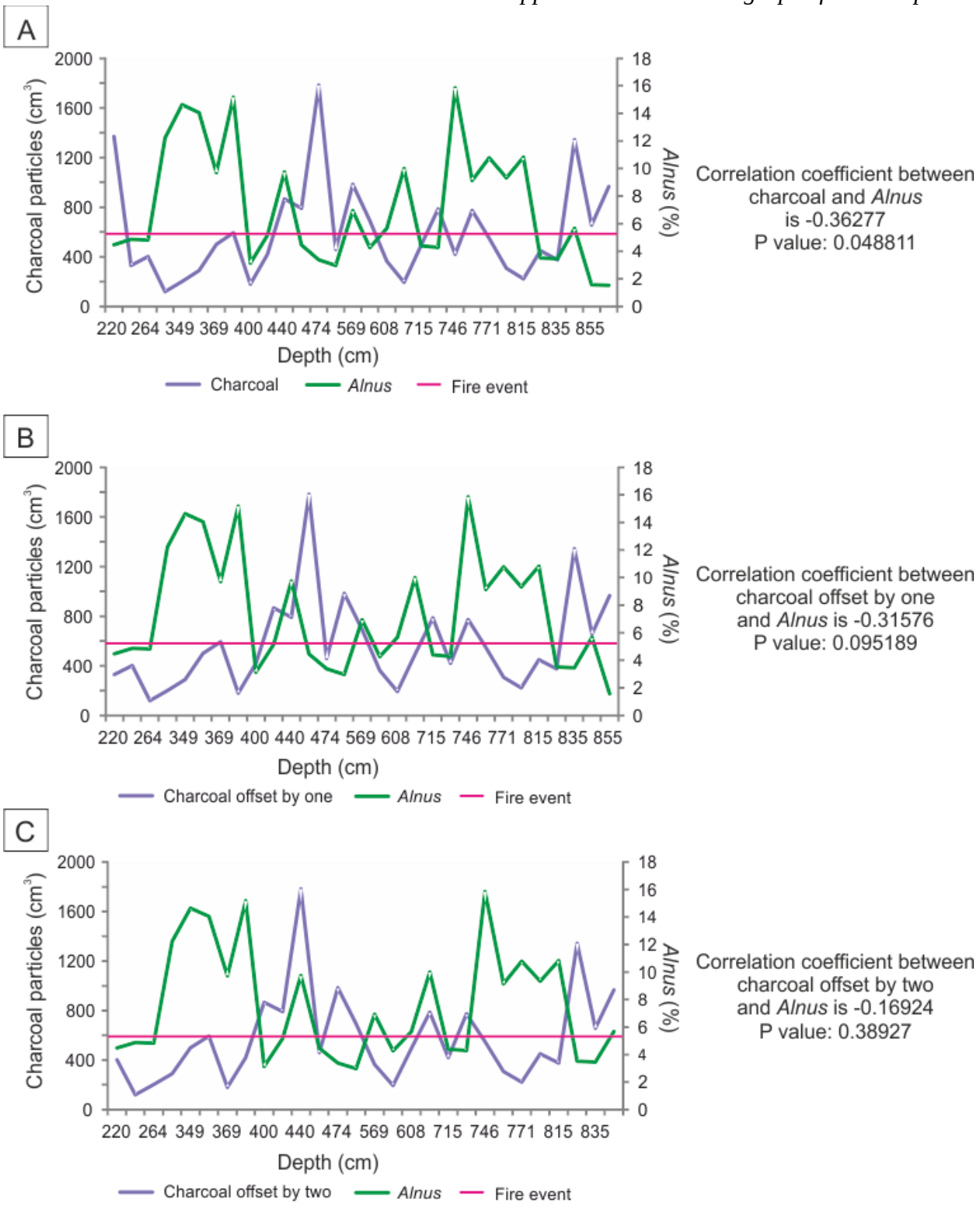

Figure A2.2: Correlation between *Alnus* and Charcoal particle concentration (cm^3) for MTW.

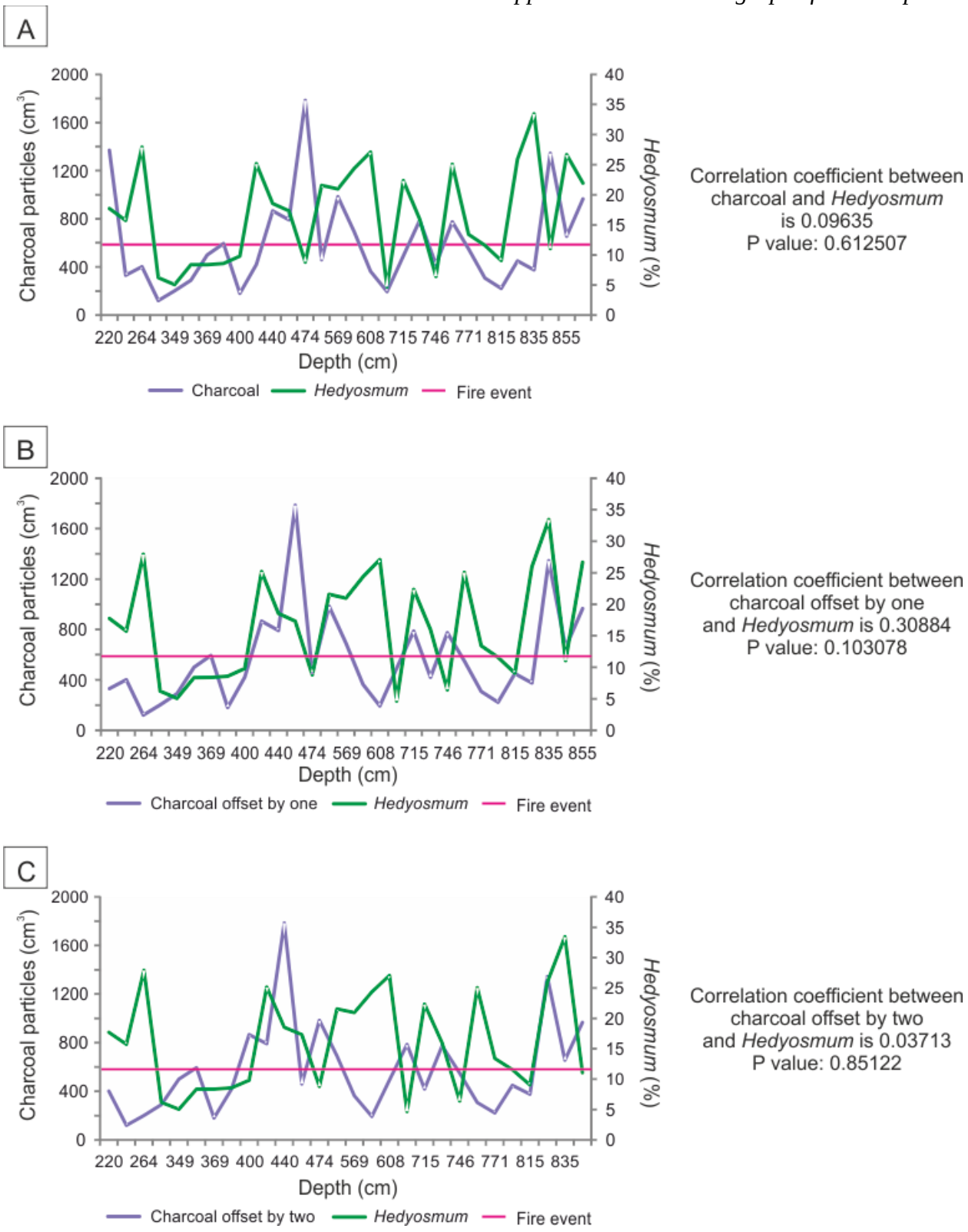

Figure A2.3: Correlation between *Hedyosmum* and charcoal particle concentration (cm^3) for MTW

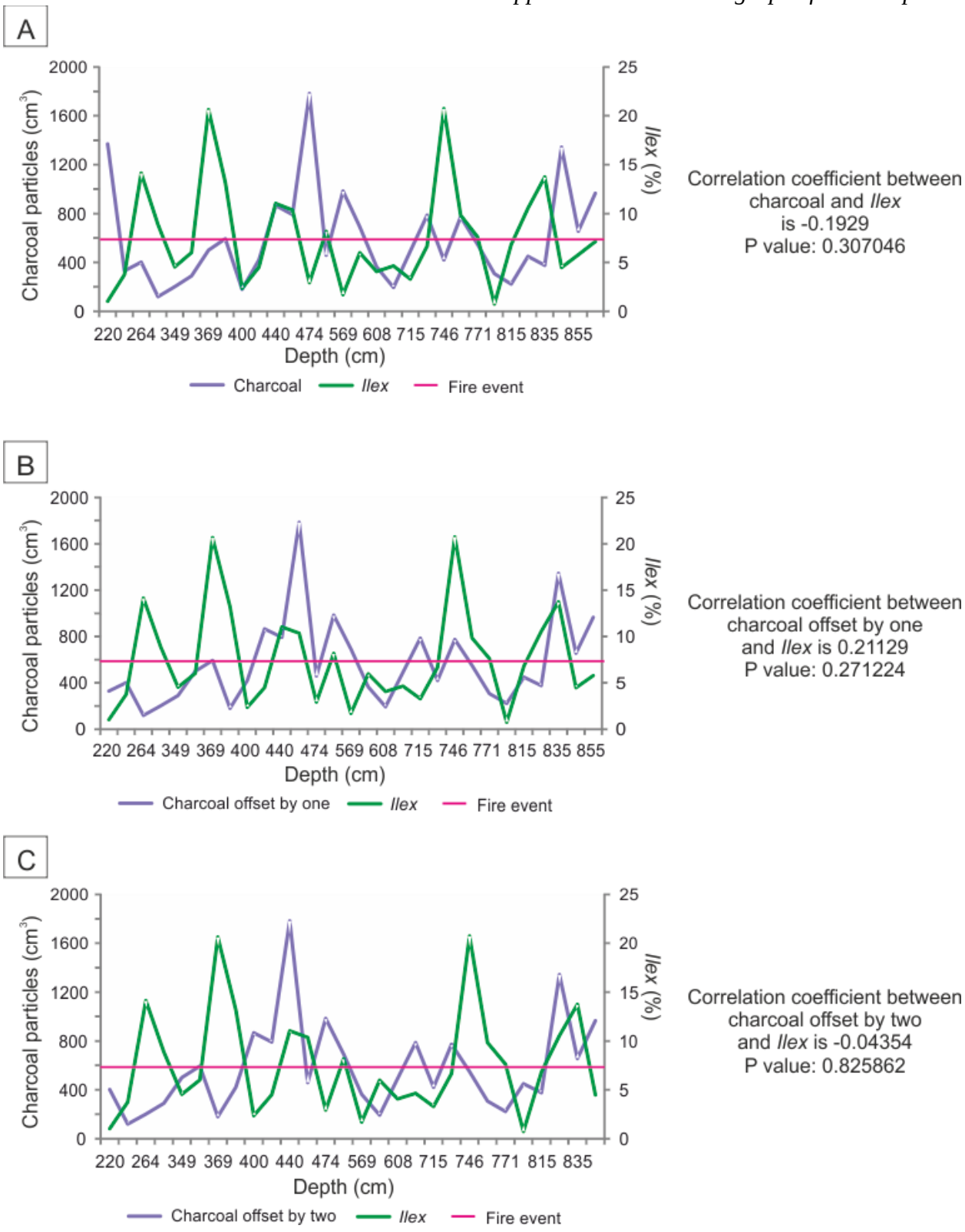

Figure A2.4: Correlation between *Ilex* and charcoal particle concentration (cm^3) for MTW.

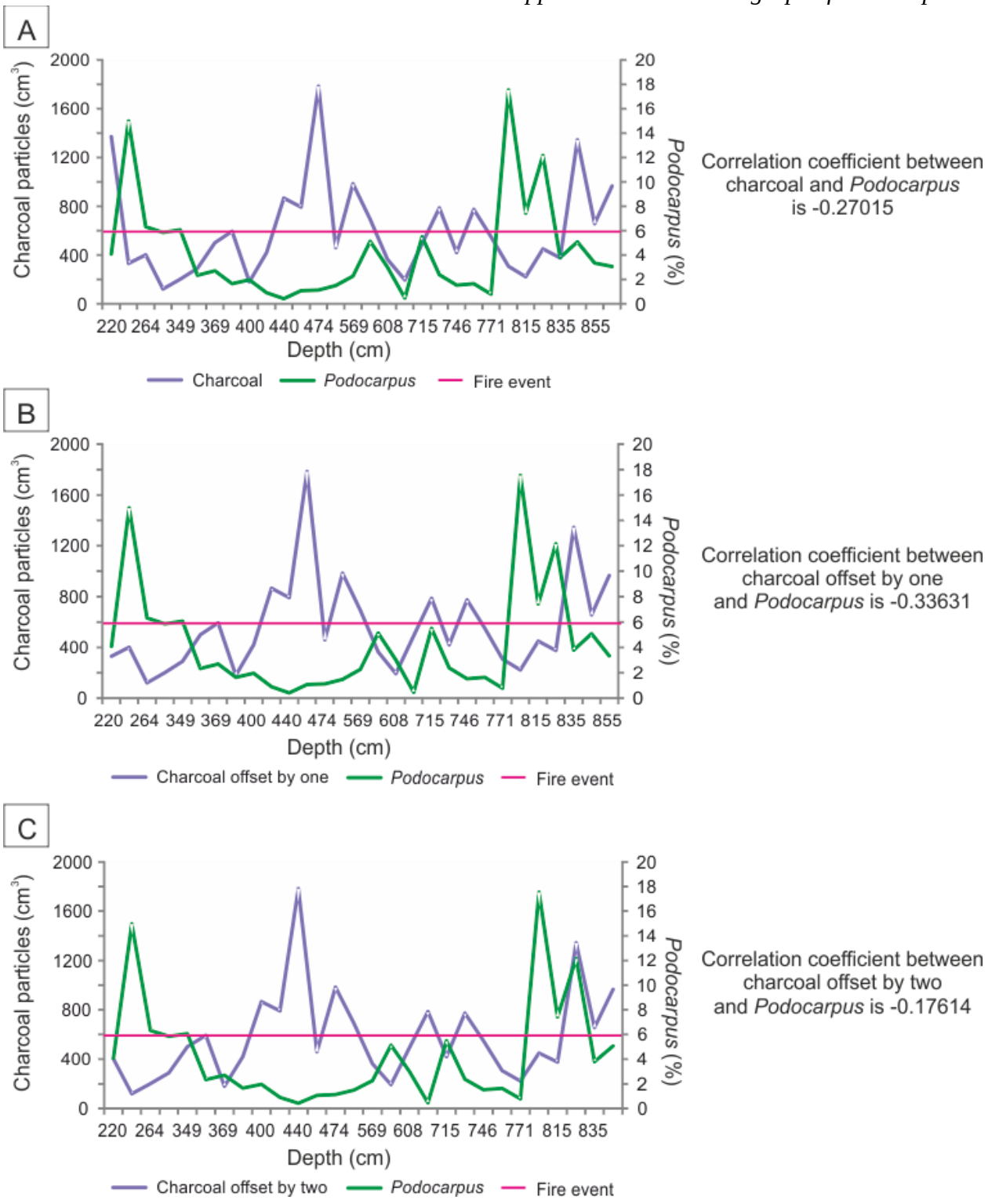

Figure A2.5: Correlation between *Podocarpus* and charcoal particle concentration (cm^3) for MTW.

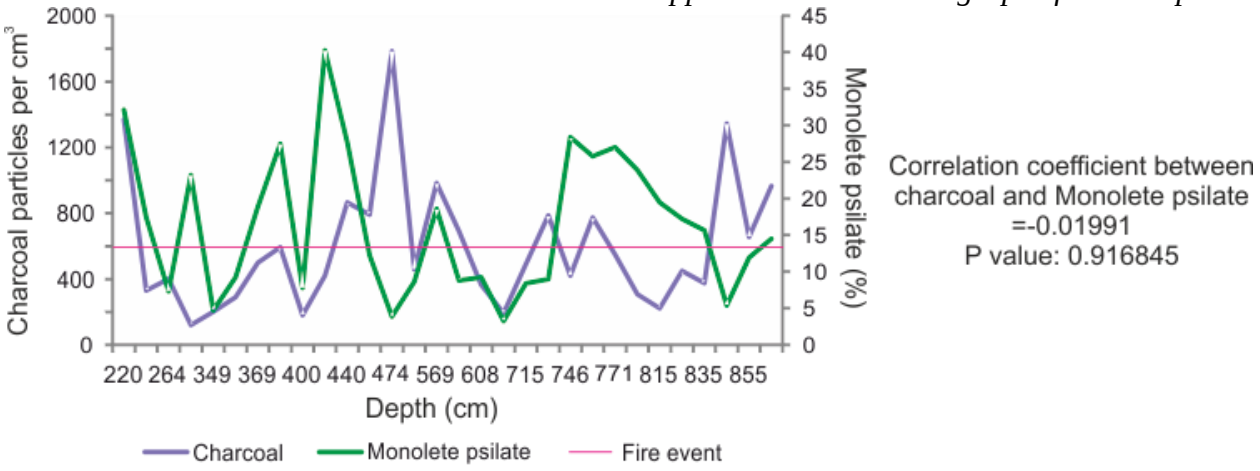

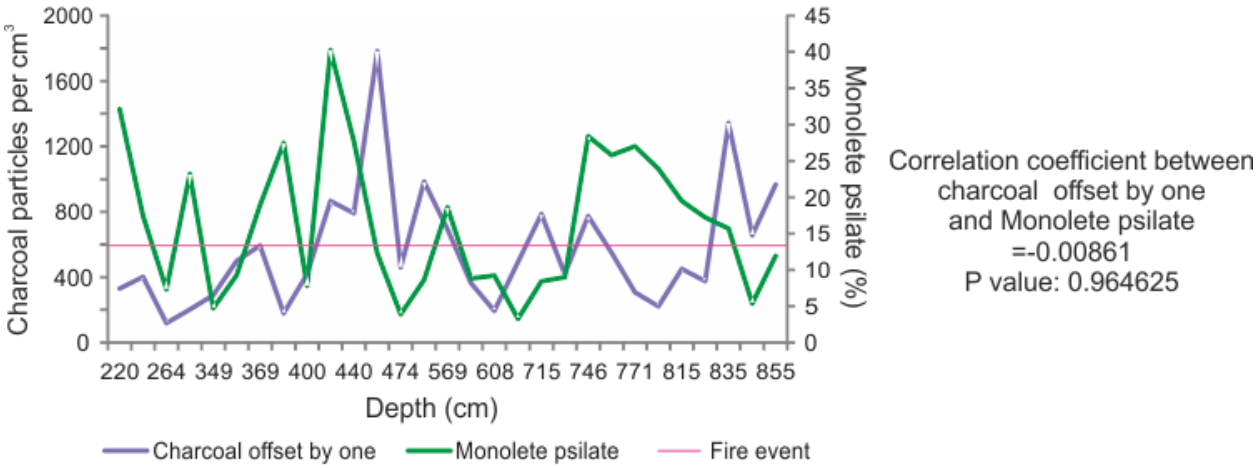

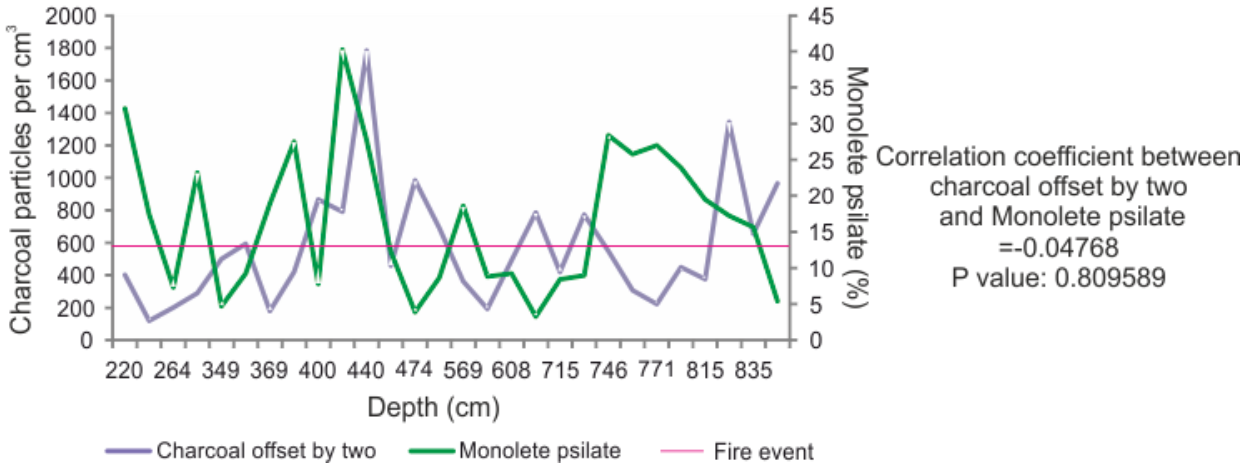

Figure A2.6: Correlation between monolete psilate and charcoal particle concentration (cm^3) for MTW.

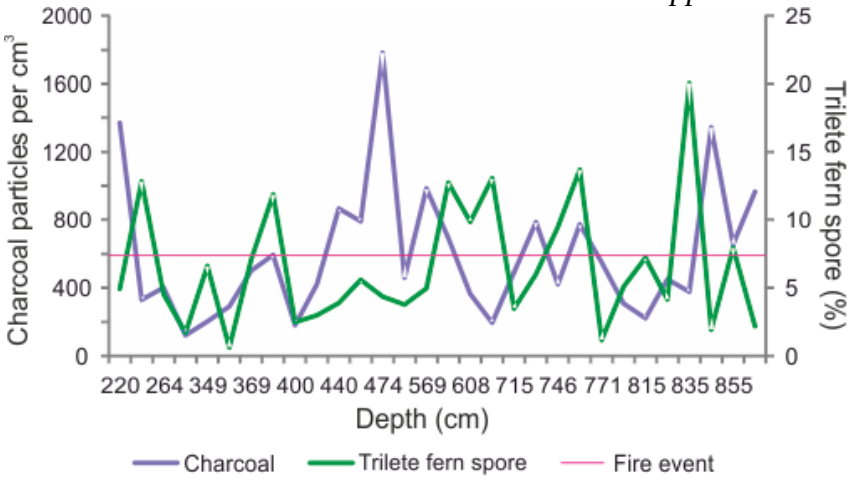

Correlation coefficient between charcoal and Trilete fern spore =-0.17159
P value: 0.364597

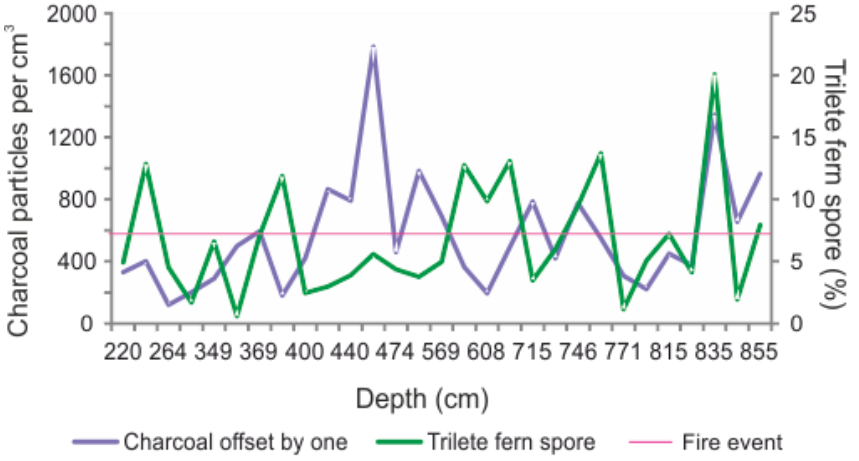

Correlation coefficient between charcoal offset by one and Trilete fern spore =0.1443
P value: 0.454889

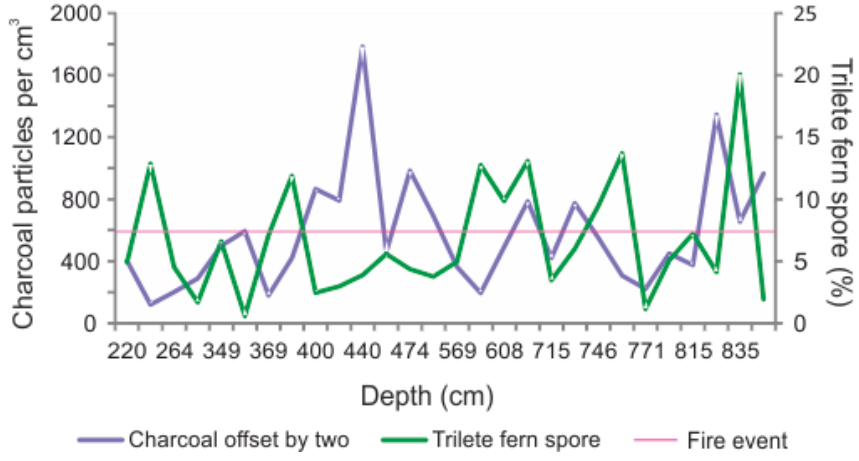

Correlation coefficient between charcoal offset by two and Trilete fern spore =-0.23537
P value: 0.227924

Figure A2.7: Correlation between trilete fern spores and charcoal particle concentration (cm^3) for MTW.

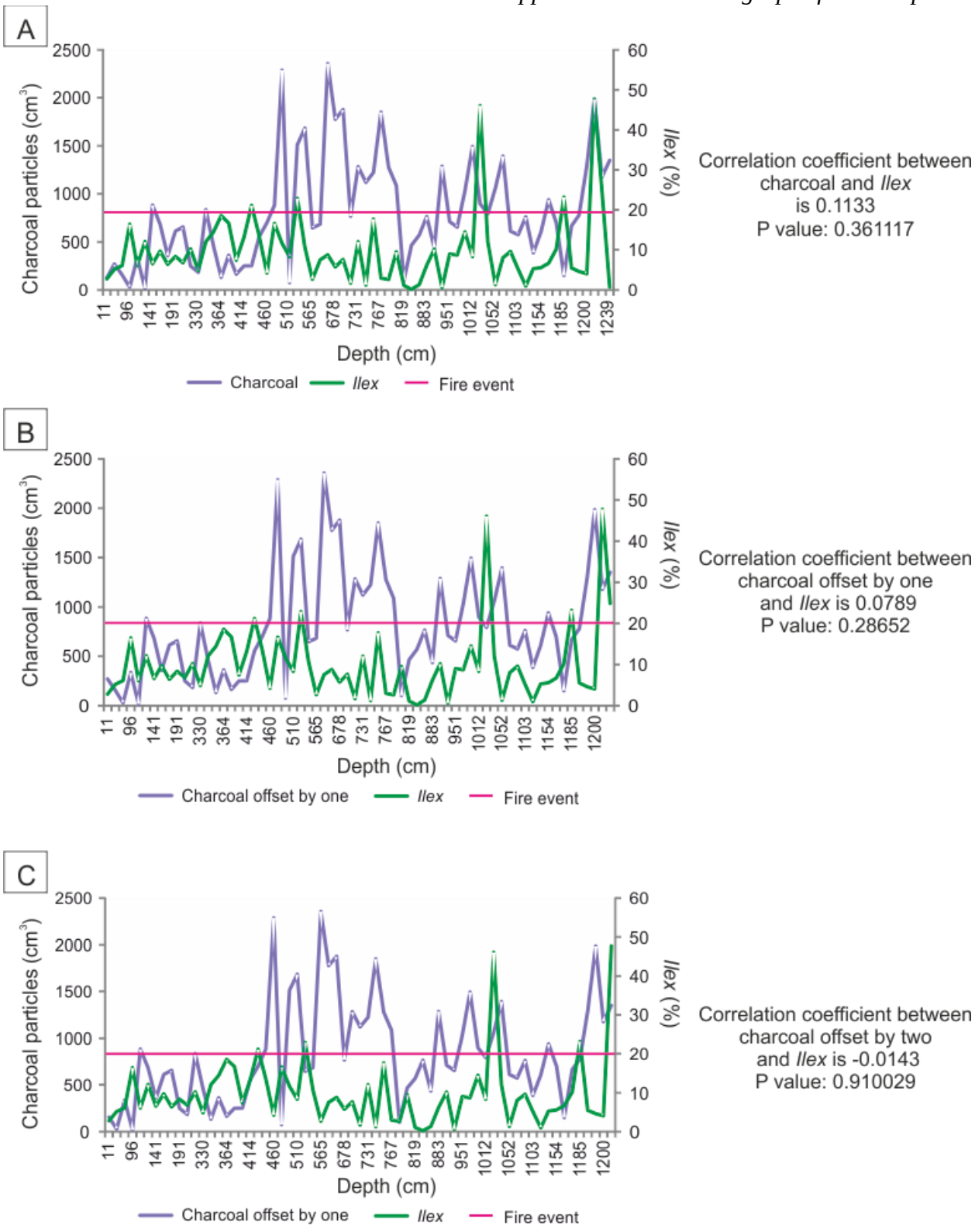

Figure A2.8: Correlation between *Ilex* and charcoal particle concentration (cm^3) for MTE

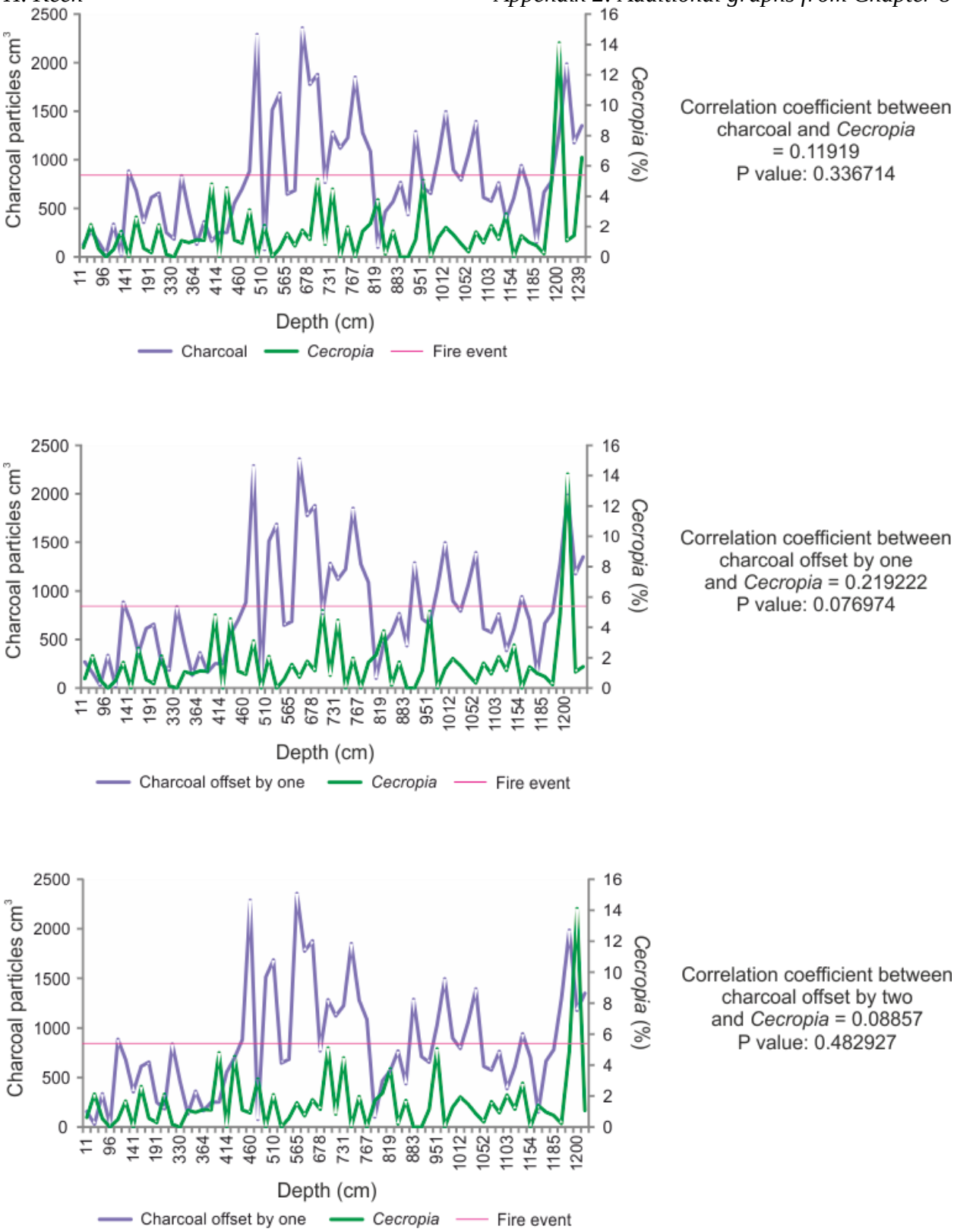

Figure A2.9: Correlation between *Cecropia* and charcoal particle concentration (cm^3) for MTE.

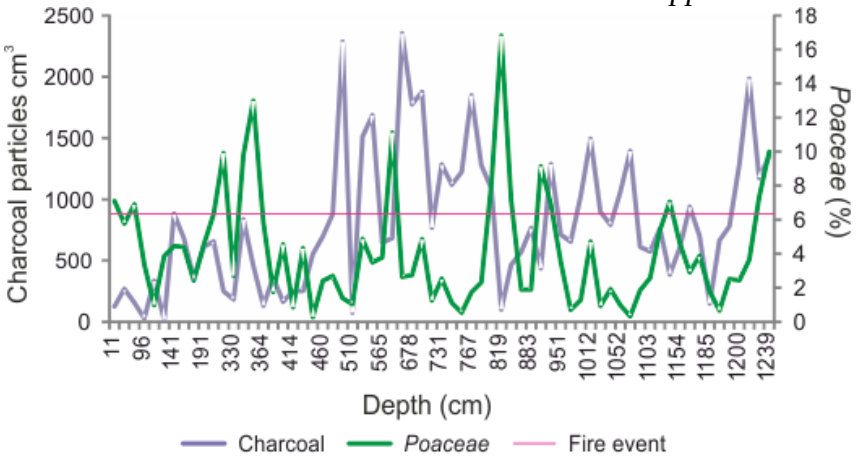

Correlation coefficient between charcoal and *Poaceae* = 0.19953
P value: 0.105483

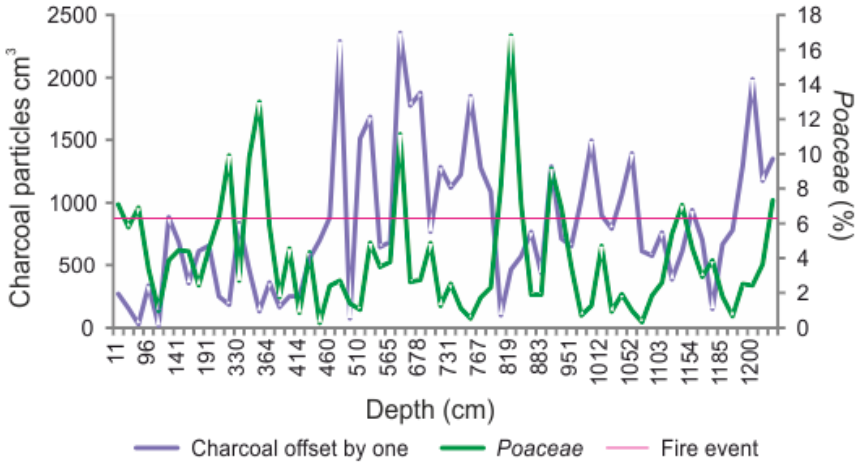

Correlation coefficient between charcoal offset by one and *Poaceae* = -0.20572
P value: 0.097501

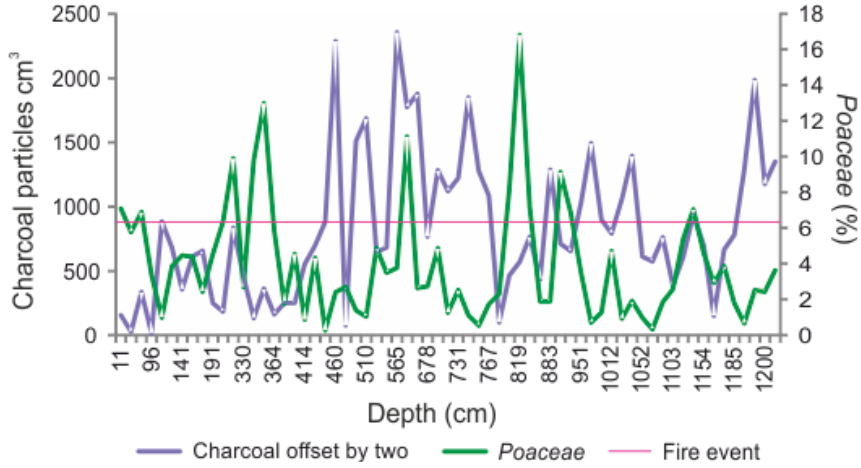

Correlation coefficient between charcoal offset by two and *Poaceae* = -0.26648
P value: 0.031894

Figure A2.10: Correlation between Poaceae and charcoal particle concentration (cm^3) for MTE.

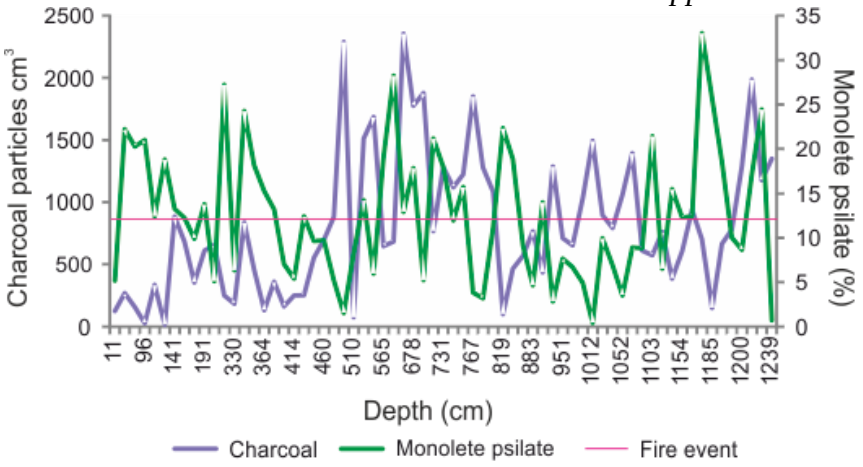

Correlation coefficient between charcoal and Monolete psilate = -0.31689
P value: 0.008982

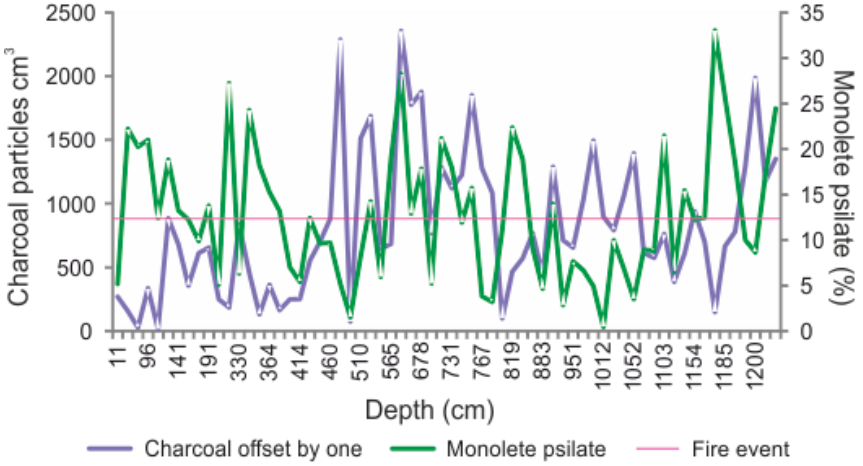

Correlation coefficient between charcoal offset by one and Monolete psilate = -0.04977
P value: 0.69147

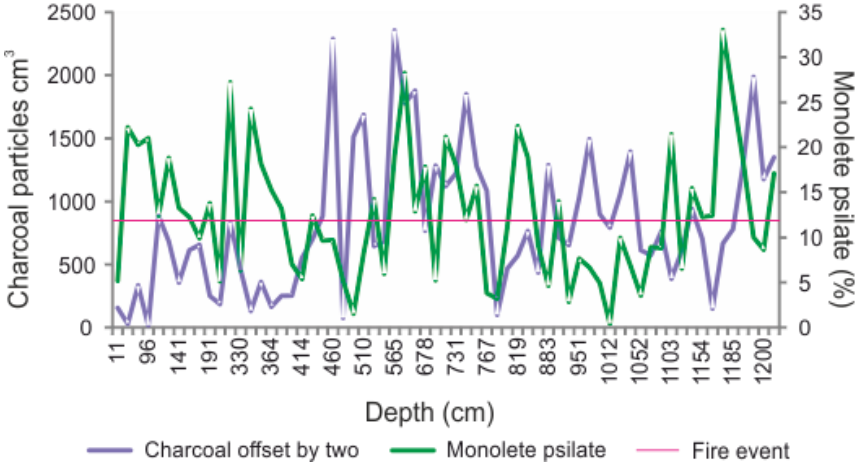

Correlation coefficient between charcoal offset by two and Monolete psilate = -0.02923
P value: 0.817206

Figure A2.11: Correlation between Monolete psilate and charcoal particle concentration (cm^3) MTE.

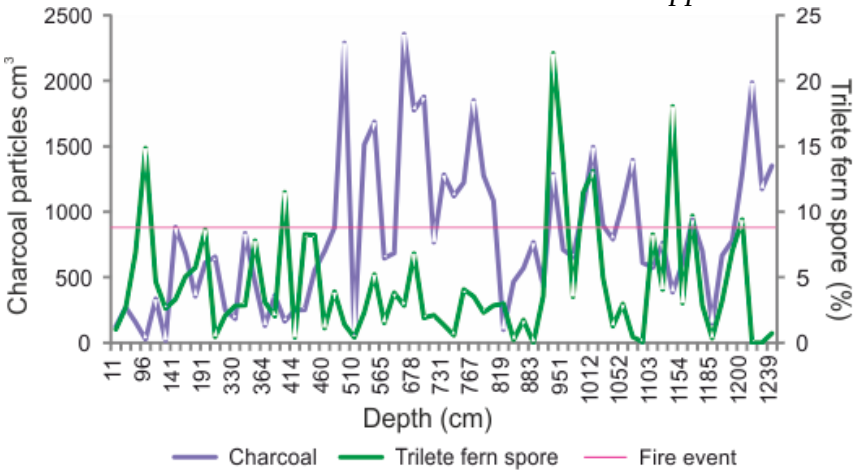

Correlation coefficient between charcoal and Trilete fern spore = -0.05968
P value: 0.631428

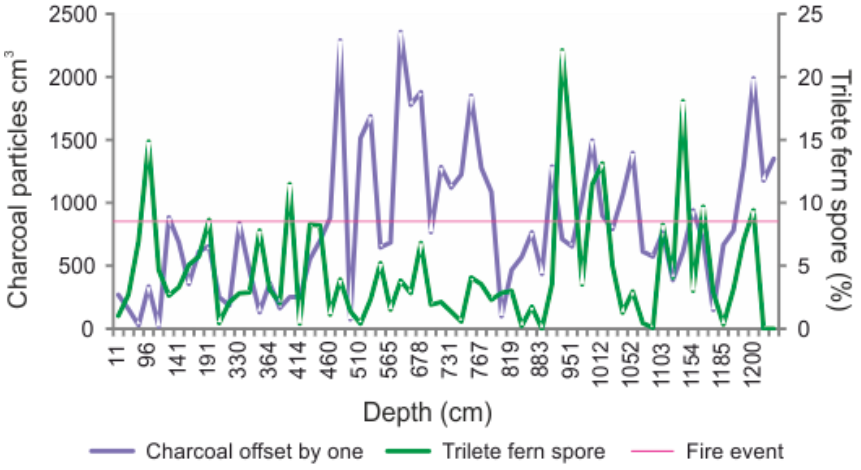

Correlation coefficient between charcoal offset by one and Trilete fern spore = -0.03045
P value: 0.808251

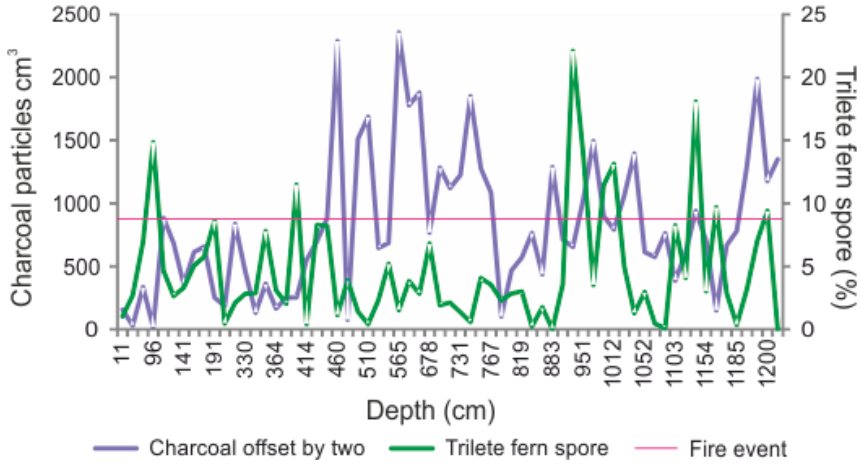

Correlation coefficient between charcoal offset by two and Trilete fern spore = -0.19251
P value: 0.124443

Figure A2.12: Trilete fern spore relation to charcoal particle concentration (cm^3) at MTE.

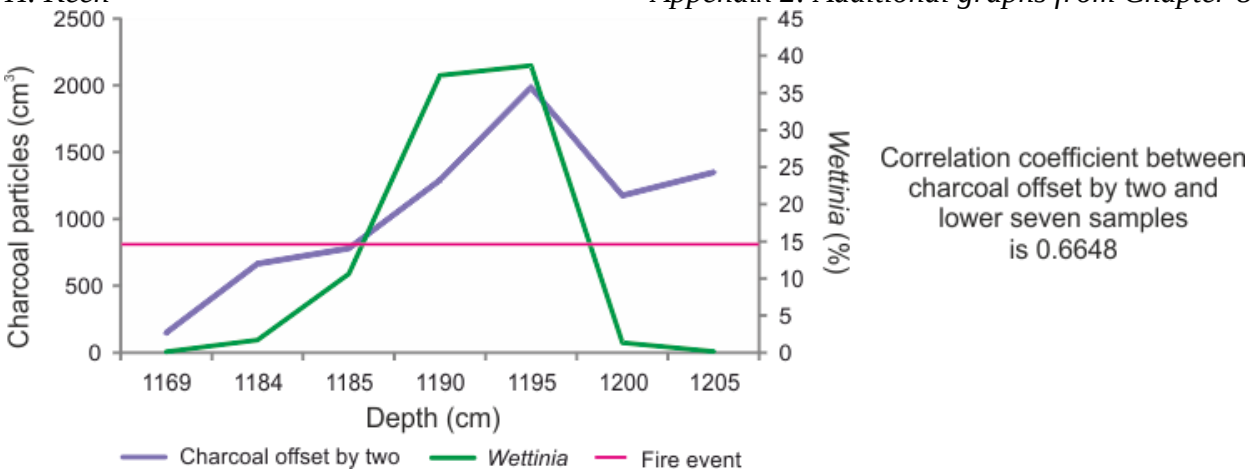

Figure A2.13: *Wettinia* (sp) offset by two (S_i +2) related to charcoal.

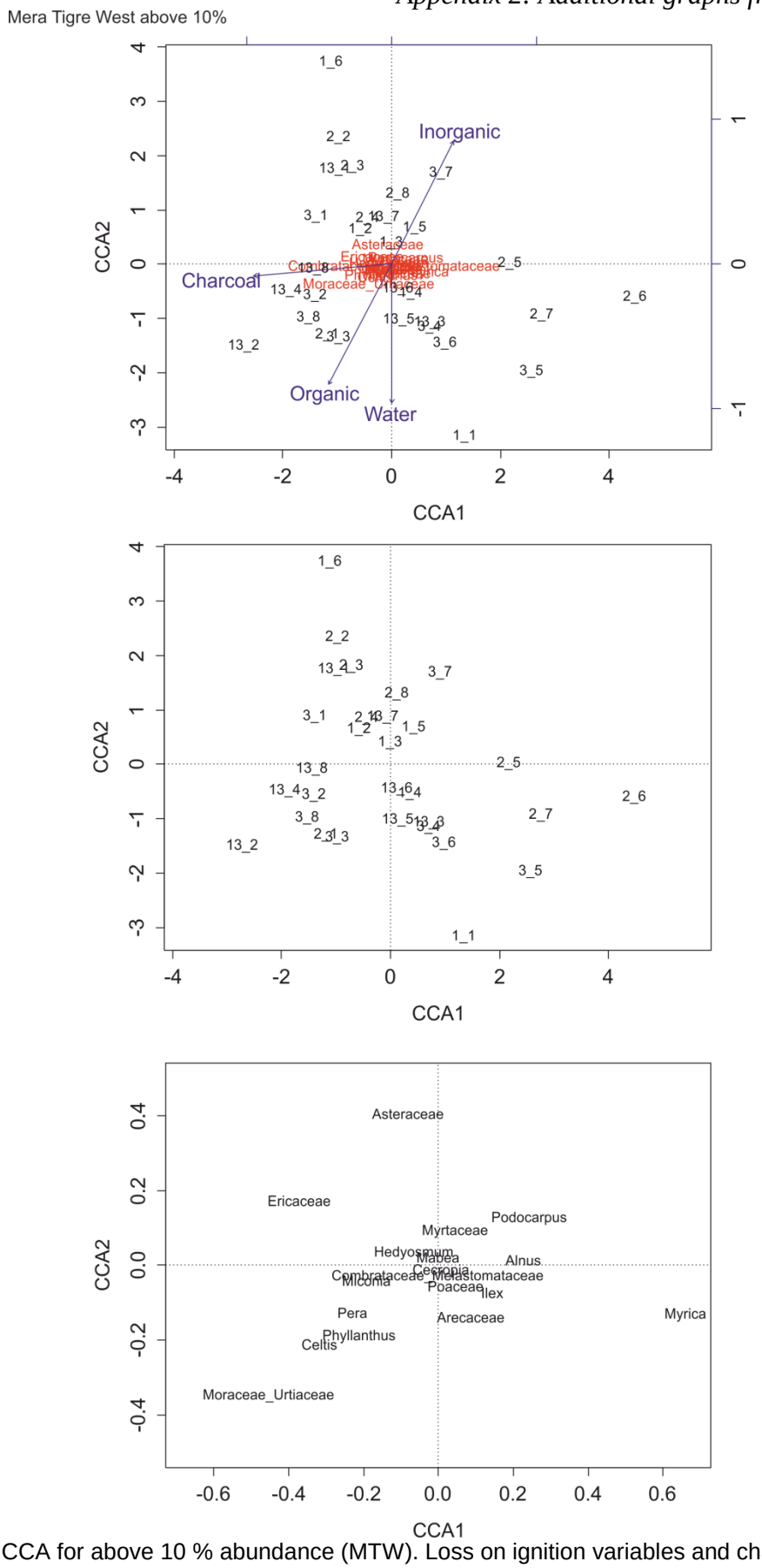

Figure A2.14: A CCA for above 10 % abundance (MTW). Loss on ignition variables and charcoal are included.

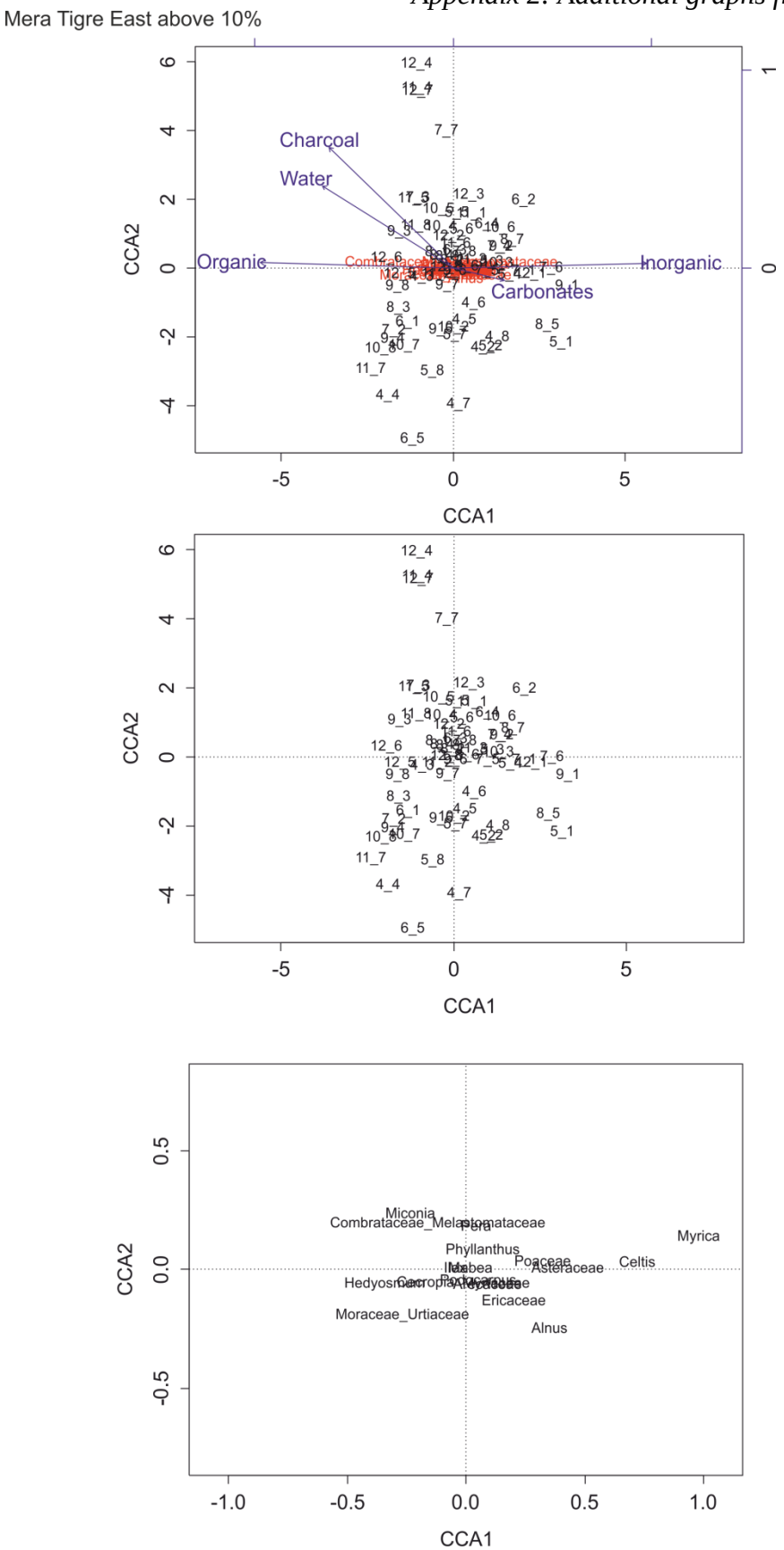

Figure A2.15: A CCA for above 10 % abundance (MTE). Loss on ignition variables and charcoal are included.

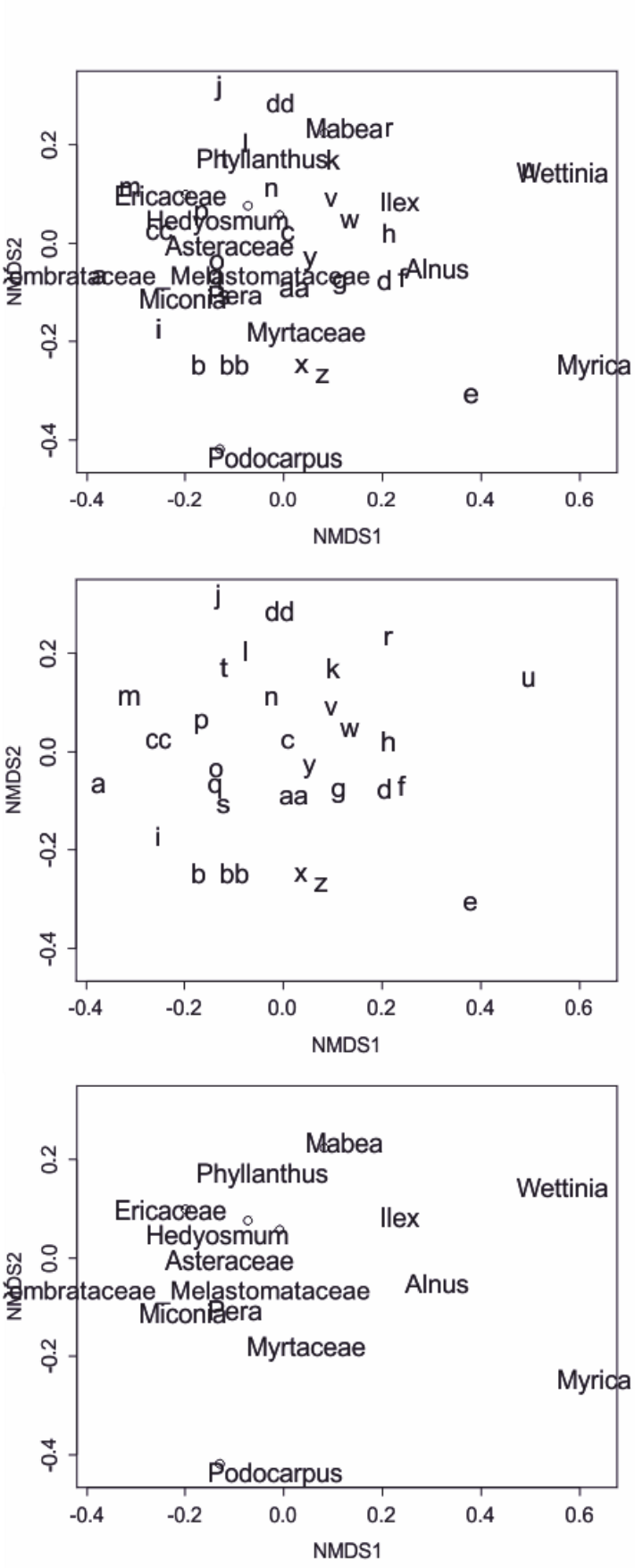

Figure A2.16: A NMDS for above 10 % abundance (MTW).

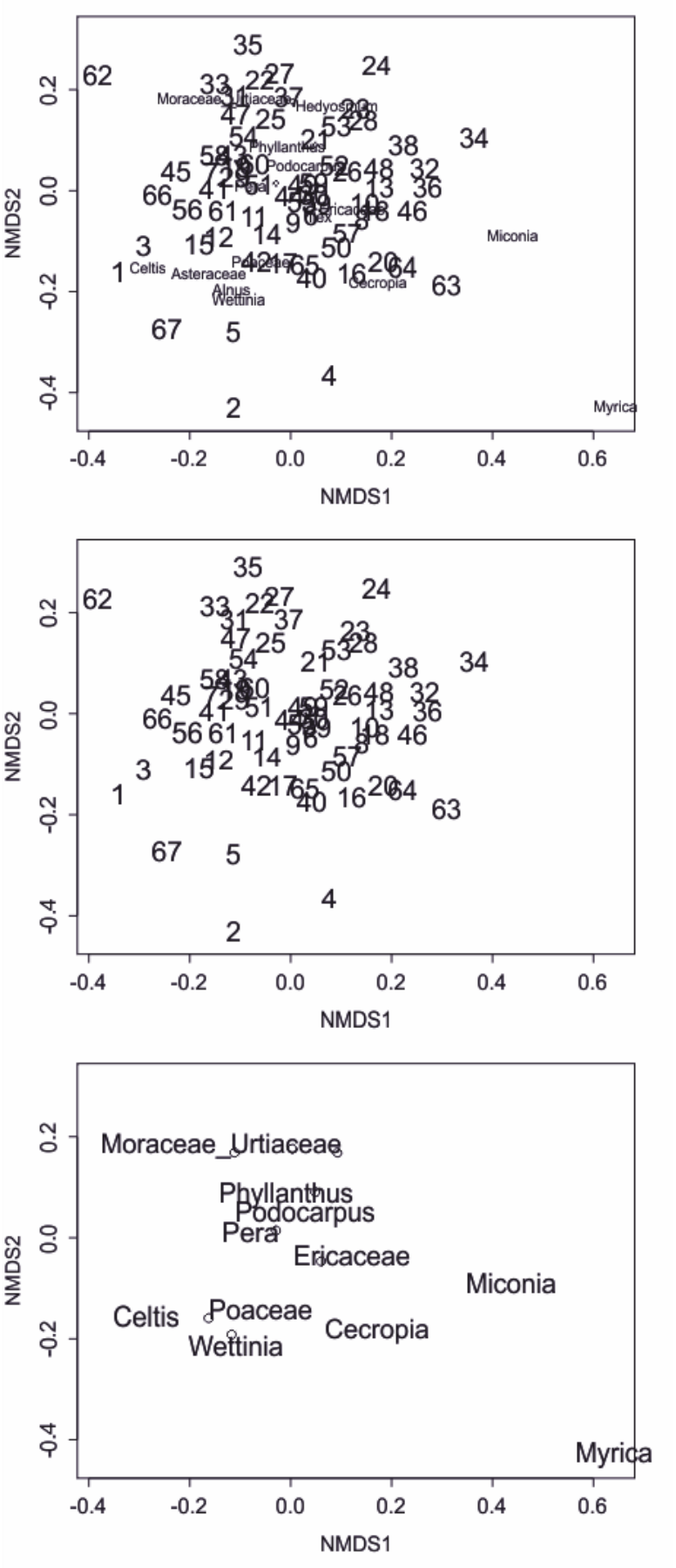

Figure A2.17: A NMDS for above 10 % abundance (MTE).

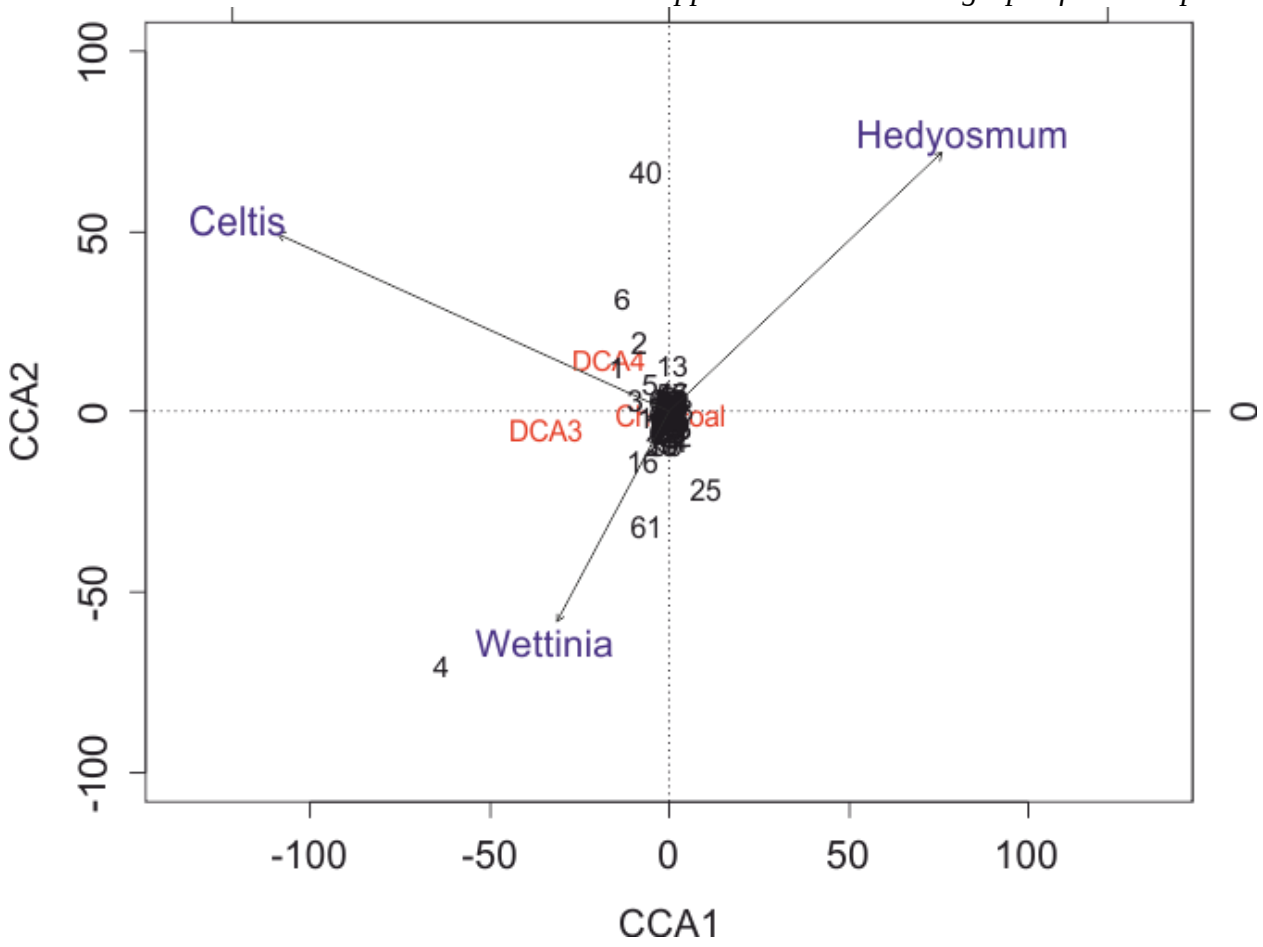

Figure A2.18: A CCA representing the correlation between DCA axes 1-4, charcoal and the three taxa included in figures 8.9 – 8.11.